The control of central nervous system myelination and the phenotypic characterisation of a novel zebrafish mutant: *akineto*^{u45}

By Thomas Hawkins

Submitted to the University of London in 2003 in partial fulfilment of the requirements for the award of Ph.D.

University College London

ProQuest LLC
789 East Eisenhower Parkway
P.O. Box 1346
Ann Arbor, MI 48106-1346

Abstract

Part 1 of this thesis addresses the control of myelination in the central nervous system (CNS). We have a sound knowledge of myelin structure, particularly the molecules and cells involved in its make-up. However, our understanding of the control of myelin formation is scanty. Myelination of CNS tracts during development follows a strictly ordered schedule suggesting local control by axons. Here I present evidence that CNS axons need to form synaptic connections before they can be myelinated. I have used myelin renewal during regeneration of the fish optic nerve as a model system: the axons withstand target deprivation and their behaviour in these circumstances is well characterised from earlier studies of synaptic plasticity. Depriving the regenerating optic nerve of its primary target, the contralateral optic tectum, delays myelination until the regenerating axons find the intact ipsilateral tectum and form synapses there. Facilitating this process hastens the onset of myelination and denying the axons of any opportunity to form synapses abolishes it. I investigated possible mechanisms by which the synaptogenesis-timed signal is mediated and also compared myelination during regeneration and development.

Part 2 describes the phenotypic characterisation of a novel zebrafish mutant: *akineto* (*akn*^{u45}). *Akn*^{u45} mutant embryos cannot contract their skeletal muscles. Here I show that this is caused by incomplete sarcomere assembly. Myofibrils of mutants lack properly assembled thick filaments. Our understanding of the process of myofibrillogenesis, particularly relating to thick filament assembly, is mostly speculative at present. Although the *akn*^{u45} gene is unidentified so far, I am currently engaged in efforts to identify it. Subsequently the *akn*^{u45} mutation may become a useful tool to further unravel the process of myofibrillogenesis.

Acknowledgements

There is a danger here that I will unintentionally mimic Halle Berry and tearfully confess that I want to thank "Everybody in the whole world" before concluding that I also love everybody in the world like some old hippy soak. However, I will try and retain composure and make some attempt at being specific about thanking those who have helped get me here, wherever that is.

Logically the first people I must thank are my parents for putting me on this planet in the first place. I'm also grateful to them for raising me in the countryside where I was surrounded by biology which must have contributed in some way to my loony inclination to study it (once I got past the torturing spiders stage). Whilst on the subject of family, my brother Jon also deserves a mention for his support and lunches in Beetroot, as do the myriad of cousins that seem to all have gravitated to London following my move here.

Now I come on to people who have actually helped me on my way to producing this volume. The most important amongst these is undoubtedly my supervisor John Scholes. I do not believe that one could find a better Ph.D. supervisor anywhere. He is simply superb, he has always available for discussion, he notices when I'm in the doldrums, egging me on with beer and crisps. His breadth of knowledge is something I believe I can only aspire too basically he is an all round first rate geezer. Steve Wilson also fits this category partly for keeping me solvent in this last year but also for providing a vibrant sociable environment. He is also who I blame for my imminent trip to California, blame not quite the right word there perhaps. Various members of the zebrafish group have been invaluable both socially and academically, particularly Pavlina Haramis (of course), Lukas Roth, Marina Mione, Will Norton, Masa Tada, Filippa Barbosa, Zsolt Lele and of course the ever dependable Diz. I would like to mention more but space does not allow. Ph.D. comrades have been a constant source of support, especially those in Jon Clarke's and Paul Martin's group: Dave Lyons, Adam Guy, Manuel (Marcel) Tawk, Mike Redd, Philippa Bayley and Lisa Cooper who have all been great company in the YMCA, the housman and the JB (when we temporarily forget about the landlady).

Outside of work, I have been lucky enough to have been blessed with understanding mates who don't mind me disappearing for months on end whilst counting cells or writing this tome. Ben Rhodes, Tom Armstrong and Robin Tudge particularly deserve mentioning in this regard.

This leaves the most important person in my life, Abby, my betrothed, since you moved to London my life has taken on new purpose and direction and has become about a zillion times more fun. Thank you for putting up with the trauma of Tom and his madcap PhD scheme, I only hope the art dealing pays off because science might not.

Table of contents

List of Figures and Tables

Part 1: The control of central nervous system myelination

Chapter 1: Introduction

Chapter 2: Materials and methods

Chapter 3: No target : no myelination

Part 2 : The Phenotypic characterisation of a novel zebrafish mutant: *akineto*^{u45}

Chapter 7: Introduction

Chapter 9 : Results

Chapter 10 : Discussion

Part 1

The control of central nervous system myelination

Preface

In this part of the thesis, I describe experiments that examine how the production of myelin in the CNS is controlled. Myelin is vital for the normal electrical function of the vertebrate nervous system. We have a sound knowledge of its structure including its molecular and cellular nature. However, our understanding of the mechanisms that control myelin production during development is incomplete. Here, I provide evidence that growing CNS axons need to form synaptic connections before they can be myelinated.

Chapter 1: Introduction

This introduction reviews myelin, including its structure, a résumé of the history of its discovery and information on the molecular and cellular biology of myelin and myelinating cells. Following this, I describe how myelin develops in the nervous system and review what is known about the control of CNS myelination, and in particular the theories that exist to explain the observed timing of myelination in the CNS. Then I provide a brief description of the principal experimental system employed here: the Teleost visual system, evaluating its utility as a model system in myelination.

1.1 Myelin.

1.1.1 Structure and function

Myelin[§] is a fatty insulating material that envelops the majority of axons in the central nervous system (CNS) and about 30% of peripheral nervous system (PNS) axons. It is vital to the normal function of the nervous system because it enables the fast propagation of action potentials over long distances by saltatory conduction. This is achieved by its discontinuous structure, in which the myelin sheath is interrupted at regular intervals by structures called nodes of Ranvier. These short stretches (<1μm) of exposed axon membrane contain sodium channels and generate the propagated action currents, which are channeled longitudinally by the myelinated internodes to activate adjacent nodes. Internodes are the units of myelin; they are made differently between the PNS and CNS and their dimensions vary widely according to the axonal diameter (Figure 1.1).

Each internode of the myelin sheath is made from a continuous flattened lamella of plasma membrane that spirals through many turns round the axon, from a Schwann cell in the PNS (1 cell per internode) or an oligodendrocyte in the CNS (up to 20 internodes per cell). This wrapping is compacted by the exclusion of cytoplasm. The compacted intracellular leaflet is called the major dense line (MDL) because of its dense appearance in the transmission electron microscope (TEM). The extracellular leaflets form the intraperiod line (IPL)

[§] The term myelin comes from the Greek: μυέλινος = *myelinos* = marrowy, this is most probably descriptive of the yellow, fatty nature of the tissue.

Figure 1.1 The structure of the myelin sheath.
A & B: Schematic diagrams (adapted from Hudson (1990)) of how the myelin sheath is constructed in the central (CNS; **A**) and peripheral (PNS; **B**) nervous systems. Oligodendrocytes are the myelinating cells of the central nervous system, they extend multiple processes and form units of myelin (internodes) on multiple axons. The bare segments of axons between the internodes are the nodes of Ranvier. A partially unravelled internode is illustrated (**A;** top right) to show how each internode is constructed from a spirally wrapped membrane lamella at the end of a process. In the PNS the myelinating cell is the Schwann cell and each internode is constructed by a separate Schwann cell. The electron micrographs on the right show the structure of the spiral wraps of the compact myelin membrane which are very similar in structure between the CNS and PNS. Major dense lines (MDL; white arrows), comprising highly compacted intracellular surfaces, alternate with the interperiod lines (IPL; black arrows) which comprise the closely apposed extracellular membrane surfaces. The IPL can sometimes be resolved as a double line.
C: The components of a CNS myelin sheath (adapted from Peters et al (1991) p277). In cross section, a CNS myelin sheath comprises the inner and outer loop of uncompacted cytoplasm (IL & OL) and the intervening spirally wrapped compact myelin (CM).
D: A schematic diagram of an unravelled PNS myelin internode (adapted from Raine (1984) p10 (not to scale)). This shows how the cytoplasmic components of a myelin sheath are arranged. The compact myelin region of the sheath (CM) takes up the majority of the membrane, however, there are thin veins of cytoplasm that run along the edges of the myelin sheath these form the inner and outer loops (OL & IL) and the paranodal loops (PL; see below). Sometimes (particularly in the PNS) additional veins of uncompacted cytoplasm run through from the cell body to the inner loop, these are known as Schmidt-Lanterman incisures (S-L).
E & F: The nodes of Ranvier. **E:** Electron micrographs of longitudinal sections through the nodes of Ranvier in the PNS and CNS (adapted from Peters et al (1991) p249 & p251), **F:** a schematic diagram of the same structure (adapted from Raine (1984) p31). The nodes of Ranvier (N) are flanked by specialised structures where the lamellae of the compact myelin sheath form tight seal against the axonal membrane. These are the paranodal loops (PL) and contain uncompacted cytoplasm. The outermost of the paranodal loops of Schwann cells forms multiple microvillar-type structures surrounding the nodal surface.
Scale bars: **A & B** = 0.1μm; **C** = 0.5 μm; **E** = 0.5 μm.

A. CNS

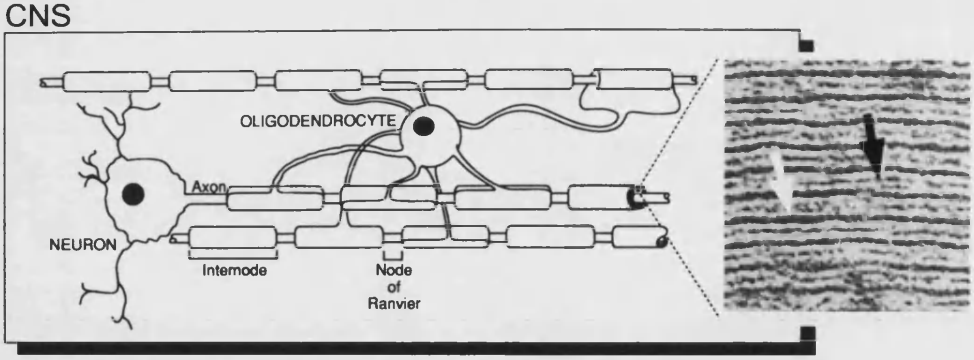

B. PNS

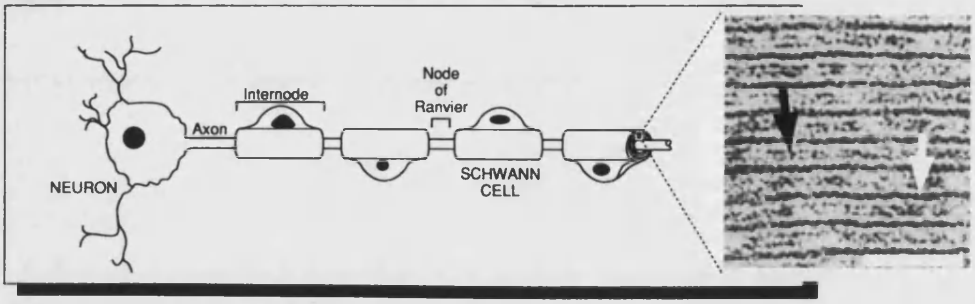

C

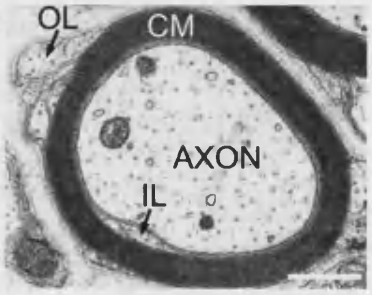

D

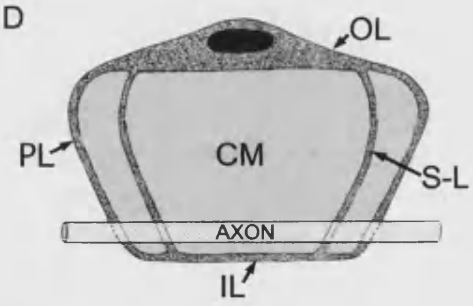

E

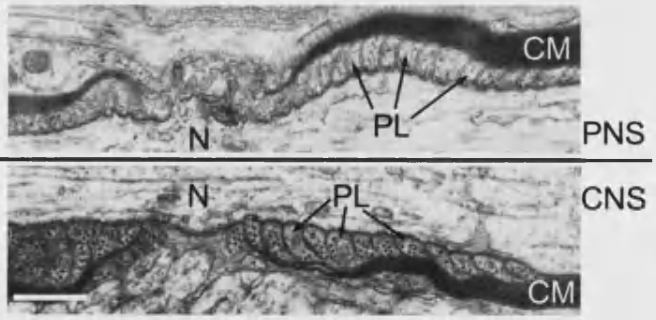

F

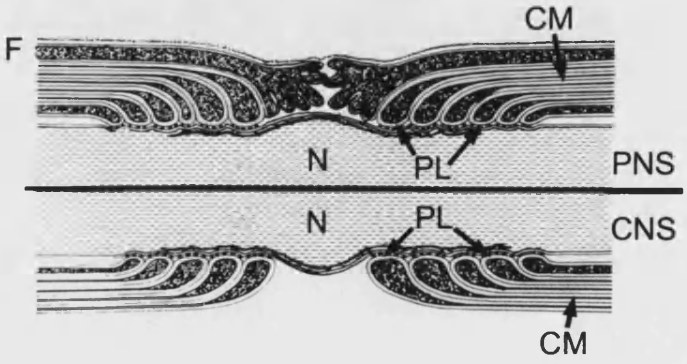

which can sometimes be visualised as two lines in the EM (Figure 1.1 A-C). Cytoplasm is not completely excluded from the compacted lamella: cytoplasm-filled veins run from the parent cell round its margins, forming the inner, outer and paranodal loops of the myelin sheath (Figure 1.1 D). Bordering the node (the paranodal region) the sheath tapers off where the paranodal loops adhere in sequence to the axonal surface (Figure 1.1 E & F), sealing the internodal axon membrane from the extracellular space and localising the sodium channels.

1.1.2 History of myelin discovery

Most reviewers (Penfield, 1932; Windle, 1958; Raine, 1984; Somjen, 1988; Peters et al., 1991; Compston et al., 1997; Baumann and Pham-Dinh, 2001) credit Virchow (1846; 1854; 1858) with the discovery and naming of myelin and the description of neuroglia[†]. Some commentators argue (Windle, 1958; Somjen, 1988) that since he described it as a connective tissue and did not acknowledge its cellular and modular nature he did not fully describe it. Credit for this may fall to Deiters (1865) who first described non-neuronal cells in the central nervous system. Following these original descriptions, undoubtedly the greatest advances in the understanding not only of glia but of the cellular nature of the nervous system occurred with the advent of the heavy metal cell impregnation techniques originally discovered by Camillo Golgi (1873; 1885). These techniques allow the visualisation of a subset (1-5%) of brain cells. With this technique and variations of it Golgi (1885), Santiago Ramón y Cajal (1913a, b) and later Pio Del Rio-Hortega (1919; 1920; 1921) and Wilder Penfield (1924, 1932) were able to fully describe and categorise the glia of the nervous system.

The glia were divided by morphology into protoplasmic and fibrous astrocytes (Andriezen, 1893; Kölliker, 1893) (classical neuroglia or macroglia) and a 'third element' first described by Cajal which did not stain as successfully (Cajal, 1913a, b). Before Cajal published this work and apparently without Cajal's knowledge (see Penfield, 1924) the Scottish pathologist W. Ford Robertson had managed to stain the processes of some of the cells belonging to this third element which he referred to as 'mesoglia' because he considered them to be of mesodermal origin (Robertson, 1897, 1900). The use of his term, mesoglia

[†] The term neuroglia was coined later, the original term used was *nervenkitt*: German for nerve-glue or perhaps more correctly nerve-putty (Somjen, 1988). Subsequently the term "neuroglia" employing the Greek γλία = glue, became the norm.

persisted for several years. However, using a silver carbonate stain Pio Del Rio-Hortega managed to differentiate Cajal's 'third element' into two cellular elements which he named microglia (Del Rio-Hortega, 1919) and oligodendroglia (Del Rio-Hortega, 1921). His observations were confirmed by Wilder Penfield whilst studying in the Cajal institute in Madrid (Penfield, 1924). Having also seen Robertson's preparations, Penfield confirmed that Rio-Hortega's oligodendroglia and Robertson's mesoglia were one and the same. The term mesoglia was doubly confusing because it turned out to be the microglia that are mesodermal, whereas the oligodendroglia arise in the neuroectoderm. It was dropped in favour of the new term oligodendrocyte[‡] (or oligodendroglia) describing cells that have few processes compared to neurones and astrocytes. The myelinating cells of the peripheral nervous system, the Schwann cells, were discovered much earlier than the oligodendroglia. Named after Theodor Schwann (1839) their accessibility facilitated their study, and it was in the PNS that features such as the nodes of Ranvier (Ranvier, 1872, 1878) and Schmidt-Lantermann incisures (Schmidt, 1874; Lantermann, 1877) were described. The birefringence of myelin sheaths (Gothlin, 1913), along with X-ray diffraction of peripheral nerves, allowed the concentric membrane structure to be deduced (Schmitt et al., 1935; Schmitt and Bear, 1939; Schmitt et al., 1941). Finally, electron microscopy (EM) allowed the first ultrastructural description of myelin (Sjostrand, 1949; Fernandez-Moran, 1950, 1954).

Although it was understood that myelin is made by Schwann cells and oligodendrocytes, it many years before any explanation was offered as to how the cells made the myelin. Geren (1954) was the first to describe the spiral wrapping of the Schwann cell mesaxon around the axon and the compaction of the myelin lamellae. Later, Peters confirmed that CNS myelin has a similar spiral structure (Peters, 1960, 1962). However, the thin outer tongue of cytoplasm in CNS myelin indicated that the parent cell is distant from the sheath, as expected if the dendritic (Penfield, 1924) and axon-parallel (Weigert, 1895; Robertson, 1900) processes of oligodendrocytes are the connecting structures.

These slender connections were first identified in the electron microscope by Bunge et al. (1961, 1962) when studying remyelination in the cat spinal cord.

[‡] The term (oligodendro)cyte or glia comes from Greek: ὀλίγος = oligos = few, δένδρον = dendron = tree/branches.

Subsequent studies have fully resolved the three dimensional structure of oligodendrocytes (Peters, 1964; Stensaas, 1977; Nagashima, 1979; Remahl and Hildebrand, 1990; Remahl and Hildebrand, 1990; Hildebrand et al., 1993; Ankerhold and Stuermer, 1999).

1.2 The molecular biology of myelin

1.2.1 Myelin lipids

Myelin, being largely composed of membrane, has a very large lipid content (70% lipid: 30% protein: table 1 (Norton and Cammer, 1984)), with a different lipid composition from that in normal cell membranes. It contains a much larger ratio of glycosphingolipids to glycerophospholipids (Norton and Cammer, 1984), comprising mainly two species, galactocerebroside (GalC; also called cerebroside: 23-32% d.w.) and its its sulphated derivative galactosulphocerebroside (also called sulphatide: 4-7% d.w. : Norton and Cammer, 1984). Myelin also has a very much larger cholesterol content, which is thought to keep the highly saturated glycosphingolipids in a more fluid state (Lee, 2001). These constituents can be localised asymmetrically in the lipid bilayers. Cholesterol and the galactosphingolipids are preferentially localised to the extracellular side which forms the interperiod line whereas the intracellular side contains more glycerophospholipids, resembling a normal plasma membrane (Braun, 1984; Marcus and Popko, 2002). Far from being a passive component of myelin, the lipids, and particularly the galactosphingolipids, play a crucial structural role in sheath assembly, particularly in the CNS. Mice mutant for the enzyme needed to produce galactosphingolipids (Bosio et al., 1996; Coetzee et al., 1996) have structural defects in their CNS myelin but not in PNS myelin. The reason is that a key CNS specific myelin structural component (proteolipid protein (PLP)) is not able to properly integrate into the myelin membrane without galactosphingolipids.

1.2.2 CNS Myelin proteins

The protein composition of myelin differs between the CNS and the PNS (Table 2). The major (50%) CNS structural protein is Proteolipid protein (PLP) which is highly conserved (near to 100%) amongst higher mammals (Diehl et al.,

Table 1. Composition of central nervous system myelin

Substance	Myelin			White matter		Grey matter	Whole brain
	Human	Bovine	Rat	Human	Bovine	(human)	(rat)
Total protein	30.0	24.7	29.5	39.0	39.5	55.3	56.9
Total lipid	70.0	75.3	70.5	54.9	55.0	32.7	37.0
Cholesterol	27.7	28.1	27.3	27.5	23.6	22.0	23.0
Total Galactolipid	17.5	29.3	31.5	26.4	28.6	7.3	21.3
Cerebroside	22.7	24.0	23.7	19.8	22.5	5.4	14.6
Sulfatide	3.8	3.6	7.1	5.4	5.0	1.7	4.8
Total Phospholipid	43.1	43.0	44.0	45.9	46.3	69.5	57.6
Ethanolamine phosphoglycerides (PGs)	15.6	17.4	16.7	14.9	13.6	22.7	19.8
Choline PG	11.2	10.9	11.3	12.8	12.9	26.7	22.0
Serine PG	4.8	6.5	7.0	7.9	11.4	8.7	7.2
Inositol PG	0.6	0.8	1.2	0.9	0.9	2.7	2.4
Sphingomyelin	7.9	7.1	3.2	7.7	6.7	6.9	3.8
Plasmalogen	12.3	14.1	14.1	11.2	12.2	8.8	11.6

Total protein and lipid figures are in percentage dry weight; all others are in percentage total lipid weight.

Table taken from Norton & Cammer (1984) page 155

Table 2: Myelin proteins

Myelin gene	Alternatively spliced isoforms	Post translational modifications	Localisation in myelin	Functions & proportions of total protein (if known)
Proteolipid protein (PLP/DM20)	24 kDa (PLP) 20 kDa (DM20)	Acylated	Compact myelin CNS: transmembrane (PNS: cytoplasmic)	PLP: Structural (50% of CNS myelin) DM20: Possible receptor for differentiation signals
Myelin basic protein (MBP)	21.5 kDa 20 kDa 18.5 kDa 17 kDa (x2) 14 kDa	Phoshorylated, glycosylated, GTP-binding protein, deiminated (Arg), acylated, lipid-linked, methylated.	Compact myelin: cytoplasmic face	Structural: compaction of MDL? (30% of CNS myelin; 5-15% of PNS myelin)
2',3'-cyclic nucleotide 3'-phophodiesterase (CNP)	48 kDa 46 kDa	Amidated, phosphorylated, polyisoprenylated, ?GTP-binding protein, Acylated	Noncompact myelin: cytoplasmic	Axonal support?
Myelin associated glycoprotein (MAG)	72 kDa 67 kDa	Glycosylated, phosphorylated acylated (72 kDa)	Noncompact myelin: transmembrane	Axon - myelin sheath adhesion
Protein zero (P_0)	25 kDa	Glycosylated, phosphorylated acylated	Compact myelin: transmembrane	Structural (compaction of both IPL and MDL) (50% of PNS myelin; not present in CNS)
P2 Basic Protein (P_2)	14 kDa	Amidated	Compact myelin: cytoplasmic	Assembly? lipid transport
Myelin oligodendrocyte glycoprotein (MOG)	52 kDa	Glycosylated, GPI-linked	Noncomact myelin: extracellular face	? Cell adhesion

Table adapted from Hudson (1990) page 486

1986; Macklin et al., 1987; Macklin, 1992). The full length PLP molecule evolved from a splice variant called DM20 by the incorporation of mRNA coding for an extra 35 amino acids into exon 3 (Nave et al., 1987; Yoshida and Colman, 1996). PLP is heavily acylated (on 6 residues) making it very hydrophobic and so it was originally quite a challenging protein to study. The PLP molecule has four transmembrane α-helices, with a large extracellular loop between loops 3 and 4 which is considered to mediate interactions across the intraperiod line. Most of our understanding of the function of PLP comes from the study of both natural and induced mutants of the PLP/DM20 locus (Nave, 2001). The role that the alternative splice variant DM20 has in myelin is still unclear. However, it has been suggested to play some part in the generation of oligodendrocytes because of its expression at early stages in the development of these cells.

Another key myelin protein component is myelin basic protein (MBP) which has several different splice isoforms (de Ferra et al., 1985; Takahashi et al., 1985) and comprises 30-40% of mouse CNS myelin and 10-20% of PNS myelin (Lees and Brostoff, 1984). MBP localises to the major dense line of the myelin sheath (Omlin et al., 1982) analysis of mice mutant for this protein (*shiverer*) (Roach et al., 1985) show that it probably serves a role in the compaction of the intracellular half of the myelin leaflets into the major dense line (Privat et al., 1979; Rosenbluth, 1980). mRNA for MBP migrates from the cell body of oligodendrocytes to the myelin sheath for local translation as needed during membrane compaction (Colman et al., 1982; Trapp et al., 1987; Amur-Umarjee et al., 1990; Landry et al., 1994; Hardy et al., 1996). The MBP molecule appears to have evolved by the intragenic insertion of a novel transcription initiation site within a larger gene. The MBP gene is part of a larger gene (called GOLLI-MBP: gene expressed in the oligodendrocyte lineage) (Grima et al., 1992; Campagnoni et al., 1993). This larger gene is not expressed exclusively in the oligodendrocyte lineage but has been found in the immune system and in neurons (Pribyl et al., 1993; Zelenika et al., 1993; Pribyl et al., 1996).

Aside from these principal structural components of myelin, there are many other lesser components (by weight) that serve functions which I will not discuss in any detail here. 2',3'-cyclic nucleotide phosphodiesterase (CNP) which is not exclusive to myelin comprises 4-5% of myelin protein (Braun et al., 1988). It is not localised to the compacted membrane component but to the cytoplasmic

parts of the sheath (Braun et al., 1988; Trapp et al., 1988). The role of CNP is somewhat enigmatic. It is expressed very early in oligodendrocyte development (see below) and recent knockout studies suggest that it may be important for glial-mediated axonal support/survival signals (Lappe-Siefke et al., 2003; Popko, 2003).

Another lesser component is myelin-associated glycoprotein (MAG) which comprises 1% of CNS myelin and 0.1% of PNS myelin (Norton and Cammer, 1984). It has been assigned several different roles based on the production of mice mutant in different portions of the molecule (Schachner and Bartsch, 2000; Baumann and Pham-Dinh, 2001), such as adhering the sheath to the axon, compaction, and determining if an axon has been previously ensheathed (Schachner and Bartsch, 2000; Baumann and Pham-Dinh, 2001). MAG has also been shown to inhibit axon regeneration in the CNS via the NoGo receptor which is a focus of research aiming to promote post-injury regeneration in the human CNS (Hunt et al., 2002).

1.3 Oligodendrocyte development

The myelinating cells of the CNS are oligodendrocytes. They fit into around 4 morphological classes in the adult, according to their size and the number of axons that they myelinate (Del Rio-Hortega, 1921; Penfield, 1932; Stensaas, 1977) (Figure 1.2).

Oligodendrocytes have been extensively studied *in vitro* as a model system to address questions about cell lineage, differentiation and the control of cell number (for reviews see: (Pfeiffer et al., 1993; Compston et al., 1997; Raff et al., 1998; Rogister et al., 1999; Baumann and Pham-Dinh, 2001; Richardson, 2001; Miller, 2002)). Oligodendrocyte precursor cells (OPCs) will differentiate *in vitro* in the absence of axons. Important cell intrinsic and cell extrinsic regulators of this process have been identified. However, the interactions of developing OPCs with the axons that they have to myelinate *in vivo* are less well understood.

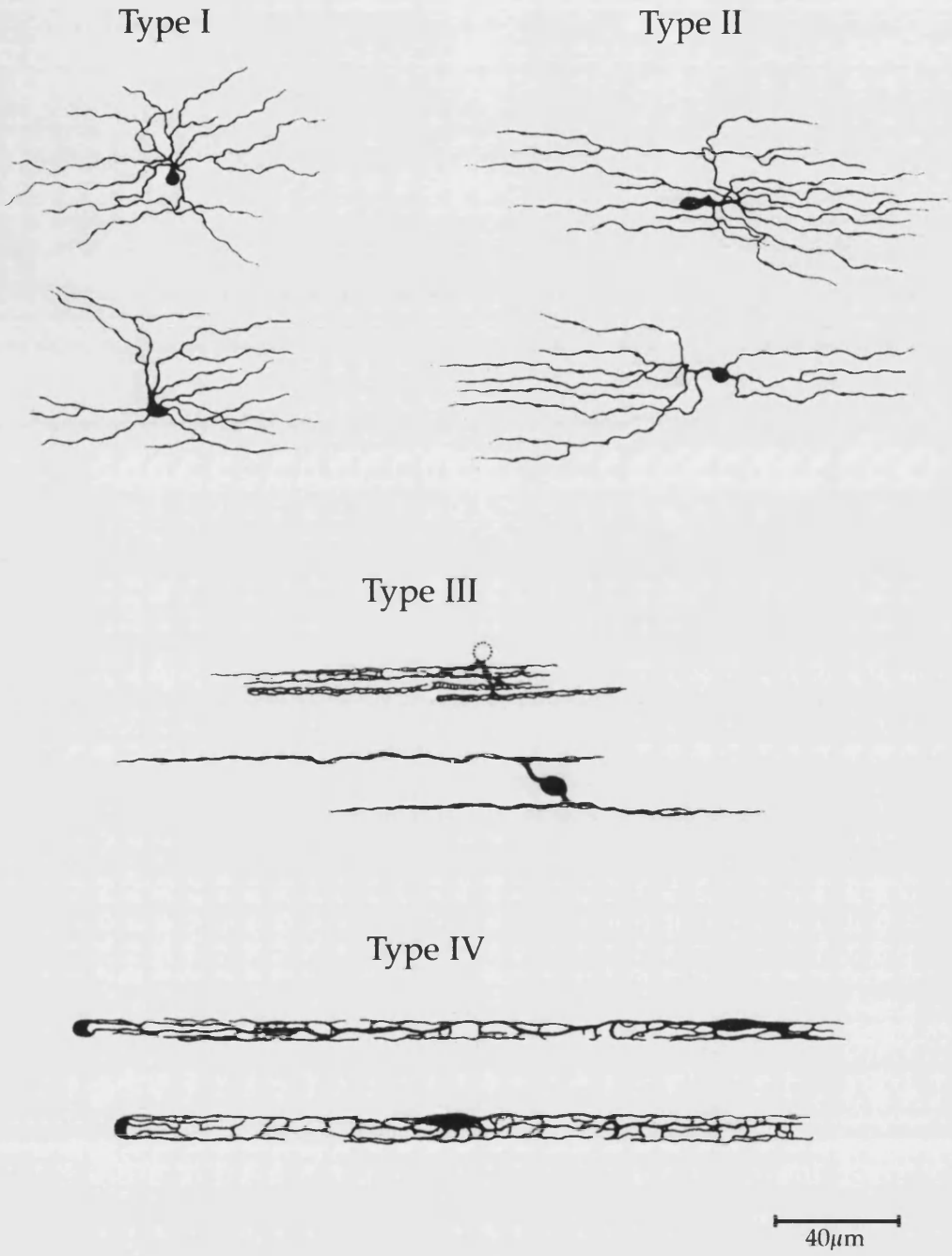

Figure 1.2 Classes of oligodendrocytes. (Adapted from Stensaas & Stensaas (1977)). Oligodendrocytes can be grouped into 4 classes according to their morphological features. Types I & II myelinate many axons of smaller diameter and have an extensive network of cell processes. Types III & IV myelinate either one (IV) or a small number (III) of larger diameter axons.

1.3.1 Stages in oligodendrocyte differentiation.

Study of oligodendrocyte development *in vitro* and *in vivo* has shown that there are several distinct stages in this process. These stages are identified by the expression of stage-specific marker molecules, by morphology and by the propensity of the cells to migrate or proliferate (Figure 1.3).

The early specification of cells fated to become oligodendrocytes occurs in focal areas of the ventral neuroepithelium under the control of factors downstream from hedgehog signalling by the notocord/floorplate (Richardson et al., 2000; Richardson, 2001). The earliest point at which an oligodendrocyte lineage cell can be distinguished from other neuroepithelial/subventricular zone precursors is when the cells begin to express the platelet-derived growth factor receptor-α (PDGFRα) (Pringle et al., 1992), DM20 (Ikenaka et al., 1992; Timsit et al., 1992; Timsit et al., 1995; Dickinson et al., 1996) and CNP (Yu et al., 1994). They also show PSA-NCAM (Hardy and Reynolds, 1991; Grinspan and Franceschini, 1995), vimentin (Grinspan et al., 1990) and nestin (Gallo and Armstrong, 1995) expression. This early stage is generally referred to as the pre-GD3 stage because the cells do not yet express the GD3 antigen (Hardy and Reynolds, 1991).

Following pre-GD3 stage the cells assume a bipolar morphology and commence expression of the antigens GD3, A2B5 and NG2 (Hardy and Reynolds, 1991; Fok-Seang and Miller, 1994; Nishiyama et al., 1996a) in addition to the pre-GD3 markers. At this stage, the cells are highly migratory and proliferative (Small et al., 1987; Pfeiffer et al., 1993; Warrington et al., 1993) and are named oligodendrocyte precursor cells or OPCs. They were earlier termed O-2A progenitors because of their capacity to produce either oligodendrocytes or type-2 astrocytes under different conditions *in vitro* (Raff et al., 1984; Temple and Raff, 1985). However, this capacity appears not to be expressed *in vivo* where transplantation of labelled O-2A progenitors only produces oligodendrocytes (Espinosa de los Monteros et al., 1993). OPC/O-2A cells have QK-type glutamate receptors (Barres et al., 1990; Wyllie et al., 1991) and can be labelled with cobalt, which made it possible to trace how their bipolar morphology becomes more complex during development and how their number decreases during development as mature oligodendrocytes differentiate from them (Fulton et al., 1992).

Figure 1.3 The oligodendrocyte lineage, markers and morphology. The development of the oligodendrocyte lineage is illustrated with sketches of the morphology of the cells at the five principal stages *in vivo* (left) and *in vitro* (right). The stage names are written in the centre along with features of the cellular behaviour (eg proliferation and migration) Markers expressed by the cells are also listed. mRNA markers detectable by *in situ* hybridisation are listed in blue, proteins detectable by immunohistochemistry are listed in green.
1. **Pre GD3 stage**: *in vivo,* the cells are part of the sub-ventricular zone SVZ and are morphologically indistinct from other SVZ cells. However, they can be identified by marker expression (red). *In vitro,* cells of this stage also have a fairly indistinct morphology but some isolated cells have a unipolar morphology.
2. **OPC/O2As**: This is a highly motile and proliferative stage where the cells take on a bipolar morphology both *in vivo* and *in vitro.* However, some *in vivo* cells appear unipolar and some markers of this stage are only expressed *in vitro.*
3. **Pro-oligodendrocytes**: These cells are still proliferative but are less motile. They are characterised *In vivo* by the formation of strings of cells with increasingly complicated networks of processes. *In vitro* they elaborate their bipolar processes further.
4. **Pre-myelinating oligodendrocytes**: These are post-mitotic oligodendrocytes. They are characterised both *in vitro* and *in vivo* by increasingly elaborate cell processes. *In vivo, they* often have a very dense, nest-like network of processes. Although not drawn, they are still often found in rows *in vivo* as at the previous stage.
5. **Myelinating oligodendrocytes**. This is the final stage of oligodendrocyte differentiation which culminates in the formation of myelin. Myelinating oligodendrocytes *in vivo* extend processes longitudinally along the axons that thicken and enwrap the axons. The nest of processes concurrently becomes less dense. *In vitro,* cells at this stage produce large flat segments of membrane that adhere to the substratum.

Abbreviations:
PDGFαR = Platelet-derived growth factor alpha receptor
CNP = 2',3'-Cyclic nucleotide phosphodiesterase
PSA-NCAM = Polysialated neural cell adhesion molecule
GAP-43 = Growth associated protein 43
POA = Pro-oligodendrocyte antigen
MBP = Myelin basic protein
GalC = Galactocerebroside
PLP/DM20 = Proteolipid protein and splice isoform DM-20
GS = Glutamine synthase

Morphology
In vivo

Stage & markers expresed

Morphology
In vitro

1. Pre-GD3

Both:
PDGFRα
Nestin
DM20
CNP
PSA-NCAM
Vimentin

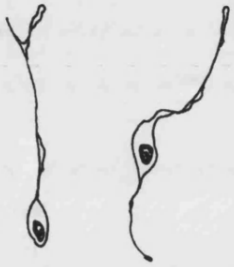

2. OPC/O-2A
proliferative &
highly motile

Both:
DM20
CNP
GD3
A2B5
NG2
PDGFRα

***In vitro* only**
vimentin
GAP-43

3. Pro-Oligodendrocyte
proliferative
but less motile

Both:
DM20
CNP
POA (O4 or A007)
GD3
NG2
PDGFRα

4. Pre-myelinating Oligodendrocyte
Post-mitotic

Both:
DM20
CNP
MBP
GalC

5. Myelinating Oligodendrocyte

Both:
GalC
PLP & DM20
MBP
CNP
GS

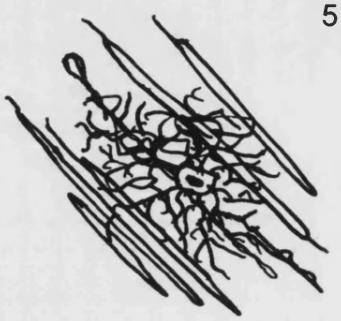

After the OPC stage, the cells reach their destinations in the prospective white matter tracts where they settle but continue proliferating (Pfeiffer et al., 1993) to form strings of cell bodies aligned with the axons (Del Rio Hortega, 1920; Penfield, 1924), that persist in the white matter into adulthood (Suzuki and Raisman, 1992, 1994). At this stage they are post-migratory. In contrast to OPC cells, they are unable to spread and colonise the CNS when transplanted into hypomyelinated hosts (*shiverer* mutant mice: Warrington et al., 1993). This change is marked by an alteration in antigenic phenotype and by elaboration of the formerly simple bipolar cell processes (Hardy and Reynolds, 1991). These cells are referred to as pro-oligodendrocytes, and are identified by pro-oligodendrocyte (POA) antigen recognised by the antibodies O4 and A007 (Sommer and Schachner, 1981; Bansal et al., 1992). Pro-oligodendrocytes become progressively unresponsive to PDGF despite continued expression of PDGFRα (Hart et al., 1989; Hall et al., 1996).

These cells finally cease division and commence terminal differentiation as immature or premyelinating oligodendrocytes (Hardy and Reynolds, 1991; Baumann and Pham-Dinh, 2001 Reynolds, 1991 #305), recognised by complex processes and the expression of myelin sheath molecules such as galactocerebroside (GalC or GC), myelin basic protein (MBP) and 2',3'-cyclic nucleotide 3'-phosphohydrolase (CNP) (Knapp et al., 1988; Reynolds and Wilkin, 1988; Gard and Pfeiffer, 1989). The use of antibodies which are specific for DM20 and PLP have shown a transition from the DM20 isomer to the PLP isomer as the cell transits from an immature oligodendrocyte to a mature and myelinating one (Kronquist et al., 1987; Gardinier and Macklin, 1988; LeVine et al., 1990; Trapp et al., 1997).

The transition from an immature oligodendrocyte to a mature myelinating cell is really only well characterised by morphology. The up-regulation of certain antigens like PLP on myelinating processes and glutamine synthase has been shown by some observers (Hardy and Reynolds, 1991; Trapp et al., 1997) but morphology is the best way to distinguish cells at this late stage of development. *In vitro*, so-called mature oligodendrocytes have widely spreading processes that form lamellipodia-like structures which are taken as the *in vitro* equivalent of myelin sheaths (Sarlieve et al., 1983; Knapp et al., 1988; Amur-Umarjee et al., 1990; Hardy et al., 1996).

There are many EM studies of the formation CNS myelin sheaths (for review see: Peters et al., 1991 pp 234-242), but few on the behaviour of myelinating oligodendrocytes. Hardy and Friedrich (1996) studied them immunohistochemically and showed that initially they have an extremely dense net of thin processes among the surrounding axons. As myelination proceeds, a subset of the processes thicken and spread along selected axons preparatory to enwrapment and the fine processes are lost as the oligodendrocyte forms sheaths around these axons.

Remahl and Hildebrand (Remahl and Hildebrand, 1990; Remahl and Hildebrand, 1990; Hildebrand et al., 1993) reconstructed myelinating oligodendrocytes by serial section EM, and noticed that early oligodendrocytes only myelinate axons close to the cell body, where later on these axons are more widely spread out. The myelination process may be dynamic such that oligodendrocytes change axons to arrive at the final array, or it could be intercalated growing axons that progressively space out the array.

1.3.2 Control of differentiation in the oligodendrocyte lineage

(i) A cell intrinsic timer.

The oligodendrocyte progenitor *in vitro* (O-2A) can control its further differentiation through a cell-intrinsic timer. O-2A progenitors isolated from the rat optic nerve and maintained in defined medium will passage through several rounds of cell division (up to 8) before undergoing differentiation into mature oligodendrocytes (Raff et al., 1984; Temple and Raff, 1985). Moreover, when the progeny of one round of division are isolated in individual culture vessels they undergo an identical number of divisions before differentiating (Temple and Raff, 1985), thus revealing an internal clock. The cellular machinery underlying the clock is beginning to be understood. It is affected by inhibitors of cyclin-dependent kinases (CDKs). Both $p27^{Kip1}$ and $p18^{Ink}$ have been shown to build up in cells over successive cell cycles (Durand et al., 1997; Gao et al., 1997; Tokumoto et al., 2002) in step with the clock (Gao et al., 1997). Tokumoto et al (2002) have shown that artificially raising the level of both $p27^{Kip1}$ and $p18^{Ink}$ causes the premature differentiation of O-2A cells.

The bHLH transcription factor inhibitors Id2 and Id4 have also been implicated in the timer mechanism (Kondo and Raff, 2000b; Wang et al., 2001).

They inhibit bHLH transcription factors by forming heterodimers with them. Id2 translocates from nucleus to cytoplasm as O-2A cells differentiate (Wang et al., 2001) and the level of Id4 expression decreases over the same timescale (Kondo and Raff, 2000b). Increasing the level of Id2 or Id4 expression in O-2As *in vitro* decreases the propensity of these cells to differentiate (Kondo and Raff, 2000b; Wang et al., 2001). These and other findings suggest the presence of an unidentified bHLH trnscription factor that promotes oligodendrocyte differentiation. A possible candidate is Mash1 which increases as the timer runs (Kondo and Raff, 2000a), but O-2As derived from Mash1 null mice show no change in their ability to differentiate (Wang et al., 2001).

(ii) Thyroid hormone

A supply of thyroid hormone (more specifically T3 or triiodothyronine) is crucial for the clock to run as removing it from the medium halts differentiation (Barres et al., 1994a). Thyroid hormone is thought to be an 'effector', promoting differentiation based upon a readout from the clock. Thus, when TH-deprived O2A cells are given TH, they differentiate rapidly and synchronously, indicating that the timer has still been running but could not be acted upon (Barres et al., 1994a). That thyroid hormone is implicated in the control of oligodendrocyte differentiation fits well with many studies showing myelin deficits in hypothyroid rats; thyroid hormones are also only released into the blood around the time of birth which is the same period that myelination commences (for review see: (Rodriguez-Pena, 1999)).

(iii) Oligodendrocyte precursors arise in focal areas of the neuroepithelium

In the spinal cord a 'singularity' of PDGFRα mRNA expression in the ventral ventricular zone at embryonic day 14 (E14) days of development in rat development marks the focal origin of the OPCs in this region of the CNS (Pringle and Richardson, 1993). These cells then rapidly proliferate and spread throughout the spinal cord (Pringle and Richardson, 1993; Ono et al., 1995; Orentas and Miller, 1996). Similar focal origins of OPCs have been described in more rostral brain areas (Pringle and Richardson, 1993; Spassky et al., 1998; Perez Villegas et al., 1999; He et al., 2001; Olivier et al., 2001; Spassky et al., 2001; Tekki-Kessaris et al., 2001). However, these are not always ventral areas like in the

spinal cord. For example, a source of oligodendrocytes has been described in the olfactory bulb (Spassky et al., 2001).

(iv) Oligodendrocyte precursor origin is controlled by mechanisms which also regulate neurogenesis.

The ventral origin of OPCs in the spinal cord suggested that they might be specified by the well known mechanism underlying motor neuron differentiation in this region, namely sonic hedgehog (shh) produced by the notocord and floorplate. This was confirmed by notochord transplants producing ventral fates including ectopic oligodendrocytes, in dorsal regions of the spinal cord (van Straaten et al., 1985a; van Straaten et al., 1985b; Yamada et al., 1991), and by notochord ablation, which eliminates oligodendrocytes (Maier and Miller, 1997). The focus of oligodendrocyte precursor cells identified by Pringle & Richardson (1993) arises in the same expression domain as the cells that produce somatic motor neurones (the pMN domain) (Sun et al., 1998; Lu et al., 2000; Lu et al., 2002). They appear after the motor neurons and the switch restricting them to the oligodendrocyte lineage (Kessaris et al., 2001; Zhou et al., 2001) includes the down-regulation of neurogenins and the subsequent spread of more ventral marker domains (e.g. nkx 2.2) into the olig2 motor neuron expression domain (Kessaris et al., 2001; Zhou et al., 2001). However, it is unclear whether this involves neuroblasts switching to oligodendrocyte production or glioblasts springing to life.

(v) Glial restricted progenitors (GRPs) may represent an alternative lineage of oligodendrocytes.

The ventral (or 'focal' in areas of the CNS other than the spinal cord) origin of the PDGFRα expressing OPCs and their fast spread through the nervous system may not be the only source of oligodendrocytes. There is evidence that cells throughout the developing CNS that can give rise to oligodendrocytes (albeit fewer). These cells can be isolated by immunopanning with A2B5 (Rao and Mayer-Proschel, 1997; Rao et al., 1998) and are called glial restricted progenitors (GRPs). They differ from O-2As because they can give rise to both types of astrocytes and oligodendrocytes *in vitro* (Rao et al., 1998) and after transplantation *in vivo* (Herrera et al., 2001). They also appear to utilise a

different arsenal of survival/differentiation factors and mitogens than O-2As. For example, GRPs are unresponsive to PDGF (Rao et al., 1998).

Whether these progenitors represent an entirely different lineage to the OPC/O-2A lineage or an earlier step within it is currently under debate. GRPs can give rise to O-2A-like cells and thus may be 'pre-progenitors' of this lineage (Gregori et al., 2002). However, they arise throughout the neuroepithelium and produce more astrocytes than oligodendrocytes when transplanted back into the CNS (Herrera et al., 2001). GRPs may not be not a homogenous population (Gregori et al., 2002). For example, the sonic hedgehog-dependent emergence of oligodendrocytes in the olfactory bulb seems to be via a PDGF unresponsive GRP-type lineage (Spassky et al., 2001).

Adult oligodendrocytes are far from a homogenous population of cells, showing wide variation in morphology depending on axon size (Figure 1.2) with associated biochemical differences (Butt et al., 1995; Butt et al., 1998). Miller (2002) has suggested that these oligodendrocyte sub-types may arise from the different GRP and OPC/O-2A lineages.

(vi) Mitogens and survival factors exerting control at different stages in the oligodendrocyte lineage.

A variety of factors control the progression of cells through the oligodendrocyte lineage by regulating survival, proliferation and differentiation at different stages.

(a) Platelet derived growth factor (PDGF)

PDGF is required for cultured OPCs to divide and advance their mitotic clock (Noble et al., 1988; Raff et al., 1988; Richardson et al., 1988), and acts as a survival factor as well (Raff et al., 1988; Barres et al., 1992; Grinspan and Franceschini, 1995). It can be supplied *in vitro* by co-culture with astrocytes or incubation in astrocyte-conditioned medium (Noble et al., 1988; Richardson et al., 1988). Its role *in vivo* has also been confirmed by transgenic over-expression and knockout studies resulting in an excess or dearth of oligodendrocytes (Calver et al., 1998; Fruttiger et al., 1999). Total removal of PDGF from culture media causes isolated oligodendrocyte progenitors and precursors to die, indicating that it is a survival factor as well as a mitogen.

Both neurons and astrocytes express PDGF (Raff et al., 1988; Yeh et al., 1991; Barres et al., 1992; Mudhar et al., 1993; Grinspan and Franceschini, 1995) but neurons appear to be unable to deliver PDGF via their axons (Mudhar et al., 1993; Fruttiger et al., 2000). This is perplexing when the loss of OPCs caused by TTX blockade of axon transmission can be reversed by PDGF (Barres and Raff, 1993). The answer is probably that astrocytic release of PDGF is dependant on the electrical activity of the axons, so PDGF supply is a joint effort between neurons and astrocytes (Barres and Raff, 1993; Fruttiger et al., 2000).

The chemokine GRO-α (CXCL1) (Robinson et al., 1998) is made by astrocytes and regulates the sensitivity of OPCs to PDGF, as well as acting as a stop factor to halt migratory cells where needed and encourage division (Tsai et al., 2002). The chondroitin-sulphate proteoglycan NG2 also regulates responsiveness to PDGF. It co-localises with the PDGFR and immunoprecipitates with it in extracts OPC, and anti-NG2 antibodies attenuate the proliferative responses of OPCs to PDGF (Nishiyama et al., 1996a, b).

(b) Fibroblast growth factors (FGFs)

The FGF family also controls OPCs. FGF-2 (bFGF) enhances the mitogenic effects of PDGF on OPC cells (Bögler et al., 1990; McKinnon et al., 1993; Fok-Seang and Miller, 1994), acts as a mitogen in its own right for O4+ GalC- pro-oligodendrocytes (Gard and Pfeiffer, 1993; Fok-Seang and Miller, 1994; Goddard et al., 1999) and down-regulates myelin genes in mature oligodendrocytes (Bansal and Pfeiffer, 1997). The FGFs are a huge family of factors with much redundancy and it is not clear which of them act on the oligodendrocyte lineage during development *in vivo*, as mouse mutants have so far proved uninformative (for review see: Bansal, 2002).

(c)Other survival factors

Among several other factors that have been implicated in controlling oligodendrocyte survival, insulin-like growth factor-1 (IGF-1) and neurotrophin-3 (NT-3) have been studied in detail. IGF-1 enhances the survival of OPCs *in vitro*, especially in combination with other factors (Barres et al., 1993a; Barres and Raff, 1994). However, the IGF-1 knockout mouse has minimal defects in myelination relative to the neuronal changes (Beck et al., 1995; Cheng et al., 1998) suggesting that the effect of IGF on oligodendrocyte development is minor. NT-3

promotes the survival of OPCs in the optic nerve and *in vitro* (Barres et al., 1994b), but spinal cord OPCs are unresponsive to this factor (Robinson and Miller, 1996). This might reflect a lineage difference akin to the GRP/O-2A spinal cord/olfactory bulb lineage differences mentioned earlier.

1.4 Axonal control of oligodendrocyte development.

Axons and oligodendrocytes are partners in the myelination process, and axons have been shown to control the oligodendrocyte lineage at various stages during progression towards myelin formation. In this thesis, I argue that CNS axons need to form synaptic connections before they permit the oligodendrocytes to myelinate them. To put this in context, I will review the currently understood roles of axons in oligodendrocyte development, ordering the account by the sequence of lineage progression given above (Figure 1.3).

Early progenitor to OPCs

The earliest stages of oligodendrocyte differentiation take place in the ventricular zone before axon outgrowth. The highly migratory OPC stage is when axons begin to take control, *via* the electrical activity-mediated control of astrocyte PDGF release described above (Barres and Raff, 1993).

OPCs to pro-oligodendrocytes.

OPCs have to migrate long distances among immature axons to colonise the future white matter and there are indications that the Notch/Delta system may inhibit premature differentiation at this stage. Notch receptors are expressed by OPC/O-2As and activation of these receptors prevents their further differentiation. The idea is that Notch ligand expressed by immature axons is down-regulated as the axons mature, thus releasing the OPCs for the next stage in lineage progression (Wang et al., 1998). The role of Notch in oligodendrocyte development has recently been confirmed in mice deficient in Notch signalling. Homozygous Notch null mice die before birth, but Givogri et al (2002) showed that myelination occurs prematurely in heterozygotes and ectopic myelinated axons are found in normally unmyelinated areas (e.g. the molecular layer of the cerebellum). In addition, Genoud et al (2002) developed a conditional knockout driven by CNP or PLP promoters to delete Notch in OPCs specifically that also

resulted in premature and ectopic oligodendrocyte differentiation. While these findings reveal a functional role Notch signalling in OPCs, the intriguing case (Wang et al., 1998) that growing axons show Notch ligand in a maturationally regulated manner needs strengthening. Notch inhibition of oligodendrocyte differentiation is upregulated in demyelinated plaques of multiple sclerosis (MS) (John et al., 2002). However, it is astrocytes not axons that express the Notch ligand Jagged in this case.

OPC to pro-oligodendrocyte to pre-myelinating oligodendrocyte

As oligodendrocytes mature from OPCs their survival requirements change from astrocyte-derived PDGF to axon-derived factors. Up to 50% of newly formed oligodendrocytes in the rat optic nerve normally die within 2-3 days of generation (Barres et al., 1992), but transection of the optic axons increases this attrition to more than 97% (Barres et al., 1993b). Neuron conditioned medium is insufficient to promote oligodendrocyte survival *in vitro* demonstrating that axon contact is required. In agreement, the unusually persistent distal segments of severed axons in the WLD mouse rescue many of the oligodendrocytes that normally die following optic nerve transection (Barres et al., 1993b).

There is mounting evidence that neuregulins are the axon survival signal required for the survival of newly differentiating pro-oligodendrocytes. Neuregulins (NRGs) are a large family of signalling molecules related to epidermal growth factor. Supply of soluble NRGs increases the survival of oligodendrocytes *in vitro* and *in vivo* (Fernandez et al., 2000). This effect is mimicked *in vitro* by co-culture with neurons where oligodendrocytes contacting axons survive, but die if NRG signalling is blocked (Fernandez et al., 2000). Oligodendrocyte development fails in spinal cord explants from mice lacking neuregulin and this is also reversed by soluble neuregulin supply (Vartanian et al., 1999). Deletion of the ErbB2 receptor (one of several neuregulin receptors) has no effect on the survival of O4+ pro-oligodendrocytes in spinal cord explants but dramatically attenuates the survival of later differentiating GalC+ pre-myelinating oligodendrocytes (Park et al., 2001; Kim et al., 2003). Thus the POA/O4 expressing pro oligodendrocytes may represent a susceptible stage in the transition from astrocyte dependence (OPCs needing PDGF) to axonal contact-dependence ($GalC^+$ premyelinating oligodendrocytes needing

Neuregulin). Extracellular matrix (ECM) molecules expressed on the axonal surface (e.g. laminins) can modulate the response of cells of the oligodendrocyte lineage to growth factors (e.g. NRG) via integrins expressed by oligodendrocytes. This is a possible mechanism by which axonal contact switches oligodendrocyte-lineage cells to NRG-mediated survival (Colognato et al., 2002; Baron et al., 2003).

Stevens et al (2002) showed that axonal electrical activity controls the differentiation of OPCs via activation of their adenosine receptors. They found that OPCs express a wide range of purinergic receptors and respond to electrical activity in OPC/DRG co-cultures. Supply of exogenous adenosine encourages oligodendrocyte differentiation and myelination of DRG axons *in vitro* (Stevens et al., 2002).

Pre-myelinating oligodendrocyte to mature oligodendrocyte.

Once past the transition from OPCs, oligodendrocyte numbers stabilise to match axon numbers, but the susceptibility to axotomy remains (Barres et al., 1993b; Trapp et al., 1997).

The mechanisms by which the ensheathment of axons by newly differentiated oligodendrocytes is controlled are still poorly understood. An unidentified astrocyte-derived factor can induce oligodendrocyte processes to align and adhere to axons (Meyer-Franke et al., 1999). Extracellular matrix interactions with integrins (specifically β1) expressed by oligodendrocytes are important for the construction of myelin membrane *in vitro* and *in vivo* (Buttery and ffrench-Constant, 1999; Relvas et al., 2001), as are cell-cell interaction mediated by adhesion molecules such as N-cadherin (Schnadelbach et al., 2001). However, how oligodendrocytes are triggered to produce myelin membrane and enwrap axons is unknown. A possible mechanism is that immature axons negatively regulate ensheathment by the expression of PSA-NCAM. This axon surface molecule is expressed in early fibre tracts and down-regulated at the time of myelination (Bartsch et al., 1990; Oumesmar et al., 1995). Removal or masking of the PSA moieties of PSA-NCAM promotes axon contact by oligodendrocyte processes *in vitro* (Meyer-Franke et al., 1999) and enhances myelination *in vitro* and *in vivo* (Charles et al., 2000). This may be of interest in myelin disease as PSA-NCAM is upregulated in MS lesions (Charles et al., 2002).

However, masking PSA-NCAM does not induce precocious myelin formation on its own. Charles et al (2000) found that electrical activity was required as an additional positive signal. Although activity-dependent adenosine release may act by influencing OPC/O-2A differentiation more than directly promoting myelin enwrapment of the axons, adenosine treatment of OPC/DRG co-cultures did result in the formation of compact myelin (Stevens et al., 2002). These studies have shown that CNS axons control their myelinating cells in different ways at different stages during the progression from OPCs to mature oligodendrocytes. This culminates in ensheathment itself, which occurs in a precisely timed schedule from one fibre tract to the next, but how a neuron times the up or down-regulation of these various mechanisms in order to regulate the myelination of its axon is not clear.

1.5 The timing of myelination during development

During human development myelination of the tracts of the central nervous system proceeds in a highly ordered schedule. This was originally shown by studies of white matter development using histological methods on pathological specimens. The study of myelination in pathological brain specimens has a long history. Flechsig (1901; 1920) was the first to make a detailed account and two other comprehensive studies were published later in the 20th century (Yakovlev and Lecours, 1967; Brody et al., 1987).

In a particularly meticulous study, Yakovlev & Lecours (1967) surveyed human white matter development from the onset of myelination at around 6 months before birth until the third decade of life. The earliest CNS tracts to commence myelination are the midbrain tracts of the stato-acoustic system, the medial lemniscus, and the inner division of the inferior cerebellar peduncle at 3 months gestation. In contrast, myelination of the corpus callosum does not begin until four months after birth (Figure 1.4). Whereas some pathways (e.g. the optic radiation) are completed in the first year of life, others (e.g. in association cortex) appeared incomplete even in the 3rd decade (Figure 1.4 A: (Yakovlev and Lecours, 1967)).

Several recent studies have re-examined white matter development *in situ* using magnetic resonance imaging (MRI) in live human infants from birth and in premature births (Van der Knaap and Valk, 1995; Paus et al., 1999; Paus et al., 2001). Little new information has emerged from these studies. They essentially reconfirm the earlier post mortem studies (Figure 1.4 B). However, MRI is non-invasive and can efficiently sample normal healthy subjects. Although resolution is poor at present, as this improves MRI will likely further refine our detailed knowledge of the sequence of myelination in the human brain.

There have also been many detailed histological and immunochemical studies on myelin development in the brain and spinal cord of laboratory animals (Chung and Coggeshall, 1984; Looney and Elberger, 1986; Rozeik and Von Keyserlingk, 1987; Schwab and Schnell, 1989; Hamano et al., 1996). These studies generally recapitulate what was found in the studies in humans; different fibre tracts in the brain and spinal cord are myelinated in specific sequences.

In one of the most thorough of these studies, Schwab and Schnell (1989) examined the developing rat spinal cord with antibodies for myelin proteins from birth to 14 days of development and in the adult. They found that myelin appears in the white matter tracts in a strictly ordered sequence and that this sequence broadly matures in a rostro-caudal pattern of development (Figure 1.5). An interesting case in point is myelination of the dorsal columns. Both Schwab and Schnell (1989) and before them Schreyer and Jones (1982) noted that the cuneate fasciculus of the dorsal columns commence myelination before the gracile fasciculus despite the tracts being tightly abutted against each other.

The universal principle which emerges from these anatomical studies is that the onset and progress of myelin formation, while influenced by systemic factors such as thyroid hormone, is controlled locally with sharp discrimination between nearby tracts. The outstanding question is, how do oligodendrocytes decide to myelinate one tract whilst leaving a neighbouring tract untouched?

As recognised at the turn of the 20th century by Flechsig (1901), the most likely answer to this question is that the fibre tracts myelinate in the order of their functional maturation. This suggestion was examined by many subsequent observers in the early 20th century (reviewed by Langworthy, 1933) who noted that the order and speed of myelination appears to reflect an order of priority in

Figure 1.4 Myelination of the human brain occurs in a strictly timetabled fashion. Examination of myelination of the human brain by histology on pathological specimens (**A**) (taken from Yakovlev & Lecours 1967) and on live brains by magnetic resonance imaging (MRI; **B**) (taken from Van der Knaap & Yalk 1995). **A**: The temporal schedule of myelination in 25 tracts of the brain is shown by the black tapering bars. Myelination commences 5 months pre-birth and continues into the 3rd decade of life. **B**: MRI studies largely corroborate the findings by histological study of pathological specimens. Increasing myelination is indicated by 1 to 3 plus signs. The MRI data only describe infant development up to one year post natal. However, the authors note (as did Yakovlev & Lecours (**A**)) that myelination of some higher tracts continues for many years.

A

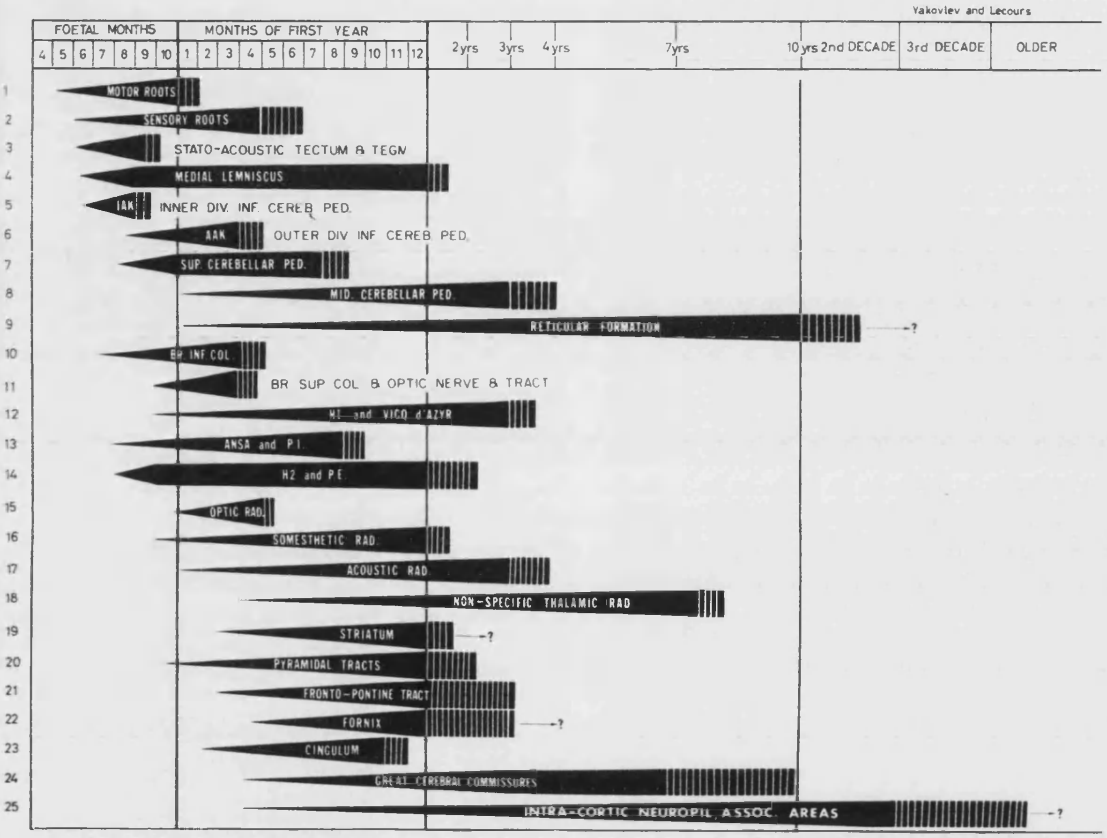

B

Regions of CNS	Fetal age in months					Postnatal age in weeks					Postnatal age in months			
	24	28	32	36	40	4	8	12	16	20	6	9	12	>12 months
Cerebellar peduncles		+	+	++	+++	+++	+++	+++	+++	+++	+++	+++	+++	Further refinement of myelination in the subcortical arcuate fibers continues for several years
Tegmentum pontis				+	+	++	++	+++	+++	+++	+++	+++	+++	
Basis pontis							+	+	++	+++	+++	+++	+++	
Medial lemniscus						+	++	++	+++	+++	+++	+++	+++	
Pyramidal tracts								+	+	+	++	++	+++	
Optic nerve					+	++	++	+++	+++	+++	+++	+++	+++	
Optic radiation						+	+	++	+++	+++	+++	+++	+++	
Stato-acoustic system	+	+	+	++	++	++	++	+++	+++	+++	+++	+++	+++	
Intern. caps. post. limb			+	++	+++	+++	+++	+++	+++	+++	+++	+++	+++	
Intern. caps. ant. limb								+	+	++	+++	+++	+++	
Corpus call. splenium							+	+	++	++	++	+++	+++	
Corpus call. genu										+	+	++	+++	
Parieto-occip. WM						+	++	++	+++	+++	+++	+++	+++	
Frontal WM												+	++	
Temporal WM													+	

WM, white matter

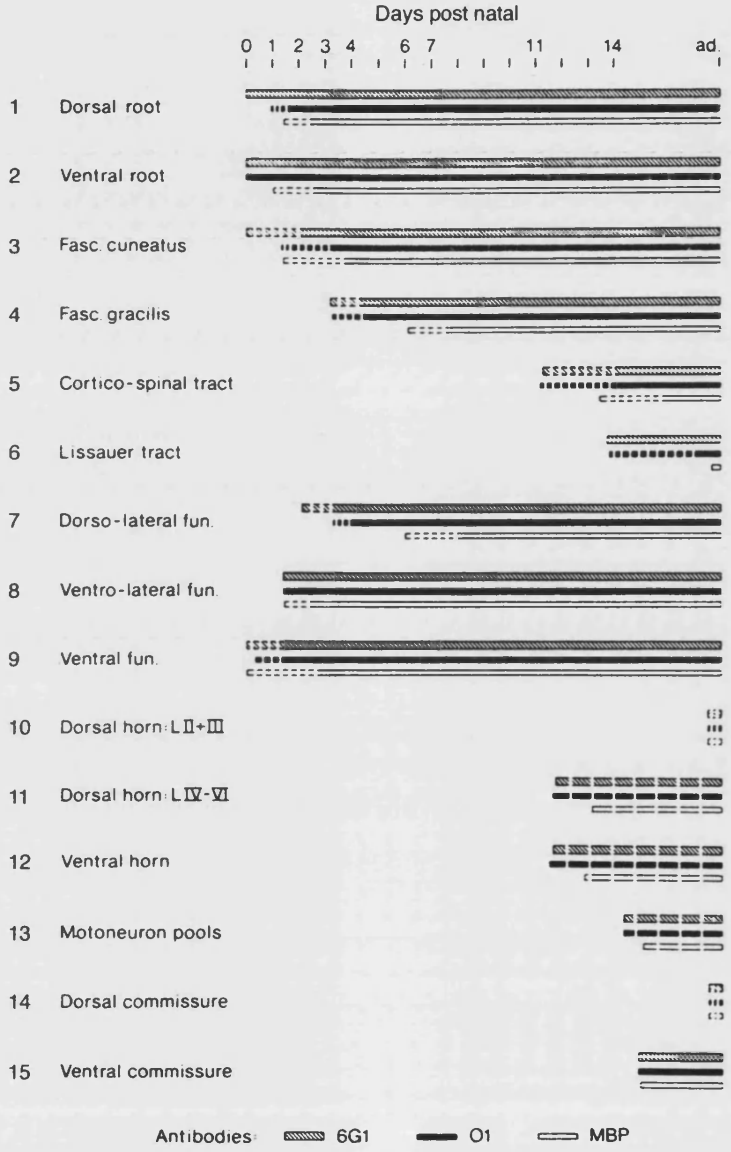

Figure 1.5 Myelination of white matter tracts of the rat spinal cord occurs in a region-specific manner (adapted from Schwab and Schnell (1989)). When the rat spinal cord is examined at several stages of postnatal development between birth and adulthood (ad.) with immunohistochmistry using antibodies specific for myelin components (6G1, O1, MBP). The white matter tracts of the spinal cord are myelinated at widely differing times. For example, the fasciculus cuneatus of the dorsal columns (**3**) begins expression of myelin components three to four days before the closely neighbouring fasciculus gracilis (**4**).

the functional maturation of systems in the CNS. The idea was also clearly foremost in the mind of Yakovlev who refers to myelination as a "morphological criterion of the functional maturity of a conduction path." ((Yakovlev and Lecours, 1967)p68).

This is probably best exemplified by the fibre-sharp selective myelination patterns in the dorsal columns of the rat (Schwab and Schnell, 1989). Presumably the cuneate is myelinated before the gracile because of (i) the rostro-caudal sequence of spinal cord development and (ii) the shorter distance that axons must traverse from the cuneate dorsal root entry points to the dorsal column nuclei.

The Notch/Delta mechanism by which axons can control the differentiation of oligodendrocytes from OPCs has been proposed as a mechanism to by which axons might mediate their myelination once they have matured. The proposal is that the release of OPCs from axon-mediated inhibition permits the differentiation of myelinating oligodendrocyte which myelinate the tract (Wang et al., 1998). This is backed up by mouse mutant data (Genoud et al., 2002; Givogri et al., 2002). However, it seems unlikely that the Notch pathway acts alone in the control of myelination. The control of CNS myelination is more likely to be a cooperation between the other axonally-derived mechanisms that have been shown to influence myelination (PSA-NCAM, Adenosine, ECM/integrin interactions) and probably other as yet unidentified mechanisms.

Despite knowing that myelination closely correlates with the functional maturation of a CNS fibre tract and having at hand some possible molecular signalling mechanisms, it is still not known what aspect of the functional maturation of axons is required for myelination to proceed. One possibility and a reason why myelin would be required, is that the axons of a tract signal for myelination once they have become synaptically connected in their target brain area, but this has not been successfully experimentally tested. This is probably because of the difficulty of keeping axons that are deprived of their target neurons alive.

1.6 The regenerating fish visual system as a model.

In the regenerating teleost visual system when axons are severed they will regenerate even when deprived of their targets. Thus I have used this system to test the influence that target-connection has on myelination because it neatly circumvents the difficulties normally caused by the death of axons deprived of their targets.

1.6.1 Anatomy of the fish visual system

The fish visual system is built on the vertebrate pattern (Figure 1.6). Two eyes containing laminated retinae project from the retinal ganglion cell layer via the optic nerve to the opposite side of the brain. The eyes of most fish point sideways from opposite sides of the head, thus the optic nerves project entirely to the opposite side of the brain without any mixing of axons at the chiasm. The forebrain of fish is a poor relative of its mammalian counterpart and although it does receive some visual input via the diencephalon (Braford and Northcutt, 1983; Northcutt and Wulliman, 1987; Burrill and Easter, 1994), the majority of the retinal axons leaving the eye project to form connections in the tectum of the midbrain, which still exists as a lesser visual pathway in mammals.

(i) The Teleost optic nerve.

The fish optic nerve resembles a pleated ribbon in cross section (Figure 1.6 B), this structure being produced by the growth of the visual system over time. The eyes and brain continue growth throughout life (in step with the growth of the fish itself), although in older fish, this growth is very slow. The retina grows at the cilliary margin adding new photoreceptors, retinal interneurons and retinal ganglion cells in an anular tree ring-like manner (Figure 1.6 A). The new projection cells send axons accross the retina to the optic nerve head where they pass into optic nerve. The optic axons are arranged by age accross the width of the ribbon with the oldest axons on one edge and the newest axons at the other edge. The different quadrants of the retina are ordered accross the thickness of the ribbon (Scholes, 1981). The very newest axons projecting from the eye at one extreme end of the nerve are unmyelinated whereas axons in the rest of the nerve are all myelinated (Figure 1.6 B) (Scholes, 1981).

Figure 1.6 Features of the fish visual system. **A.** A diagram representing the fish eye and a section cut through the plane illustrated. The brain of fish continually grows throughout life, in the retina new cells arise in the germinal zone (**GZ**; darker blue) at the cilliary margin. As a result the retina is composed of chronological annuli of cells with consecutive birthdates (**1-6**; colours). The oldest cells are near the optic nerve exit point (**1**; cyan) and the youngest are adjacent to the germinal zone (**6**; lavender). **B.** The fish optic nerve resembles a pleated ribbon in cross section (T/S). As new retinal ganglion cells are added at the retinal edge they project axons along the optic whereby across the width of the ribbon the axons are in age-sequence in step with retinal growth (**1-6**; colours). All axons in the nerve are myelinated except for those at the extreme youngest end of the ribbon (**UM**).
C. Once the optic axons reach the optic tectum (**TeO**) they branch and course obliquely over the tectum in arcuate bundles, this is illustrated by the dotted lines in the right tectal lobe which is illustrated with a segment cut away to demonstrate the layering of the tectum. The fibre bundles are restricted to a superficial layer of the tectum called the *stratum opticum* (**SO**; detail in section on right). Axons leave the bundles in the SO to enter and arborise in the synaptic layer beneath, the *stratum fibrosum et griseum superficiale* (**SFGS**). The SO and the SFGS are not the only layers in the tectum but the other layers are not illustrated here for simplicity. TeO: Optic tectum; FB: forebrain (ghosted so that the optic nerves are shown); Cb: cerebellum; Val: valvula; Teg: tegmentum; HB: hindbrain.

A Eye

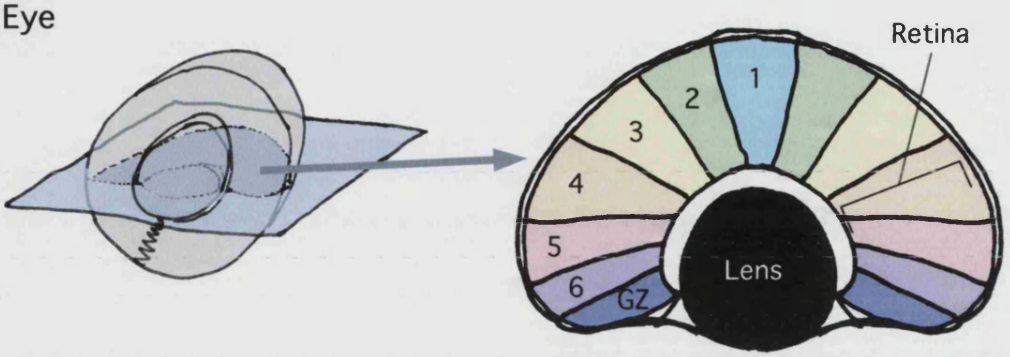

B Optic nerve

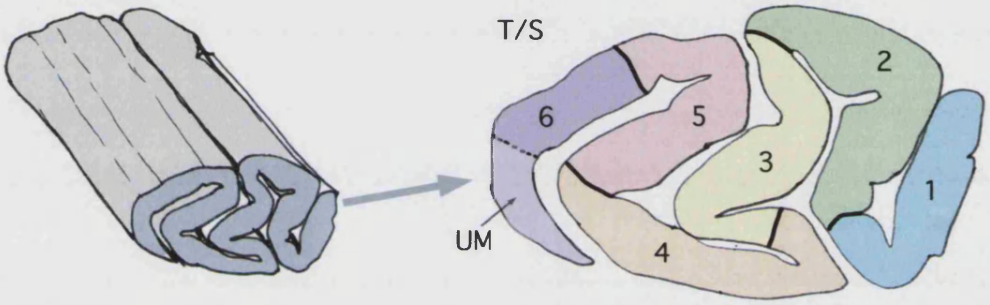

C Tectum

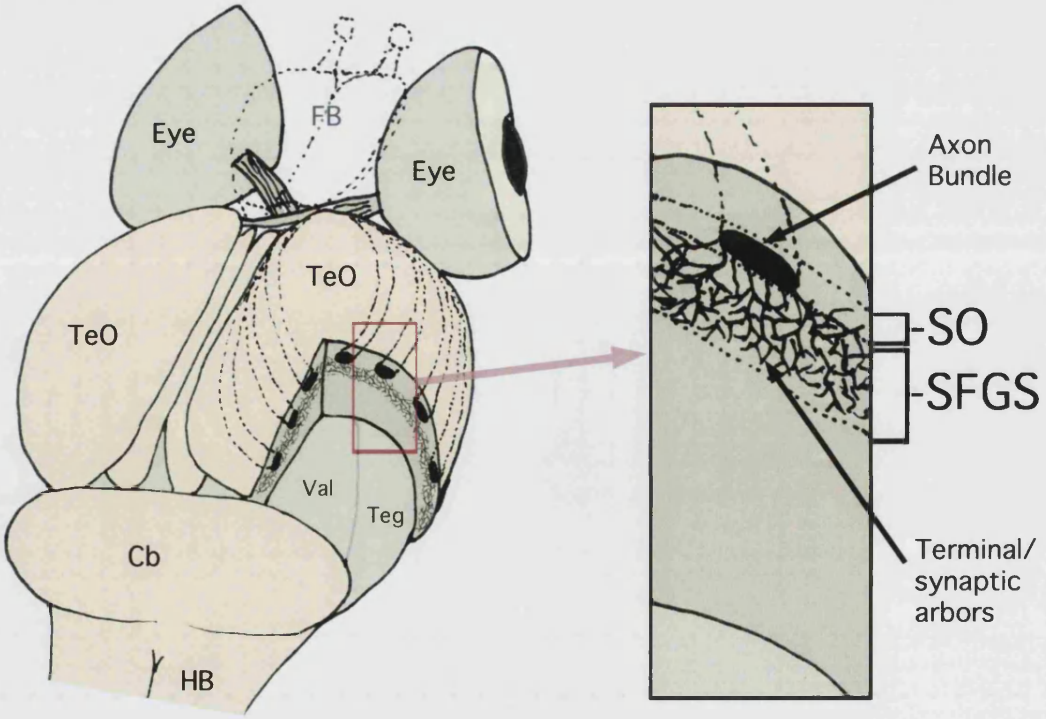

The fish optic nerve contains astrocytes and oligodendrocytes. Unlike astroglia elsewhere in the fish CNS, and unlike in mammals, the astrocytes lack the vertebrate astroglial marker, glial fibrillary acidic protein (GFAP). They appear to be a phylogenetically archaic form of astrocyte which utilise cytokeratin instead of GFAP. They form a dense meshwork investing the optic axons, which may be important for protection during the fast saccades of the eye (Scholes, 1991).

(ii) The optic tectum.

At the entrance to the tectum, the optic nerve/tract splits to form two fibre brachia which hug the tectum on its medial and lateral sides. These brachia get thinner from anterior to posterior as bundles of axons branch off from them in arcs to innervate the surface of the tectal hemisphere. The tectum is a highly laminated structure and two layers are important for this study (Figure 1.6C), namely the *stratum opticum* (SO) and underlying it the *stratum fibrosum et griseum superficiale* (SFGS) (Vanegas, 1984). The bundles of optic axons run across the surface of the tectum in the SO. They gradually attenuate as individual axons leave them at appropriate locations to synapse with the dendrites of tectal neurons. The optic synapses are formed almost exclusively in the SFGS, which accounts for about one third of the vertical extent of the dendrites of the tectal neurons (Figure 1.6C).

1.6.1 Regeneration and the Teleost visual system.

The chief advantage of the fish visual system for the studies presented here is its capacity for regeneration. When the axons of the optic nerve are severed by crushing of the nerve behind the eye they regenerate across the lesion site and re-grow up the optic nerve to reconnect with the tectum (Sperry, 1948) within two to three weeks. Myelin sheaths then begin to appear in the optic nerve, but it takes 2-3 months before myelination is completed (Murray, 1976; Nona et al., 2000), possibly by the same oligodendrocytes as before (Ankerhold and Stuermer, 1999). A key advantage is that the axons will regenerate through the optic nerve even when the optic tectum they are regenerating toward is removed (Sharma, 1973; Levine and Jacobson, 1975; Springer and Cohen, 1981).

In the normal fish visual system, the retinal projection maps topographically onto the tectum. During regeneration, as the axons make their

way into the tectum this map is initially scrambled but is then slowly re-established. This appears to happen in two stages. The first is navigation to the approximate area or tectal zone that contains their final map position (Meyer, 1980). This is an activity-independent process (Meyer, 1983) most likely mediated by molecular axon guidance cues. During the second phase, optic fibres select more precise locations, refining the spatial accuracy of the map. The refinement process can be followed by focal injection of retrograde tracer into the tectum at different times and revelation of labelled ganglion cells in the retina, which become clustered into smaller groups as time passes (Rankin and Cook, 1986).

This system has been used for many studies on axonal pathfinding and synaptic plasticity (for review see (Debski and Cline, 2002)). To explore mechanisms of adaptive change, many studies examined what happened when either a whole tectal lobe or parts of it were removed from the path of the regenerating axons. If a segment of the tectum is removed, the retino-tectal projection forms a compressed map in the remaining available tectal tissue (Yoon, 1976). If the whole tectal lobe is removed then the regenerating axons eventually invade the opposite tectal lobe where their terminals capture eye-specific territories from the pre-existing innervation (Sharma, 1973; Levine and Jacobson, 1975; Springer and Cohen, 1981; Boss and Schmidt, 1984).

To achieve these adjustments, the fish optic axons can evidently withstand lengthy target-deprivation and find alternative targets by pioneering new pathways. In what follows, I have exploited this unique capacity to ask whether the regenerating axons acquire myelin sheaths as a matter of course, or need to form synapses first. It would be very difficult to test this question in any other context than the regenerating fish nervous system. Besides the difficulty of access to early CNS pathways, cell death is the certain sequel to target deprivation during development in the mammalian CNS (Oppenheim, 1991). Only one attempt to ascend this North face has been reported in abstract form. Dugas *et al.* (2001) tried an explant approach, seeding rat retinal ganglion axons with purified optic nerve oligodendrocytes in the presence and absence of slices of the superior colliculus. They found an increase in myelin basic protein (MBP) immuno-reactivity on axons with colliculus slices and no MBP in cultures lacking target-tissue. However, no further study describing actual myelin ensheathment

has yet been published to extend these initial findings. My use of the regenerating fish nervous system neatly circumvents these difficulties and using this system I have found evidence that synaptic target-connection is required before myelination proceeds.

1.6.2 Are fish a good model?

The results in this part of the thesis all come from the regenerating fish visual system. To extrapolate them to myelination during development in other vertebrates it is important to be aware of differences that might affect this.

(i) Myelin.

Biochemically speaking, CNS myelin in fish and higher vertebrates differs in two ways. Firstly, In higher vertebrates proteolipid protein (PLP) makes up 50% of CNS myelin protein (Campagnoni, 1988). Fish, however, completely lack PLP, and its place is taken by P_0 which is confined to the PNS in higher vertebrates.

There are similarities between the roles of P_0 and PLP in myelin structure. They are both implicated in the formation of the interperiod line (IPL) of the myelin sheath, although P_0 also acts in the stbilisation of the major dense line (MDL). Because of these similarities in their roles it was previously thought that PLP is an exclusive invention of higher vertebrates, superseding the role that P_0 had in the CNS of lower vertebrates such as fish. Recently, however, it has been shown that the smaller splice variant of PLP, DM20 (also found in higher vertebrates) is present in the CNS of bony and cartilagenous fish (Yoshida and Colman, 1996). From amphibians onward the full PLP protein is present, having evolved from the DM20 locus by activation of a cryptic splice site to insert an extra 35 amino acids into exon 3 (Nave et al., 1987; Yoshida and Colman, 1996). Although the co-expression of PLP and P_0 is seen in the CNS of some amphibia (Yoshida and Colman, 1996), the absence of P_0 from the CNS terrestrial vertebrates suggests a phylogenetic replacement of P_0 by PLP as the protein of choice for the CNS in higher vertebrates. This may have occurred by the transposition of the fish P_0 promoter onto the DM20/PLP gene (Jeserich et al., 1997). However this remains to be fully proven. As pointed out by L. D. Hudson (1990), this situation where apparently unrelated proteins (e.g. P_0 and PLP) evolve to fulfil similar roles is reminiscent of the crystalins of the eye where

widely differing proteins can perform a crystaline function in the lens (Piatigorsky and Wistow, 1989).

The second main biochemical difference between fish and higher vertebrates is the presence of a 36 kDa protein (thus called 36K) originally characterised in the Trout (Jeserich, 1983). This seems to be a fish-specific component of CNS and PNS myelin (Waehneldt and Jeserich, 1984; Jeserich and Waehneldt, 1986; Waehneldt et al., 1986). It is predicted to be a member of the short-chain dehydrogenase/reductase (SDR) family from its sequence (Moll et al., 2003; Morris et al., 2003) and so may have some biochemical role in lipid biosynthesis. However, the protein is also heavily expressed in the myelin sheath and may thus serve a structural role there (Moll et al., 2003). The utility of this protein must have been lost or superseded by other proteins in higher vertebrates, and its function remains unknown at present. It appears that this could be another protein seemingly unrelated to other myelin structural components that has been conscripted 'off the peg' for use in the construction of the myelin sheath.

Despite these biochemical differences the morphology of myelin in the CNS of fish is essentially identical to higher vertebrates. There are subtle differences in the distance between the myelin lamellae (Kirschner and Blaurock, 1992) but the principal morphological features of myelin (including spiral wrapping, multiple ensheathment by oligodendrocytes, nodes of Ranvier, *etc...*) are consistent between fish and higher vertebrates

(ii) Regeneration.

Is regeneration a good model for development? Regeneration is inherently less orderly than development. During the continual growth of the Teleost CNS new axons fasciculate to guide each other to the target brain areas which grow in step to accommodate them. This synchronised progression is totally lost during regeneration where all the axons in a nerve or tract must sprout and grow simultaneously to their targets. However, given time, much of the initial disorder of regeneration is resolved by the recapitulation of developmental mechanisms such as activity-dependent refinement. Is myelination during regeneration also a recapitulation of developmental myelin formation? This question is thoroughly addressed in the discussion (chapter 6) in the context of

the results I have obtained in chapter 5. Briefly, it appears that the same factors do govern the onset of myelination during development and regeneration. However, the balance between these factors differs during development and regeneration.

Chapter 2: Materials and methods.

I have divided the description of the materials and methods employed in between the two parts of the thesis. However, where there are common protocols (for example, electron microscopy) which are described in this section, with any differences being listed in the methods chapter of part 2 (chapter 8).

2.1 General information

Chemicals

Unless otherwise listed, all chemicals used were obtained from the Sigma-Aldrich Company Ltd, Poole, UK.

Microtomy

All cryosections were cut using a Reichert-Jung Frigocut 2800E cryostat (Reichert-Jung, Chicago, IL, USA). All resin-embedded preparations were sectioned using an LKB 2088 Ultratome V (LKB, Bromma, Netherlands).

Microscopes/photography

The main compound light microscope used was a Zeiss Axioplan (Carl Zeiss Ltd, Welwyn Garden City, UK) micrographs were taken using a Zeiss MC 100 spot camera. The film was either Kodak Ektachrome 64T EPR or Ektachrome 100 EPN and was electronically scanned using a Polaroid sprintscan 35 35mm film scanner (Polaroid (U.K.) Ltd, Luton) at 2700 dpi. The main dissecting microscope used was a Zeiss Stemi SV11 (Carl Zeiss Ltd, Welwyn Garden City, UK). Some photographs were taken via the photo-tube on this microscope using an Olympus OM-2 camera (Olympus Optical Co. (UK) Ltd. Southall, UK) with the same film as above.

All electron microscopy used a Jeol JEM-1010 transmission electron microscope (Jeol UK Ltd, Welwyn Garden City, UK) at 80kV. Electron micrographs were taken using Kodak 4489 electron microscope film. These were processed on-site using Kodak D19 developer and were electronically scanned at 1200 dpi using an Epson Perfection 1240U scanner with a transparency adaptor (Epson UK, Hemel-Hempstead, UK) and printed using an Epson colour photo 900 printer.

All images were handled using either Adobe Photoshop 7 or Adobe Illustrator 10. Planimetry was carried out using NIH image (freely downloadable from http://rsb.info.nih.gov/nih-image/).

2.2 Animals.

The carp (*Cyprinius carpio*) were obtained from a local ornamental koi farm. They measured from 50-62mm (nose to base of tail) and were maintained in glass tanks measuring 1200x300x400mm with under-gravel filtration at 22°C ± 3°C. The tanks were kept in a room which had a controlled light cycle of 14 hours light/10 hours dark. The golden orfe (*Leuciscus idus*) were obtained from a local aquarium shop. They measured 64-76mm and were maintained in the same conditions as the carp.

The zebrafish (*Brachydanio rerio*) were obtained from the in-house zebrafish facility in the Department of Anatomy and Developmental Biology at University College London. They were maintained in 12 litre tanks with a water temperature of 28°C. The light cycle was 14 hours light/10 hours dark. The tanks were supplied with a constant feed of filtered water from a gravel bed/fluidised sand filtration plant and were constantly aerated. The fish were fed twice a day on a mixture of cultured brine shrimp and powdered flake fish food (Tetra-Min UK)

The larval zebrafish used in chapter 5 were obtained from the natural daily spawning of the breeding colony of the same facility. They were raised for the first 6 days in water containing 0.001% w/v methylene blue at 28°C. Following this they were transferred to the nursery where they were maintained in 1 litre tanks that were drip fed with filtered water. They were fed cultured paramecia and finely powdered fish embryo food (ZM Ltd, UK). The age of the larvae was counted from the day of fertilisation.

2.3 Surgery

Anaesthesia.

For all operations fish were anaesthetised using 3-Aminobenzoic acid ethyl ester: methansulfonate salt (MS-222) at a concentration 0.1g/L in tank water. All procedures were licensed by the UK Home Office.

Optic nerve lesions.

To induce regeneration of the optic nerve it was crushed at its exit from the eye. Following induction of anaesthesia, the fish were removed from the water and held vertically in a cut sponge soaked in anaesthetic-containing water. Adult zebrafish were additionally supplied with aerated water containing anaesthetic through the gills via a gravity fed system. The operations were carried out using a dissecting microscope. To access the optic nerve, the dorsal part of the membrane attaching the eye to the orbit was cut and the eye was gently rotated down and out of the orbit. This revealed the optic nerve, retinal artery and the muscles of the eye. Using a dedicated set of fine forceps (Dumont Biologie No. 5) the optic nerve was crushed at its exit to the eye. Care was taken to avoid injury to the retinal artery. To totally remove innervation from one eye, the optic nerve was revealed as above but instead of crushing with forceps, it was cut with fine spring scissors and a length of the nerve was removed. Following these operations the eye was gently replaced in the orbit and the fish were returned to fresh water for recovery. Revival from anaesthesia was aided by irrigating the gills and the fish were returned to their tank and left to regenerate for the required period.

Tectal ablation.

Tectal ablations were carried out between 5 and 7 days following optic nerve crush. To remove one tectal lobe, the fish were anaesthetised and placed upright in a sponge mould. The midline of the skull overlying the tectum was cut using a small scalpel and further incisions were made using small curved spring scissors to open a skull flap that hinged laterally over the tectal lobe to be removed. The tectum was removed using an aspirator under low pressure with a fine tip. Suction was applied to the caudal half of the tectum and as the tissue was pulled away from the brain the tip of the aspirator was moved out and

rostrally to ensure that the whole tectum was detached from underlying structures. The complete tectum was then sucked into the fine tip of the aspirator. A quick inspection was made to ensure that the lesion had been complete before the skull flap was re-engaged and the skin was sealed with cynoacrylate (RS components Ltd, Corby, UK). To remove both tecta the same procedure was carried out on each side of the brain. The fish were revived in fresh water and returned to their tank for the required period of regeneration as before.

Anterograde tracer injection

To trace the destination of the regenerated axons an anterograde tracer was injected into the eye 24 hours before sacrifice. The fish were anaesthetised and laid on their side. For the injection, a Hamilton syringe (Hamilton GB Ltd, Camforth, UK) was adapted by fitting with a 12.7x0.33mm needle from an insulin syringe (Micro-fine+ brand; Becton-Dickinson, Dublin, Ireland) This was filled with the tracer (see below). The needle was inserted into the eye from a ventral angle through the area of the 'pupil' above the choroid fissure. 3-5μl of tracer was then injected into the vitreous compartment of the eye. The needle was withdrawn and the fish revived.

Implantation of elvax

To insert Elvax slow release polymer implants containing dAPV and lAPV, a very similar procedure to tectal removal was employed. Fish were anaesthetised, a skull flap was opened and the tectum was revealed. Connective tissue and oil globule deposits were removed from surrounding the tectum and the Elvax implant was placed onto the surface of the tectum. The skull flap was re-engaged and sealed with glue and the fish were recovered in fresh water.

Perfusion with fixative.

Sacrifice was carried out by terminal anaesthesia followed by perfusion through the heart with fixative (for adult fish) or decapitation (for larval zebrafish). The fixative was chilled 2% w/v paraformaldehyde, 2.5% w/v glutaraldehyde in 0.1M sodium cacodylate buffer (pH 7.3). Terminal anaesthesia was induced using >0.2g/L 3-Aminobenzoic acid ethyl ester:methansulfonate salt (MS-222) in tank water. To perfuse through the heart with fixative the fish

was terminally anesthetised, and was held upside down using an anaesthetic soaked sponge. The pericardial cavity was opened and a syringe fitted with a 30 gauge needle containing fixative was inserted into the right ventricle of the heart. A hole was made in the left atrium to allow blood to escape as pressure was applied to the syringe. Perfusion was continued until there was no more blood emitted from the left atrium. This usually required approximately 10 ml of fixative for the fish used here. Larval zebrafish were decapitated under terminal anaesthesia with spring scissors and placed in fixative.

2.4 Anterograde tracing.

The anterograde tracer employed was n-hydroxysuccinimido biotin. This was first dissolved in dimethyl sulfoxide (DMSO) 100mg per ml. This solution was mixed 1:1 with absolute ethanol to make a final concentration of 50mg per ml. 3-5 μl of this solution was injected into the eye 24 hrs before sacrifice (as described above). Following perfusion, the brains and the optic nerves were removed and immersed in the same fixative (2% w/v paraformaldehyde, 2.5% w/v glutaraldehyde in 0.1M sodium cacodylate buffer (pH 7.3)) for 24 hrs at 4°C. After rinsing in 0.1M Sodium cacodylate (pH 7.3) the optic nerves were removed from the brains and processed for electron microscopy (see below). The brains were transferred to 0.1M phosphate buffered saline (PBS; pH 7.3). Following several rinses with PBS the brains were incubated overnight in PBS containing 20% w/v Sucrose. Following this the brains were incubated in a 1:1 mixture of 20% w/v sucrose/PBS and OCT cryoembedding solution (Agar Scientific, Stansted, UK) for 2 hours. The brains were then mounted on cryostat stubs in the same solution and snap frozen using liquid nitrogen. 60μm coronal sections were made on the cryostat set at -24°C with a specimen temperature of -18°C. Sections were placed in serial order in microwell plates containing PBS with 0.1% v/v Triton X100 (PBTr). To reveal the location of the anterogradely traced axons an avidin/horseradish peroxidase kit (Vectastain ABC kit; Vector Labs UK ltd, UK) was used on selected sections. The chromogen was 0.05% w/v diaminobenzine (DAB) with 0.001% w/v Nickel and 0.001% w/v chromium ions ($NiCl_2$; $CrCl_3$) added to the reaction to darken the hue obtained. Following the colour reaction sections were washed several times in PBTr and were

mounted on gelatin-coated PTFE multiwell slides (C.A. Hendley (Essex) Ltd, Loughton, UK). The sections were examined and photographed at low power using the dissecting microscope and at high power using the compound microscope.

2.6 Electron Microscopy

Optic nerves

Following dissection from the brain, optic nerves were post-fixed in 0.1M sodium cacodylate buffered (pH 7.3) 1% w/v osmium tetroxide (OsO_4) (Johnson-Matthey PLC, London, UK) overnight at 4°C. They were rinsed several times in 0.1 M Sodium cacodylate buffer (pH 7.3) followed by 0.1M Sodium Acetate (pH 7.3). The nerves were then *en bloc* stained for 1 hour using 2% w/v uranyl acetate in 0.1M sodium acetate (pH 7.3). Following rinses the nerves were dehydrated using an ethanol series, washed in propylene oxide and slowly infiltrated with Agar 100 epoxy resin (Agar Scientific, Stansted, UK) before polymerisation at 60°C overnight. Segments of the nerve taken from standard levels: 1. 1.5mm proximal to the optic chiasm, 2. At the optic chiasm, 3. 1mm proximal to level 1, were mounted on stubs in preparation for sectioning. Semithin (1μm) sections were cut, these were mounted on plain glass slides and stained with toluidine blue solution (1% w/v toluidine blue (Agar Scientific, Stansted, UK), 1% w/v sodium tetraborate for 15 seconds on a hot-plate at 80°C. The stained sections were sealed with coverslips (No 1, 40 or 50mm x 22mm) using DPX mountant. These sections were examined and photographed using the compound microscope.

Ultrathin sections (80-100 nm) were made from the blocks at standard level 1 (1.5mm proximal to the optic chiasm). These were mounted on Athene old 400 grids (Agar Scientific, Stansted, UK) contrasted with lead citrate and examined and photographed using the electron microscope.

Zebrafish larvae.

Preparation of the zebrafish larvae for electron microscopy was carried out in the same way as for the nerves. Parasagittal sections of the heads of the larvae

were made from the midline to incorporate a cross section of both optic nerves at the midline chiasm.

2.7 Quantification and statistics.

The total numbers of myelinated and unmyelinated axons in each optic nerve was estimated by sampling transverse EM sections from the standard level 1 (1.5mm proximal to the optic chiasm) mounted on mesh grids. Some tests were carried out to determine a suitable magnification and number of sample points. Three options were tried: 10 sample points at 5,000 x magnification (approximately 6.2% of total axon number), and 20 sample points at 5,000 x and 10,000 magnification (12.3% & 3.9% of total axon number respectively). The percentage of myelinated fibres found with these different methods did not vary greatly (Figure 2.1) so 10 sample points at 5000 x magnification was chosen as the standard method to minimise the number of micrographs required but maximising the sample of fibres (over all fish this averaged 3.5 % of all axons). To eliminate any bias in the choice of sampling points, sample grids from each nerve were shuffled so that the experimental group was not known during taking of the micrographs, also, the random way sections were orientated on the grid was used to eliminate bias in the choice of sample points across the nerve section. Sections covered between 15 and 40 grid squares and micrographs were taken at 10 points in a randomly chosen pre-determined even pattern across these points. The total number of myelinated and unmyelinated axons in each micrograph was counted. To eliminate bias in counting that may have arisen from the micrographs being grouped the micrographs were shuffled into a random order. To extrapolate this number to an estimate for the total number of axons in the optic nerve, the outline cross-sectional area of the nerve (excluding the sheath) was traced from toluidine blue-stained sections using a *camera lucida* attached to a Zeiss photomicroscope 4. The areas were determined by planimetry using NIH Image. The fraction of the electron micrographs that was taken up with glial fibres varied considerably between micrographs. To account for this, the axon fascicles were traced and the fraction of the micrograph that they took up was determined by planimetry using NIH image. An accurate estimation of the total number, N, of axons in the nerve was then calculated as

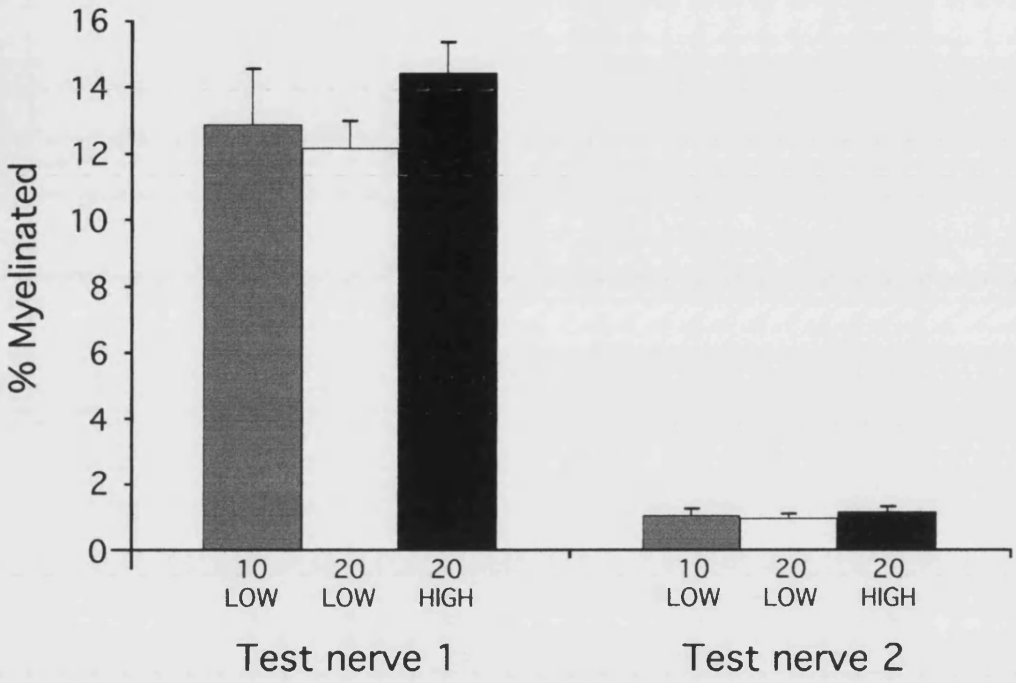

Figure 2.1 Testing of different methods of sampling from the nerve. Two optic nerves nerves (test nerves 1 & 2) were sampled at low and high magnificaiton (5000x ('LOW') and 10,000x ('HIGH')) with 10 or 20 micrographs. The number of myelinated and unmyelinated axons was counted from these micrographs and myelination was expressed as the percentage of counted axons that were myelinated. There was llittle or no difference in the figure obtained using the different methods of sampling.

$N = abn$ where a= the outline cross section area of the nerve, b= the fractional area of axon fascicles and n = the number of myelinated or unmyelinated axons per unit area. The figures obtained were tested for significance using T-tests, accepting $p<0.05$ as a significant difference.

2.8 Nearest neighbour analysis

The spatial distribution of the first myelin sheaths in larval zebrafish and regenerating carp optic nerves was subjected to a nearest neighbour analysis (Wässle and Riemann, 1978). Electron micrographs of cross sections of the 20 day larval zebrafish optic nerve and the target-deprived regenerating adult carp optic nerve at 30 days were prepared. The percentage of myelinated fibres was the same in both cases (5%). The distance of each myelinated axon from its nearest neighbour was measured and expressed in units of the number of intervening unmyelinated axon profiles. The observed distribution of nearest neighbour distances was compared with a random distribution calculated by substituting the fraction of myelinated axons, d = 5% into Wässle and Riemann's (1978) formula, $p(r) = 2\pi dr\ exp(-\pi dr^2)$, in which $p(r)$ is the probability density of the nearest neighbour distances, r.

2.9 Elvax preparation.

To prepare implants of slow release Elvax 40P polymer containing d- or l-APV 20mM solutions of d-APV and l-APV were prepared and mixed 1:1 with 2% w/v fast green solution to make a solution of 10mM APV and 1% w/v fast green. The fast green was included to make it easier to verify that good mixing takes place between the Elvax and the drug solution. Beads of Elvax 40P were obtained as a gift from Vicky Stirling (Department of Zoology, University of Western Australia, Nedlands, Western Australia). They were washed for a week in repeated changes of pure ethanol to remove any toxic residues from their manufacture. 10 mg of beads for each of the drug isoforms were removed from the ethanol and dried on filter paper. The beads were placed in custom manufactured glass tubes (UCL Chemistry Department glass workshop) which had a flat bottom and an internal diameter of 10mm. 900μl of methylene chloride

was added to the tube to dissolve the Elvax. Glass tubes were obligatory as methylene chloride dissolves plastic, and the size was chosen with the dimensions of the fish tecta in mind. Once the Elvax beads had fully dissolved in the solvent 100μl of the drug/Fast Green solution was added and the tube was vortexed for 3 minutes to finely suspend the drug solution in the Elvax. A spatula with a right-angled end was placed in the mixture and the tube was then quickly plunged into acetone that was cooled with dry ice. The tubes were placed in a -70°C freezer for 3 hours and then the frozen slug of Elvax/drug was removed from the tube using the pre-placed spatula. The Elvax slug and spatula were placed on a pre-cooled glass petri dish and returned to the -70°C freezer for a further 4 days to allow the solvent to slowly evaporate. Following this, the petri dish containing the Elvax slug was transferred to a -20°C freezer for a week and placed in a dessicator for another week. After this treatment the Elvax slug was removed from the spatula and trimmed into shape ready for the preparation of thin sections using a cryostat. The Elvax/drug pellet was embedded in pure OCT cryoembedding compound and 120μm sections were cut at -40°C. The cut implants were stored dry in microwell plates at -20°C. 48 hrs before they were required they were placed in sterile saline which was changed frequently. These implants were cut to size as required and placed over the tectum as described above (2.3 surgery).

2.10 *In situ* hybridisation

2.10.1 Riboprobe preparation.

Plasmid DNA for Notch genes and pax2.1 (positive control) was obtained from the sources listed below (Table 1). The plasmids were linearised using the appropriate restriction enzyme to generate anti-sense riboprobes (Table 1) in the following reaction: 5μg plasmid DNA, 5μl 10x restriction enzyme buffer, 2μl of restriction enzyme (20 units) (Promega UK, Southampton, UK) in a total volume of 50 μl water, this mixture was incubated for 3 hours at 37°C. The linearised template was cleaned by adding the same volume again of Phenol/chloroform/isoamyl alcohol (25:24:1) mixture, vortexing for 2 minutes and centrifuging for 5 minutes at 13,000 x in a Sanyo MSE microcenataur benchtop microcentrifuge (Sanyo, Japan). The aqueous phase was removed and

DNA was precipitated adding 1/10th of the volume of 3M sodium acetate and incubating at -20°C for 30 minutes. The DNA was pelleted by centrifugation at 13,000x for 15 minutes. The supernatant was removed and the pellet was washed with 70% v/v ethanol solution. This pellet was air-dried for 30 minutes and re-suspended in 10μl or RNAse-free water and the concentraiton was determined by UV absorption. Riboprobes were generated using the following mixture: 1μg of linearised template (2μl of 0.5μg/μl), 4μl of 5x transcription buffer (appropriate for the enzyme), 1μl 0.1M DTT (Promega UK, Southampton, UK), 2μl RNAse inhibitor (Promega UK, Southampton, UK), 2μl DIG labelled nucleotide mix (Roche Diagnostics Ltd, Lewes, UK), 8.5μl RNAse-free water, 2μl RNA polymerase (appropriate for the template (e.g. T3, T7 or SP6) Promega UK, Southampton, UK). This mixture was incubated for 3 hours. Then 10 units of RNAse-free DNAse (Promega UK, Southampton, UK) was added to destroy the template. This mixture was run through an RNAse-free Sephadex G50 column (Amersham Pharmacia Biotech Ltd, Amersham, UK) to remove proteins and unpolymerised nucleotides. An equal volume of formamide was added and the probe was stored at -70°C until required.

Table 3. DNA templates and enzymes used for probe production

Gene	Clone name	DNA Source	Plasmid Linearising Enzyme	RNA Polymerising Enzyme	Genbank Accession (if known)
Notch 1a	E4.1	J. Campos-Hortega	HindIII	T3	X69088
Notch 1b	AE 26	M. Lardelli	Bam H1	T3	Y10352
Notch 5	AE 22	M. Lardelli	Bam H1	T3	Y10353
Notch 6	BJ 1	M. Lardelli	Bam H1	T3	Y10354
Serrate A	SerA	J. Lewis	Xba1	T7	
Serrate B	SerB	J. Lewis	Bam H1	T7	AF090432
Delta A	DeltaA	J. Lewis	Xba1	T3	AF030031
Delta B	DeltaB	J. Lewis	Xba1	T3	Y11760
Pax 2.1	pzf paxb	S. Wilson	Bam H1	T7	

2.10.2 In situ hybridisation.

(a) Sectioning.

Optic nerves/retinae

The optic nerves of zebrafish were crushed as described above (2.2 surgery) and two weeks later the fish were perfused through the heart with 4% w/v paraformaldehyde in PBS. The eyes and brains were further fixed in the same solution overnight (the eyes were pierced to equalise the osmolality inside and outside). The eyes and brains were then washed in PBS and incubated overnight in PBS/20% w/v Sucrose and then for 3 hours in 1:1 mixture of 20% w/v sucrose/PBS and OCT cryoembedding compound (Agar Scientific, Stansted UK). The tissue was then snap frozen in the same mixture using liquid nitrogen. The tissue was orientated within the block so that longitudinal sections of the optic nerve and transverse sections of the eye could be easily cut and mounted on the same slide. Efforts were made from this point onwards to prevent RNAse contamination that might reduce the sensitivity of the process (glassware was baked for 8 hours at 200°C and RNAse-free water was always used). 10μm sections were cut on the cryostat. The sections were lifted off from the knife onto Superfrost Plus slides (Merck Sharp & Dohme, Hoddesdon, UK). As a positive control, additional sections of 24hr old zebrafish embryos were cut and adhered to all slides. Slides were then stored until required at -20°C.

Zebrafish embryos

Notch receptor and ligand expression was also examined in zebrafish embryos/larvae from 4 days to 20 days development. Embryos/larvae were killed by terminal anaesthesia/decapitation and were fixed by immersion in 4% w/v paraformaldehyde in PBS. Following washes in PBS the embryos were treated identically to the optic nerves/retinae (above). The heads of the larvae were orientated in the frozen block so that cryosections were horizontal.

(b) Pre-hybridisation preparation

The slides were prepared for hybridisation by pre-treatment in the following solutions: 4% w/v paraformaldehyde for 20 minutes, 3x strength PBS for 5 minutes, PBS for 5 minutes, RNAse free water for 30 seconds followed by 20 minutes treatment in proteinase K solution (1μg/μl in 0.1M Tris-HCL and 50mM

EDTA). The slides were then treated with 4% w/v paraformaldehyde for 5 minutes followed by 3xPBS for 5 minutes, PBS for 5 minutes and water for 30 seconds. Then the slides were transferred to a trough containing 0.1M triethanolamine 250μl of acetic anhydride per 100ml of triethanolamine was added dropwise whilst constantly stirring. Following addition of all of this solution, the slides were incubated in the solution for a further 10 minutes. The slides were then rinsed twice in RNAse-free water and stored in a solution of 50% v/v formamide and 3x Standard Sodium Citrate (SSC; 1x = 0.15 M Sodium Chloride and 0.015 M Sodium Citrate) until hybridisation was organised.

(c) Hybridisation

The hybridisation mixture was: 50% v/v deionised formamide, 5 x SSC, 10mM β-mercaptoethanol, 10% w/v dextran sulphate, 2 x Denhardt's Solution, 250μg/ml yeast RNA (Roche diagnostics Ltd, Lewes, UK), 50 μg/ml Salmon Sperm DNA. This solution was mixed 200:1 with the prepared DIG labelled riboprobe. 100μl of the 1:200 mixture per slide to be hybridised was pre-heated up to 65°C. Small slips of Parafilm (American Can Co., Greenwich CT, USA) large enough to cover the sections were cut. 100μl of the hybridisation mixture and riboprobe was placed on this parafilm slip and the slides were used to pick up the parafilm containing the mixture. The slides were incubated in a hybridisation oven at 55°C overnight.

(d) post-hybridisation washes

Following hybridisation, the parafilm was removed by immersion in a solution of 2xSSC at 55°C and the slides were then placed in 2xSSC, 50% v/v formamide 1mM EDTA mixture at 55°C. They were twice washed in 2xSSC for 30 minutes and then treated with RNAse, to a solution of 2xSSC and 1mM EDTA was added 20μg/ml RNAse A and 1units/ml of RNAse T1 (Promega UK, Southampton, UK). This was incubated at room temperature for 30 minutes, followed by two 30 minute washes with 2xSSC/50% v/v formamide 1mM EDTA at 55°C, and two 5 min washes in 0.2 x SSC.

(e) DIG detection

To then detect the DIG labelled hybridised riboprobe, the slides were incubated with anti-digoxygenin antibody. The slides were transferred to maelic

acid buffer with 0.1% v/v tween-20 (MABT; 0.1M Maelic acid, 0.15M Sodium Chloride (pH 7.5)). The sections were encircled with a hydrophobic ring using a PAP pen (Agar Scientific, Stansted, UK). Non-specific binding was inhibited by incubation for 1 hour in 2% w/v blocking reagent (Roche diagnostics Ltd, Lewes, UK) and 10% v/v normal sheep serum (NSS; ICN Ltd., Basingstoke, UK) in MABT. This solution was then replaced with MABT containing 2% w/v blocking reagent, 1% v/v sheep serum and 1:2000 concentration of alkaline phosphatase (AP) conjugated Anti-DIG antibody (FAB-fragments; Roche diagnostics Ltd, Lewes, UK), the slides were incubated overnight in a humid chamber at room temperature.

(f) Colour reaction

To detect the alkaline phosphatase labelled DIG-hybridised transcripts, a colour reaction using Bromo-chloro-indoryl phosphate (BCIP; Invitrogen Ltd, Paisley, UK) and Nitro Blue Tetrazolium (NBT; Invitrogen Ltd, Paisley, UK) was carried out. The slides were rinsed twice with MABT to remove antibody, they were then transferred to the BCIP/NBT buffer: 0.1M Tris-HCL pH 9.5, 50mM $MgCL_2$, 0.1M NaCl, 0.1% v/v Tween-20. After two washes this was replaced with the same buffer containing BCIP (4.5μl/ml) and NBT (3.5μl/ml). The slides were incubated in this mixture away from light for several hours until coloured precipitate appeared. The colour reaction was then stopped by washing in PBS containing 0.1% v/v tween-20 and 0.05M EDTA.

(g) Slide finishing.

Slides were then sealed using aqueous permanent mountant (Agar Scientific, Stansted, UK) and were examined and photographed using the compound microscope.

Chapter 3: No target : no myelination.

3.1 Introduction.

Myelination of the tracts of the CNS follows a strictly ordered schedule during development (Flechsig, 1901; Langworthy, 1933; Yakovlev and Lecours, 1967; Schwab and Schnell, 1989; Van der Knaap and Valk, 1995; Paus et al., 1999). But how is this schedule directed? Different fibre tracts seemed to early authors (Flechsig, 1901; Langworthy, 1933; Yakovlev and Lecours, 1967) to myelinate in the order that they come to function, suggesting a link between myelination and maturation.

In this chapter I describe experiments that perturb the normal course of myelination of the regenerating teleost optic nerve. In line with the proposition that myelination is linked to the formation of functional connections I show that timely myelination depends on the presence of the principal synaptic target of the regenerating optic axons, the contralateral optic tectum of the midbrain.

The majority of these experiments used juvenile carp (*Cyprinus carpio*). However, to test the generality of my findings I have also used other fish species. I first describe the results obtained with the carp before briefly describing the experiments in the other species.

3.2 Target-deprivation retards myelination.

3.2.1 Regeneration and remyelination in the fish visual system.

The visual pathway of fish is completely crossed at the optic chiasm. All right eye axons terminate in the left optic tectum and *vice versa*. Apart from the small cohort of unmyelinated axons at the growing edge of the nerve (Marotte, 1980; Scholes, 1981), the optic nerve of a mature fish is totally myelinated. If the optic axons are severed by crushing the optic nerve, the axons and and their myelin sheaths degenerate distal to the lesion and are cleared phagocytically by macrophages and astrocytes. Concurrent with this, the severed proximal axon stumps sprout and regenerate to re-innervate their primary synaptic target, the contralateral optic tectum. Innervation of the tectum by the regenerating axons is achieved within a couple of weeks in the young carp (50-60 mm) used here.

However, myelination of the regenerated optic nerve is a slower process. The first myelinated fibres appear after about 3 weeks but it takes several months before all the regenerated optic axons acquire myelin sheaths (not shown).

3.2.2 Target-deprivation and myelin formation.

To initiate regeneration in the carp visual system the right optic nerve was crushed with fine forceps just distal to its exit from the eye. To test if target innervation is necessary for myelination of the regenerating axons the left optic tectum of the midbrain was removed a few days later from a subset of the fish by aspiration (Materials and Methods).

Following 30 days of regeneration, the fish were perfused with fixative and their brains and eyes were removed from the skull. To examine the destination of the regenerated axons the right eyes were injected with the anterograde tracing compound n-hydroxysuccinimido biotin 24 hours before sacrifice (Materials and Methods). Following removal of the brains, the optic nerves were examined to compare the progress of myelination in the target-deprived and target-intact fish.

An initial indication of the extent of myelination is gleaned through examination of the optic nerves by transmitted light. This is because mature myelinated axons are more opaque than unmyelinated axons, which are very translucent. Examples of trans-illuminated brains are shown in Figure 3.1. Target deprivation resulted in less myelin opacity in the regenerated optic nerves. In fact, the target-deprived nerves were often nearly completely transparent: the tips of forceps could be seen through them during dissection.

What is the destination of the regenerated axons when they have no contralateral tectum to innervate? To answer this question, the brains were processed separately to examine the distribution of the anterogradely labelled axons. Thick coronal cryostat sections were taken and the trajectories of the labelled axons from the right eye were revealed by biotin/avidin/peroxidase histochemistry (Materials and Methods). Examples of these sections are shown in Figure 3.2 (C & D). In the target-intact fish, the labelled right eye axons were found exclusively in the contralateral tectum where they spread throughout the optic radiation and its underlying synaptic layer (the *stratum opticum* and the *stratum fibrosum et griseum superficiale* respectively).

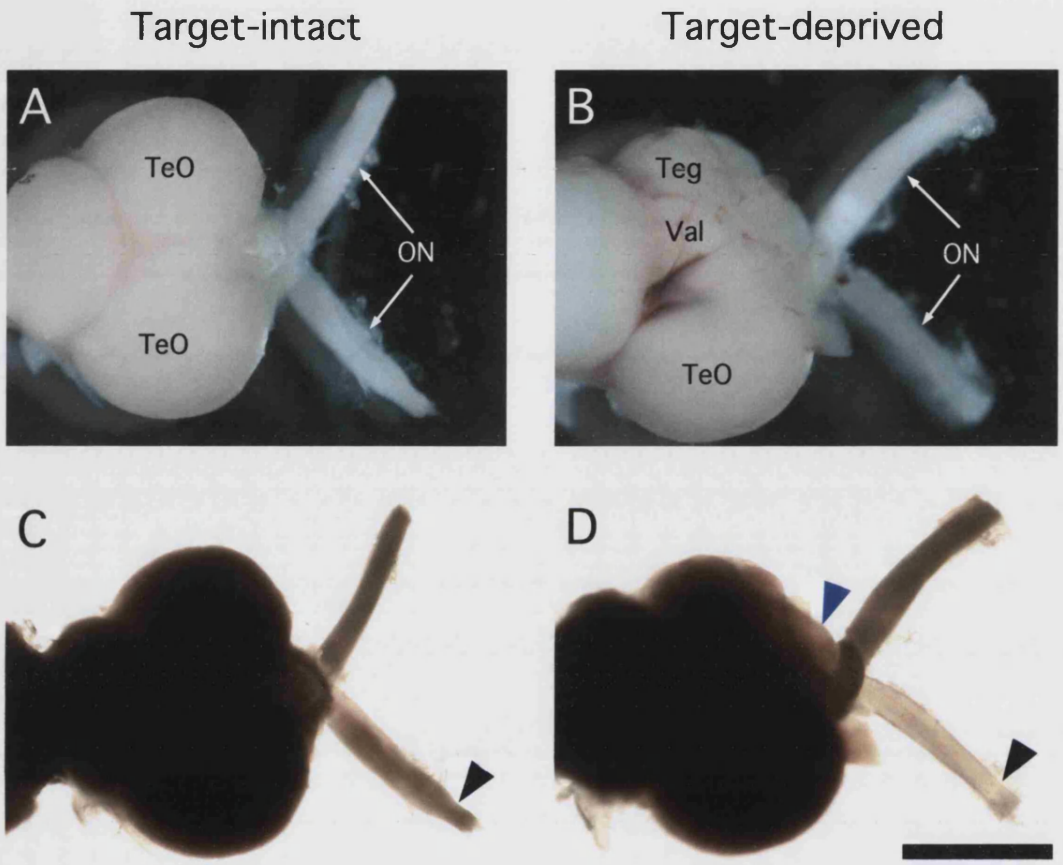

Figure 3.1 Myelination in target-deprived nerves is retarded at 30 days. Illuminated optic nerves (ON) and mid-brains (forebrain removed) from carp with intact right optic tecta (**A**, **C**) and from carp with the right optic tectum removed (**B**, **D**).
A & **B**: Both optic tecta (TeO) are intact in the target-intact brain (**A**). In the target-deprived brain the left optic tectum is removed and the underlying structures of the valvula of the cerebellum (Val; **B**) and the tegmentum (Teg; **B**) are visble.
C & **D**: The lesion site in the optic nerve is visible as a pinched or more translucent segment of the nerve (black arrowheads). The target-deprived right nerve (**D**) is more translucent than the target-intact right nerve (**C**), indicating less myelination. The neuroma that forms in place of the extirpated tectum is also transluscent (blue arrow-head;**D**). Scale bar = 2mm.

In the target-deprived fish, the regenerating axons formed a large neuroma[§] at the normal optic fibre entry point to the contralateral tectum. This neuroma was conspicuous in surface view because of its translucency (Figure 3.1 D), and showed as a tangled mass of anterogradely labelled axons in the stained sections (Figure 3.2 D). Aside from the heavily labelled neuroma at the site of the extirpated left tectum, some anterograde label was also present in the intact right tectum, indicating that a minority of axons had reached this alternative ectopic target.

To confirm the initial indications that target deprivation curtailed myelination, the optic nerves were prepared for electron microscopy (Materials and Methods). It was clear from semi-thin (1μm) sections using the light microscope that the more transparent target-deprived nerves contained substantially fewer myelin sheaths (not shown). This was confirmed by examination of ultra-thin sections by transmission electron microscopy (TEM; Figure 3.2 E & F). Whereas the target-intact optic nerves were substantially myelinated by 30 days, the target-deprived nerves contained only small numbers of myelinated axons among very large numbers of unmyelinated axons.

3.2.3 Quantification.

It quickly became apparent that to compare the degree of myelination in the target-deprived and target-intact regenerating optic nerves is a non-trivial task. First, in the small carp used here, the optic nerve normally contains about 130,000 axons. Growing or regenerating unmyelinated axons are about 0.1 - 0.3 μm in diameter and the majority of myelinated axons measure only 0.5 - 1 μm. They can therefore only be distinguished by electron microscopy. At the magnification required (and quite apart from the counting task), it would need several hundred micrographs to cover just one optic nerve. Sampling was therefore obligatory.

Second, regeneration of the optic nerve is a more disorderly process than earlier studies have ever properly shown, leading to substantially varied

---

[§] The definition of a neuroma is: "A swelling or tumour growing upon a nerve or in nerve-tissue," (OED) or "A benign tumour or tumourlike lesion composed of a mass of nerve fibres," (Churchill's medical dictionary). It is often used to refer to neoplasmic tumours originating from the nerve sheath (neurofibromas) but can also be used to describe a generic growth in nervous tissue as seen here.

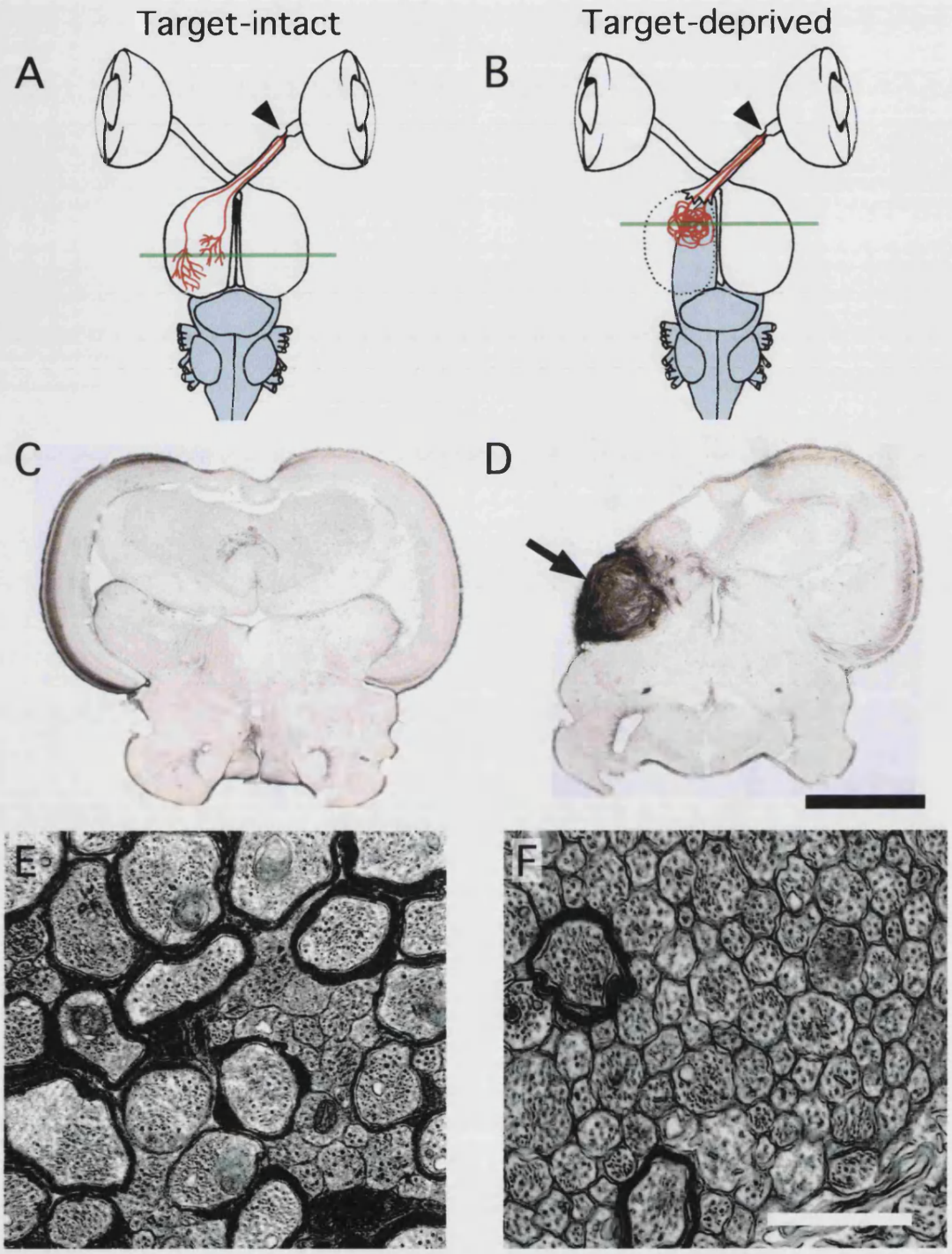

Figure 3.2 Optic nerve regeneration and myelination at 30 days. By this time the regenerating optic nerve axons in target-intact nerves (**A**,**C**,**E**) have reached the left tectum and myelination is well underway. However, in target-deprived nerves (**B**,**D**,**F**) they form a neuroma and myelination fails.
A & **B**: Diagrams of the fish visual pathway indicating the optic nerve lesions (arrowheads) and the behaviour of regenerating optic axons (red) with an intact-target (**A**) and deprived of a target (**B**).
C & **D**: Anterograde tracing (approximate levels of green lines on **A** & **B**) showing the destinations of the regenerating axons. Target-intact axons innervate the tectum (**C**) whereas target-deprived axons form a neuroma (arrow;**D**) although some pioneer axons also reach the intact tectal lobe. (see weak staining of the right tectum in **D**)
E & **F**: Representative electron micrographs showing regenerated axons and their myelin sheaths. Scale bars **B** & **C**, 1mm; **E** & **F** 1 μm.

outcomes. The cross-sectional areas of the regenerated nerves varied nearly four-fold in different fish, with varied retention of their original folded pattern. Extensive astrogliosis occurred, resulting in nearly two-fold variation in the percentage of the optic nerve cross-section that was occupied by axon bundles. The density of glial processes also varied locally, and the distribution of myelinated fibres often did so as well, showing hot-spots in different parts of the nerve. These factors necessitated a comprehensive and objective sampling procedure.

Another possible source of variation is that CNS tracts usually myelinate in a proximo-distal sequence (Skoff, 1978; Skoff et al., 1980; Colello et al., 1995). However, this variation was small (Figure 3.3), and to eliminate it I always sampled from a fixed point in the nerve (1.5 mm proximal to the optic chiasm).

I decided to estimate the total number of myelinated and unmyelinated axons in each optic nerve. This was in preference to the conventional procedure of simply determining the percentage of myelinated axons from micrographs, which would not take account of the different sizes of the nerves. In order to estimate the total number of axons in each nerve, counts at several different sampling areas were extrapolated using measurements of the entire nerve area. To control the variation in myelination across the cross-sections of the nerves and any bias in choice of sample points, the EM sample grids were shuffled by a third party to blind me from knowing which experimental group they belonged to and sample areas were chosen at random by taking micrographs from an evenly distributed pattern of grid squares (Figure 3.4 C). To eliminate any possible bias that might be caused by counting the axons from grouped sets of micrographs, the micrographs were also shuffled before counting.

To extrapolate from the numbers of myelinated and unmyelinated axons counted in the micrographs required measurements of the cross-sectional areas of the different nerves and the proportion of these areas that were occupied by axon fascicles rather than glial processes. The nerves were measured by tracing using a *camera lucida*: their cross-sectional areas varied from 0.04 mm^2 to 0.16 mm^2 (Figure 3.4 B). The proportion of the nerve area occupied by axon fascicles was determined from the sample micrographs by planimetry using NIH image (Figure 3.4 D & E). It varied from 45.1% to 80% between the different nerves sampled. These corrections were then applied to the axon counts to estimate the

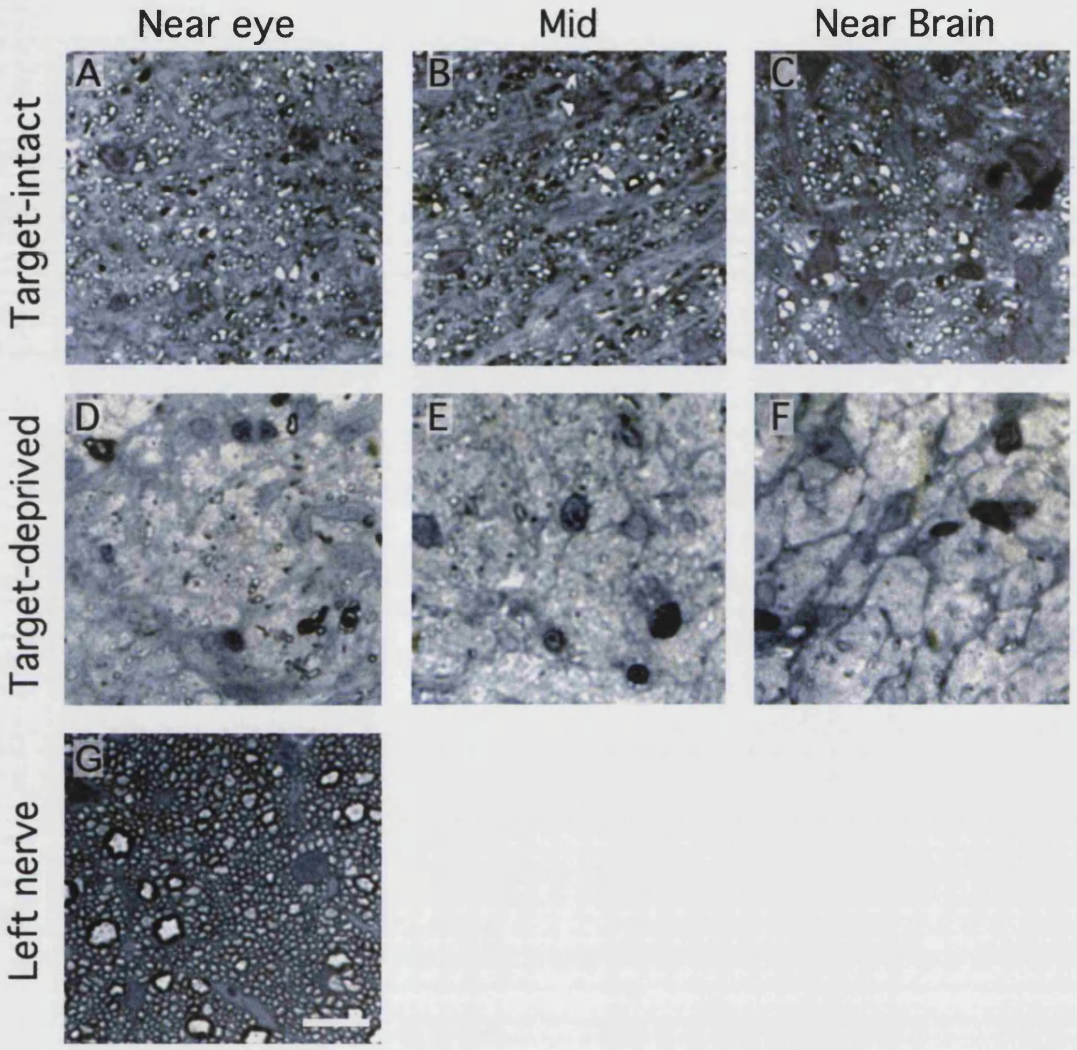

Figure 3.3 Myelination following regeneration does not vary substantially in a proximo-distal fashion. Representative light micrographs of toluidine blue sections from a target-intact (**A-C**) and a target-deprived optic nerve (**D-F**) after 30 days regeneration; and a non-lesioned left nerve (**G**).
Micrographs of sections from three different levels along the optic nerve are shown. In the both target-intact and target-deprived nerves (**A-F**) there was little or no difference in the myelination at the different levels: near to the eye (**A** & **D**), midway between the eye and brain (**B** & **E**) or near to the brain (**C** & **F**).
Myelination was substantially underway in the target-intact nerve although the nerve contained a greater density of glial filaments and the myelin sheaths were thinner than in the non-lesioned left nerve. In contrast, the target-deprived nerve was almost totally devoid of myelin sheaths although there were marginally more nearer the eye (**D**).
Scale bar: 15μm

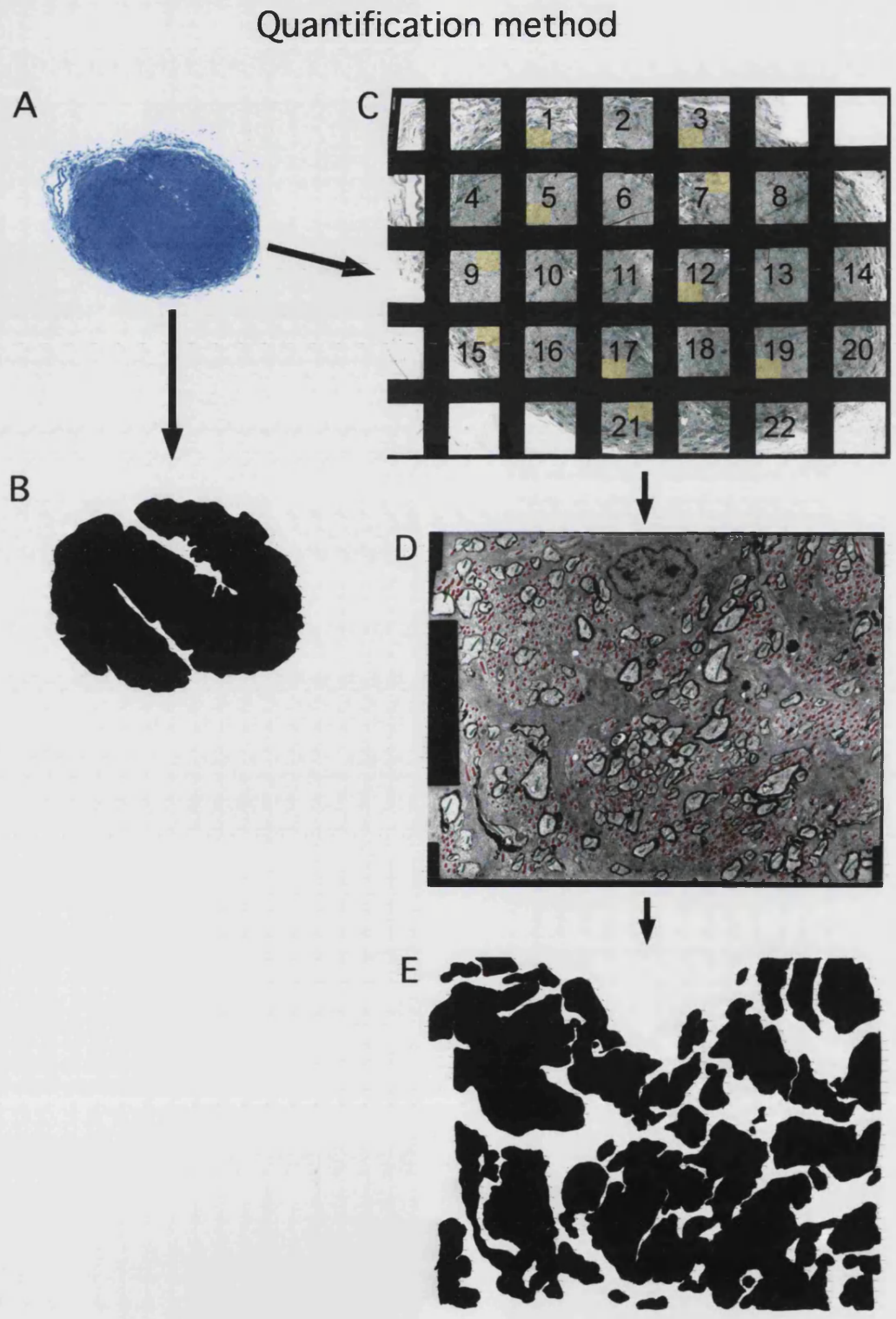

Figure 3.4 Quantification. The total area of the nerve (**A**) was determined by tracing using a *camera lucida* and planimetry of the traced outline (**B**) using NIH image. Sample points (yellow rectangles; **C**) were chosen using a randomly selected pattern of evenly spread EM grid squares (**C**). The numbers of myelinated (Green; **D**) and unmyelinated (red; **D**) axons were counted from the sample point micrographs, an example of one of these micrographs is shown (**D**). The fraction of the micrographs taken up by axon fascicles was traced and calculated by planimetry using NIH image (**E**). An estimate for the total number of myelinated and unmyelinated axons for the whole nerve could then be calculated.

total number of myelinated and unmyelinated axons in the nerves (Materials and Methods).

3.2.4 Target deprivation ninefold retards myelination at 30 days.

The fraction of myelinated fibres in the target-deprived nerves was reduced to 2.5% compared with 38.2% in the target-intact nerves. There were nine times fewer myelinated axons in the target-deprived nerves (8,606 vs 80,471 myelinated axons; Figure 3.5). This difference is highly statistically significant ($p<0.001$), demonstrating that myelination is substantially retarded by target deprivation.

Target deprivation could adversely affect the viability of the regenerating axons and affect myelination for this trivial reason. Surprisingly, however, this appeared not to have occurred. Quite to the contrary, the optic nerves of both the target-deprived and target-intact groups consistently contained more axon profiles than were present in the non-lesioned left nerves. This is presumably due to branching of the regenerating axons proximal to the sample point, rather than to proliferation of retinal ganglion cells.

Moreover, the total number of axon profiles in many of the target-deprived nerves was similar to that in the target-intact group (Table 4). In some cases, however, the number of axon profiles was greatly increased in the target-deprived nerves (Table 4, bold).

Table 4: Total number of axons in the regenerated right optic nerves of target-deprived and target-intact fish.

Target-intact	Target-deprived
157,601	166,599
108,063	202,526
182,575	209,443
240,745	253,351
251,077	**373,069**
262,989	**560,795**
	624,056

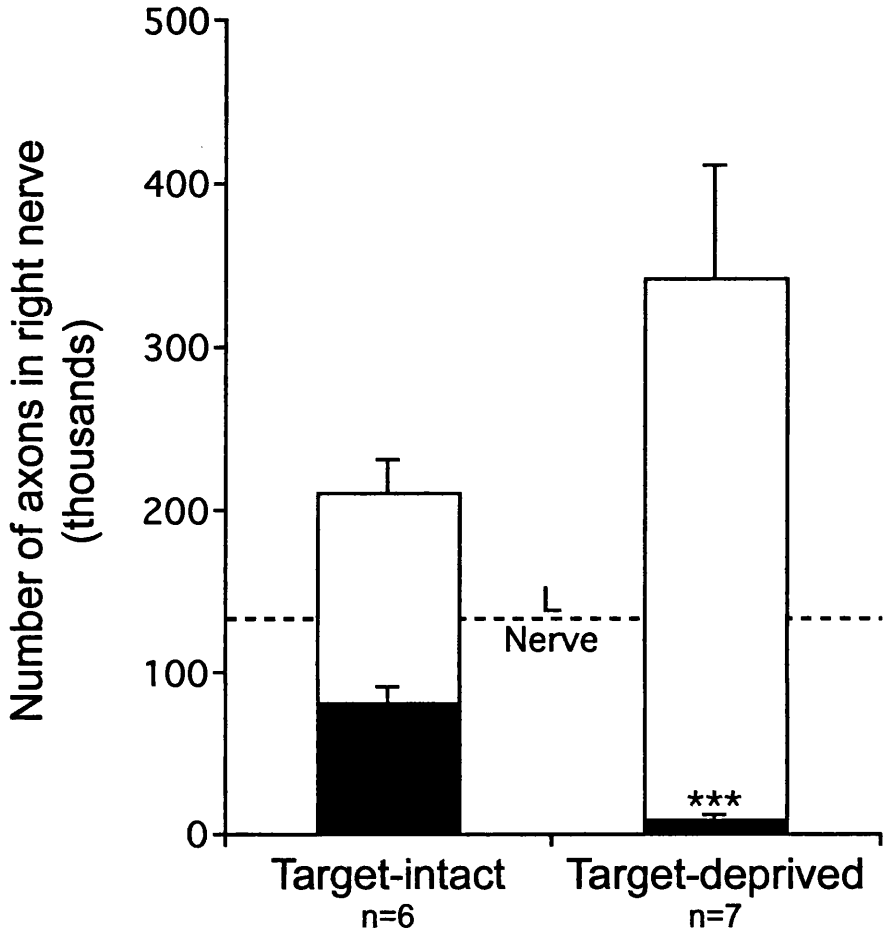

Figure 3.5 Target-deprivation ninefold retards myelination in regenerating optic nerves. Estimates (+/- SEM) of the number of myelinated axons (black) and unmyelinated axons (white) in target-intact and target-deprived regenerated optic nerves at 30 days. At 30 days the target-deprived nerves were nine times less myelinated than the target-intact nerves (asterisks:$P<0.001$). In both cases the total number of axons (myelinated plus unmyelinated) is greater than the non-lesioned left nerve (dashed line) and the total number of axons in target-deprived nerves is greater than target intact nerves.

In these outliers, the large axon counts may have resulted from excessively exuberant branching and/or from extended branch persistence, perhaps due to exceptional conditions at the site of the extirpated left tectum.

3.2.5 What accounts for the minority of myelinated axons in the target-deprived nerves?

Target deprivation does not completely abolish myelination of the regenerating nerve. After 30 days regeneration, the target-deprived optic nerves contained a small number myelinated fibres, albeit nine times fewer than in target-intact nerves (Figures 3.2 F & 3.5). Why was the nerve not completely devoid of myelin?

The most likely explanation is that the myelinated axons were axons that had reached and ectopically innervated the intact ipsilateral tectum as anticipated from earlier studies (Sharma, 1973; Levine and Jacobson, 1975; Springer and Cohen, 1981). This was confirmed from the anterograde fibre tracing (Figure 3.2 C & D). In the target-intact fish no fibres had reached the ipsilateral tectum, but in the target-deprived fish numerous bundles of anterogradely labelled axons were present throughout this structure.

Although innervation of the ipsilateral lobe is the most likely reason for the small amount of myelination of the target-deprived nerves, there are two other possible explanations. Firstly, the tectal ablations may have been incomplete. However, the fish brains were serially sectioned for anterograde fibre tracing, and this permitted examination of the extent of the lesion in all cases. There were never any fragments of the contralateral tectal lobe remaining for the axons to connect to. Secondly, optic axons connect not only to the tectum but also to other brain structures such as the diencephalon. Normally these pathways are very much bridleways in comparison to the 10 lane motorway of the tectal projection, and there was no evidence from the fibre tracing that they were expanded in the target-deprived animals.

The small minority of optic nerve axons that became myelinated in the target-deprived nerves considered here may represent an exception that proves the rule that these experiments sought to test. They may be one and the same axons as the pioneers that extended across the midline from the neuroma to reach the ipsilateral tectum. In the next chapter, I use the capacity of the regenerating

axons to innervate this alternative target for more critical tests of the possibility that synaptogenesis is required to trigger myelination.

3.3 Other fish species

3.3.1 Orfe: increasing axon size does not inevitably trigger myelination.

The first other species I used was the Orfe (or Ide: *Leuciscus idus*). This is a commonly available ornamental fish with large eyes and tecta relative to body size. Regeneration was induced in the optic nerve, and the opposite tectal lobe was also removed in a subset of the fish. After 50 days of regeneration (longer than the carp because of the orfe's larger size) the regenerated optic nerves were examined for signs of myelination. Examination of semithin and ultrathin sections showed that removal of the tectum substantially attenuated myelination of the regenerated optic nerves (Figure 3.6).

One of the original theories for how CNS myelination is controlled is that axon diameter is crucial (Vogt and Vogt, 1908; Duncan, 1934; Matthews and Duncan, 1971). Axons are myelinated when their diameter reaches a critical point. Micrographs from the target-deprived nerves of the orfe show that the diameter of many non-myelinated axons considerably exceeded the diameter of nearby myelinated axons (Figure 3.6). Thus, axon diameter is not the triggering factor that controls myelination.

3.3.2 Zebrafish: The possibility of screening for axonal myelin-permissive signals.

The zebrafish (*Brachydanio rerio*) is a small (max. length ≈ 40mm) tropical fish native to the Indian subcontinent. George Streisinger (1981) began work on this fish as a model vertebrate for molecular genetics. The principal reason for its use is the ease of carrying out large-scale genetic screens for genes involved in vertebrate development (Driever et al., 1996; Amsterdam et al., 1999) (See also part 2 of this thesis). The properties that facilitate this are the fecundity and fast development of the zebrafish (from egg to swimming larva in 6 days). The transparency of the embryo also makes it particularly useful to examine cellular movements. The worldwide research effort into zebrafish development (including large scale genetic screens, EST databases and genome sequencing)

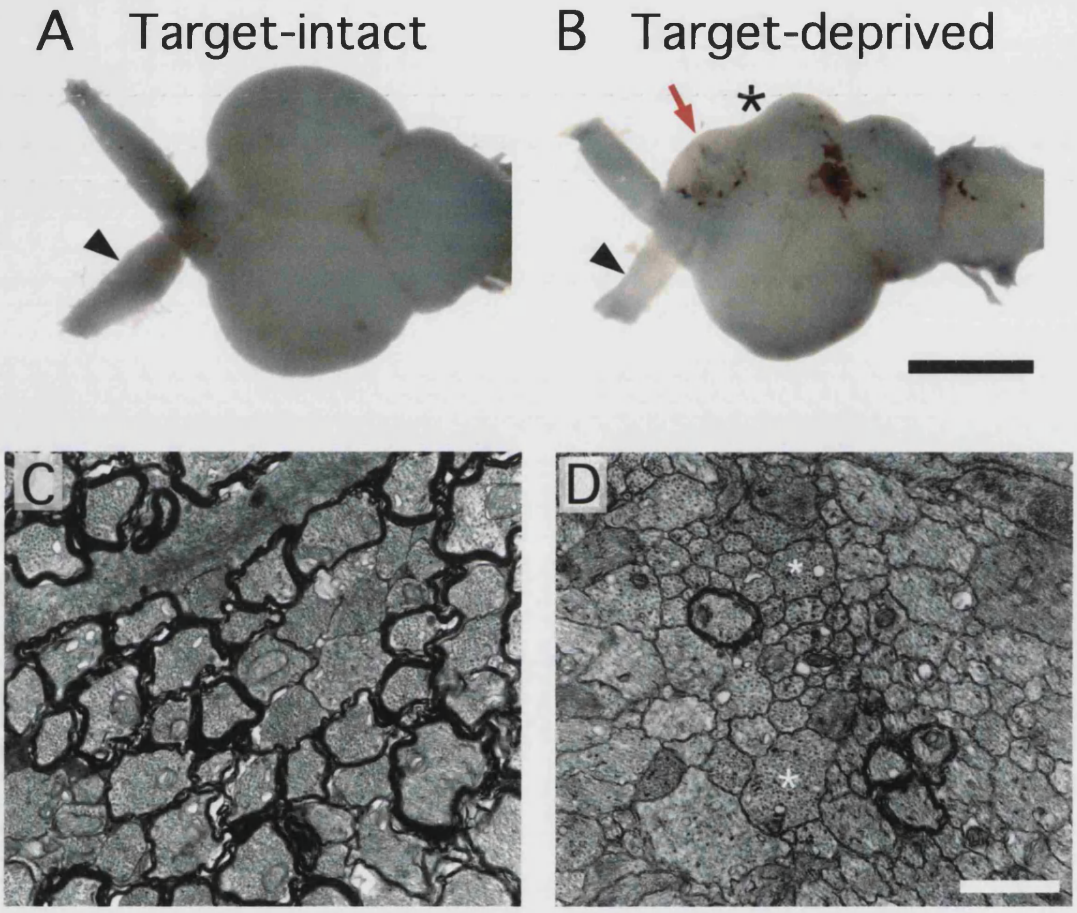

Figure 3.6 Fibre diameter does not trigger myelination. Target-deprivation of the regenerating left optic nerve in golden orfe resulted in a highly translucent optic nerve (**A**, **B**; arrowheads) with very little myelin, as confirmed by electron microscopy (**C**, **D**). In the electron micrographs many unmyelinated axons have a greater diameter than myelinated axons (e.g. **D**; asterisks), demonstrating that increasing axon diameter does not trigger myelination. Scale bars: **A**, **B** = 2mm; **C**, **D** = 1µm.

makes the zebrafish an ideal organism in which to look for molecular signals underlying myelination.

To determine if the target deprivation approach might provide a basis of future examination of molecular mechanisms controlling myelination, I tested if it worked in zebrafish. On account of the small size of the zebrafish the surgery was more challenging than it was in the carp, but with practice both optic nerve lesions and tectal removals were performed successfully. Firstly I conducted a time-series to determine the course of regeneration and myelination in the visual system of these fish, which is fast (Figure 3.6). This could be due to the small size of the zebrafish and their maintenance at tropical temperatures.

I then proceeded to determine if the target-deprivation experiment would work. Target-deprivation indeed delayed myelination of the regenerated optic nerve (Figure 3.7). This technique (target$^+$/target$^-$) could form the basis of a differential molecular screen for axonal signals controlling myelin formation.

3.4 Chapter Summary.

We know from the literature that myelination of different (often neighbouring) CNS tracts occurs in a strictly ordered sequence during development (Yakovlev and Lecours, 1967; Schwab and Schnell, 1989). This strict order appears to relate to the functional maturation of each tract following innervation of its target area (Flechsig, 1901; Yakovlev and Lecours, 1967), suggesting that CNS myelination may depend upon target innervation.

Axons deprived of their targets during development normally die because of the lack of trophic support, and this may be why the developmental correlation between target innervation and myelination has never been successfully tested.

In this chapter I have made use of the regeneration competence of the adult fish visual system to test the possibility that axons must first innervate their target brain area before they can be myelinated. In the next chapter I explore the possibility that, to permit myelin formation, CNS axons must not only reach their target but also form synapses there.

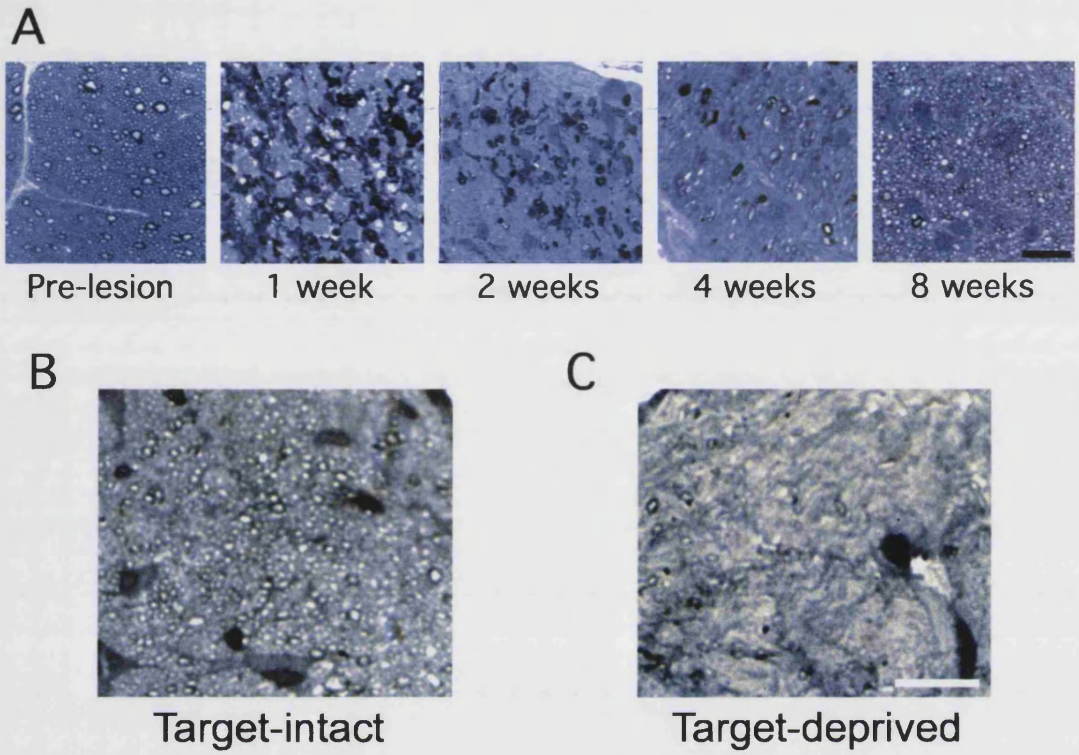

Figure 3.7 Regeneration and remyelination in the zebrafish. Light micrographs from toluidine blue stained 1µm sections.
A: A time-series of regeneration in zebrafish optic nerves. Before the crush lesion the optic nerve is fully myelinated. 1 week following the lesion many palely stained fascicles of regenerated unmyelinated axons are surrounded by darkly stained myelin debris from the degenerating fibres. After 2 weeks of regeneration, much debris has been cleared, although some still remains. The newly regenerated axons are still largely unmyelinated although occasional thinly myelinated profiles are present. 2 weeks later, almost all the debris has been cleared and many newly myelinated fibres are present. At 8 weeks most regenerated axons are myelinated, but the nerve still has a different appearance to an unlesioned nerve because it contains more glial processes.
B, **C**: Target-deprivation retards myelination in zebrafish. After 4 weeks regeneration, target-intact optic nerves (**B**) contain many more myelinated profiles than target-deprived nerves. Scale bars = 15 µm.

Chapter 4 : Evidence that CNS myelination is triggered by synaptogenesis.

4.1 Introduction.

The experiments described in chapter 3 showed that myelination of the regenerating carp optic nerve was greatly reduced at 30 days when the growing axons were deprived of their primary synaptic target, the contralateral optic tectum. However, a small fraction of the axons acquired myelin sheaths under these conditions, and anterograde tracing showed that this could be because the axons involved had reached the intact ipsilateral tectal lobe. In agreement, I show in this chapter that target-deprivation by removal of the contralateral optic tectum simply delays myelination by the time that it takes the regenerating axons to reach and form synapses in the remaining intact optic tectum. I go on to demonstrate that enhancing or eliminating the opportunity for synaptic connection with the remaining tectal lobe respectively accelerates or abolishes myelination of the regenerating optic nerve.

4.2 Target deprivation delays myelination.

Target-deprived and target-intact carp were allowed to regenerate for a further 3 weeks until 50 days following the initial optic nerve crush. After 50 days, the fraction of myelinated axons in the target-deprived optic nerves (44.1%: 88,840) had increased to a similar level found in the target-intact optic nerves at 30 days (38.2%: 80,471), as shown in Figure 4.1. Removing the contralateral tectum thus delays myelination by about 3 weeks, but it proceeds rapidly once contact with the ipsilateral tectum is achieved.

Figure 4.1 also shows that the average total number of axons in the target-deprived nerves fell from 341,406 axons at 30 days to 201,517 axons at 50 days, a value equivalent to that seen in the target-intact group at 30 days (210,508). Evidently, the intervening 3 weeks were sufficient for the excessive axon branching seen in some target-deprived group fish at 30 days to be eliminated. However, the total number of axons in the target intact nerves still exceeded that present in the normal left optic nerve. Moreover, the number of myelinated

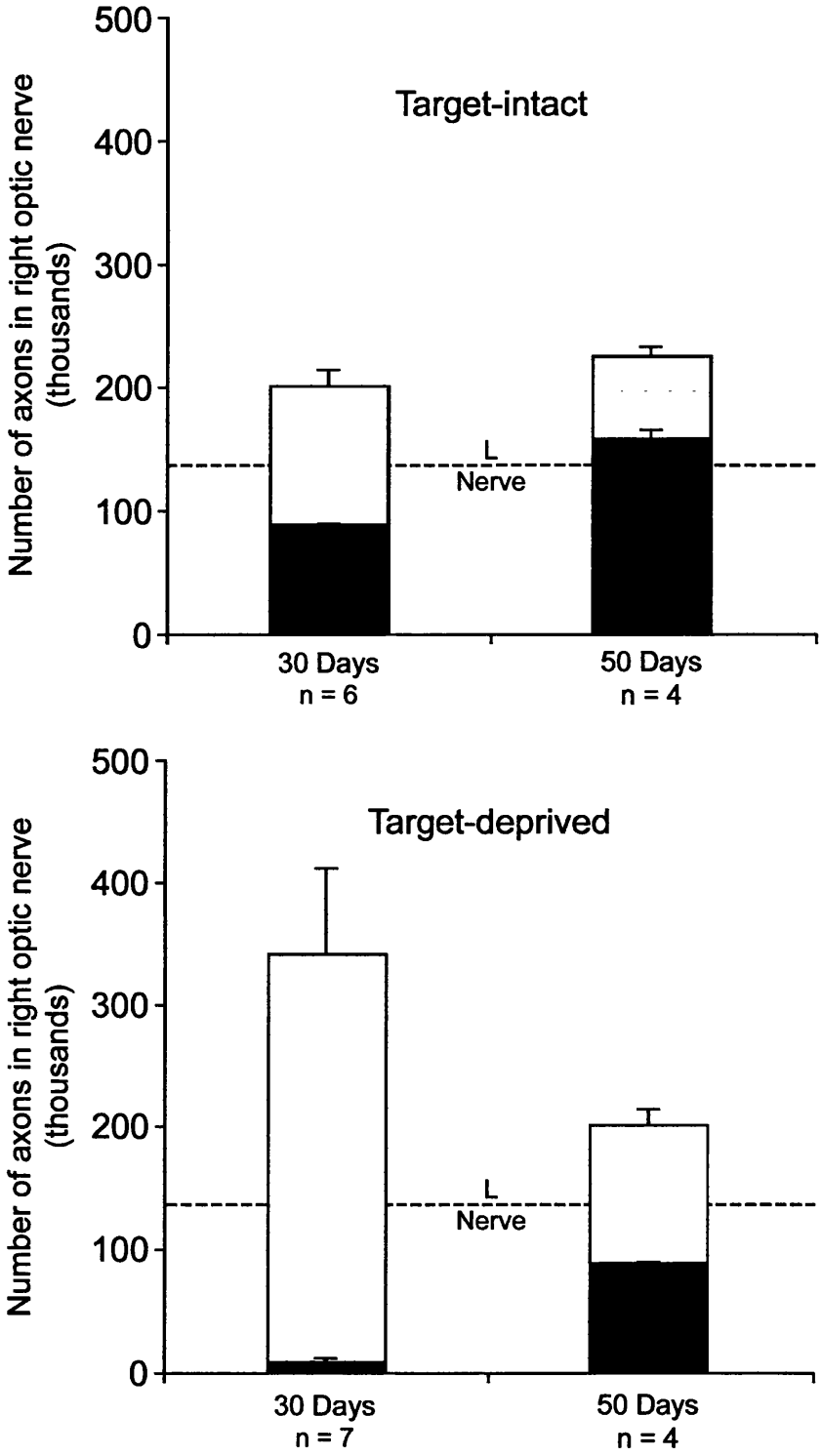

Figure 4.1 Myelination is delayed by 20 days in target-deprived optic nerves.
In target-intact nerves (top), the number of myelinated axons (black) increases by 78,286 between 30 and 50 days. Myelination of the target-deprived nerves (bottom) increases by 80,234 axons in the same time-interval. The number of myelinated axons in target-deprived nerves at 50 days therefore approximately equals that in target-intact nerves at 30 days, indicating that target-deprivation causes a 20 day delay in myelination. The total number of axons (myelinated (black) plus unmyelinated (white)) in regenerated nerves exceeds that in the non-lesioned left nerves (dashed lines) in all cases. At 30 days there are more axons (in total) in the target-deprived nerves, however, by 50 days this excess has gone and the number of axons in target-deprived and target-intact nerves is approximately equal.

fibres also exceeded the normal value. Assuming that the excess of regenerating axons is due to branching, this suggests that some branches as well as parent axons acquired myelin, and that one retinal ganglion cell may have multiple functional connections with the tectum.

4.3 Evidence that myelination depends on synapse formation.

The regenerating fish visual system has been used extensively as a model system to examine the formation and refinement of synaptic connections. A well documented phenomenon from these studies is the formation of ocular dominance patches in the optic tectum. In fish and amphibia two eyes can be induced to share one tectal lobe, either by the removal of the other tectum (Levine and Jacobson, 1975; Springer and Cohen, 1981) or by surgically implanting an additional eye in the early embryo (Constantine-Paton and Law, 1978). The axon terminals from the two eyes segregate into separate territories in the tectum by an activity-dependent process that is driven by the differing input from the two eyes and is dependent upon the NMDA receptor (Cline et al, 1987; Cline and Constantine-Paton, 1989; Schmidt, 1990). The segregated eye-specific territories are called ocular dominance patches.

The 3 extra weeks regeneration (from 30 to 50 days) necessary for the myelination of target-deprived nerves to catch up were also sufficient for the regenerating axons to carve out synaptic territory and form ocular dominance patches in the ipsilateral tectum. Ocular dominance patches were clearly visible as dense areas of anterogradely labelled axons in the intact tectum (Figure 4.2 B).

High magnification comparison of the anterograde labelling in target-deprived group fish after both 30 and 50 days regeneration showed important differences in the character and distribution of the staining in the retinorecipient layers of the tectum. At 30 days the majority of traced axons in the ipsilateral tectum were restricted to fibre bundles. These bundles ran mainly in the in the optic fibre layer of the tectum (the *stratum opticum* (SO)), although some were also found in the optic synapse layer of the tectum (the *stratum fibrosum et griseum superficiale* (SFGS)) (Figure 4.2 C).

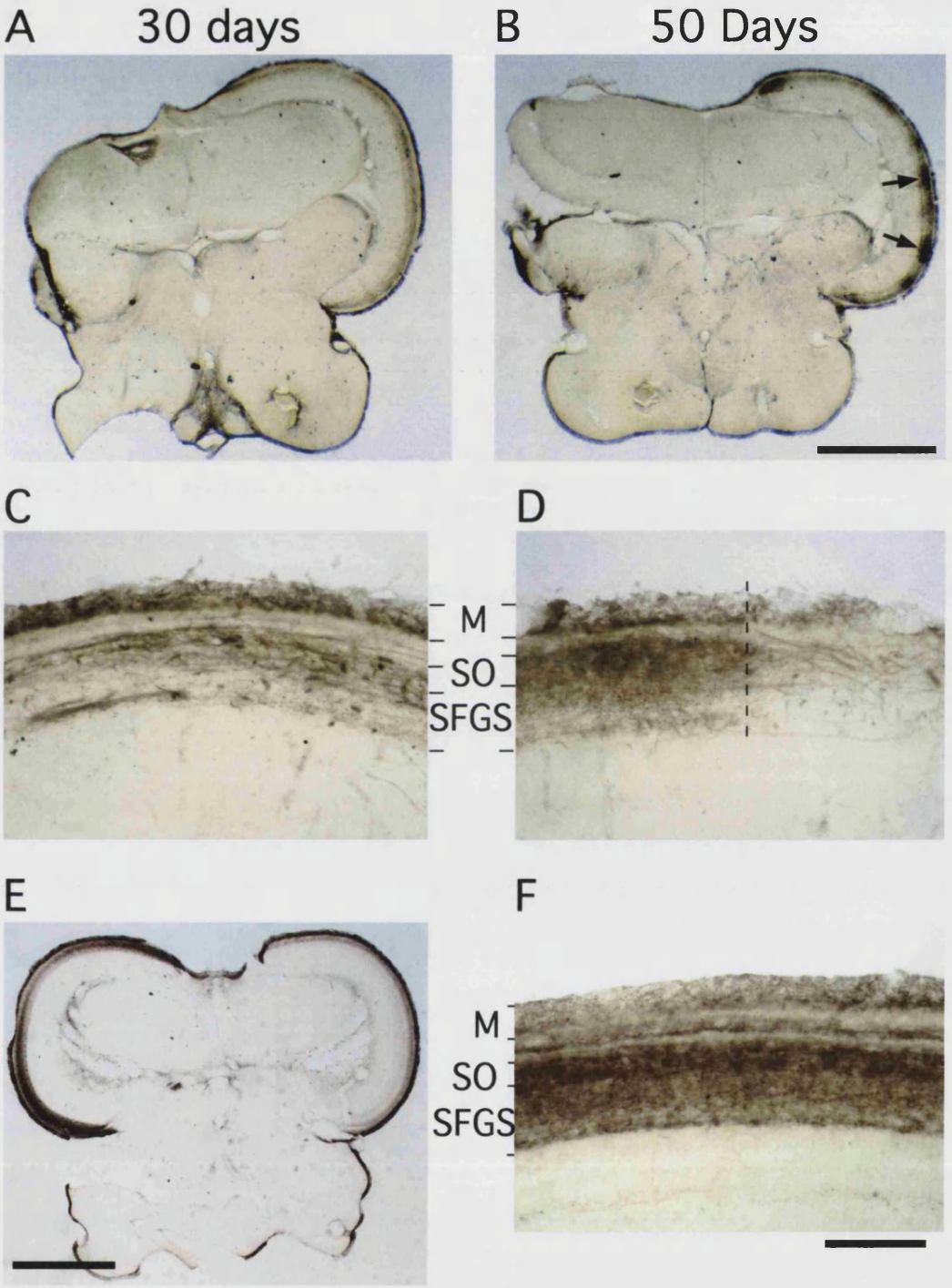

Figure 4.2 Anterograde fibre tracing showing that the 20 day delay in myelination in target-deprived optic nerves (Figure 4.1) is the time taken for regenerating axons to invade the remaining intact tectum and form synapses there.
A & **C**: At 30 days the labelling is confined to scattered fibre bundles found mostly in the optic fibre layer, the SO.
B & **D**: By 50 days, ocular dominance patches have formed (arrows; **B**). Within the patches dense synaptic arborisations are present in the synaptic layer, the SFGS (left of dashed line; **D**). Outside of the patches, labelled axons are restricted to fibre bundles in the SO (right of dashed line; **D**).
E & **F**: For comparison, after 50 days regeneration with both tecta intact, labelled axons are found throughout the contralateral tectum (**E**) Dense granular synaptic arborisations are found throughout the SFGS (**F**).
Scale bars **A**, **B** & **E**: 1mm, **C**, **D** & **F**: 100µm; M: non-specific meningeal staining.

After 50 days, ocular dominance patches had formed in the ipsilateral tectum. Within the patches, labelled bundles of axons were still found in the SO but a different, dense granular quality of staining had appeared in the SFGS, indicating synapse formation there. Between the patches where synaptic connections had not developed, the tracer was only present in fibre bundles mainly running in the SO, in a pattern resembling that seen at 30 days (Figure 4.2 D).

Little or no tracer was found in the ipsilateral tectum of the target-intact group fish after either 30 or 50 days regeneration (Figure 4.2 E; also Figure 3.2 C). This suggests that exploratory behaviour by regenerating growth cones continues only until they reach a suitable target, i.e. the intact contralateral tectal lobe, if it is present, or the ipsilateral tectum in its absence.

Ocular dominance patch formation is a competitive Hebb-type activity-dependent process (Cline, 1991) that inherently requires the formation of synapses, so that they can be selected for or against. The fact that myelination of the target-deprived optic nerves takes off concurrently with the formation of ocular dominance patches (Figures 4.1 & 4.2) is the best indication so far obtained that synapse formation by growing axons triggers myelination in the CNS.

To test this correlation critically, two possible approaches were considered. Firstly, the implication is that any isolated myelinated axon in the regenerating optic nerve (e.g. Figure 3.2 F) differs from its unmyelinated neighbours in having formed synapses centrally. This could be tested directly if there were a method of selectively labelling or visualising the entire length of axons that have formed synapses, but the fact is that no such method exists. The second possibility is to encourage or block synaptogenesis, to see if the oligodendrocytes produce or withhold myelin coordinately. This could be by using some blunt pharmacological or genetic strategy needing development from scratch. However, the capacity of unilaterally target-deprived fish optic axons to infiltrate the intact opposite tectum provides a uniquely refined test-bed for answering this question (Figure 4.3).

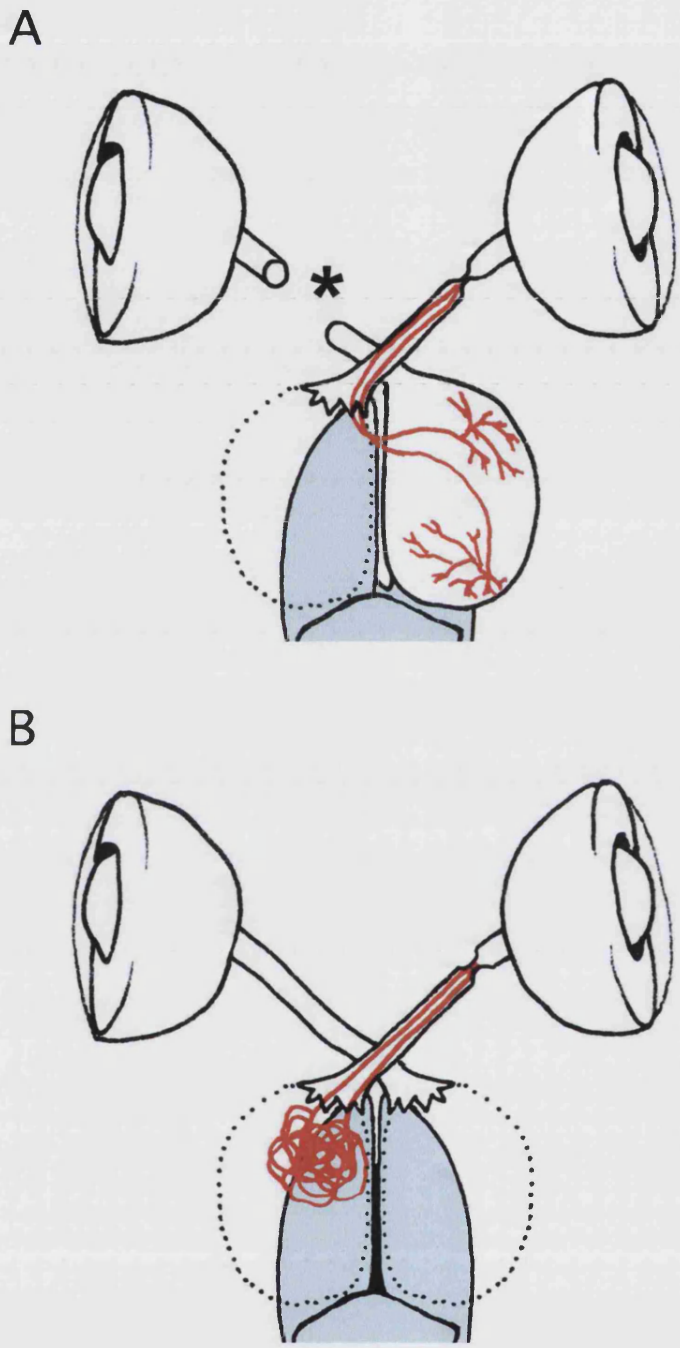

Figure 4.3 Two tests of whether myelin formation depends upon synaptogenesis.
A: To accelerate the formation of synapses by target-deprived axons in the intact ipsilateral tectum (**A**) the intact tectum was permanently denervated by removal of a length of the left optic nerve (asterisk; **A**). The intention was to expedite formation of synaptic connections by regenerating axons (red) in the remaining intact tectal lobe.
B: To totally remove the possibility for synaptic connection, both tectal lobes were removed.

4.4 Expediting synaptogenesis speeds up myelination.

The formation of ocular dominance patches is a slow process in which the infiltrating axons have to displace the existing presynaptic terminals to annexe their own input to tectal neurones. An early behavioural study (Davis and Schlumpf, 1984) using this system showed that removal of the pre-existing innervation of the ipsilateral tectal lobe speeded up the recovery of vision *via* the target-deprived regenerating optic nerve. To see if vacating the intact ipsilateral tectum to facilitate synapse formation in this way would accelerate myelin renewal in the target-deprived regenerating optic nerve, the left eye innervation of the intact right tectum was removed by extirpation of a lengthy segment of left optic nerve 2 weeks after the right optic nerve crush (Figure 4.3 A). The carp were sacrificed after 30 days of regeneration to compare the extent of myelination with the earlier result where target-deprived nerves had innervated the ipsilateral tectum with occupied synaptic sites.

30 day regenerating axons formed bundles in the optic fibre layer (the SO) of the intact ipsilateral optic tectum, but were excluded from the underlying synaptic layer (the SFGS: Figure 4.2 C; Figure 4.4 A). In the denervated 'vacant' tecta, however, they were already admitted to the SFGS by 30 days (Figure 4.4 B), forming the same dense granular pattern of anterogradely labelled synaptic arbors as took up to 50 days to appear in the OD patches of the normally innervated ipsilateral tectum (Figure 4.2 B). Thus, removal of the pre-existing innervation expedites synapse formation by the ectopically regenerating axons.

Facilitating synaptogenesis in this way significantly enhanced myelination of the right optic nerves (Figure 4.4 C). After 30 days there was a nearly four-fold increase in the number of myelinated axons over that in fish in which the normal innervation of the ipsilateral tectum was intact (from 8,606 to 32,462 fibres: $P = 0.013$). Considering that the axons had to escape from the site of their normal target and cross the midline, this compares very well with the level of myelination found during normal regeneration into the intact contralateral tectum (80,471 after 30 days regeneration). The overall density of anterogradely labelled fibre bundles in the ipsilateral tectum appeared greater in pre-vacated tecta than in the occupied tecta. This suggests that denervation may have attracted more regenerating axons via a long range signalling mechanism. In

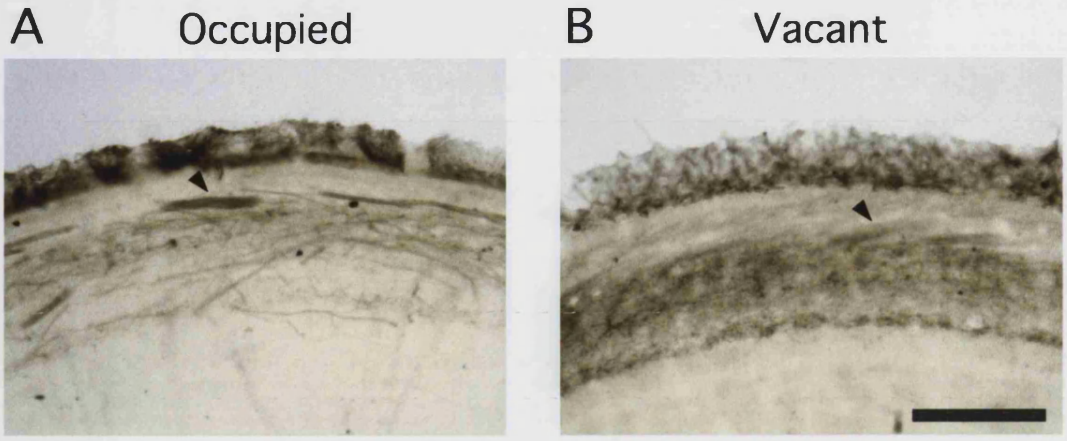

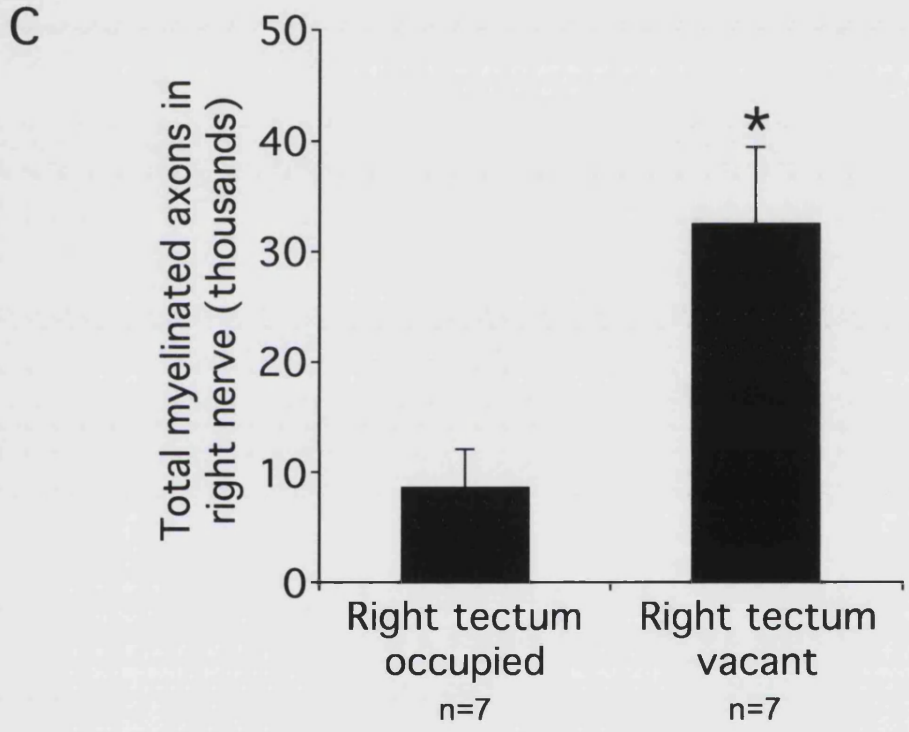

D

	R tectum occupied	R tectum vacant
Total axons	341,406 (± 69,700)	225,680 (± 24,449)
Myelinated axons	8,606 (± 3469)	32,462 (± 6,933)

Figure 4.4 Freeing up synaptic space promotes myelin formation.
A & **B**: Anterograde tracing showed that vacating the synaptic sites on tectal neurones allowed axons to escape the fibre bundles of the SO (arrowheads; **A** & **B**) to form dense granular staining arborisations in the in the SFGS (**B**).
C & **D**: Facilitating synaptogenesis in this way produced a significant (asterisk; p=0.0132; **C**) nearly fourfold increase (**D**) of myelinated fibres in the regenerating optic nerves. Exuberant branching of regenerating axons had not occured as extensively in the right tectum vacant group as there was a smaller total number of axons in these nerves (**D**). Scale bar: **A** & **B** = 100μm

agreement, I noticed that large neuromas at the site of the extirpated right tectum (e.g. Figure 3.2 D) were less common in the (ipsilateral) tectum-vacated group of fish.

4.5 Preventing synaptogenesis abolishes myelination.

Expediting synaptogenesis enhances myelination of the regenerating nerve. What happens if the opportunity for the axons to form synapses is totally removed? The simplest way to achieve this is to remove all tectal tissue from the path of the regenerating optic axons (Figure 4.3 B).

I removed both the ipsilateral and contralateral lobes of the tectum of four carp a few days after they had received right optic nerve crushes (Materials and Methods). Despite the complete lack of any visual function the fish were able to forage for food successfully and remained perfectly healthy. I examined the optic nerves of these fish as before, using electron microscopy. Two fish were examined after 30 days of regeneration and the remaining two after 50 days. Examples of micrographs from the two time-points are shown in Figure 4.5.

In contrast to unilaterally target-deprived optic nerves, the bilaterally-deprived nerves completely lacked any myelin after 30 days regeneration. Comprehensive examination of the cross sections of the both nerves failed to reveal a single myelin sheath (Figure 4.5). Most of the axons appeared healthy, but a minority showed early signs of degenerative change (eg., mitochondrial swelling, blebbing membranes), suggesting that removal of both tectal lobes had withdrawn some required trophic support.

After 50 days, small numbers of myelinated axons were found in the regenerated optic nerves. However, these myelinated axons were very rare and the vast majority of the axons were still unmyelinated. The initial signs of axonal degeneration seen at 30 days had now become widespread, involving most axons in the nerve and indicating that they have a long-term requirement for trophic support from tectal tissue. The rare myelinated axons were all healthy and a subset of the unmyelinated axons also appeared viable, presumably having found some alternative target. Evidently, the optic nerve supports axon growth from the lesion to the brain: the tectum is not needed for this process (Figures 3.2, 4.1, 4.2 & 4.5 A). Moreover, on arrival at the brain, the axons can survive unilateral target deprivation for long enough to escape from the neuroma

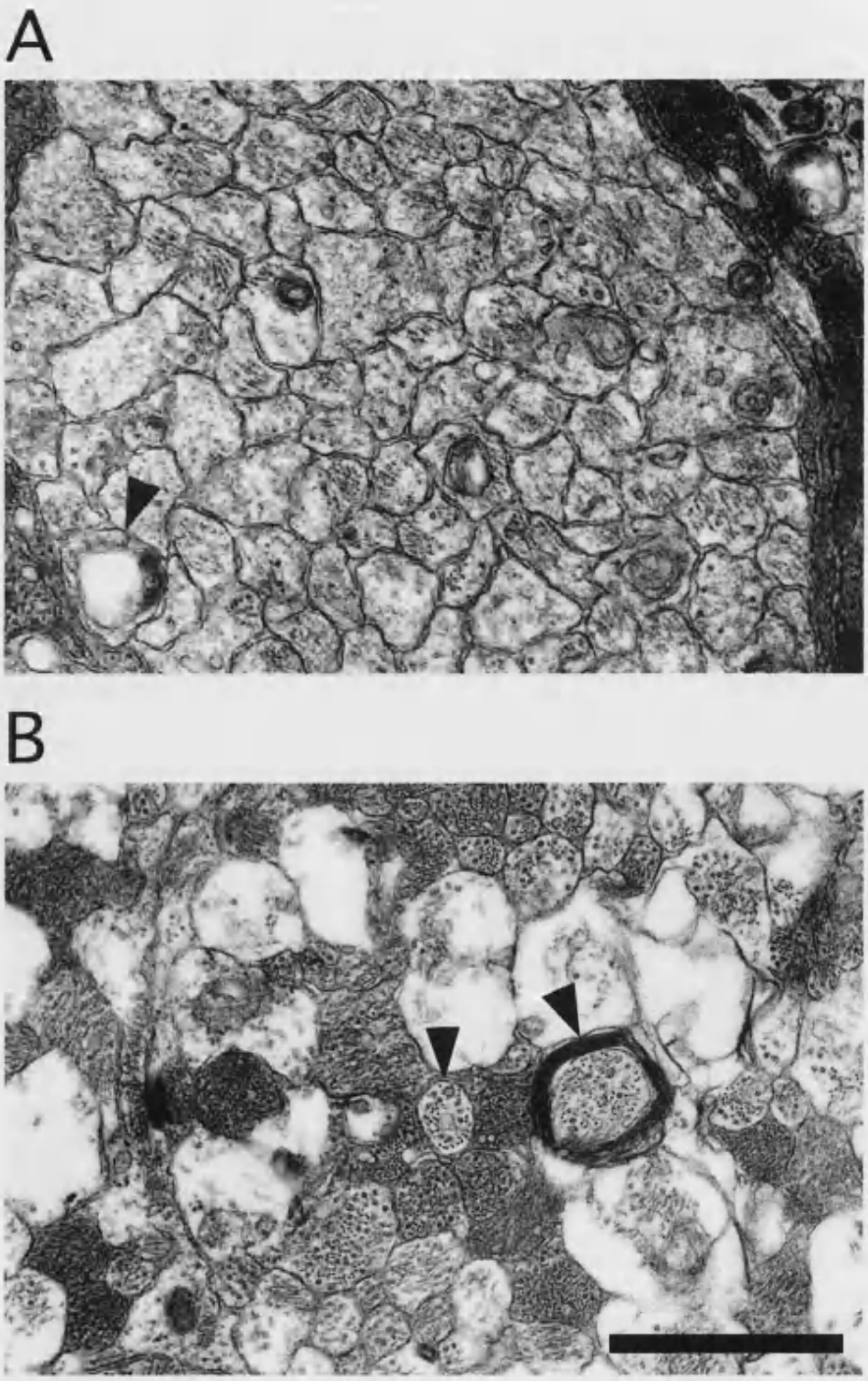

Figure 4.5 Total removal of all opportunity for synaptic connection prevents myelination. Example micrographs of regenerated optic nerves after 30 days (**A**) and 50 days (**B**) from carp which had both tectal lobes removed. After 30 days there were no myelinated axon profiles whatsoever (**A**). At this stage some axons had a slightly unhealthy appearance (e.g. swollen mitochondria; arrowhead). By 50 days regeneration, many axons were degraded. A minority of more healthy axon profiles remained and a small subset of these were myelinated (arrowheads; **B**). Scale bar: 1µm

(Figure 3.2) and reach the opposite optic tectum without apparent losses (Figure 4.1 & 4.2). How they are supported during this extra journey across the midline is unknown. One possibility is that the attractant is a diffusible trophic factor which works over a long distance i.e. from the ipsilateral tectal lobe to the neuroma. Another possibility is that the axons form synapses with the ipsilateral tectum before their long term requirement for support becomes critical.

The small percentage of healthy axons that survived 50 days of bilateral target deprivation had presumably found an alternative source of support. There are minor pathways by which retinal ganglion cell axons connect to locations other than the tectum (e.g. the diencephalon), or some unnoticed tectal tissue may have regenerated from the tectal germinal zone for these axons to innervate. A striking aspect of the axonal degeneration that resulted from bilateral target deprivation is that it does not attract macrophages. Following axotomy of the optic nerve, Wallerian degeneration normally occurs whereby very large numbers of macrophages/microglia proliferate in the fish visual pathway to clear away the debris of the degenerating distal axon segments and their myelin sheaths. However, during the degeneration seen after 50 days regeneration with bilateral tectal removal I saw no evidence of macrophage-mediated clearance of of the degenerating axons. Thus this appeared to be a form of "silent" axonal death whereby the degenerating tissue does not emit cytokines capable of initiating macrophage clearance.

4.5 Summary.

In this chapter I have shown that after 50 days of regeneration the myelination of target-deprived optic nerves reaches the level seen after 30 days of regeneration in target-intact optic nerves. Thus, removing the contralateral tectum of the regenerating optic nerve simply delays myelination by 20 days. The delay is the time required for the axons to cross the mid-line, compete for synaptic territory in the intact ipsilateral tectum and form ocular dominance patches there.

To test this indication that that myelination is triggered by synaptogenesis, I facilitated synapse formation in the ipsilateral tectum by removing the pre-existing innervation. This hastened synaptogenesis and significantly advanced

the progress of myelination of the regenerating optic nerve. Conversely, bilateral target deprivation totally abolished myelination in the regenerated optic nerve at 30 days.

These experiments build on evidence from the basic target-deprivation experiments described in chapter 3. The results offer an answer to the question of whether simple target infiltration or synaptogenesis stimulates myelination. Myelination appears to be triggered not just by the arrival of the regenerating axons in the target tissue. The formation of synaptic connections is required. In the next chapter I address the question of how this process might be regulated.

Chapter 5: What is the control mechanism for myelination?

5.1 Introduction

I have shown that the onset of myelination in the regenerating fish visual system is dependent upon the formation of synaptic connections by the growing axons. This finding raises various important questions, for example, how do the axons signal to the oligodendrocytes, what aspect of synaptogenesis initiates this signalling and to what extent is the supply of oligodendrocytes influential in the timing of myelination? Here I describe three lines of work intended to address these questions.

5.2 Does the Notch/Delta system regulate myelination in fish?

Whereas oligodendrocytes *in vitro* will differentiate from their precursors (OPCs) in the absence of axons, I have shown here that myelination *in vivo* depends on the formation of synaptic connections by the axons concerned. It would clearly be of great interest to identify the axonal signals involved, and I tested whether the Notch/Delta signalling pathway is active during myelination in the developing and regenerating fish visual pathway.

Notch receptors are expressed by rat optic nerve OPCs and Notch ligand binding arrests further differentiation of these cells *in vitro* (Wang et al., 1998). Wang *et al.* suggested that Delta on the surface of immature optic axons may inhibit OPC development until the axons are ready, when they down-regulate the Notch-ligands, releasing the oligodendrocytes to differentiate further (Wang et al., 1998). Interfering with the Notch pathway affects oligodendrocyte development in zebrafish (Park and Appel, 2003) as well as in mammals (Genoud et al., 2002; Givogri et al., 2002).

I decided to see if this mechanism controlled the myelination in fish in a synaptogenesis-timed manner. A number of different Notch receptors and ligands have been cloned in the zebrafish (Bierkamp and Campos-Ortega, 1993; Westin and Lardelli, 1997; Haddon et al., 1998; Itoh et al., 2003). I used *in situ* hybridisation to examine the expression of mRNA for these during regeneration of the visual system in adult zebrafish and also during development of the

Figure 5.1 Notch expression in the regenerating and developing zebrafish brain indicates that it may not be involved in myelin development.

A, B, C, & F: No expression of mRNA for notch receptors (example shown Notch 1a) was found fibre tracts (f) in longitudinal sections of control non-lesioned optic nerves (**A**) or regenerating optic nerves two weeks post lesion (**B**). Positive controls of embryos that are known to express mRNA for Notch ligands were included on the same slides which were positive for Notch ligand expression (not shown). Additionally a probe for pax2.1 mRNA was used to ensure that the *in situ* hybridisation protocol did work on sections of optic nerve. Pax 2.1 mRNA was expressed by the astrocytes (arrowheads; **F**) surrounding the fascicles (f) of axons, and in sections of 24 hour zebrafish embryos its expression was restricted to the optic stalk (arrowhead; **F**) and mid-hind brain boundary (arrow; **F**), as expected from an earlier study (Macdonald et al, 1997).

D & E: The expression of mRNA for notch ligands was examined in the retina of control and post-optic nerve regenerating zebrafish. No expression of mRNA for any Notch ligand was found in the retinal ganglion cells in either control or regenerating zebrafish. Examples of *in situ* hybridisations for Serrate A mRNA in non-lesioned control (**D**) and regenerating (**E**) are shown. The retinal ganglion cell layer (RGCs) was negative in both cases.

G, H, J & K: During the developmental period in which myelination commences no expression of mRNA for Notch ligands was found in retinal ganglion cells of the retinae of zebrafish embryos. No Serrate A mRNA was detectable in the retina at 4 days (**G**). Low levels of Serrate B mRNA were found in the inner nuclear layer of the retina at 4 days (arrowheads; **H**). mRNA for Delta A and B was restricted to the periphery of the retina in the retinal ganglion cell germinal zone (arrowheads; **J & K**). Low levels of Delta b mRNA were also expressed in the inner nuclear layer (arrow; **K**).

I & L: Notch receptors are expressed only in germinal zones of the brain and retina and not in fibre tracts. If the Notch system is involved in myelination, one would expect the expression of Notch receptors by oligodendrocytes in fibre tracts. Upon examination of the developing fibre tracts of the zebrafish brain at periods when myelination is underway I found no expression of mRNA for Notch receptors in fibre tracts of the zebrafish brain (for example, Notch 1a; **I**; f=fibre tracts). Notch receptors were only expressed at high levels in the germinal zones of the retina and brain (arrowheads; **I & L**).

Scale bars: **A - C & F**= 100μm; **D & E** = 50μm; **G, H, J, K & L** = 50μm; **I** = 100μm.

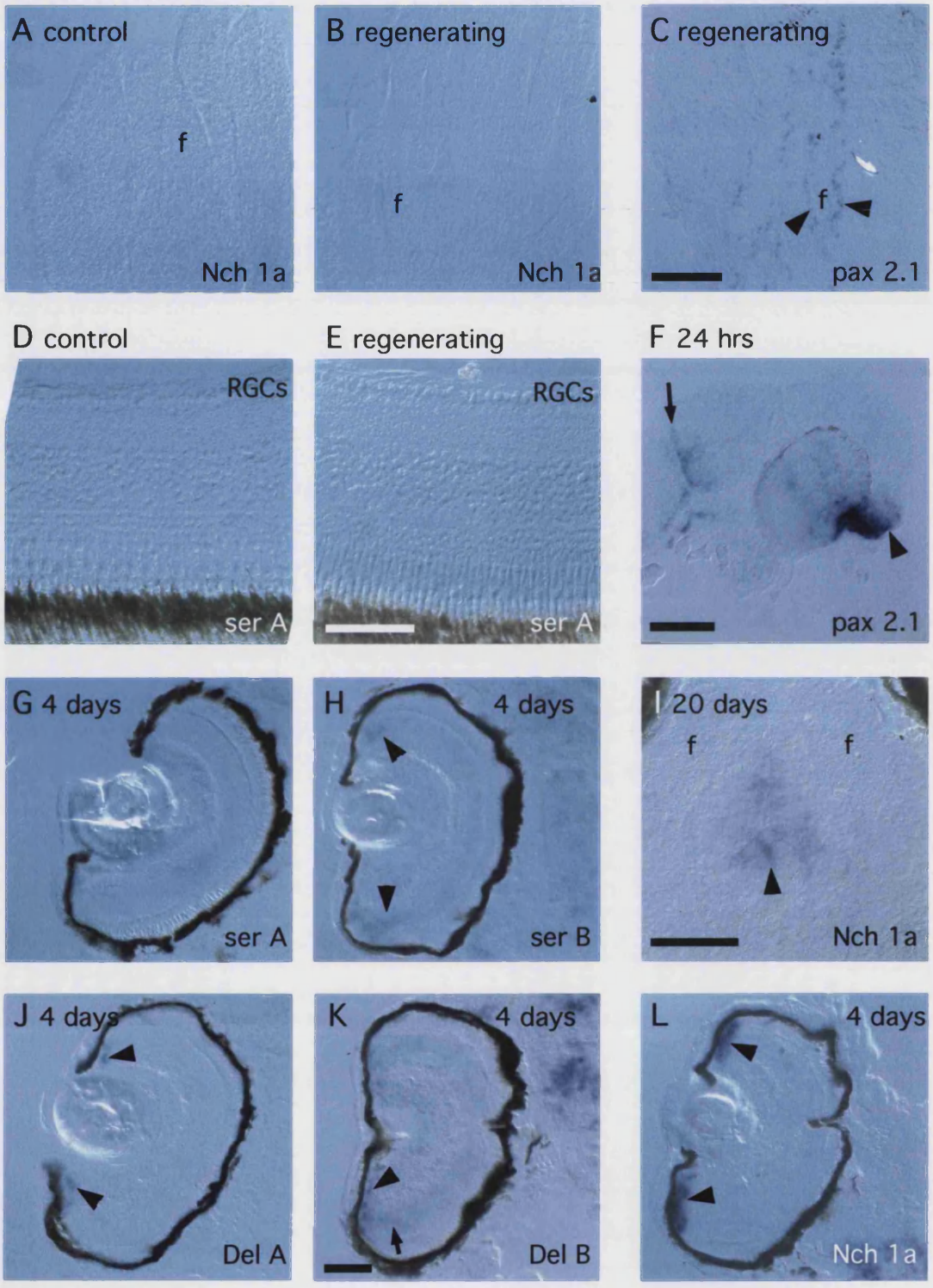
A control
f
Nch 1a
B regenerating
f
Nch 1a
C regenerating
f
pax 2.1
D control
RGCs
ser A
E regenerating
RGCs
ser A
F 24 hrs
pax 2.1
G 4 days
ser A
H
4 days
ser B
I 20 days
f
f
Nch 1a
J 4 days
Del A
K
4 days
Del B
L
4 days
Nch 1a

zebrafish. Figure 5.1 shows a selection of micrographs of these *in situs*. There was no up-regulation of Delta A or B, or Serrate A or B expression in the retinal ganglion cell layer of the retina during regeneration (2 weeks after optic nerve crush, when myelination has only just started (*cf* Figure 3.7). Moreover, I detected no Notch receptor expression in longitudinal sections of the optic nerve during regeneration.

Perhaps regeneration is a special case. To examine whether the Notch pathway is active during myelination of the developing zebrafish CNS, I examined zebrafish at the stage when the brain and optic nerve is starting to be myelinated (Brösamle and Halpern, 2002). mRNA for the Notch ligands Serrate A and B and delta A and B was found in the retina of developing zebrafish (Figure 5.1). However, expression of these transcripts was not seen in the retinal ganglion cell layer. Serrate B and Delta B were expressed at low levels in the inner nuclear layer of the retina. Expression of the other Notch ligands examined was limited to the germinal zone at the periphery of the retina. Corresponding mRNA for Notch receptors was expressed at high levels in the periphery of the retina but no Notch receptor transcripts were found in fibre tracts of the developing brain or the optic nerve (Figure 5.1).

These experiments show that the expression patterns of the Notch ligands and receptors examined show no hint of involvement in myelin formation in fish. Although I examined all Notch receptors so far cloned (1a, 1b, 5 and 6; (Bierkamp and Campos-Ortega, 1993; Westin and Lardelli, 1997) Materials and Methods) I did not examine every Notch ligand so far identified, omitting Delta C & Delta D because DNA to make the riboprobes was unavailable. There also may be other Notch ligands and receptors yet to be identified in zebrafish. It could also be informative to search with antibodies against these molecules.

5.3 Synaptogenesis or refined connections?

In the normal adult fish visual system, the terminal arbors of retinal axons are arranged in a precise neighbourly manner over the tectal surface forming an accurate point to point map of the visual field (Meyer, 1980; Easter et al., 1981; Stuermer and Easter, 1984; Rankin and Cook, 1986). When the optic fibres reach the tectum during regeneration of the fish visual system, they initially branch

and synapse widely over the tectal surface forming a low resolution map which is gradually refined with time. This process is slow. In the Goldfish (where the majority of experiments examining this process have been carried out) , it takes 2-3 months (Rankin and Cook, 1986). The time course of myelin renewal in the optic nerve is very similar, suggesting an association between the two processes. Perhaps individual axons take widely varying times to refine their arbors, and only permit myelination when this is achieved.

Map refinement is certainly mediated by the same activity-dependent NMDA receptor-driven mechanism (Meyer, 1983; Olson and Meyer, 1991) that segregates target-deprived optic axons into OD patches (Schmidt, 1990) when they are made to compete for the intact optic tectum belonging to the other eye (Figure 4.2).

Would blocking OD patch formation by NMDA receptor blockade therefore prevent myelination? To address this question, I locally administered the NMDA-blocking drug APV to the tectum using the slow-release polymer Elvax 40P (Materials & Methods). This method has been used before on several occasions to block ocular dominance patch formation in the tectum of frogs (Cline et al., 1987; Cline and Constantine-Paton, 1989; Scherer and Udin, 1989; Udin et al., 1992) and rats (Simon et al., 1992). The drug is suspended in thin slices of the polymer which are implanted over the required brain region, where it is slowly released over several months after an initial peak (Cline and Constantine-Paton, 1989). Carp right optic nerves were made to regenerate in the absence of the left tectum. After 18 days I then placed Elvax implants containing d-APV or its inactive isomer l-APV over the right tectum. To allow time for the formation of ocular dominance patch formation the fish were sacrificed 50 days following the initial optic nerve lesion. 24 hours before sacrifice, the right eyes were injected with anterograde tracer to ascertain whether ocular dominance patch formation had taken place and the nerves were prepared separately for TEM.

An example of anterograde tracing from a d-APV fish is shown in Figure 5.2. Unfortunately, ocular dominance patches had formed in the presence of Elvax implants containing d-APV, and the experiment had therefore failed. This may have been because the method of drug delivery was ineffective or because NMDA receptor antagonists do not prevent ocular dominance patch formation in

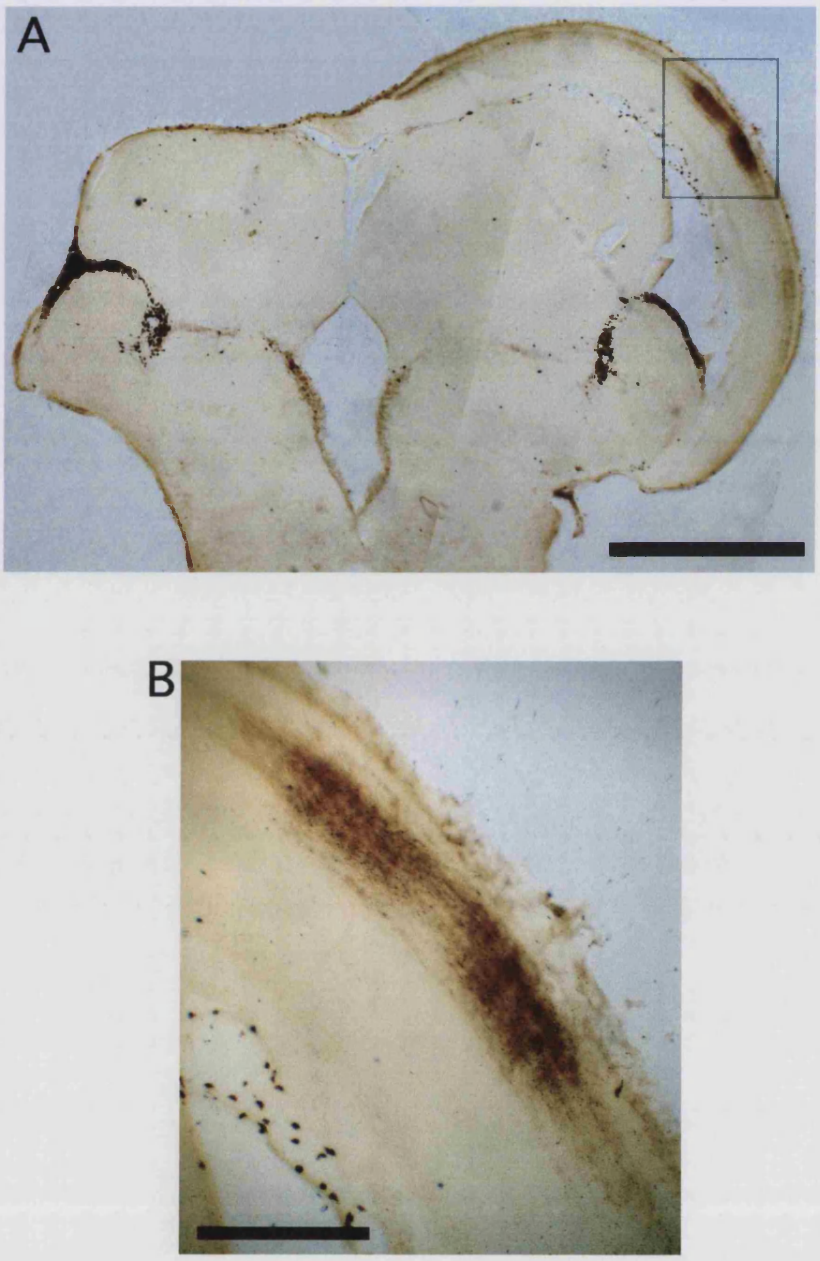

Figure 5.2 Blockade of the NMDA receptor with dAPV in slow-release Elvax polymer was unsuccessful. Images of anterograde tracing of regenerated target-deprived right-eye axons from a fish that had an Elvax implant containing the NMDA antagonist d-APV (10mM) placed over the remaining right tectum. The drug implant did not prevent the formation of ocular dominance patches (Box; **A**). High magnification examination of the ocular-dominance patches revealed that the axons had arborised in the SFGS (**B**). Scale bars: **A** = 1mm, **B** = 250µm.

fish as this has never been shown. Further efforts are required to improve the drug delivery method or find a better one. For example, Schmidt (1990) used osmotic mini-pumps to block the process of map refinement. The advantage of blocking ocular dominance patch formation is the simple anatomical readout it provides on the success (or otherwise) of the drug treatment.

5.4 Demand and supply in myelination.

The experiments I described in the previous chapters show that the optic axons determine (demand) when optic nerve myelin formation begins during regeneration. For example, facilitating synapse formation in the ipsilateral tectum hastened myelination, which would only be possible if there were sufficient oligodendrocytes to implement this change of schedule. However, examining myelination during development of the zebrafish visual system I found indications that the supply of oligodendrocytes is outstripped by axonal demand.

In agreement with Brösamle and Halpern (2002) I found that thin myelin sheaths start to appear in the larval zebrafish optic nerve after around 6 or 7 days of development. Their number steadily increased at the further time-points I examined (10, 15, 20 and 25 days of development). However, even at 25 days the majority of axons were still unmyelinated.

Axons sprout from the zebrafish eye at around 30-32 hours post fertilisation (hpf) (when incubated at 28.5°C) (Burrill and Easter, 1994; Easter and Nicola, 1996). These axons reach the tectum by 48 hpf and start to connect up from 72 hpf (Stuermer, 1988; Burrill and Easter, 1994; Easter and Nicola, 1996). This coincides with the first recordable eye movements and 24 hours later (96 hpf) the optokinetic and vetibulo-ocular reflexes are indistinguishable from the adult response (Easter and Nicola, 1996, 1997). The presence of directed eye movements proves that the retina and tectum are synaptically connected after only 4 days of development, well in advance of myelination in the optic nerve. If the axons are functionally connected, what accounts for their failure to be myelinated?

I found that the first myelin sheaths in the optic nerve appear in patterns indicating that the axons are ready but there are insufficient oligodendrocytes to myelinate them. At 20 days of development (when the nerve is 5% myelinated)

the myelinated axons were characteristically clustered in neighbour groups (Figure 5.3 A; *myelinating units*: Hildebrand et al., 1993) each belonging to the same oligodendrocyte. These groups of myelinated axons were separated from one another by large expanses of unmyelinated axons, suggesting that oligodendrocytes find themselves surrounded by axons which are all ready to be myelinated (because they are synaptically connected up) and simply myelinate the closest at hand. This was confirmed by nearest neighbour analysis of the distances between the myelinated axons (Figure 5.3 C). The developmental pattern differed from that seen in regenerating carp optic nerves where the myelinated axons were more frequently found in isolation, as if individually singled out for myelination from the surrounding axons which were not yet ready (Figure 5.3 B & D).

Although the supply of oligodendrocytes appears in this way to be the rate limiting step for myelination of the zebrafish visual system, there were indications that in this case, as in regeneration that synaptogenesis is a pre-condition for myelin formation. The visual system of the zebrafish larvae was growing rapidly and in cross-sections of the whole optic nerve the region that contained the most recent axons was identifiable by the presence of growth cone profiles. The array of new axons in this region was completely unmyelinated (Figure 5.3 E-G). Presumably because they had not yet formed synaptic connections in the tectum. Thus myelination during development is also contingent upon axons forming synaptic connections but is held back by a restriction in the supply of competent oligodendrocytes.

Axons and oligodendrocytes are partners in the myelination process but these observations suggest that in different circumstances either can lead the other in the control of myelination. The reason that myelination during regeneration is axonal demand-led could be that the pre-existing oligodendrocytes survive in readiness. Why it appears to be oligodendrocyte supply-limited during development could be that wiring up to the tectum is a simpler task in the tiny fish larva than during regeneration.

Figure 5.3 Optic nerve myelination proceeds in different patterns during development and regeneration.

A & B: During zebrafish development, newly myelinated axons in the optic nerve were in clustered neighbourly groups (**A**). In contrast, during regeneration in the carp, the myelinated axons were more evenly distributed (**B**). The percentage of myelinated axons was about the same in both cases (5%)

C & D: Quantification of the nearest neighbour distances confirmed that during development (**C**) the newly myelinated axons were more tightly clustered than during regeneration (**D**). In both cases, however, the patterns differed from the expected random distribution (curves).

E, F, G: Newly grown axons were not myelinated in the developing zebrafish optic nerve. **E**: A cross-section of an optic nerve and a segment of the other optic nerve of a 20 day old zebrafish larva. Areas of new growth of the nerve (box f; **F**) and the neighbouring optic nerve (box g; **G**) were identified by the presence of growth cone profiles (GC; **F & G**). The new axons neighbouring the growth cones were all unmyelinated.

Scale bars: **A & B** = 1μm; **E** = 5μm; **F & G** = 2μm.

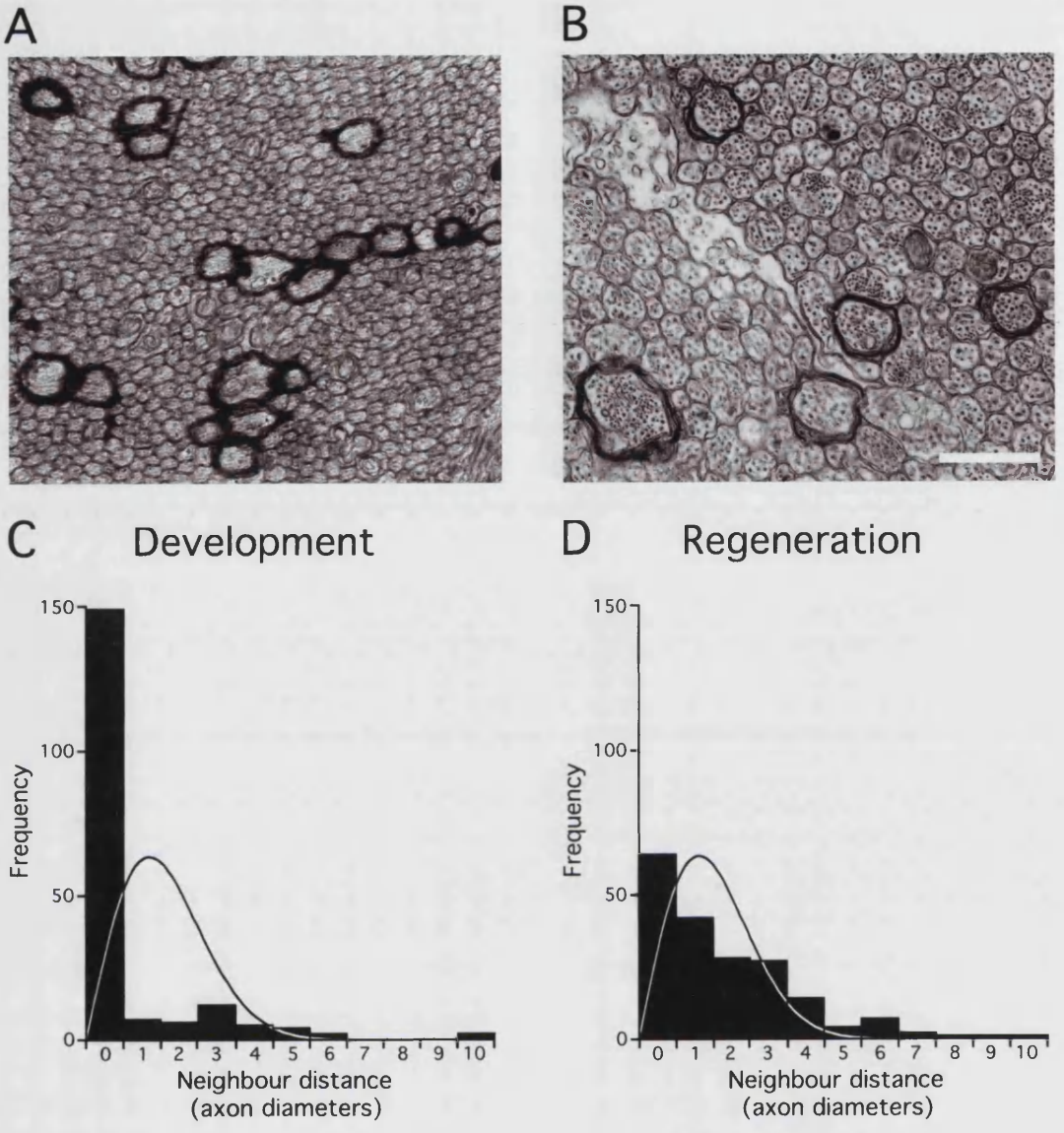
A
B
C
Development
D
Regeneration
150
100
50
0
Frequency
0 1 2 3 4 5 6 7 8 9 10
Neighbour distance
(axon diameters)
150
100
50
0
Frequency
0 1 2 3 4 5 6 7 8 9 10
Neighbour distance
(axon diameters)
E
G
F
F
GC
G
GC

5.5 Summary.

In summary, I have examined three aspects of the control of myelination in the fish visual system.

I first examined whether Notch signalling has a role in myelination of the fish optic nerve. Notch activation can inhibit differentiation of mammalian oligodendrocytes, but I found no indication that it is involved in the control of myelination during regeneration or development of the fish visual system.

I then tried to test whether myelination in the regenerating visual system is dependent upon NMDA-mediated synaptic refinement. Unfortunately, NMDA blocking failed and requires development before further attempts to address this important question are made.

Lastly I provided evidence that the timing of myelination is not always exclusively dependent upon axonal demand for myelin, as it is during regeneration of the fish visual system. During development of the zebrafish visual system, the supply of oligodendrocytes appeared to be more influential in determining the spatial pattern of the first myelin sheaths.

Chapter 6: Discussion.

6.1 Summary of results.

Chapters 3 and 4 described tests of the proposal that CNS myelination is dependent upon synaptogenesis. Using the regenerating fish optic nerve, I first showed that myelination is delayed when the optic axons are deprived of their principal synaptic target, the contralateral optic tectum. This delay corresponds to the time that it takes for the regenerating axons to innervate the intact ipsilateral tectum, displace the native innervation and form synapses there. Once they connect up ectopically in this way, myelination of the nerve progresses rapidly.

I then used this system to obtain more critical evidence that the formation of synaptic connections is the crucial step that triggers myelination. I opened the gates for the regenerating target-deprived right eye axons to form synaptic connections by removing the native left eye innervation of the intact ipsilateral tectum. This allowed the regenerating axons promptly to form synapses in the SFGS, which resisted innervation when the native innervation was intact (Figure 4.4). Under these conditions, myelination in the optic nerve was four-fold enhanced. Conversely it failed completely when the axons were prevented from forming any synaptic connections.

In chapter 5, I described attempts to identify an axon to oligodendrocyte signal that might mediate this synaptogenesis-timed behaviour, and to interfere pharmacologically with synapse formation. Finally, I examined fish optic nerve development and found indications that myelination is dependent both on the formation of synaptic connections by the axons and availability of sufficient oligodendrocytes.

These findings build on extensive hints from the literature which suggest that myelination is dependent upon the functional maturation of fibre tracts in the brain (Flechsig, 1920; Langworthy, 1933; Yakovlev and Lecours, 1967). This idea was originally proposed as far back as 1901 (Flechsig, 1901) but despite an abundance of circumstantial support (e.g. Schwab and Schnell, 1989), the possibility that CNS myelination is dependent on synapse formation has never been tested experimentally before.

The results presented here suggest that when axon outgrowth culminates in synapse formation, the axon is retrogradely modified to signal permissively to the oligodendrocytes for myelin formation. The target$^+$/target$^-$ approach used here could be used in the future to identify molecular components of this signalling mechanism.

6.2 Is optic nerve regeneration in fish a special case?

The regenerative competence of the fish visual system was crucial in my experiments to address how axonal target-deprivation affects myelination. However, it is important to consider whether regeneration might be a special case. Do these findings reflect a general rule applicable to CNS myelination during development in other species, particularly mammals and birds which cannot regenerate CNS connections? In support of this, the older literature contains a number of scattered indications that CNS myelination only begins after synaptogenesis is underway, and never before (Lund and Lund, 1972; Skoff et al., 1976a, b; Rager, 1980; Sefton and Lam, 1984; Warton and McCart, 1989). In most cases, the issue was clearly not foremost in the experimenters' minds and the correlation has to be extracted from multiple papers. Below, I have summarised examples from studies on development in the chick and rat visual systems.

6.2.1 Myelination in the developing chick and rat visual system.

Rager (1980) examined the number of axons (myelinated and unmyelinated) in the chick optic nerve through the course of development and measured their physiological properties as well. Although he did not directly describe a correlation between synaptogenesis and myelination, it is apparent in his data, which I have rearranged in Figure 6.1A. The total number of axons in the optic nerve increases until the embryo is 11 days old (stage 37) and then falls back and begins to plateau at 14 days of development (stage 40). This decrease corresponds with the elimination of excess retinal ganglion cells in the retina (and presumably also with the elimination of excess axonal branching) (Rager, 1980). Presumably, the axons that remain are stabilised by receiving trophic support after forming synaptic connections in the tectum. Concurrent with this

Figure 6.1 Synaptogenesis precedes myelination in development of the visual system of chicks and rats. Data extracted from **A**: (Rager, 1980), **B**: (Sefton & Lam, 1984; Warton and McCart, 1989; Skoff 1976a,b).
A: In the chick, the total number of axons in the optic nerve (*black*) first rises to a peak and then drops back to a plateau. In the period that the number of axons in the nerve starts to plateau the conduction velocity (*brown*) increases. As the plateau is reached myelinated axons appear in the nerve (*blue*), myelination proceeds slowly and is all but complete by 119 days of development. Inset traces show tectal recordings which start to mature at the peak of axon number in the nerve (10-12d)
B: In the rat the shape of the trace of axon number in the optic nerve over development (*black*) is remarkably similar to the chick with an initial peak falling back to a plateau. As in the chick, myelination of the nerve (*Blue*; n.b.percentage myelinated in this graph) only starts once axon number approaches the plateau. The number of synapses in the tectum (*red*) also starts to rise to a peak once axon number appraches the plateau.

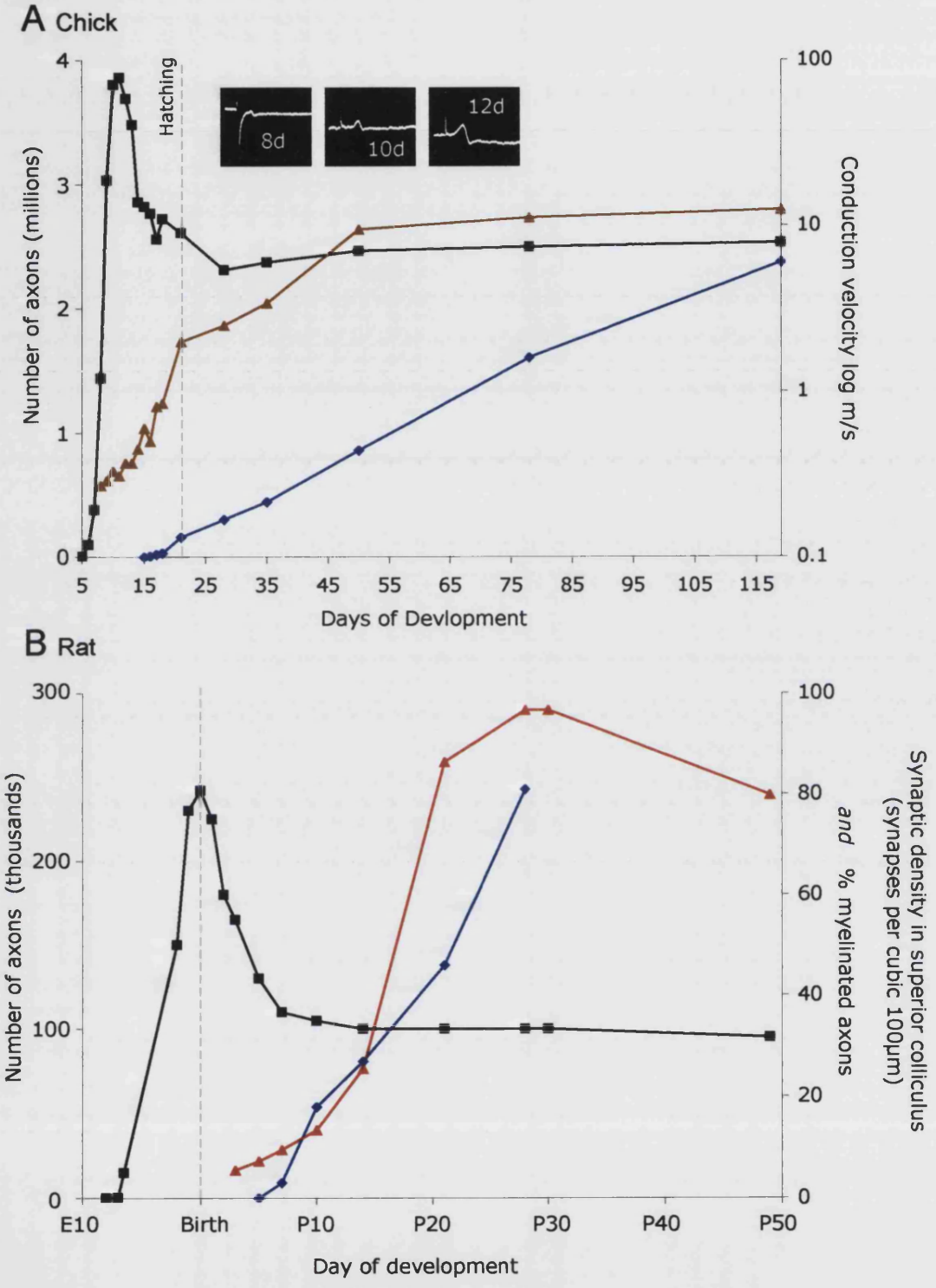
A Chick
Hatching
8d
10d
12d
Number of axons (millions)
Conduction velocity log m/s
Days of Devlopment
B Rat
Number of axons (thousands)
and % myelinated axons
Synaptic density in superior colliculus
(synapses per cubic 100µm)
E10
Birth
P10
P20
P30
P40
P50
Day of development

stabilisation in axonal number, the conduction velocity of the axons increases, the tectal neurones mature and the first myelinated axons are found in the optic nerve (Figure 6.1A). Thus the stabilisation of axon number following synaptogenesis in the tectum precedes myelination of the chick optic nerve.

The time course of axon outgrowth, synaptogenesis and myelin formation in the rat visual system is very similar. Figure 6.1B is derived from three separate studies in developing rats (Skoff et al., 1976a, b; Sefton and Lam, 1984; Warton and McCart, 1989). Sefton & Lam (1984) counted the number of optic axons in the optic nerve at times during embryonic and postnatal development, and found an initial peak followed by pruning of excess retinal axons until a plateau is reached. Likewise, the timing of myelination in the rat optic nerve is very similar to that in chick (Skoff et al., 1976a, b). Myelination commences after the initial embryonic peak in axon numbers, and progresses to near completion at P30 while the number of axons declines to its adult value. Skoff *et al.* also showed that oligodendrocytes start to appear in the optic nerve from birth, several days before the onset of myelination (Skoff et al., 1976a, b), suggesting that a further maturational changes are needed before the axons can be myelinated. Figure 6.1B also shows the time course of synapse formation by retinal axons in the superior colliculus, extracted from a quantitative EM study (Warton and McCart, 1989; see also: Lund and Lund, 1972).

These graphs show that the percentage of myelinated axons in the optic nerve rises with a remarkably similar time course to that of synaptogenesis in the superior colliculus. The formation of synapses in the colliculus precedes the onset of myelination in the optic nerve by a few days. This could represent the time that it takes to mobilise permissive signalling by the axons and or myelin formation by the oligodendrocytes. Oligodendrocyte differentiation and myelination proceeds in a slow anterograde wave (Skoff, 1978; Skoff et al., 1980; Colello et al., 1995), which could reflect a proximal to distal sequence in the insertion of whatever axonal signals are needed to initiate myelination.

The retinotectal connection is not the only visual pathway in the rat: there is also a major connection with the lateral geniculate nucleus (LGN) of the thalamus. Qualitative examination of synaptogenesis during development in the rat LGN shows that it commences on a similar time-scale to that in the superior colliculus (Aggelopoulos et al., 1989). Together, these findings demonstrate that

the formation of myelin in the rat optic nerve follows after the formation of synapses in the brain.

Correlations have also been made between neurophysiological maturation and myelination of axons in the rat corpus callosum (Seggie and Berry, 1972) and in the visual pathway and the corpus callosum in cats (Grafstein, 1963; Haug et al., 1976; Looney and Elberger, 1986).

Overall, these similarities with the sequence of events during the renewal of myelin in the regenerating fish optic nerve strongly indicate that the fish system is a valid model for CNS myelin formation.

6.2.2 Does fish optic nerve regeneration recapitulate fish optic nerve development?

Relating myelination and synaptogenesis during development in fish visual system, Jeserich (1982) showed how, much as elsewhere, the ingress of optic axons into the tectum, synaptogenesis and the myelination of the axons in the optic fibre bundles of the tectum follow in sequence during trout (*Salmo gairdneri*) development. The first optic axons reach the tectum at 10 days, synaptogenesis follows the ingress of axons into the tectum and is substantially underway in the optic tectum by hatching a few days later (Vernier, 1969; Jeserich and Rahmann, 1977) (Figure 6.2).

However, myelinated fibres only start to appear in small numbers in the axon bundles of the SO at hatching and their number increases at a snail's pace thereafter, comprising a mere 46% of axon bundle fibres after a year of development (Jeserich, 1981). This lengthy delay between synapse formation and the appearance of the first myelinated fibres, and the slow progression of myelination thereafter, suggests that some further maturational step is needed before myelination can take place. This could be the provision of myelin-ready oligodendrocytes, as to be considered below.

6.2.3 Oligodendrocyte supply.

The observations in chapter 5 on myelination in the developing zebrafish visual system, suggested that axon connectedness may not be the only factor which affects myelination during development. Oligodendrocytes are more than equal partners in this process, and the supply of mature oligodendrocytes must be an important determinant of the developmental timing of myelination. The

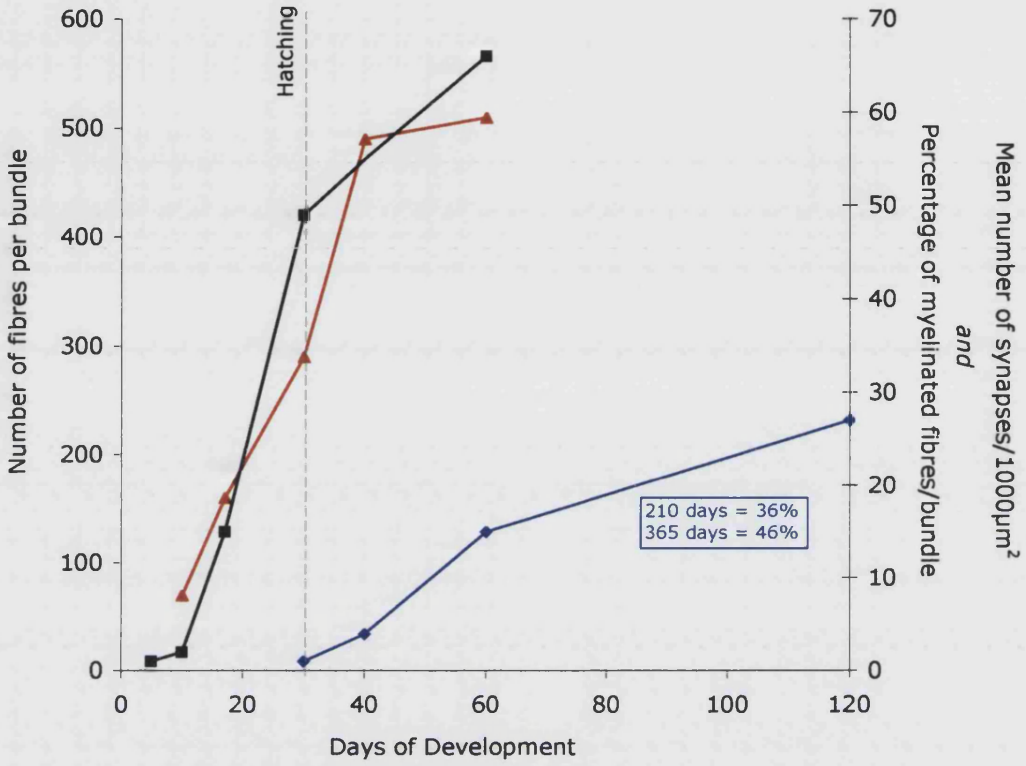

Figure 6.2 Myelination in the trout (*Salmo gairdneri)* visual system follows long after fibre in-growth and synaptogenesis in the tectum. Data extracted from (Jeserich and Rahmann, 1977; Jeserich 1981, 1982). Fibres appear in bundles in the *stratum opticum* (SO) of the tectum from day 10 of development (Red) concurrently with the first synapses in the tectum (Black) these two properties then rise coordinately. Myelinated axons only appear in the fibre bundles of the SO from 30 days of development (Blue) and the number of myelinated axons rises slowly thereafter only reaching 46% after a year of development (inset).

supply of these cells is dependent on systemic (Barres et al., 1994a; Rodriguez-Pena, 1999) as well as local (Barres and Raff, 1993; Fernandez et al., 2000) axonal and glial factors.

Much as in trout, zebrafish retinal axons form functional connections at an early stage (Stuermer, 1988; Burrill and Easter, 1994; Easter and Nicola, 1996, 1997), well before the appearance of the first myelin sheaths in the optic nerve. In agreement, the pattern of the first myelin sheaths suggested that most axons in the nerve are myelin-competent by this stage, and that it is the oligodendrocytes that are in short supply. If it is correct to interpret the early myelination patterns in this way, the pattern in the regenerating optic nerve indicated that the balance between oligodendrocyte supply and axonal demand here is tipped more towards axonal demand. The fate of the pre-existing oligodendrocytes that were deprived of axons by the lesion is unknown, but they could have remained in place or been quickly renewed to myelinate the regenerated optic nerve. This is demonstrated by the experiment described in chapter 4 where vacating the ipsilateral tectum and facilitating synaptogenesis promoted myelin renewal in the regenerating optic nerve. This shows that there must either have been sufficient pre-existing oligodendrocytes to support this advance in the myelination timetable or adequate capacity to generate them. These observations show that myelination during regeneration is a system where axonal demand for myelination is more easily revealed because it is uncoupled from the restriction in the supply of differentiated oligodendrocytes which may affect myelination during development.

6.2.4 Are CNS axons ever myelinated without forming synapses?

Only one case where CNS axons are myelinated when not synaptically connected has been documented, in neonatal cerebellar Purkinje cells cultured in brain slices (Schnadelbach et al., 2001). In preparing the slices, the Purkinje neurons are axotomised and detached from their synaptic targets in the deep nuclei. However, they survive and the proximal segments of their axons remain in place. They fail to sprout regeneratively, but attract oligodendrocytes to myelinate them in the absence of synapses (Schnadelbach et al., 2001). This is a unique exception that may prove the rule argued in this thesis. Purkinje axons are characteristically resistant to degeneration following axotomy, but this resistance is only acquired after the axons have formed synaptic connections in

the deep nuclei during development (Dusart et al., 1997). The capacity of the axons to permit myelination may have been acquired at the same time as the resistance to degeneration (i.e., prior to slice preparation), and persist in the same way in the mature Purkinje axons.

6.3 Possible mechanisms controlling myelination.

6.3.1 Axon diameter

Paul Flechsig (1901) originally proposed that the ordered schedule of myelination in the brain might reflect the sequential functional maturation of the white matter tracts. Two other theories on the control of myelin formation were current, proposed by Vogt and Vogt (1908) and von Monakow (von Monakow, 1900, 1910). Vogt's theory was based upon observations of the larger diameter of myelinated fibres. He suggested that axons are myelinated only once they reach a critical diameter. von Monakow's theory was that myelination is triggered only once the brain area to be myelinated has been vascularised. Subsequently, little has been heard of the von Monakow theory, but the ideas of Flechsig and Vogt have fallen in and out of favour at different times during the 20th century (Langworthy, 1933; Duncan, 1934; Yakovlev and Lecours, 1967; Matthews and Duncan, 1971; Looney and Elberger, 1986).

Here, I have provided experimental evidence that CNS axons need to form synapses before they can be myelinated. I also found clear instances that refute any simple form of the critical diameter theory. In target-deprived orfe optic nerves (Chapter 3; Figure 3.6), large unmyelinated axons were routinely found adjacent to much smaller myelinated axons. When an axon synaptically connects with a target neuron, many changes in housekeeping and function must take place as it switches from supporting growth cone extension to maintaining synaptic transmission. It is interesting that, despite the importance of this topic, it has hardly been approached except in the regenerating fish visual system (Perry et al., 1987, 1990; Hieber et al., 1992; Hoover et al., 1997). The findings presented here suggest that the earliest of these changes include the expression of permissive axonal signals that initiate oligodendrocyte myelination. Increased axon diameter may be among these changes (*cf.*, (Voyvodic, 1989)), and certainly

occurs in response to ensheathment itself (Windebank et al., 1985). However, the observations in orfe clearly demonstrate that axonal diameter *per se* is not the trigger for myelination.

6.3.2 Molecular mechanisms.

Axonally expressed signalling molecules have been shown to act at different stages of oligodendrocyte lineage progression. Axon-derived neuregulin regulates the survival of early differentiating oligodendrocytes (Fernandez et al., 2000) and axons are required for the normal proliferation of these cells (Barres and Raff, 1993). Immature axons are thought to negatively regulate the differentiation of OPCs via the Notch pathway (Wang et al., 1998; Genoud et al., 2002; Givogri et al., 2002). The removal of sialylation from PSA-NCAM molecules expressed on axons induces myelination (Charles et al., 2000) and the cell adhesion molecule n-cadherin may regulate the final oligodendrocyte-axon interactions that lead to ensheathment (Schnadelbach et al., 2001).

Any or all of these axonal signals could be activated in a synaptogenesis-related manner. In Chapter 5 I concentrated on the Notch pathway as a possible regulator of myelination in the fish visual pathway. However, no expression of Notch receptors or ligands at appropriate locations and times during regeneration or development of the zebrafish visual system was found. The survey was not completely exhaustive, but suggests that some other pathway regulates the onset of myelination in the context considered here. In mammals, the Notch pathway operates *in vitro* at an early stage in oligodendrocyte lineage progression, which is upstream from, and may not be influential, in the production of myelin sheaths as assayed here. Confirming this suggestion in zebrafish Notch appears only to be active during the earliest stages of oligodendrocyte specification in the spinal cord germinal zone (Park and Appel, 2003).

It would be useful to examine other signaling mechanisms identified as important in CNS myelination (*e.g.* PSA-NCAM or n-cadherin), to see if they regulate myelination in the regenerating fish visual system. The target deprivation technique I have used here works in the zebrafish and because the zebrafish is genetically pliable and bioinformatically accessible, a dissection of

molecular mechanisms controlling myelination would be easier in this organism. This could firstly take the form of a differential molecular screen using subtractive hybridisation or oligonucleotide microarrays, applied to the target$^+$/target$^-$ approach I have developed. This could identify genes that are up- or down-regulated in the retinal ganglion cells (and oligodendrocytes) when synapses are formed. It would exclude regeneration-associated genes, but include a very wide spectrum of genes activated in nerve cells as their axons switch from growth to synaptic transmission. Another less precise way to look for signaling mechanisms controlling myelination might be genetic screening for induced mutations affecting myelination. At least one such zebrafish screen is in progress (W. Talbot, personal communication) but it is not easy to see how mutagenesis screening could address the problems considered here.

6.3.3 Axonal activity

A direct mechanism by which the control of myelination could be mediated is through the changes in axonal impulse activity which occur once an axon is synaptically connected. This was first suggested by the description of a correlation between the developmental opening of the eyes and myelination of the optic nerve in mammals (Gyllensten and Malmfors, 1963). Surgically-induced early opening of the eyes accelerates the onset of myelination (Tauber et al., 1980).

By use of the sodium channel blocking molecule tetrodotoxin (TTX), Barres & Raff (1993) demonstrated that the survival of oligodendrocyte precursor cells (OPCs) in the rat optic nerve is dependent upon axonal conduction, although this is probably mediated indirectly via the induction of astrocyte release of PDGF (Fruttiger et al., 2000). Stevens et al (2002) showed that axonal impulse activity affects development of the oligodendrocyte lineage. They demonstrated that activity in dorsal root ganglion (DRG) cell axons exerts promyelinating effects upon OPCs *in vitro* via adenosine receptors. Rather than mediating survival, adenosine release by DRG axons encouraged the OPCs to withdraw from division and differentiate, and this enhanced myelin formation *in vitro*. Thus axonal activity can affect oligodendrocyte development, but there are conflicting views in the literature over whether axonal activity has any direct role in stimulating the production of myelin by differentiated oligodendrocytes.

The use of TTX to block axonal activity has been reported to inhibit myelination both *in vitro* and *in vivo* (Demerens et al., 1996; Charles et al., 2000). However, other reports have shown that TTX does not affect oligodendrocyte-axon adhesion or myelin formation (Colello et al., 1995; Shrager and Novakovic, 1995; Meyer-Franke et al., 1999). The reason for this disparity is unclear. However, axonal impulse activity strengthens synapses and could therefore indirectly influence myelin formation by modulating the synapse-dependent axonal signaling pathway that I have identified here.

6.3.4 Are refined synaptic connections required?

Retinotopic map refinement during regeneration is a two stage process. Firstly axons grow to approximately the correct location in the tectum and branch widely forming a coarse map in an activity-independent process in which axons are guided by chemotactic cues (Meyer, 1980, 1983). Subsequently, the synaptic arbors are refined by a Hebbian-type activity-dependent processes mediated by NMDA receptor activation (Schmidt, 1990). Where in this process does the synaptogenesis-timed mechanism controlling myelination come into effect? Are the initial transient synapses which form during refinement sufficient or is the formation of a highly refined accurate map required?

In chapter 5, I described an attempt to test whether refined connections are necessary. NMDA-R antagonists block refinement of the tectal map (Cline and Constantine-Paton, 1989; Schmidt, 1990) as well as the formation of ocular dominance patches (Cline et al., 1987). I hoped to test whether NMDAR blockade would also block myelination. Unfortunately, the drug delivery technique that I used was not sufficient to block the formation of ocular dominance patches. A better technique of drug delivery should be found to test this possibility. However, there are some indications in the literature that bear on this question.

In two separate papers by Marotte (Wye-Dvorak et al., 1979; Marotte, 1980) there are hints that myelination is dependent upon the formation of refined connections. The first study examined how the season affects the compression of a retinotopic map onto a surgically halved tectum in goldfish (Wye-Dvorak et al., 1979). It was found that map compression occurs in spring/summer but not in autumn/winter. Examination of the fibre bundles in the SO of the remaining

half-tectum showed that, when compression had occurred in the spring/summer, all axons in the bundles were myelinated. However, when compression failed in the autumn/winter large numbers of unmyelinated axons persisted in the tectal bundles. Half-tectal map compression occurs via the same Hebbian-type mechanism as developmental or regenerative tectal map refinement and the formation of ocular dominance patches. Although the reduction of myelination in this case could be directly due to seasonal hormonal related effects, the correlation found by Wye-Dvorak et al., (1979) is a tantalising suggestion that myelination will only proceed once refined connections are made with tectal neurones.

In the other study, Marotte examined developmental myelination in the goldfish at two different stages, 19 mm and 70 mm (Marotte, 1980). She found that the optic nerve was only 70% myelinated at the younger stage but at the later stage it was completely myelinated. She then examined synapse formation in the tectum and found that the total number of synapses in a complete rostro-caudal section of the tectum increased from 15,000 at 19mm to 50,000 - 80,000 at 70mm. However, despite this overall increase in number the density of the synapses decreased over the same timescale from 1.8 synapses/μm^3 in a 19mm length fish to 1.1 synapses/μm^3 in a 70mm fish (Marotte, 1980). Although Marotte does not make this explicit connection, the decrease in synaptic density might coincide with the pruning of axon branches during the refinement of accurate retinotopy in the tectum. Myelination of the optic nerve may follow the maturation of the synapses as they form an accurate retinotopic map.

The two studies described above suggest that myelination is dependent upon a refined synaptic connection with the tectum. However, a study by Hayes and Meyer (1989) indicates that synapse formation *per se*, as opposed to refinement, is sufficient to trigger myelination. Hayes and Meyer studied the role of axonal activity in retinotopic map formation during regeneration in the goldfish. They used chronic intra-ocular TTX administration to block impulse activity in the retinal ganglion cells. They then studied the numbers of synapses formed in the SFGS of the tectum and the numbers of axons in the optic nerve. TTX treatment did not significantly affect the elimination of exuberant axonal branches nor the formation and morphology of synapses in the tectum. The optic nerves of TTX-treated fish also had a normal level of myelination (Hayes and

Meyer, 1989). From other studies it is known that TTX prevents map refinement during regeneration (Olson and Meyer, 1991) so in this case myelination must have progressed in the absence of map refinement. This shows that the process of contacting the target neurone and constructing a synapse can occur in the absence of impluse activity and this is enough to trigger myelination.

Further experiments need to be carried out to more precisely dissect at which stage of synaptogenesis myelination is triggered. These could include a quantification of synapse formation in the tectum, and this could also preferably be combined with the determination of the stage of refinement of the retino-tectal map. If some method of imaging single axons from their origin to where they form synaptic connections could be devised this method would allow direct examination of synaptogenesis, refinement and myelin formation.

6.4 A comparison of myelination in the central and peripheral nervous systems.

Myelination of the peripheral nervous system (PNS) proceeds differently to myelination in the CNS. In the PNS, axons do not need to be connected to their targets for the Schwann cells to myelinate them. This was shown by the observations of Speidel (1964). When examining the growth of axons in the developing tadpole tail he recorded Schwann cells constructing internodes on the proximal stretch of an axon that was still growing distally. During regeneration in the PNS, myelination also follows the same pattern, with myelin sheaths forming in a wave following some distance behind the front of regenerating growth cones (Pellegrino and Spencer, 1985; also unpublished observations on the regenerating mouse facial nerve). Thus myelination is the default behaviour of Schwann cells in the PNS. Schwann cells automatically form myelin internodes once they have proliferated in sufficient numbers to envelop single axons rather than small clutches of axons (Webster et al., 1973).

The axons that Schwann cells myelinate do not always have an exclusively PNS origin. Frequently axons have both a CNS segment myelinated by oligodendrocytes and a peripheral segment myelinated by Schwann cells. The difference in the way that the formation of myelin proceeds between the PNS and

CNS (target-dependent in the CNS and default in the PNS) suggests that Schwann cells may be insensitive to axonal signals which precipitate oligodendrocyte myelination in the CNS following target innervation.

Although severed CNS axons will not normally regenerate, they can be stimulated to do so by grafting lengths of peripheral nerve into the PNS (Richardson et al., 1980). Consistent with the possibility that Schwann cells are unresponsive to target-dependent myelin signals, the Schwann cells in these peripheral nerve grafts myelinate the CNS axons (Bray et al., 1987; Vidal-Sanz et al., 1987) and this occurs even in blind ended grafts which have no opportunity to innervate any target (Campbell et al., 2003).

Another study suggests that the PNS environment may be important in determining the behaviour of the Schwann cells. When the optic nerve in goldfish is crushed, ectopic Schwann cells populate and myelinate the lesion site (Nona et al., 1992). If a second crush is made following regeneration of the first crush then two patches of ectopic Schwann cells can be produced at different locations in the CNS optic nerve (Nona et al., 2000). These patches of Schwann cells appear to respond to axons in a target-related manner. When myelination gets underway after the second lesion then the two patches of Schwann cells respond by proliferating simultaneously. This proliferation is synchronised between the two patches, suggesting that axonal signals are responsible (Nona et al., 2000). The axonal signals most probably correspond to the target-dependent signals I have identified. Thus, Schwann cells found ectopically within the boundaries of CNS tissue may respond differently to those in peripheral nerve grafts where the surrounding tissue is of peripheral origin.

The only recorded case where the myelination of axons in the PNS is affected by innervation of the axonal target is the sympathetic innervation of the rat salivary gland. If the relative gland territory an individual axon must innervate is experimentally enlarged then more axons are myelinated (Voyvodic, 1989). The reason for this probably stems from increased trophic support. The larger gland territory must enhance trophic support for axons and Schwann cells enabling them to proliferate in large enough numbers to bring the axon to Schwann cell ratio down to 1:1 allowing the Schwann cells to myelinate more axons.

I have characterised a profound difference between the CNS and PNS in the way myelin is produced. However, the reasons for this difference are unclear. Holding back myelination until the axons are ready seems like logical behaviour because of the large numbers of axons that are eliminated during neural development. Although I have demonstrated that this rule applies to the behaviour of oligodendrocytes, the evidence is that Schwann cells are not as discerning over choosing whether or not to myelinate an axon. Why does this difference exist? It may be that it is simply a result of the different ways Schwann cells and oligodendrocytes develop in relation to the axons they will myelinate. Schwann cells might not need to sense whether an axon is connected up because, by the time they have proliferated in sufficient numbers to begin myelination the elimination of excess axons may have already occurred. Oligodendrocytes do not need to proliferate in such large numbers because they can myelinate multiple axons. They may be present in readiness where the elimination of excess axons is still incomplete. To prevent oligodendrocytes from wasteful ensheathment, a target-related myelinating programme may have evolved in the CNS.

6.5 Trophic support and silent axonal death.

In chapter 4, I described experiments where complete tectal ablation abolished myelination of the regenerating optic nerve. After 30 days without tectal tissue to innervate there was no myelination, and after 50 days there was only very limited myelination of the remaining healthy axons. The degeneration seen in the absence of all tectal tissue is interesting because it does not occur when one tectal lobe is still intact. Further investigation of this might be useful to increase our general understanding of regeneration. It is possible that there is a very long range trophic signal from the tectum which is required for the optic axons to survive. However, it seems that axons only start to require this putative signal in the period of regeneration between 30 and 50 days. Further investigation of this process might yield clues as to why fish can regenerate with ease where mammals cannot.

Another interesting aspect is that the degenerating axons fail to attract macrophages/microglia. This contrasts sharply with Wallerian degeneration

seen following axotomy, which stimulates massive macrophage proliferation. This slow degeneration is reminiscent of the reports of the C57BL/WLD^s mouse (Lunn et al., 1989). This mouse has a mutation resulting in a chimeric Ube4b/Nmnat gene that prevents Wallerian degeneration following axotomy by acting on ubiquitination or pyridine metabolism (Mack et al., 2001) although the exact mechanism by which this delays Wallerian degeneration remains unknown.

My observations that the degeneration of completely targetless axons in the fish does not trigger an inflammatory response might be related to the lack of myelination of the degenerating axons and thus this might be highly relevant to the disease processes of multiple sclerosis (MS) where myelin in the CNS is stripped from axons by immune cells. The phenomenon of 'silent' axonal death that I have described may warrant a more extensive investigation.

6.6 Future directions.

I have shown that CNS myelination will only proceed once axons are synaptically connected with target neurones. However, many questions remain unresolved.

Firstly, identification of the axonal signalling mechanism(s) which underlies the synaptogenesis-timed control of myelination I have identified is the most obvious next step. As I have mentioned before, molecular screening methods should be employed in this effort and because I have shown my manipulations to be successful in zebrafish, trawling for molecules involved may be easier. However, there remains the possibility that the signalling mechanism is not mediated by molecular interactions but directly by axonal activity. The literature is not clear on whether axonal activity is necessary for myelination, and there are several indications that it is important. Therefore, molecular screens should be conducted concurrently with investigation of possible neurophysiological mechanisms that might trigger myelination.

Secondly, what aspect of synaptic connection is necessary? Myelination may simply require the formation of synapses, or a refined topographic mapping of these synaptic connections may be required to trigger myelination. I

attempted to test whether refined connections are required for myelination to proceed. For technical reasons this experiment was not successful, overcoming these technical issues would permit resolution of this question. This may also offer intriguing suggestions about the role of synaptogenesis in timing axon maturation, a question which is surprisingly neglected in the literature.

Lastly, the precise role that the supply of oligodendrocytes has in the timing of myelination during development is still not clear. It appears that the supply of oligodendrocytes may be the major rate-limiting step in myelination of the fish visual system. This differs from regeneration, where oligodendrocyte supply is not an issue and axonal demand is thus more easily revealed as a factor influencing myelination. This means studying myelin renewal during regeneration in the fish may be perfectly suited to identifying target-dependant axonal molecular mechanisms regulating myelination. However, this would still leave our understanding of the control of developmental myelination incomplete. It would be useful, for example, to be able to visualise the proliferation, migration and differentiation of cells in the oligodendrocyte lineage *in vivo*. The transparent zebrafish embryo may be an ideal place to do these experiments. Transgenic zebrafish which express fluorescent genes under the control of oligodendrocyte stage specific markers would allow the direct visualisation of differentiating oligodendrocytes as they interact with the axons.

Part 2

The phenotypic characterisation of a novel zebrafish mutant:

akineto^{u45}

Preface

Here I describe the phenotypic characterisation of a novel zebrafish mutant *akineto*^{u45} (*akn*^{u45}) which was identified in a mutagenesis screen at UCL. The principal phenotype of *akn*^{u45} mutant embryos is that they do not move their skeletal muscles. Evidence I present here demonstrates that this immobility is caused by a lack of thick filaments in the myofibrils of the skeletal muscle, an interesting molecular cell-structural defect. However, the mutant also exemplifies one of the disadvantages of the mutagenesis/forward genetics approach frequently used in the zebrafish system. This is that the mutated gene has proved to be very elusive to map and is not known at present. However, once it is identified, this mutant may be a valuable tool for the investigation of myofibrillogenesis, the process of the assembly of the contractile apparatus of muscle.

Chapter 7: Introduction.

7.1 Isolation of *akineto* in an ENU mutagenesis screen.

The mutant *akineto* (*akn*^{u45}) was identified through a forward genetic screen in zebrafish, following well established methodology (Mullins et al., 1994; Driever et al., 1996; Haffter et al., 1996). Mutagenesis is induced in spermatogonia by immersion of adult male fish in a chemical mutagen, ethylnitrosourea (ENU). They are returned to their tanks to recover for three weeks then paired with non-treated females. The three week time-period allows existing sperm directly affected by the toxicity of the mutagen to be eliminated and permits the maturation of the spermatogonia with mutated genes to increase the likelihood of mutations in F1. The F1 of this pairing are raised and crossed to found an F2 family. Developmental mutations are then screened for by random in-crosses of the F2 families and examination of the F3 embryos produced (Figure 7.1).

Zebrafish lend themselves well to mutagenesis screening because of the large numbers of embryos produced by any individual pairing and the short time that it takes to grow the fish to breeding maturity (3-5 months). Additionally, screening the F3 embryos through all stages of development is possible because of external fertilisation and the transparency of the egg cases and the embryos themselves.

A key criterion in any mutagenesis screen is the method by which one screens for defects. Screening F3 embryos whilst retaining the heterozygote parents is useful because it allows for the identification of mutations in genes important for development but that prevent the development of viable adult fish. The majority of mutants identified using ENU mutagenesis in zebrafish do not survive to adulthood. When homozygote adults are not viable, as is usually the case, mutant lines can be maintained by a cycle of out-crossing or in-crossing of hetereozygote carriers with subsequent screening to identify carriers of the mutation.

The UCL screen used *in situ* hybridisation with a cocktail of probes to examine early embryonic patterning, as well as antibody staining for acetylated β-tubulin to reveal defects in the early axonal scaffold of the CNS (Wilson et al.,

Figure 7.1 Scheme showing the protocol followed for mutagenesis in the screen at UCL. Male zebrafish were treated with ENU resulting in fish which had mutations in their haploid germ-line (**red sperm**). These mutagenised males are paired with non-treated females. Some members of the resultant **F1** generation will therefore be heterozygote for recessive mutations (**red embryos**; a minority will be dominant mutations and will result in lethal phenotypes as indicated by the crossed out malformed red embryo). The **F1** are grown up to breeding age and are intercrossed to found individual **F2** families. The individual families are in-crossed and embryos in the **F3** are examined for phenotypes. If the **F2** founder fish do not carry any recessive mutations then the resulting **F3** will not have any observable phenotype (**'all normal'**). However, some of the **F1** will have been heterozygote for mutated genes (**red fish**) which results in heterozygotes in the **F2** families founded by those fish (1/2 of the fish). In-crossing of one of these **F2** families will produce a phenotype in the **F3** embryos in 1/4 of the pairings.

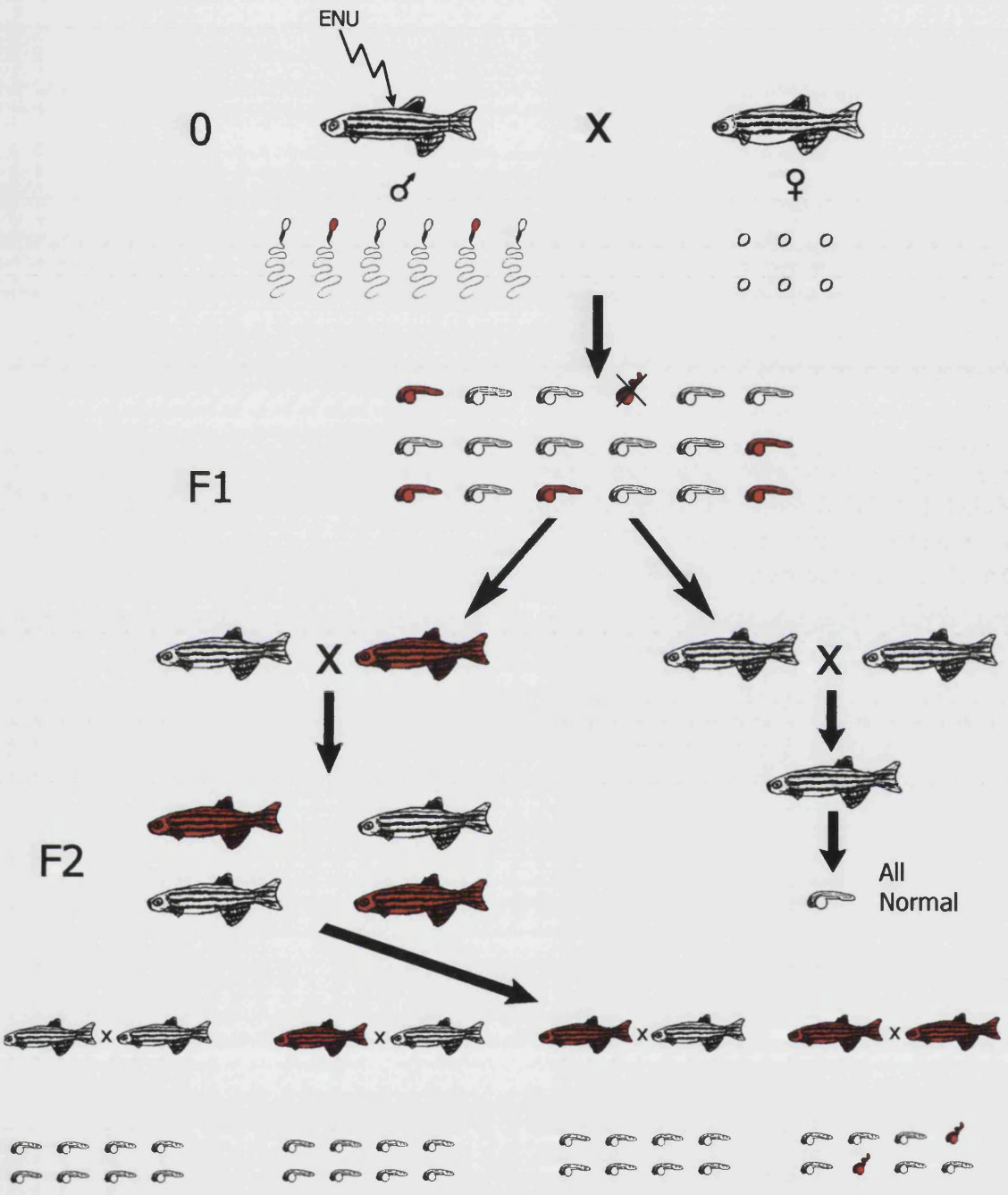

F3 - Screen for phenotypes

1990). However, embryos were also examined prior to fixation and the *akn*^{u45} mutation was identified separately by the lack of any movement.

7.2 The phenotype of *akineto*

Embryos homozygous for the mutant allele of *akineto* (*akn*^{u45}) do not move. Spontaneous movement normally commences in wild-type zebrafish at around 20 hpf, but at this stage *akn*^{u45} mutants remain immobile. They have no spontaneous or stimulus-evoked movements involving skeletal muscle at any stage of development. However, the heart beats normally resulting in blood circulation, and at 24 hpf there are no obvious morphological differences between mutants and wild-type (WT) siblings. After 3-4 days of development a minority of mutants develop pericardial oedemas and fail to inflate their swim bladders, presumably because they cannot gulp air to accomplish this. Because of their lack of ability to swim, find food and eat, *akn*^{u45} mutants die after around 6 days of development once the yolk is exhausted.

The lack of skeletal muscle movement in the mutant could be caused in a number of ways. The muscle fibres might lack proper innervation, the innervation might be defectively coupled to the contractile apparatus or there might be a defect in the contractile apparatus.

Pavlina Haramis isolated *akineto*^{u45} [†] in the screen at UCL in 1999 and carried out the initial phenotypic characterisation of the mutation, including a demonstration that muscle fibre excitation-contraction coupling is normal. I have subsequently shown (chapter 9: Results) that the nervous input to the muscles in *akn*^{u45} is normal, and that the defect that causes the lack of movement is incorrect myofibril assembly. Before describing these results, I will describe Haramis' unpublished findings so far.

7.3 Initial characterisation of *akn*^{u45} by Pavlina Haramis.

7.3.1 The morphology of muscle cells is abnormal in akn mutants.

The myotomes of zebrafish develop in a wave which follows somitogenesis in a rostral to caudal progression (Kimmel et al., 1995; Costa et al.,

[†] From the Greek: ακίνητο = immobile or quiescent

2002). In Teleosts most of the somite comprises dermamyotome, and only the ventromedial part differentiates as sclerotome (Morin-Kensicki and Eisen, 1997; Currie and Ingham, 1998). Prior to the segmentation of the somites, a group of cells named adaxial cells differentiates in the presomitic mesoderm adjacent to the notocord (Thisse et al., 1993; Weinberg et al., 1996; Currie and Ingham, 1998). The adaxial cells are crucial in the regulation of sonic hedgehog signalling to produce myotomal cells of different lineages (Wolff et al., 2003). In zebrafish, there are thought to be four separate different lineages of cells in the myotome. The first lineage to differentiate are the slow myoblasts, which differentiate under the influence of high sonic-hedgehog exposure in the region neighbouring the notocord and are fated to become superficial slow twitch myofibres. Cells amongst this population which receive the highest concentration of hedgehog signal differentiate as a separate lineage called 'muscle pioneer' cells identified by the expression of zebrafish *engrailed* homologues (Felsenfeld et al., 1991; Hatta et al., 1991; Ekker et al., 1992). They are fated to become the cells of the horizontal myoseptum of the myotome in later development. The muscle pioneers remain in the region adjacent to the notocord, but the slow myoblasts migrate out to the lateral surface of the myotome. At this time (around 18hpf), a lower level of hedgehog signal causes the remaining cells of the myotome to differentiate as fast myoblasts, fated to become fast twitch myofibres in the muscle. The migration of the slow myoblasts causes a small population of the fast myoblasts to become exposed to high levels of hedgehog signal which induces engrailed expression in these cells. This is the fourth lineage of cells in the myotome, the engrailed positive fast-myofibres (Wolff et al., 2003). In zebrafish, the superficial slow muscle cells are mononucleate and fast muscle cells fuse to become multinucleate. Roy et al (2001) demonstrated this by showing that slow muscle myosin heavy chains are localised in mononucleate cells and that transplanted labelled cells can be incorporated into fast muscle fibres by fusion events.

Because the developing muscle cells in one myotome are in very close proximity it is difficult to clearly examine the morphology of individual cells. To surmount this problem and examine the detailed morphology of individual muscle cells in *akn*^{u45} Haramis (unpublished) used mosaic analysis with rhodamine-labelled cells transplanted into the embryo at the 64-120 cell stage.

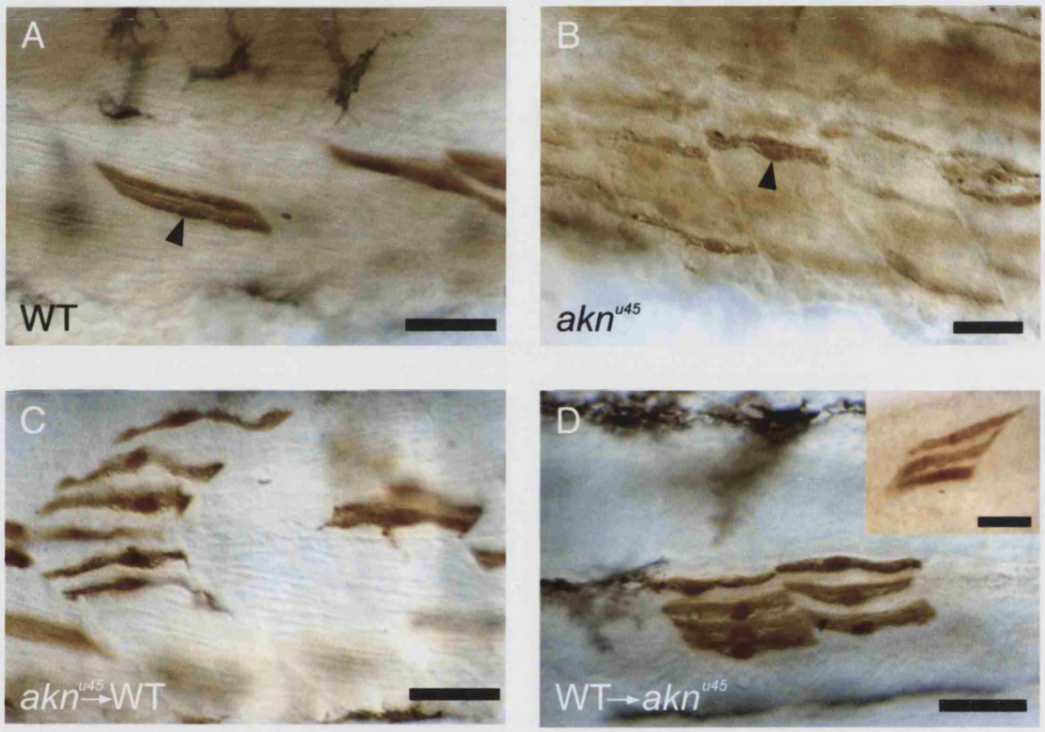

Figure 7.2. Mosaic studies and transplantation studies of muscle in wild-type (WT) siblings and akineto mutants (*akn*^{u45}). Data from Pavlina Haramis.
The morphology of individual muscle fibres was revealed by mosaic analysis. WT muscle fibres had a highly regular morphology (**A**; arrowhead). They were straight, had an even morphology along their length, tightly aligned with neighbouring fibres and they formed crisp attachments at the myotomal boundaries. In *akn*^{u45} embryos the muscle fibres (**B**; arrow-head) were very variable in their morphology; they had an irregular shape, their association with neighbouring fibres was not regular and the attachments formed at the myotomal boundaries were indistinct.
Transplantation studies suggest that the *akn*^{u45} gene acts cell autonomously. *akn*^{u45} cells transplanted into WT hosts (**C**; *akn*^{u45}- WT) adopted a mutant-like morphology. However, WT cells transplanted into *akn*^{u45} hosts (**D**; WT-*akn*^{u45}) resulted in muscle fibres that were more regular but did not have a totally wild-type morphology. Moreover, transplanted WT cells which were in neighbourly groups had a more regular appearance (**D**; inset). (Scale bars: 20μm).

This allowed the detailed examination of the morphology of isolated muscle cells at later stages.

The morphology of differentiating muscle cells is highly abnormal in *akn*^{u45} embryos. At the stage examined (24-30 hpf) (Figure 7.2 A, B) the muscle cells of WT siblings are aligned with each other and stretch across the whole myotome forming sharp attachments at each end. In contrast, the muscle cells of *akn*^{u45} embryos are irregular and wavy. Neighbouring cells have very different appearances and are not neatly aligned with each other. The cells have clearly made an attempt to elongate and attach to the myotome boundaries, but the attachments that are formed are not as crisp as those in WT siblings. Additionally the muscle cells are all mononucleate indicating either a failure of fusion or that the cells are all specified as slow muscle.

7.3.2 The akn^{u45} *mutation acts cell autonomously*

In addition to visualising the morphology of individual cells using rhodamine injections, Haramis also examined the morphology of prospective mesodermal cells transplanted before differentiation from mutants into wild-type embryos and from wild-type embryos into *akn*^{u45} mutant embryos.

Transplantation of mutant cells into wild-type hosts produced cells with an abnormal morphology (Figure 7.2 C & D), much as was seen in the mutant cell labelling experiments described above, indicating that *akn* acts intrinsically to the cell. From this, one would expect wild-type cells to have a normal morphology when transplanted into mutant hosts, but they also appear abnormal. This is probably a secondary effect moulded by the highly abnormal morphology of the surrounding mutant cells of the host. In agreement, neighbour-groups of transplanted wild-type cells show a more wild-type morphology (Figure 7.2 D inset).

7.3.3 Muscle cells are specified and commence differentiation normally in akn.

Somite formation is well understood in zebrafish. In particular, patterns of gene expression involved in the differentiation of the somites from paraxial mesoderm to myotome and sclerotome have been thoroughly characterised (reviewed in Stickney et al (2000)). A new somite is formed every 20 minutes between 10 and 12 hours and then every 30 minutes for the remaining somites

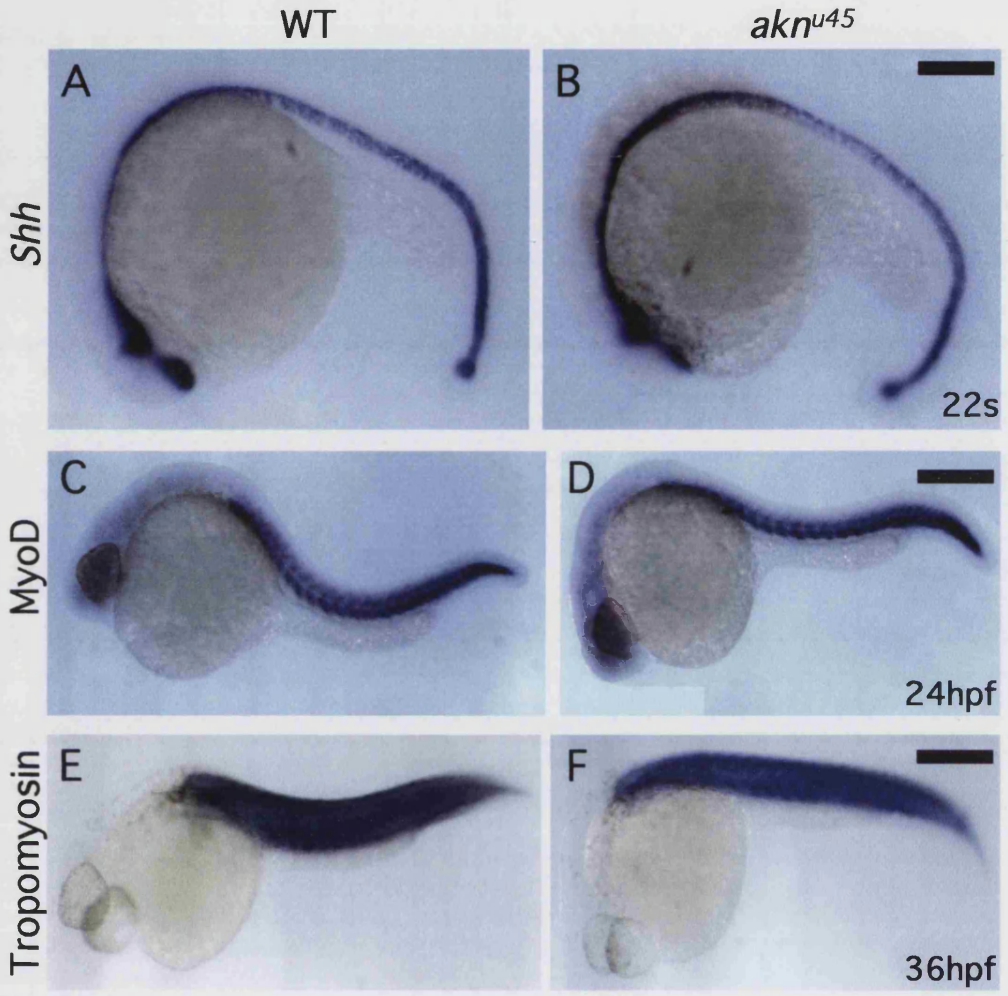

Figure 7.3
Examination of genes involved in muscle differentiation revealed no differences in *akn*^{u45} mutants. Data from Pavlina Haramis.
In situ Hybridisation of three genes involved in muscle differentiation. Sonic hedgehog (*Shh*) (**A** & **B**), MyoD (**C** & **D**) and Tropomyosin (**E** & **F**). At 22 somite stage (22s) comparision of the of Shh expression between WT and mutants showed no differences. MyoD expression is also normal in *akn*^{u45} at 24hpf (**C** & **D**). Tropomyosin expression at 36hpf (**E** & **F**) was slightly reduced in *akn*^{u45} mutants in comparison to WT siblings. However, levels of expression were high enough to indicate that muscle cells differentiate normally in *akn*^{u45} mutants. (Scale bars: **A** & **B** = 100 µm, **C**-**F** = 200 µm)

(Kimmel et al., 1995). The presomitic mesoderm is pre-patterned by clock-like oscillations of gene expression (Holley et al., 2000; Jiang et al., 2000; Lewis, 2003). The formation of furrows between somites and the epithelialisation of the individual somites is regulated by ephrin/eph signalling (Barrios et al., 2003). Patterning into sclerotome and myotome and into fast and slow muscle within the myotome commences before the onset of somitogenesis under the influence of hedgehog signals from the notcord.

To determine whether the abnormalities in muscle morphology seen in *akn*^{u45} mutants are caused by incorrect muscle cell specification or differentiation Haramis (unpublished) screened with *in situ* probes for abnormal patterns of *Shh, fgf8, paraxis* and *MyoD*, at the 3 somite stage (12hpf). There were no differences from wild-type embryos, showing that somitogenesis proceeds normally (not shown). *MyoD* also marks differentiating myoblasts at 24 hrs (Weinberg et al., 1996), and appeared normally in *akn*^{u45} mutants at this stage (Figure 7.3). These nascent myoblasts also showed normal expression of *tropomyosin* (Figure 7.3), a component of the sarcomere (Ohara et al., 1989; Xu et al., 2000).

7.3.4 Excitation-contraction coupling is normal in akn mutants

The coupling between the plasma membrane and the contractile apparatus is elegantly arranged to facilitate synchronous contraction across the whole muscle fibre. Invaginations of the external membrane called T-tubules associate with the sarcoplasmic reticulum to form triad complexes at each Z-disc of the sarcomeres (Peachey, 1965). The T-tubule transmits the action potential into the interior of the muscle fibre, triggering calcium release from the sarcoplasmic reticulum to activate the contractile machinery.

The excitation-contraction coupling between the T-tubule matrix and the cisternae of the sarcoplasmic reticulum is composed of voltage sensitive dihydropyridine (DHP) receptors on the T-tubule membranes, linked with ryanodine receptor-type calcium channels on sarcoplasmic reticulum membrane at the triads (Rios and Pizarro, 1991). The action potential causes a conformational change in the DHP molecules which is mechanically transduced to the ryanodine receptor in the membrane of the sarcoplasmic reticulum (Figure

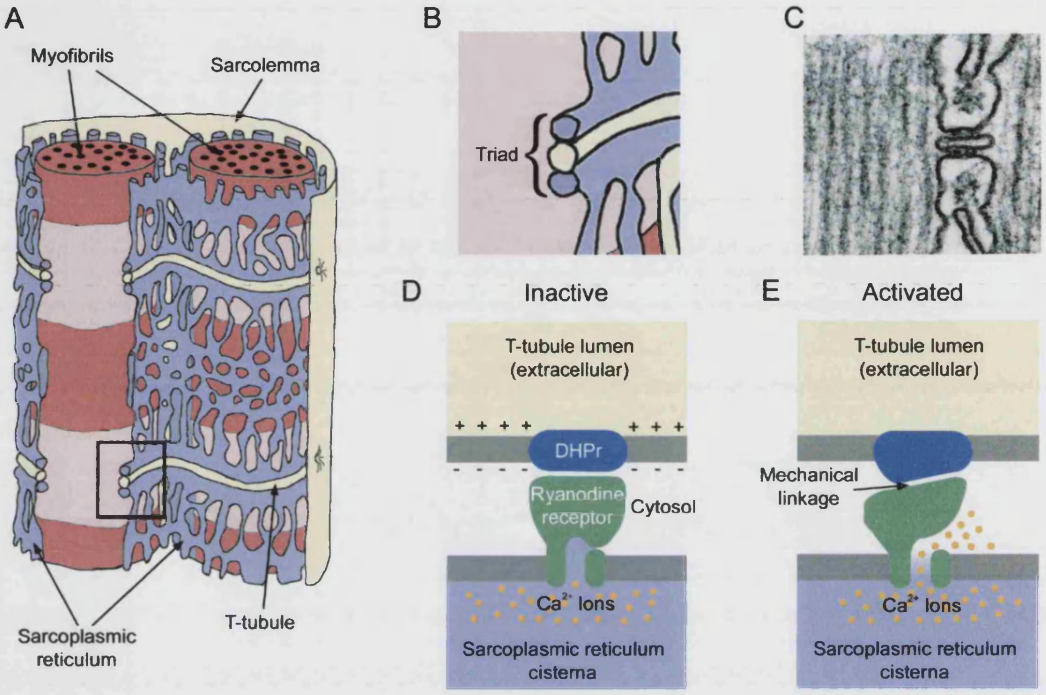

Figure 7.4
The T-tubule excitation-contraction coupling system
Panels **A** - **E** are diagrams showing the structure and function of the excitation-contraction coupling system of striated skeletal muscle adapted from Alberts et al. (2002).
A. Myofibrils consisting of alternating bands of thick (red) and thin (pink) filaments are surrounded by a mesh-like matrix of the sarcoplasmic reticulum (blue). Multiple myofibrils are bundled together in a muscle fibre by the external membrane or sarcolemma (yellow). At regular intervals along each myofibril (near Z-lines in zebrafish) transverse invaginations of the sarcolemma form hoops around individual myofibrils called transverse tubules or T-tubules. T-tubules are closely associated with large cisternae of the sarcoplasmic reticulum in structures called triads (box in **A**; **B** & **C**). The T-tubules and sarcoplasmic reticulum cisternae are closely linked by voltage sensitive di-hydropyridine receptors (**D;** DHPr (blue)) on the T-tubule membrane and ryanodine receptors (**D**; Green) which act as calcium channels in the sarcoplasmic reticulum membrane. In the resting state the T-tubule membrane is polarised and the sarcoplasmic reticulum has a high concentration of calcium ions within (**D**; Inactive) maintained by ion pumps. When an action potential spreads over the external sarcolemma it simultaneously spreads down the T-tubules. The DHPr conformationally changes in response to the voltage change, and this is mechanically linked to the Ryanodine receptor/channel causing it to open (**E**), flooding the fibre with calcium ions and initiating contraction of the myofibrils as myosin heads 'walk' along the thin filaments.

7.4), it thus opens, releasing stored calcium from the sarcoplasmic reticulum and activating the associated myofibrils (Martonosi, 2000).

To establish whether this system functions normally in *akn*^{u45} mutants, Pavlina Haramis collaborated with Rachel Ashworth to use a system developed by her in the Physiology Department at UCL (Zimprich et al., 1998). This uses the calcium-sensitive dye (BAPTA oregon green-dextran), which fluoresces in response to increases in calcium concentration. The dye is injected during early development into cells which are fated to become muscle, to record calcium fluorescence signals when they differentiate.

Recordings of spontaneous Ca^{2+} transients from *akn*^{u45} mutants showed no difference from wild-type siblings (Figure 7.5), except that the mutants showed slightly larger transients because movement in the wild-types took the dye-containing cells out of focus.

7.3.5 Primary sarcomeric components show defective expression in akn.

A defect in the nervous input to the muscles could not be ruled out as the primary defect in *akn*^{u45} at this stage. However, the cell autonomous morphological defects and the normal spontaneous calcium transients in *akn* mutants suggested that the defects are intrinsic to the contractile apparatus.

The sarcomeric apparatus within muscle fibres that is responsible for the actual contraction of the muscle is well characterised and understood. In skeletal muscle it consists of the linear arrangement of repeated units called sarcomeres, the length of which is between about 1 and 3 μm. The sarcomere (Figure 7.6) is primarily composed of three types of filament (reviewed by Squire, 1997; Pollard, 2000; Clark et al., 2002).

The first are thin filaments, which are lengths of F-actin together with with associated molecules. They are capped on either end by tropomodulin and capZ and aligned by the z-lines. The thin filaments extend from the Z-line into the A-band of the sarcomere where they associate with thick filaments in a hexagonal lattice arrangement (Squire, 1997). The length of the actin filaments in skeletal muscle is determined by a yardstick molecule called nebulin. Variations in length of the thin filaments are correlated with the size of nebulin (Kruger et al., 1991). Periodically arranged thin filament-associated proteins permit

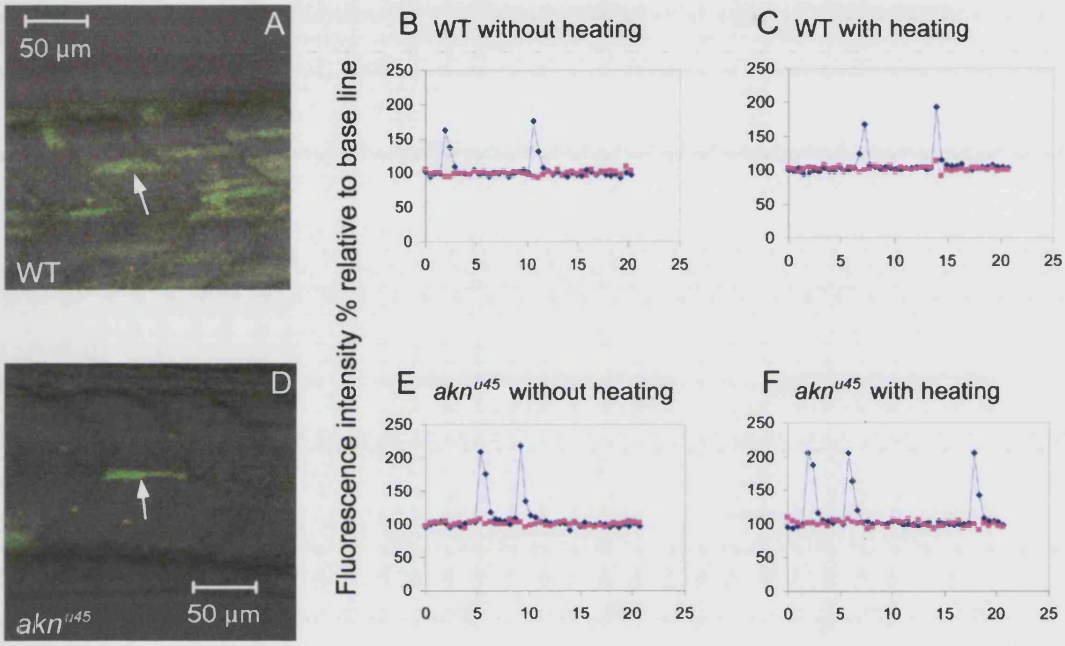

Figure 7.5
akn^{u45} mutants have a normal excitation-contraction system.
A - F. Recordings of calcium flux from WT siblings and *akn*^{u45} mutants. Data from Pavlina Haramis & Rachel Ashworth.
Micrographs show muscle fibres labelled with BAPTA buffered Oregon green dextran in WT (**A**) and *akn*^{u45} (**D**). Panels **B** & **C** and **E** & **F** show recordings of fluorescence of the Oregon green wavelength (blue trace) and Rhodamine wavelength (red trace) which was co-injected as a negative control. Several peaks of fluorescence in the Oregon green are seen in both WT and *akn*^{u45} without (**B** & **C**) and with (**E** & **F**) heating which was provided as an external stimulus. Slight perturbations in the rhodamine trace at the time of Oregon green peaks and the slightly lower level of peak seen in the WT were due to movement of the embryo taking the muscle fibre in and out of focus.

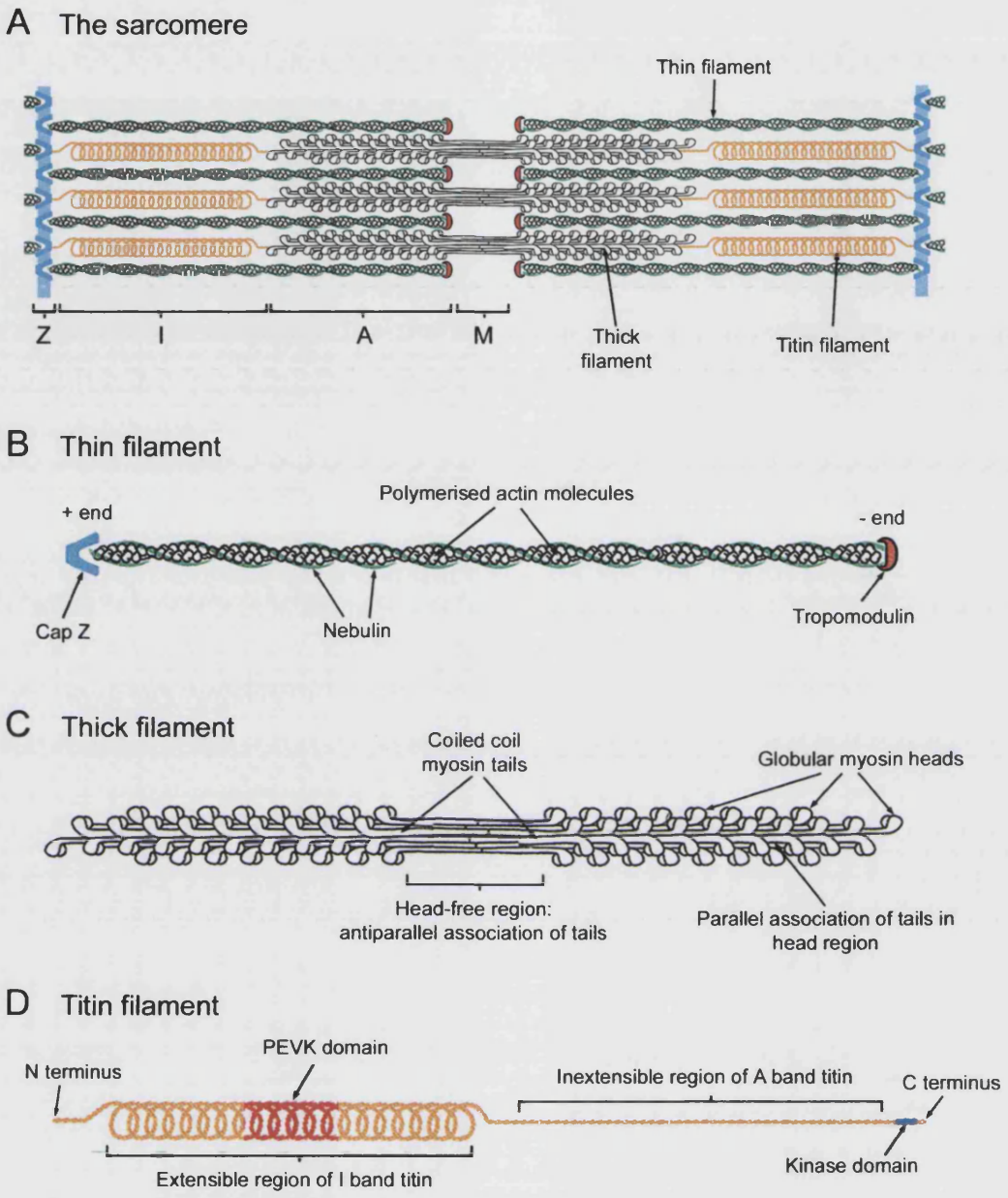

Figure 7.6 The molecular structure of the sarcomere and its constituent elements (adapted from (Alberts et al, 2002)). The sarcomere (**A**) comprises 4 bands: Z, I, A and M. There are three main filaments: thick, thin and titin filaments. Thin filaments (**B**) run from z-line to M-line and comprise a polymerised actin cable capped on the positive end at the z-line by cap-Z protein and at the negative end at the A-M band interface by tropomodulin. Thick filaments (**C**) are symmetrical structures which occupy the A and M bands. Thick filaments are constructed from parallel and anti-parallel associations of myosin molecules which are configured so that the myosin head portions point outward. The M-band is where the coiled coils of the myosin tails associate and it is free of myosin heads. Titin filaments (**D**) are composed from a single molecule that runs from Z band to M band; the molecule can be broadly divided into two domains. An extensible domain runs between the z-band and A-I interface, and its extensibility is thought to be responsible for the passive elasticity in muscle. A domain called the PEVK domain appears particularly important for this extensibility. The inextensible region of the titin filament runs from A-I junction to the M line and lies in very close association with the thick filaments.

interaction with the myosin heads of the thick filaments. These are the tropomyosin and troponin complexes which regulate the binding of myosin to actin in a calcium dependent manner (Potter and Gergely, 1974; Phillips et al., 1986). The array of actin filaments makes up the majority of the I-band, so named because of its isotropic effect on polarising light.

The second filament type is the thick filament. These are mainly made from myosin II molecules, which have a globular head region and a long tail region. The thick filaments are built by parallel association of the tail portions of myosin molecules arranged mirror symmetrically on either side of the M-line (Squire, 1997). Within the A-band, the exposed myosin heads that protrude from the thick filaments consume ATP to walk along the thin filaments (Vale and Milligan, 2000), a process regulated via the thin filament proteins troponin and tropomyosin by calcium release from the sacroplasmic reticulum (Gordon et al., 2000).

The third type of filament, titin, is a comparatively recent discovery (Maruyama et al., 1977; Wang et al., 1979; Wang et al., 1984; Maruyama, 1997; Tskhovrebova and Trinick, 2002). In contrast to thick and thin filaments, the titin filament is one molecule. It spans the sarcomere from M-line to Z-line and thus varies in length from between 1-3μm. Part of the reason for its late discovery is that it was dismissed as an artifact (e.g. caused by crosslinking) on protein electrophoresis gels because it hardly left the loading well (Wang et al., 1979) (*cf* (Etlinger et al., 1976; Porzio and Pearson, 1977)). The full sequence of the titin molecule has been determined (Labeit and Kolmerer, 1995) and from this and studies using antibodies for epitope sites along the length of the molecule (Fürst et al., 1988; Whiting et al., 1989) the regions that interact with different parts of the sarcomere have been determined. The N-terminus end attaches to the Z-line and the C-terminus end attaches to the M line. The part of the titin filament that passes through the A-band region is tightly associated with the thick filaments, and is thought to act like a ruler to determine the length of the thick filaments in a similar manner as nebulin is thought to with thin filaments (Trinick, 1994). As a result of the close association with the molecules of the thick filaments, A-band titin is inextensible (Labeit et al., 1997). In contrast, the I band region of titin does not associate with thin filaments and is elastic to cope with the varying length of the sarcomere.

The myofibrils are a highly ordered structure and therefore any abnormalities should be easily noticeable. Dr Haramis examined sarcomere structure using an antibody which recognises cardiac and skeletal myosin heavy chains (Hughes et al., 1993) and fluorescently tagged phalloidin. Phalloidin shows myofibrils within the muscle cells in wild-type embryos. The muscle cell morphological abnormalities in *akn*^{u45} mutants that were characterised by mosaic cell labelling are also visible (Figure 7.7). The striated pattern of actin in the I bands of the wild type embryo was disrupted: bright aggregates of actin were present sporadically throughout the muscle cells in mutant embryos, but none of the continuous long fibrils characteristic of the wild-type.

The anti-myosin antibody showed dense staining in wild-type embryos with striations clearly in register between neighbouring muscle fibres. In contrast, the mutant embryos were only lightly stained with this antibody, and there was no sign of striations within the muscle cells.

As to be described, I have taken up the further characterisation of *akineto*, and show here that the nervous input to the muscle is largely normal. Building on the light microscopy, I have also used EM to show that *akn*^{u45} muscle cells assemble thin filament sarcomeres complete with Z lines and associated triads, but with no thick filaments or A-band structures. The fact that this is possible suggests that thin filament/Z-line structures may be the template for sarcomere assembly. I am also engaged in efforts to identify the *akineto* gene.

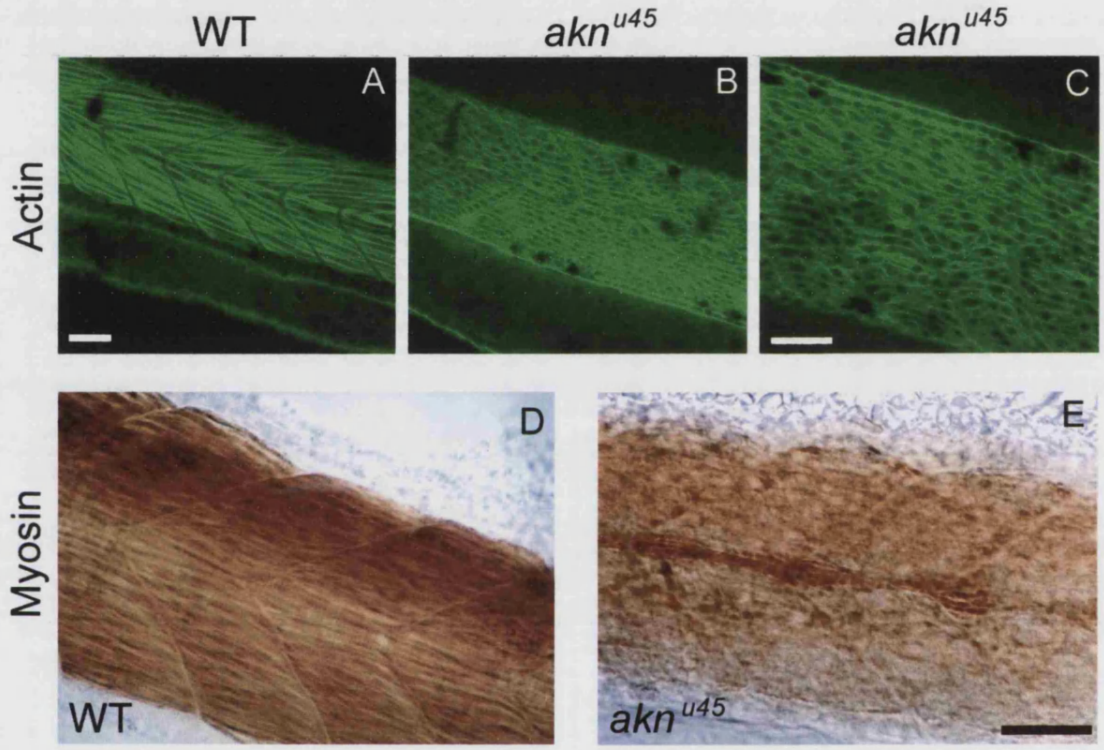

Figure 7.7 Fluorescent phalloidin revealed defects in the myofibrils of *akn*^{u45} mutant embryos. In WT myotomes (**A**; 48hpf), actin was focally located within the muscle cells in myofibrils running the length of the myotome, cell nuclei were not visible. In *akn*^{u45} mutant embryos (**B** & **C**; 48hpf) the actin was not focally organised, the staining filled the whole muscle cell which had a wavy appearance, the myofibre nuclei were visible as actin negative patches. Myosin expression was reduced in *akn*^{u45} mutants. Staining for myosin using an antibody raised against myosin heavy chain showed heavy staining in the myotomes of WT 48hpf embryos. Within the myotomes striations in register between neighbouring muscle fibres were present. In *akn*^{u45} mutant embryos (**E**) myosin was present but at much lower levels, no striations were visible but the muscle pioneer cells appeared to have a higher expression levels of myosin. (Scale bars: 20μm)

Chapter 8: Materials and Methods

As explained in chapter 2 some methods were common to both parts of this thesis and so here I describe methods specific to this part only. The general information concerning chemical sources and microscopes used (section 2.1) still applies in this section.

8.1 Animals/embryo care.

The *akn*^{u45} mutation was isolated in a screen for mutagenesis induced mutations in UCL. The mutagenesis was carried out in the Tübingen (Tü) wild-type line. Following isolation of the founder mutant carrier pairs, the pairs were outcrossed with AB wild-type background fish to establish the line. The line was then maintained by a cycle of outcrossing and screening for heterozygotes. Fish were maintained in the in-house zebrafish facility (installed by Marine biotech Inc Beverly MA, USA). Care of the fish was carried out in accordance with UK home office regulation and procedures were licensed. The zebrafish book (Westerfield, 2000) was used as reference for fish care methods. Embryos were generated by pairing of fish in breeding tanks, they were harvested shortly after the lights in the room came on (09:30). Embryos were maintained in system water with a trace of methylene chloride added to retard mould growth. Incubation at 28.5°C was standard, although embryos could be grown at higher or lower temperatures to speed-up or slow-down the rate of development embryos were staged according to (Kimmel et al., 1995). When required, 0.003% w/v Phenylthiocarbamide (PTU) was added to the medium from 16hpf to prevent pigmentation. Before fixation, embryos were anaesthetised using (MS-222(3-aminobenzoic acid ethyl ester: methansulfonate salt)) at a concentration greater than 0.2g/L.

8.2 Microscopy.

In addition to conventional microscopy, I also used the confocal microscope and polarised light microscopy. Confocal miscroscope images were acquired using Leica confocal microscopes and Leica TCS software. This

software was also used to construct z-series projections which were saved as TIF files for transfer to other computers.

Polarised light microscopy was carried out using a Zeiss photomicroscope 4 (Carl Zeiss Ltd, Welwyn Garden City, UK) and images were captured using an Olympus OM-2 camera on either Ektachrome 100 EPN or Ilford Pan-F 50 (Illford Essex, UK).

8.3 Antibodies/labelling.

In this section I used two protocols for antibody labelling and molecular marking, one used cryostat sections and the other used wholemount zebrafish embryos

8.3.1 Antibodies and molecular probes.

Primary antibodies:

1. *ZNP-1* this was obtained from the developmental studies hybridoma bank (DSHB, University of Iowa, Iowa city IA, USA) and was described in the zebrafish book (Westerfield, 2000) it labels primary motor neurones.
2. *anti-Actinin* (clone name: EA-53)(#A5044; Sigma Aldrich Co Ltd, Poole, UK)
3. *anti-Titin* (clone name: T11)(#T9030; Sigma Aldrich Co Ltd, Poole, UK)

Secondary antibodies:

This was Goat anti-mouse IgG conjugated either to alexafluor 488 or alexafluor 568 (Molecular Probes Europe BV, Leiden, Netherlands)

Molecular probes:

1. Phalloidin conjugated to alexafluor 568 (#A-12380; Molecular Probes Europe BV, Leiden, Netherlands). Stock solution concentration was 200 units/ml (6.6μM).
2. α-Bungarotoxin conjugated to alexafluor 488 (#B-13422; Molecular Probes Europe BV, Leiden, Netherlands). Stock solution was 1mg/ml.

8.3.2 Wholemount staining using ZNP1.

This was done using a protocol based on the standard antibody protocol in the zebrafish book (Westerfield, 2000) Embryos were fixed using 4% w/v paraformaldehyde in 0.1M PBS at 27 hours post fertilisation. They were fixed overnight at 4°C. All stages of the staining procedure were carried out in 1.5ml microcentrifuge tubes. Following several washes in PBS to remove the fixative the embryos were permeabilised to aid entry of the antibodies. Firstly the embryos were washed in distilled water for 5 minutes at room temperature , and then the water was replaced by pre-cooled -20°C acetone and incubation at -20°C. They were rinsed in distilled water for 5 minutes at RT and returned to PBS. To block non-specific antibody binding the embryos were then washed in PBS containing 2% v/v normal goat serum (NGS), 1% w/v bovine serum albumin (BSA) and 1% v/v dimethylsulfoxide (DMSO) for 1 hour. This was replaced with the same solution containing primary antibody (Znp1) at 1:100 concentration. The tubes were incubated overnight at 4°C with continuous gentle agitation. The primary antibody was washed out using PBS with 1% v/v DMSO, and 1% w/v BSA (PBS/DMSO/BSA) with repeated washes at room temperature over a 2 hour period using gentle agitation. The secondary antibody (anti-mouse alexa 563) was added at 1:100 concentration. To visualise the motor endplates flourescently-conjugated bungarotoxin was added at the same time at 1:1000 concentration. The tubes were incubated overnight at 4°C as for the primary antibody. After this the embryos were washed for 2 hours in PBS/DMSO/BSA for two hours and were then transferred to PBS/Glycerol containing AF-1 anti-fadant compound (Citifluor Ltd, Leicester, UK).

Mounting for confocal microscopy involved removing the yolk and placing the embryos in a drop of glycerol on their side on a 67x22mm cover slip (Merck Sharp & Dohme, Hoddesdon, UK) that had a 22x22mm coverslip glued to each end to make a cavity in the middle. This was placed on a plain microscope slide (Merck Sharp & Dohme, Hoddesdon, UK), the embryo was adjusted for orientation and the coverslip was secured using nail varnish (Rimmel, London, UK).

8.3.3 Staining of sections using anti-titin and anti-actinin antibodies.

Embryos were fixed in 4% w/v paraformaldehyde (Merck Sharp &

Dohme, Hoddesdon, UK) in PBS overnight at 4°C. Following washing in PBS they were transferred to PBS containing 20% w/v sucrose and then to a 1:1 mixture of PBS with 20%sucrose and OCT cryoembedding compound (Agar Scientific, Stansted UK). To cut longitudinal sections of the muscle the embryos needed to be correctly orientated for cryotomy. Embryos were placed in a small well made from aluminium foil so that their medial surface was parallel with the bottom of the well. This foil was placed on a liquid nitrogen-cooled metal block, the resulting slug was inverted and mounted on a cryostat stub with the embryos outward. 10μm sections were cut and lifted onto gelatin-subbed PTFE microwell slides (C.A. Hendley (Essex) Ltd, Loughton, UK).

The sections were re-hydrated using PBS with 0.1% v/v triton (PBTr) and non-specific binding was blocked using 5% v/v NGS in PBTr for 1 hour. Following rinsing, the primary antibody (anti-titin or anti-actinin) was added at 1:100 concentration and the slides were incubated at room temperature in a humid chamber overnight. Following this the slides were rinsed and washed 5 times for 10 minutes in PBTr. The secondary antibody (alexafluor 488) was then added at 1:100 concentration and the slides incubated in a humid chamber for 4 hours at room temperature. The secondary antibody was washed off in several rinses of PBTr and Phalloidin staining was carried out. This was done using 1:40 of Phalloidin stock solution (see above) in PBTr for 1 hour. The slides were rinsed and washed thoroughly before mounting under 50x22mm coverslips using Glycerol/PBS with AF-1 (Citifluor Ltd, Leicester, UK), then sealed with nail varnish (Rimmel, London, UK).

8.4 Electron microscopy

The electron microscopy procedure was essentially identical to that provided in section 2.6 The embryos were decapitated under terminal anaesthesia and were treated as described for zebrafish larvae in section 2.3. The only difference was that 5% w/v $CaCl_2$ was added to the fixative which seemed to improve myofibril definition. The zebrafish embryo tissue was also always *en bloc* stained with uranyl acetate as this reduced the dense staining of glycogen granules in the myofibres.

8.5 Complementation testing/mapping

The complementation testing was carried out in the laboratory of Uwe Strahle (IGBMC, CNRS/INSERM/ULP, Parc d'Innovation, BP 10142 67404 Illkirch Cedex, C.U. de Strasbourg FRANCE) 2 male and 2 female identified *akn*^{u45} carriers were shipped to Martine Behra, a member of his laboratory. These were tested for complementation by crossing with identified carriers of other mutations and examination of the generated embryos for mutants. If the embryos were all wild-type then the alleles had complementary function. If mutants were present then the alleles did not complement each other and the mutation must have been in the same gene.

Mapping crosses were generated by crossing of identified carriers with the mapping line (wik) carriers were identified in the resulting F1 and they were paired and given unique ID numbers so that embryos from particular pairs were known. DNA samples (tail clips) were taken from the F1 carriers and the P founder fish so that markers could be traced back through the generations and polymorphic markers could also be identified. Embryos from the F1 pairs were harvested regularly, they were grown to 72hpf and sorted into mutants and siblings. The embryos were fixed under anaesthesia using methanol pre-cooled to -20°C and were stored in the methanol at -20°C until further use. Genomic DNA was extracted by placing individual embryos in individual thin-walled PCR tubes and evaporating the methanol. 50μl of Lysis buffer was then added (10mM Tris-HCL pH 8.3, 50mM KCl, 0.3% v/v Tween-20, 0.3% v/v NP40) the tubes were placed in a PCR thermal-cycling machine (GeneAmp PCR system 9700; PE applied Biosystems, Foster city CA, USA) and the embryos were incubated at 90°C for 10 minutes. To the lysis buffer was added 5μl of proteinase K (10mg/ml) and this was incubated for 8 hours at 55°C. the tubes were heated up to 90°C for 10 minutes to denature the proteinase K and then cooled to 4°C. The DNA samples were shipped to the laboratories of Robert Geisler (Max-Planck-Institut für Entwicklungsbiologie, Abteilung III - Genetik, Spemannstrasse 35, D-72076 Tübingen, GERMANY) or William Talbot (Department of Developmental Biology, Stanford University School of Medicine, Beckman Center B315, 279 Campus Drive, Stanford, CA 94305-5329 USA) for mapping using either the SSLP or SNP protocols (see Figures 9.7; 9.8).

Chapter 9: Results.

9.1 *akn*^{u45} is not required for correct innervation of the trunk muscle.

From the unpublished work of Haramis and Ashworth (personal communication), I knew that the muscle excitation-contraction system functions normally in the muscle cells of *akn* mutants. However, the transient calcium increases shown in these experiments could have been randomly generated and myogenic in origin. The lack of movement might have been due to a lack of proper innervation to the muscle or poor development of the neuromuscular junction. To examine the innervation of the trunk muscle in *akn* mutants I used the monoclonal znp1 antibody which marks primary motor neurons in the developing zebrafish (Westerfield, 2000). Acetylcholine receptors cluster on the post-synaptic membrane of neuromuscular junctions during development, and these clusters were examined using fluorescently labelled α-bungarotoxin. (Behra et al., 2002).

Double labelling with znp1 antibody and fluorescent α-bungarotoxin showed that there are only subtle differences in trunk muscle innervation between the *akn* mutant and wild-type (Figure 9.1). Axons from the three primary motor neurones: medial, rostral and caudal (MiP, RoP, CaP) are visible exiting the spinal cord and supplying each segment of muscle. Acetylcholine receptors are focally clustered at the neuromuscular junctions distributed along the trajectories of the motor axons. In addition there is a more diffuse clustering in the synaptic furrow which is not associated with any axons but has been previously described (Behra et al., 2002). There is a subtle difference in the extent of branching in the distal CaP axon, which is slightly reduced in the *akn* mutant. This indicates that the *akn*^{u45} mutation only mildly affects the motor innervation: the motor neurons are present, their axonal trajectories are largely normal, and they cause acetylcholine receptor clustering on the postsynaptic muscle fibre membrane. Whatever the primary muscle cell-autonomous defect in *akn*^{u45} is, it has little effect on the early motor innervation in zebrafish somites.

Figure 9.1 *akn*^{u45} mutant embryos have normal muscle Innervation. Confocal microscope z-series projections of Fluorescently tagged bungarotoxin (Green; **A** & **B**) revealed the location of acetylcholine receptor clusters on muscle cell membranes endplates (**EP**) of 27hpf WT and *akn*^{u45} mutant embryos. Acetylcholine receptors were also found in the furrows between somites (SF). This has been previously described and is not artifactual although the role of the receptors at this location is not clear (Behra et al. 2002). The Znp1 monoclonal antibody revealed the trajectories of the primary spinal motor neurone axons projecting from the spinal cord (SC)(red; **C** & **D**; MiP= Medial, RoP=rostral, CaP=caudal).(*nb.* RoP axons project through the myoseptum (toward the observer here)) there were only subtle differences between *akn*^{u45} and WT in the branching at the end of the the CaP axon which was slightly reduced in mutants. Overlaying the channels (**E** & **F**) showed that acetylcholine receptors are clustered along the motor axon trunks in both WT and *akn*^{u45} embryos. These experiments show that the primary motor innervation of the musle of akn mutants was normal. Scale bar = 20μm

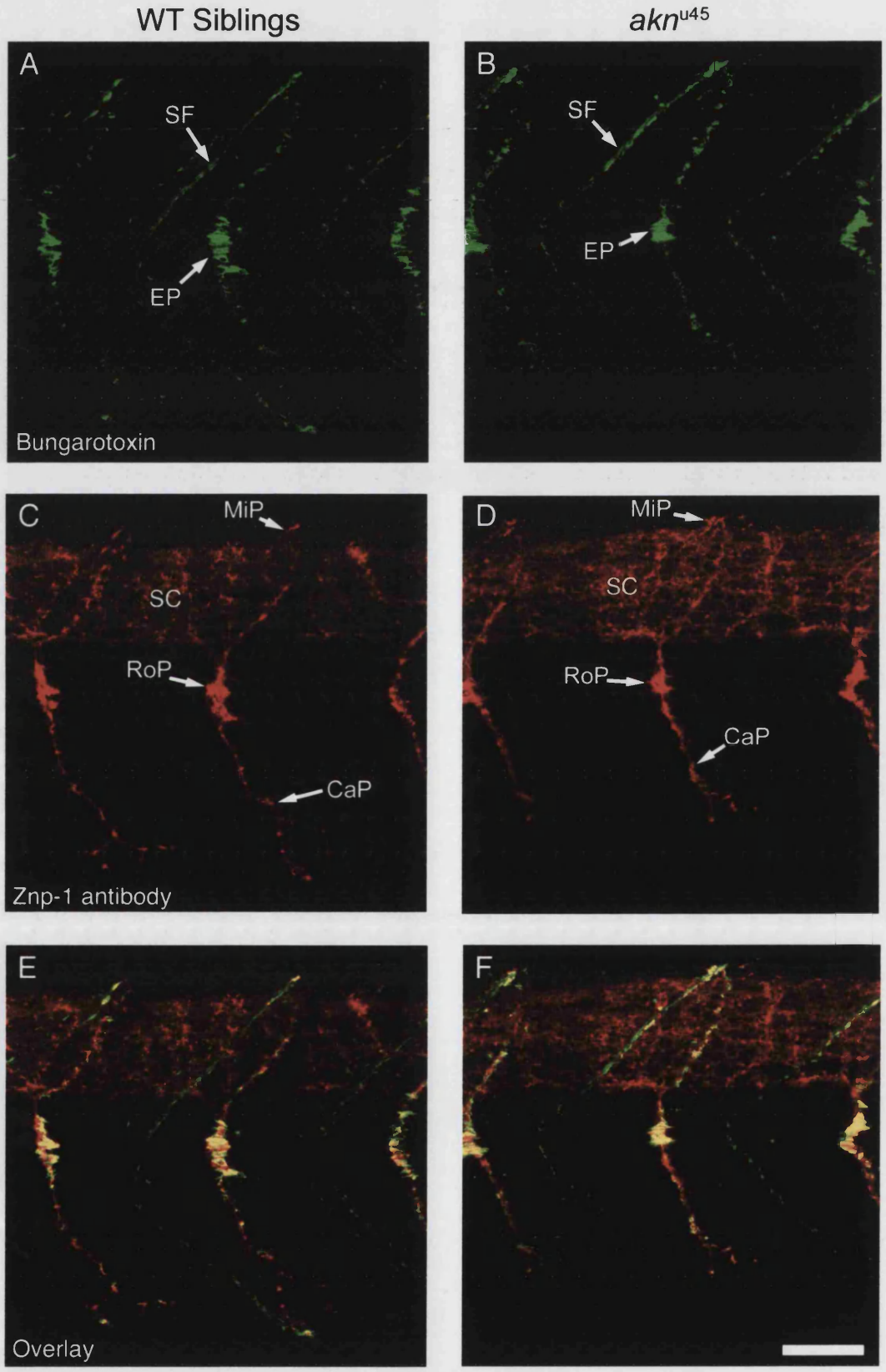
WT Siblings
akn^u45
A
SF
EP
Bungarotoxin
B
SF
EP
C
MiP
SC
RoP
CaP
Znp-1 antibody
D
MiP
SC
RoP
CaP
E
Overlay
F

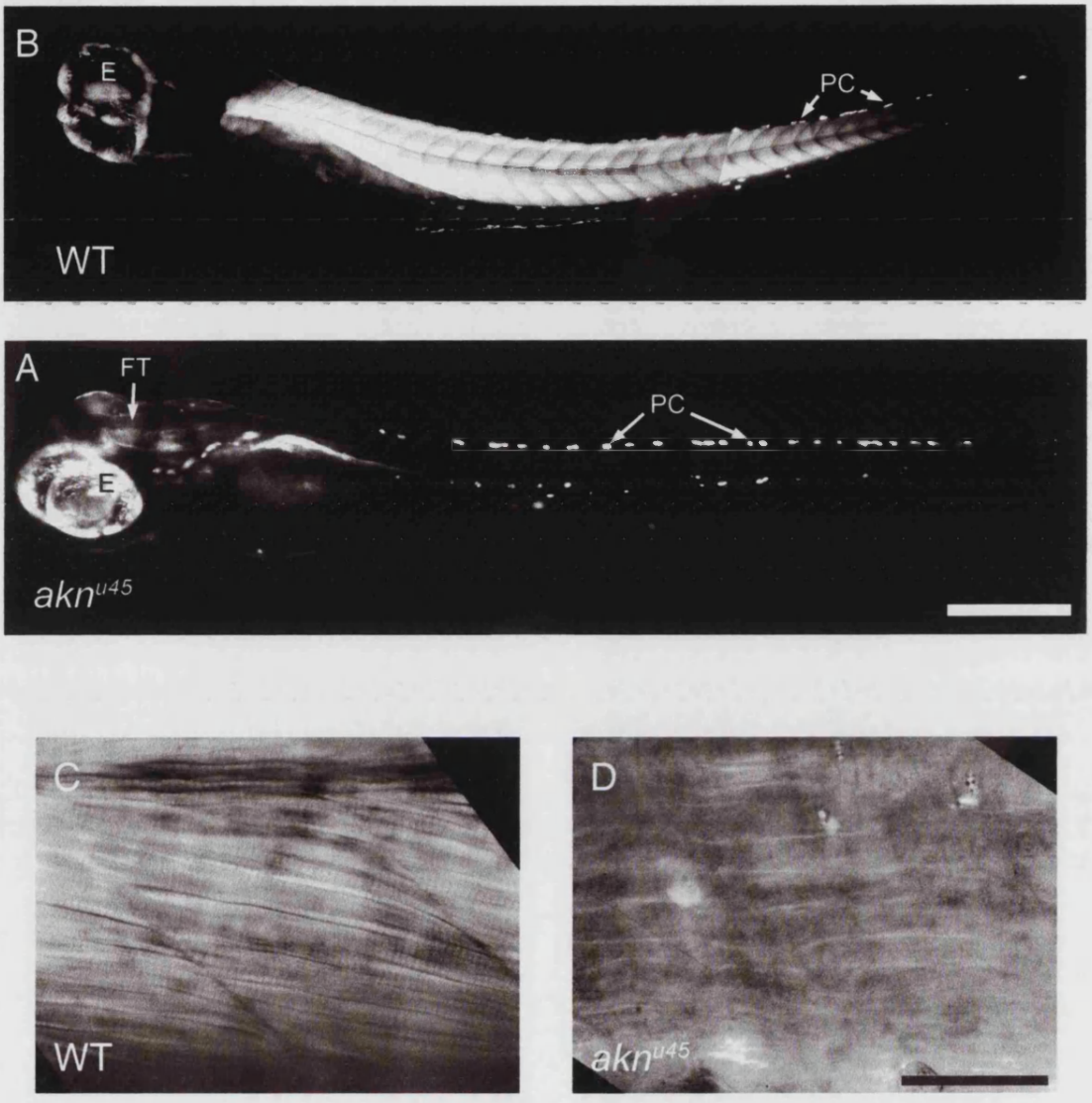

Figure 9.2
Polarised light microscopy showed that *akn*^{u45} mutants lack birefringent myofibrils.
A & B: In WT fish, the myotomes were highly birefringent (**A**), indicating the presence of anisotropic thick filaments in the sarcomeres. In contrast, the myotomes of *akn*^{u45} mutant fish had no birefringence (**B**), the only structures visible were the eyes (E), fibre tracts of the brain (FT) and pigment cells (PC).
C & D: Under high power, the birefringent striated myofibrils were visible in WTmuscle (C) The highly regular arrangement of the muscle cells was also clear. Although not birefringent, lengthy exposure at high power reveals the irregular wavy appearance of the muscle cells in *akn*^{u45} mutants. These cells totally lack striated myofibrils.
(Scale bars: A & B = 200μm; C & D = 20 μm)

9.2 Sarcomeres are incomplete in *akn*^{u45} mutants.

To gain an initial impression of the state of the sarcomere in *akn* mutants, I examined the muscle using polarised light. In the wild-type, myofibrils can be visualised when placed between crossed polarising filters because of the optical activity of the A-bands. In agreement with the observations using phalloidin and anti-myosin antibodies (Introduction), no sarcomeric structures were visible in *akn* mutant embryos suggesting incorrect myofibrillar assembly (Figure 9.2). To characterise this further I looked at the expression of additional components of the sarcomere using antibodies against α-actinin (a component of the Z-line) and fluorescently tagged phalloidin to reveal the orientation of actin filaments with respect to the actinin staining. Representative micrographs are shown in Figure 9.3. In wild-type embryos there is a highly regular pattern of staining with bright α-actinin bands regularly spaced along the myofibrils of the muscle cells. These bands are orientated perpendicular to the long axis of the cell at about 2μm intervals. The space between consecutive α-actinin bands is positively stained with phalloidin indicating that polymerised actin is present and in a few cases which are in suitable orientation, slender dark lines can be seen dividing blocks of phalloidin stain. This is consistent with the known structure of the sarcomere, with Z-lines flanked on either side by actin-positive I bands and actin-negative regions of the A and M bands showing as dark spaces in between.

The α-actinin/phalloidin staining pattern in *akn*^{u45} mutants was dramatically different. α-actinin bands are present, but they are far less numerous, shorter, less sharply defined, and poorly organised with respect to each other. The α-actinin antibody also diffusely stained other parts of the mutant muscle cells, a feature not present in the wild-type. Phalloidin staining also showed none of the regular pattern present in the wild-type. When the red and green channels are overlayed (Figure 9.3E), some wild-type features can be observed in the mutants. In some regions, α-actinin bands are arranged periodically and between these lines denser phalloidin staining is visible, suggesting that α-actinin and actin are able to associate properly. In the regions where α–actinin staining is diffuse, the phalloidin staining is also diffuse. Wherever there are bright, punctate spots of α-actinin staining, there is an increase in the density of the surrounding phalloidin staining (Figure 9.3D-F).

Figure 9.3 Confocal immunohistochemistry for sarcomere components confirmed the myofibrillar disorder in *akn*^{u45} mutants.

A-F: Double staining with anti-actinin antibody (Green) and phalloidin (red) revealed the highly ordered nature of the myofibrils in WT fish (**A-C**). Sharp actinin/phalloidin stained bands are flanked by phalloidin positive patches. Slender dark bands were sometimes visible within the phalloidin positive staining between the actinin bands (**C**; inset). *akn*^{u45} mutants had a more disorderly arrangement (**D-E**): actinin-positive bands were sometimes present aligned perpendicular to the long axis of the cell (arrowheads). These bands were sometimes found in rows and were often flanked on either side by dense patches of phalloidin (**E**; inset).

G-I: Double staining with titin (green) and phalloidin (red) revealed the orderly structure of the myofibrils in WT fish. The titin antibody usually only showed single bands but sometimes a doublet of staining was visible (**G**; inset). *Akn*^{u45} mutant embryos appeared not to express titin: no orderly bands of staining were visible above background (**J-L**). Scale bars: 10μm

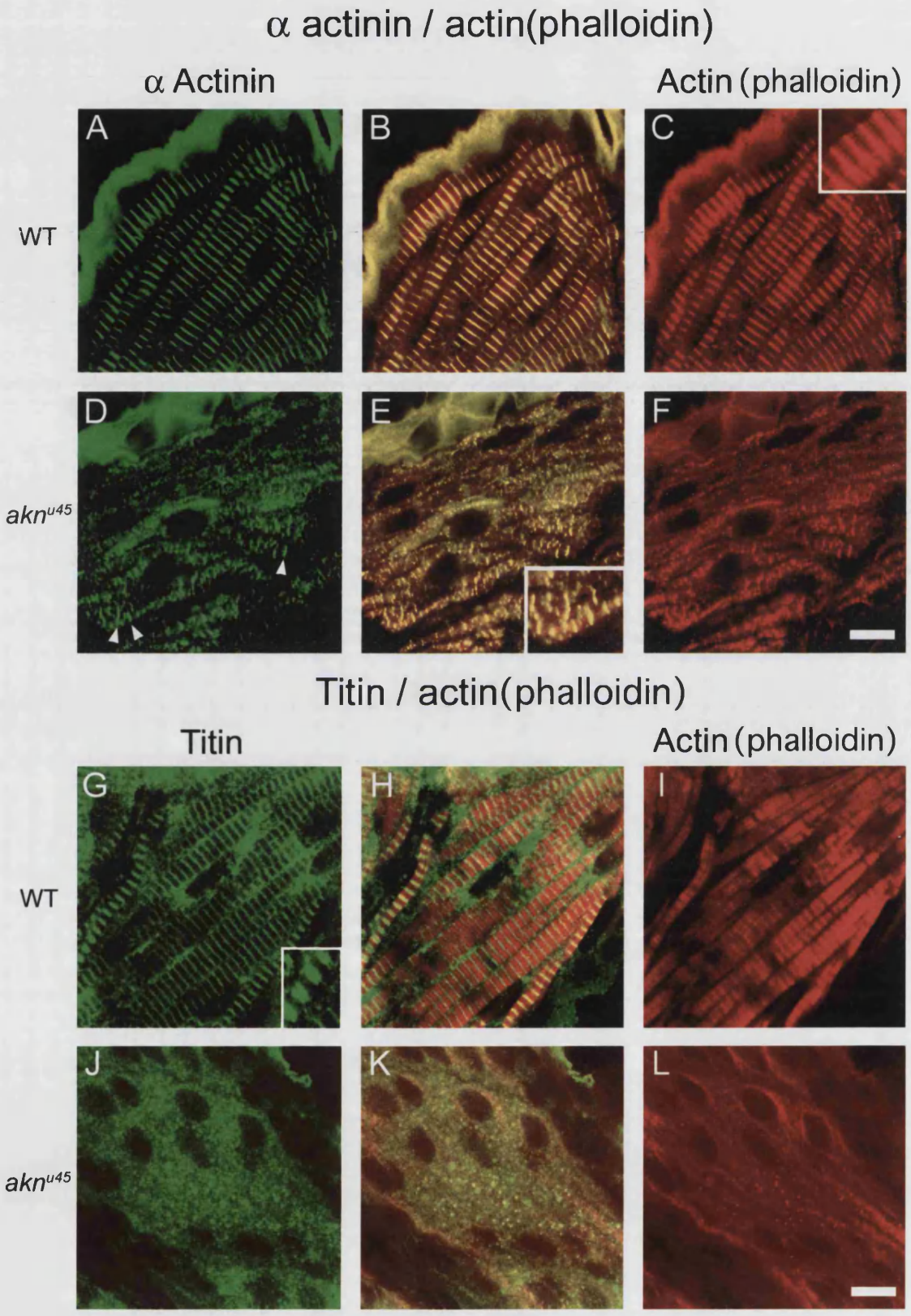
α actinin / actin(phalloidin)
α Actinin
Actin (phalloidin)
A
B
C
WT
D
E
F
akn^u45
Titin / actin(phalloidin)
Titin
Actin (phalloidin)
G
H
I
WT
J
K
L
akn^u45

I also used a monoclonal anti-titin antibody with an epitope on the titin molecule in the I band region, giving a doublet of staining either side of the Z band (Fürst et al., 1988; Costa et al., 2002). This antibody did not work as effectively as the α-actinin antibody, but stained the sarcomeres in a regular pattern in wild-type embryos. In some cases, the I band doublets were also discernible. However, in *akn*^{u45} mutants the antibody did not stain any structures recognisable above the background. This could indicate the absence of all or this part of the titin molecule (or incorrect folding so that the epitope is not exposed to the antibody). Titin may be present but because the antibody is weak and the sarcomere is disorganised, staining may have been obscured by the background.

These observations show clear abnormalities in the sarcomere structure in *akn*^{u45} mutants. The Z and I bands are present, but in fewer numbers and in a disordered arrangement. Titin filaments appear to be absent and Pavlina Haramis showed that myosin is present but depleted.

There are two main problems with examining the structure of the sarcomere by light microscopy. The first is resolution of its many components and their arrangement with respect to each other is poor, even with confocal microscopy. The second problem is antibody specificity. The molecules involved are so large that the antibodies available often only mark small regions that may be conformationally sensitive or hindered by associations with other molecules. This limits the conclusions that can be drawn about sarcomere defects in *akn*^{u45} by light microscopy. To overcome this, I embarked on a study of the muscle of *akn*^{u45} mutants using electron microscopy.

9.3 Electron microscopy confirms sarcomeric abnormalities.

Zebrafish begin spontaneous movement at around 22 hpf. This consists of slow waving of the tail, both spontaneously and in response to external stimuli. By 48 hpf, the movements develop into more patterned undulations of the trunk. An escape response occurs when the tail or head area is touched (Felsenfeld et al., 1990). I decided to fix the embryos at 24 hpf and 48 hpf to examine both the early and later stages of myofibrillogenesis (Materials and Methods).

9.3.1 Myofibrils at 24 hrs.

TEM examination of LS sections of myotomes in 24 hour WTzebrafish embryos revealed a very limited number of myofibrils (Figure 9.4). However, some of these myofibrils could be followed from the rostral myotomal boundary to the caudal boundary. There were also many examples of myofibrils that appeared to be in the process of assembling. These structures were quite often only 10 thick filaments wide (Figure 9.4 E) and consisted of only a few assembled sarcomeres. In the thin sections used for TEM it was uncertain whether these apparently partially assembled structures were oblique sections through longer, more complete structures or partially assembled structures as surmised. However, they were more frequent than in 48 hr embryos and probably represent early stages in myofibril assembly.

At the same stage of development (24 hrs), the myotomes of *akn*^{u45} mutants showed no fully assembled myofibrils. Instead of fully assembled sarcomere structures, partially assembled structures were present. These consisted of Z lines flanked on either side by bundles of actin filaments similar to structures previously characterised in the literature as I-Z-I brushes (Goll et al., 1977). No thick filaments or A-band structures were present. I-Z-I brushes were occasionally seen in linear association with other I-Z-I brushes in structures resembling sacomeres lacking thick filaments However, at this stage these incomplete sarcomeres were rare. The Z lines were orientated almost correctly (± 20-30°) relative to the long axis of the cell. I searched through the myotomes in 4 separate preparations (about 50 myotomes) to check for any evidence of myosin thick filaments as antibody staining had indicated the diffuse presence of some myosin. This search revealed some rare isolated thick filament-like structures. Some occurred in isolated groups away from the I-Z-I brushes, and in one case they were strung between adjacent I-Z-I brushes (Figure 9.4 D) suggesting an attempt at constructing an A band. However, without the use of antibodies it is impossible to say whether these structures are thick filaments or other structures that resemble them. However, a possibility is that thick filaments may be more unstable in mutant embryos and thus they are only recognisable in rare cases where they are caught before degradation.

Figure 9.4 TEM detail of sarcomeric abnormalities in *akn* mutants.

TEM of the muscle in WT embryos at 24hpf revealed the detailed structure of myofibrils (**A**, **C**, **E**, **G**). The myofibrils contain all the sarcomeric bands. There were several indications that they were recently formed. Frequently the z-lines were not perfectly straight (**A**, **E**; Arrowheads). Often the A bands appeared to have missing thick filaments (Arrowhead; **C**) and triads were only present adjacent to a minority of Z-bands (arrowhead; **G**). In contrast, the muscle of *akn*^{u45} mutant embryos (**B**, **D**, **F**, **H**) did not contain complete sarcomeres. Z-bands were present (arrowheads; **B**, **D**, **F**), but these were not as wide as in WT muscle and were also not aligned relative to each other (**A**, **D**). They were often flanked on either side by pale thin filaments, thus forming I-Z-I structures. The I-Z-I structures were aligned relative to the long axis of the cell (left to right in the micrographs) and were sometimes part of a continuous fibrous structure resembling a myofibril. However, this structure appeared frequently to completely lack thick filaments (**A**) in other cases a few sporadic structures resembling thick filaments were found in approximately correct locations between consecutive z-bands (Boxes; **D** & **B**). Occasionally, small isolated bundles of these putative thick filaments were also found (**H**). Scale bars: **A** & **B** = 1 µm; **C** - **H** = 500nm.

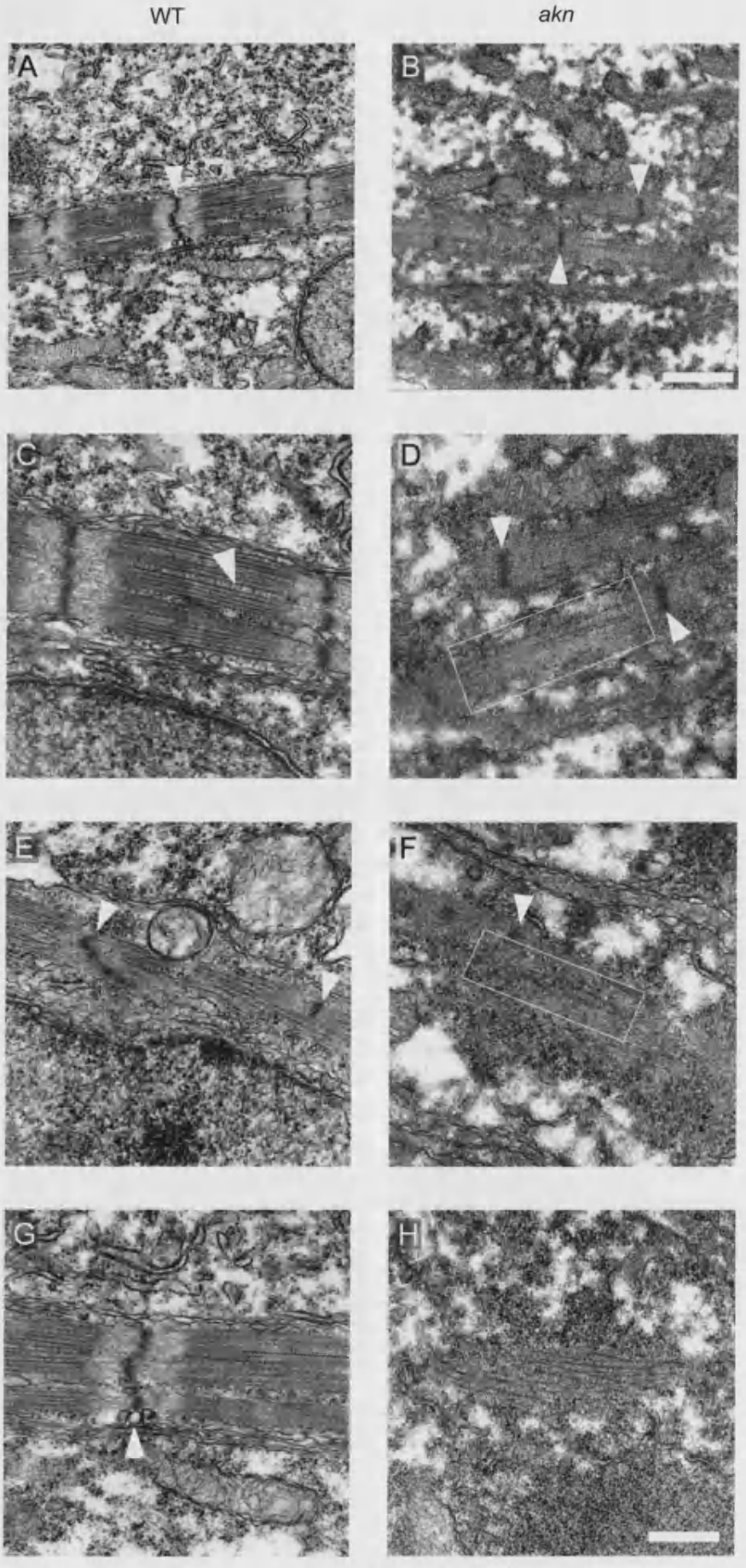
WT
akn
A
B
C
D
E
F
G
H

9.3.2 Myofibrils at 48hpf.

During the second day of development, the muscles of the zebrafish embryo develop considerably. The embryo straightens out and this coincides with the appearance of more directed movement. Wild-type embryos at 48 hpf showed myotomes tightly packed with multiple well-orientated myofibrils (Figure 9.5), well developed T-tubules and sarcoplasmic reticulum. There were still signs of ongoing myofibril assembly, but the myotomes were mostly occupied by muscle fibres containing complete myofibrils stretching from one myotome boundary to the next, showing near-crystalline orderliness in the sarcomere pattern.

In contrast, *akn*^{u45} mutant embryos have very disordered myotomal ultrastructure. At 48 hpf many I-Z-I brushes are present and they often appear to be in series with others, forming incomplete sarcomeres lacking the A band. In the wild-type, the Z-lines of the sarcomeres are found at regular intervals in register with those in adjacent myofibrils. In contrast, *akn*^{u45} mutants have infrequent Z-lines that lack regular longitudinal spacing and transverse register with neighbouring I-Z-I brushes. While the number of I-Z-I brushes is increased over that at 24 hrs, there are still far fewer than there are Z-lines in the wild-type. Occasional T-tubule-like structures are present, especially near I-Z-I brushes where poorly formed triad structures can be seen, however, these structures are rare. There is still an apparent total lack of assembled thick filaments and the structures normally associated with them. Careful survey of myotomes from multiple specimens failed to reveal the thick filament-type structures that were seen at the 24 hour stage, suggesting that there is a problem maintaining their integrity at this later stage.

Because of their increased frequency, more detailed examination of the I-Z-I brushes was possible at this stage. Several features typical of I-Z-I brush structures (Goll et al., 1977; Bullard, 1984; Chun and Falkenthal, 1988) were visible. Either side of the Z-line in the I-Z-I structure there was a more electron dense shadowy area of about 100-200 nm (Figure 9.5 B). Within this area there was more order in the thin filament array. Beyond these electron dense haloes on either side of the Z-line, the thin filaments tapered off with the more lateral filaments being shorter than the medial ones, giving the isolated I-Z-I structures a consistent diamond-like appearance in longitudinal (Figure 9.5 B) section.

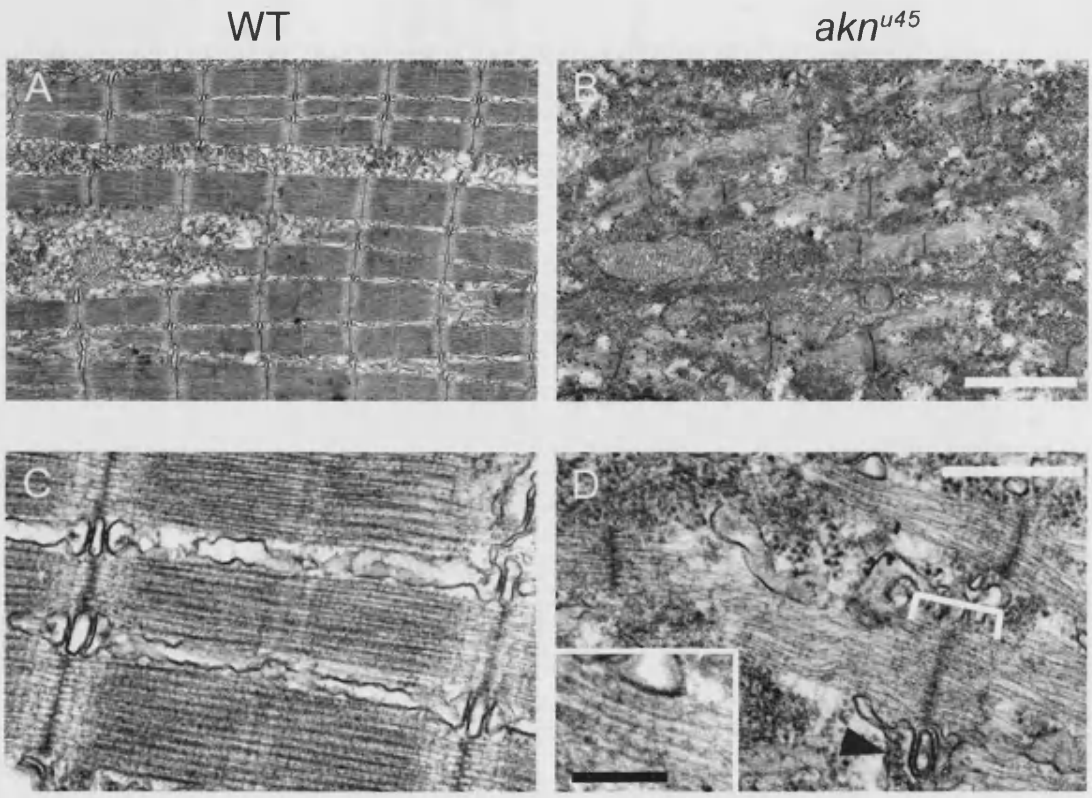

Figure 9.5 TEM at 48 hours revealed more detail of sarcomere structure in WT and *akn*^{u45} mutant embryos. There was an increase in the number of myofibrils present in the myotomes of the embryos (**A**) most of the intracellular space of the muscle fibres was now occupied by myofibrils. High power examination of these structures (**C**) revealed their highly regular organisation. The excitation-contraction coupling system was also further developed, most z-bands now had associated triad structures. In *akn*^{u45} mutant embryos, many more I-Z-I brushes have developed by 48 hours (**B**). The increased frequency of the I-Z-I brushes allowed more detail of these structures to be seen. Either side of the Z-lines there was a more electron dense region (**D**; bracket). In the thin filament domains outside of the dense regions striations were visible on the thin filaments (**D**; inset). Partially formed triads were sometimes seen in association with the Z-lines of I-Z-I brushes (**D**; Arrowhead). (Scale bars: **A** & **B** = 2µm; **C** & **D** = 500nm; **D** inset = 100nm)

However, when the I-Z-I structures are sequential there is merely a constriction of the thin filaments in the region between sequential Z-lines giving them an hourglass appearance. Although this appearance could have been due to the thin filament bundles passing in and out of the plane of section, it was a very consistent feature. It suggested that the I-Z-I brushes were partially assembled into myofibril-like structures lacking thick filaments with thin filaments instead bridging the gap betwee the Z-lines. Outside of the dense halo either side of the z-line the thin filaments of the I-Z-I brushes have a striated appearance (Figure 9.5 D & inset) of regular electron dense patches along them. These have a periodicity of approximately 30 nm which is a similar periodicity as the myosin heads in the muscle of the WT embryos. I-Z-I brushes present in the *Drosophila* myosin mutant *Ifm(2)2* show similar structures regularly distributed along the thin filament arrays, with a periodicity of 30-40nm which are thought to be troponin complexes attached to every half turn of the actin cable (Chun and Falkenthal, 1988).

9.3.3 Heart muscle structure

The heart beats normally in akn^{u45} mutants. To confirm that the ultrastructure is normal, I examined the heart muscle of both wild-type siblings and akn^{u45} mutants. As expected, normal myofibrils were found in the heart walls in WT and mutant embryos (Figure 9.6). There are differences in the structure of the heart muscle and the skeletal muscle. The heart muscle contains myofibrils that are much thinner than those found in the skeletal muscle. At the 48 hour stage they are only 5-10 thick filaments wide and there appears to be only 1 or 2 myofibrils that form a ring around the chamber of the heart. The Z-lines are much more indistinct in the heart. Also, heart muscle cells contract in several different planes so quite often both longitudinal and transverse sections through the myofibrils can be seen in one cell. The muscle cells of the heart do not fuse to form multinucleate cell syncytia. Instead, neighbouring muscle cells have junction complexes between them (Figure 9.6).

The fact that cardiac muscle has a normal function and ultrastructure may help us to narrow down the possible candidate genes for the mutation (see below).

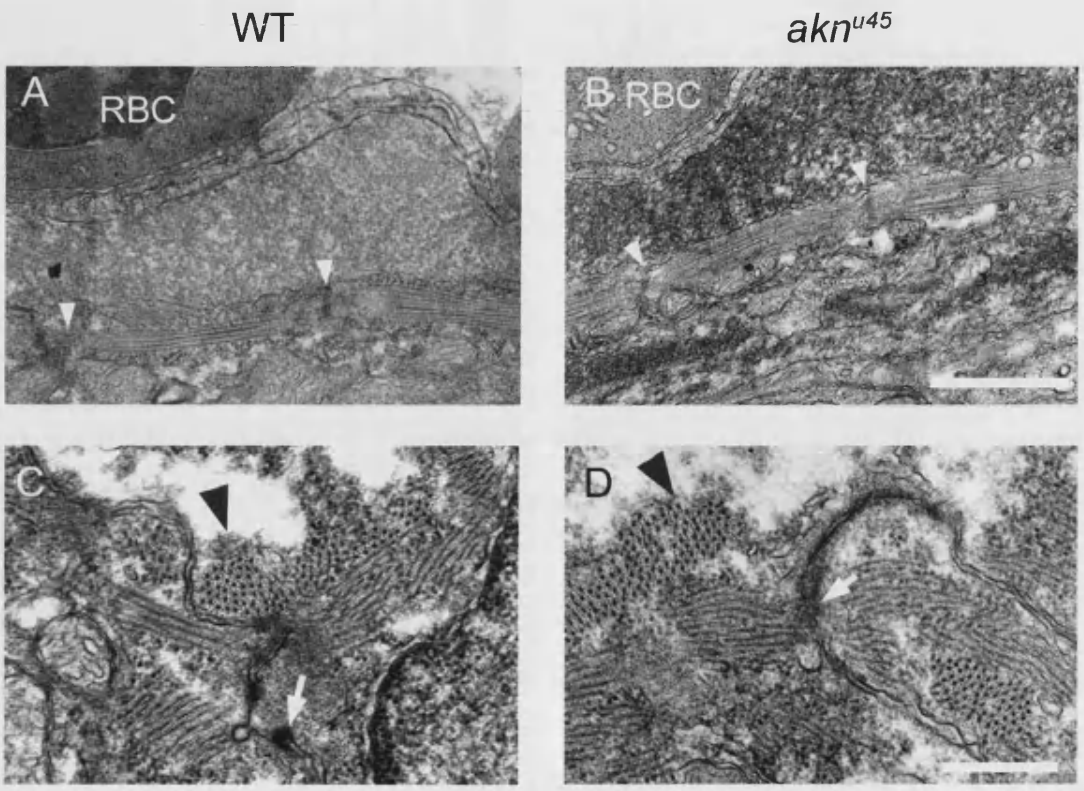

Figure 9.6 Heart muscle ultrastructure develops normally in *akn*^{u45} mutant embryos. At 48 hpf the heart walls of WT (**A**,**C**) and *akn*^{u45} mutant (**B**,**D**) embryos both contained complete sarcomeres (**A**, **B**). There were differences between the heart sarcomeres and those earlier seen in skeletal muscle. In the heart the saromeres were much thinner, comprising only 5-10 thick filaments, Z-lines (arrowheads; **A**, **B**) were more indistinct structures. Because the arrangement of sarcomeres in the heart is less ordered than in skeletal muscle transverse (arrowheads; **C**, **D**) and longitudinal sarcomere profiles are seen side by side. Junctional complexes between cells were also present (arrows; **C**, **D**). (RBC = red blood cell) (Scale bars: **A** & **B** = 1µm; **C** & **D** = 500nm)

9.4 Complementation testing and genetic mapping.

To determine an unknown mutant gene locus, the first step is to map the mutation onto the genome. In collaboration with Robert Geisler's laboratory in Tübingen a bulked segregant analysis SSLP approach was initially utilised (Figure 9.7). After two attempts with two different mapping crosses no progress was made. Next a collaboration with Will Talbot of Stanford University was set up to utilise his SNP microarray technology (Stickney et al., 2002) (Figure 9.8). Unfortunately this was also unsuccessful. Following this, heterozygote *akn*^{u45} carriers were sent to Uwe Strähle in Strasbourg to test if the mutation was complementary to any of his similar motility mutants. Fortunately it was. The mutants *paralytico* and *sloth* were both found to be in the same complementation group as *akineto*. *Paralytico* is a mutant which was generated in Strähle's lab, and found to be at the same locus as *sloth* which was generated in the earlier large-scale Tübingen screen (Granato et al., 1996). The gene for *paralytico* had been mapped by Uwe Strähle in collaboration with Robert Geisler and is located approximately 1.3cM (centimorgans) from marker z4329 on linkage group 20. Will Talbot confirmed by PCR that some of the embryos sent to him showed proximity to markers in the region (z7568 & z22144), confirming that the *akn*^{u45} gene is also in this area of the genome (and therefore is the same gene as *sloth* & *paralytico*).

The situation now is that I have generated two additional mapping crosses to commence fine mapping of the gene. From in-crosses of these families (8 pairs of fish) I have collected and sorted approximately 6,000 mutant and sibling embryos from which to extract genomic DNA for further fine mapping in collaboration with Will Talbot. I have obtained funding to go to California for three months to partake in these experiments. Uwe Strähle knows about our progress on *akn*^{u45} and is not currently working on *paralytico*, and to our knowledge nobody else is working on *sloth*, so it should be worth our while to proceed and fine map the *akn*^{u45} allele and thus (hopefully) to determine the mutated gene through a bioinformatic candidate approach as more zebrafish genome sequence becomes available through the zebrafish genome project.

Figure 9.7 SSLP mapping of *akn*^{u45}. SSLP mapping uses SSLP (simple sequence length polymorphisms) markers. These are lengths of genomic DNA (usually comprising multiple 1-6 nucleotide repeats) flanked by distinct identifiable sequences that allow for straightforward PCR isolation. The SSLPs used for mapping have been pre-determined as polymorphic in length between different WT background strains of zebrafish (e.g. wik & AB in this example). The length polymorphisms are different enough to be easily identified by their sequence length on agarose gels (right of figure).

To commence, a mapping cross (**P**) is set up with an identified heterozygote in the AB strain background and a wild-type fish from the wik mapping strain background. Examples of two markers from the different strains are illustrated on schematic chromosomes (**left; wik 1, wik 2** (black chromosomes), **AB1, AB2** (pink chromosomes)) and as bands on gels are shown on the right). In this example the AB 1 marker is closely linked to the mutation (**Mut**) whereas the AB 2 marker is on a different chromosome and is thus not closely linked. Two markers will be used as examples here for simplicity but in reality there are hundreds of markers that need to be tried to find good genetic linkage. The **F1** of this cross are screened by random intercrossing to find heterozygote carriers (half of the fish) and the non-carriers are discarded. The identified heterozygotes will now be hybrids for the two different SSLP markers (they have all markers; see gel bands on right). The **F1** heterozygotes are intercrossed, the resulting **F2** are scored for phenotypes and are sorted into pools of homozygous mutants (*akn*$^{-/-}$) and non-mutant siblings (containing both heterozygotes and homozygte WT embryos.

Crossing over during the process of meiosis in the production of F1 gametes means that the F2 individuals will possess hybrid recombinant chromosomes. This is indicated by the different coloured sections on the schematic chromosomes of the F2. Because of this process, the F2 individuals can possess any combination of markers, the approximate ratios are written above the schematic chromosome pairs. If the mutant locus (**Mut**) and a marker are nearby each other on the chromosome (closely linked; as with marker 1 here) then the marker from the original mutant heterozygote carrier background (**AB-1**) will more frequently be inherited with the mutation than the mapping cross backgound marker (**wik 1**). Thus, when genomic DNA from the homozygote mutant and sibling groups are pooled and examined by PCR for the markers then the closely linked marker will be more prevalent in the homozygote mutants and the band will be stronger on agarose gels from the mutant pooled DNA (**asterisk**) In a pool of DNA from many individual mutant embryos in some cases a recombination event will separate the mutation and the AB marker, linking the mutation instead with the wik marker (**§**) this means that in pooled DNA from many individuals then there can be a faint band on the gel corresponding to the wik marker (**asterisk**) the brightness of this band will be less the closer the mutation and marker are together. Markers which are not closely linked to the mutation (e.g. marker 2) will have no difference between the mutant and sibling pools, being present in equal ratios between the two groups and this showing no difference on agarose gels.

Further fine mapping of the mutation can be carried out by examining the genomes of individual embryos. The genetic distance between markers and mutations is calculated in centimorgans, where one centimorgan of genetic distance is a 1% probability of a recombination event in one generation (1 in 100 homozygote mutant embryos would have the wik 1 marker in this case).

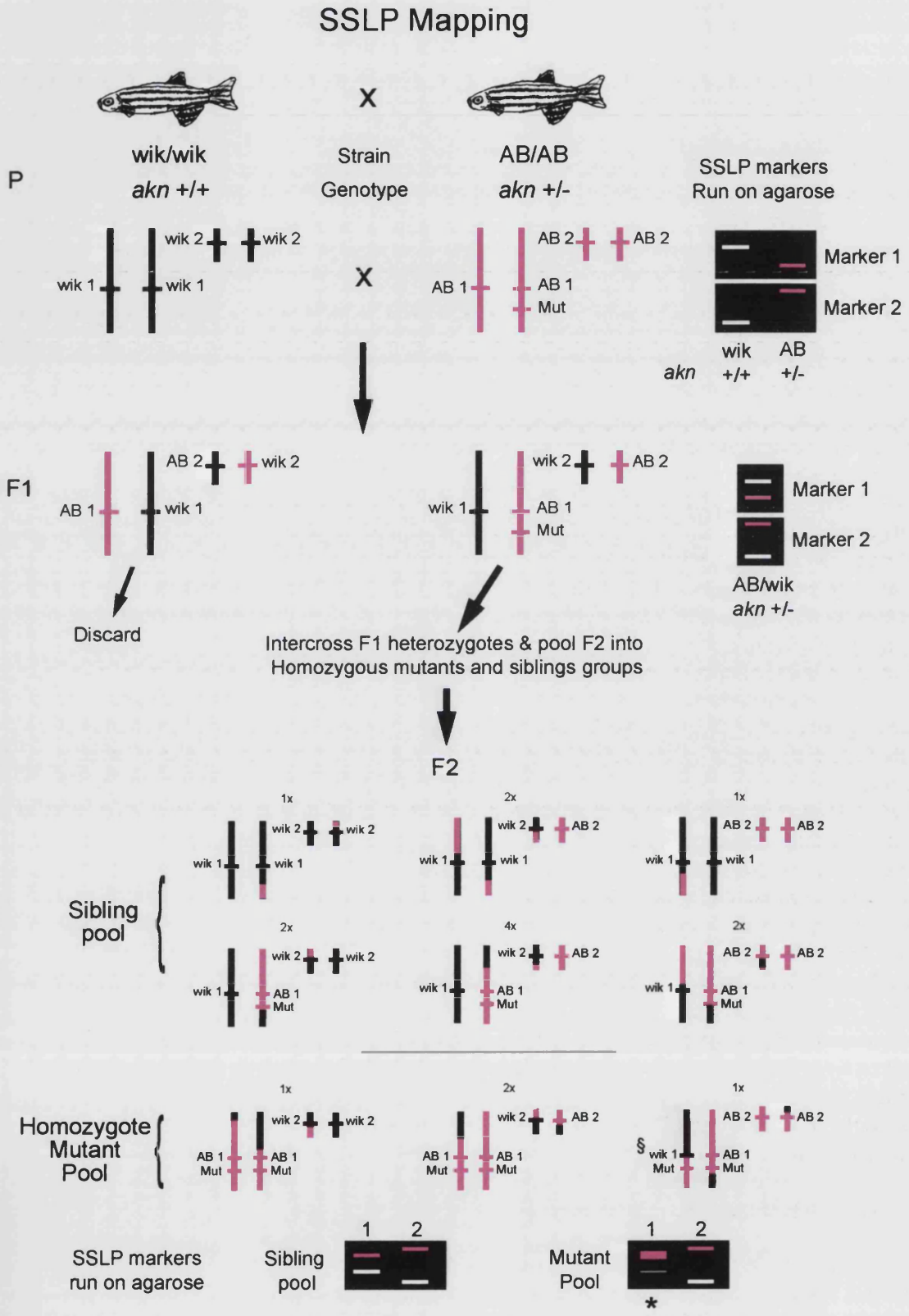
SSLP Mapping
X
P
wik/wik
akn +/+
Strain
Genotype
AB/AB
akn +/-
SSLP markers
Run on agarose
wik 1
wik 2
wik 1
wik 2
X
AB 1
AB 2
AB 1
Mut
AB 2
Marker 1
Marker 2
wik
+/+
AB
+/-
akn
F1
AB 1
AB 2
wik 1
wik 2
wik 1
wik 2
AB 2
AB 1
Mut
Marker 1
Marker 2
AB/wik
akn +/-
Discard
Intercross F1 heterozygotes & pool F2 into
Homozygous mutants and siblings groups
F2
Sibling
pool
1x
2x
4x
Homozygote
Mutant
Pool
§
SSLP markers
run on agarose
Sibling
pool
Mutant
Pool
1
2
*

Figure 9.8 SNP mapping. Diploid SNP mapping uses a similar crossing schedule to SSLP mapping (**P, F1, F2**), however, the polymorphic markers employed here are not lengths of DNA but single nucleotide polymorphisms (SNPs) differing between strain backgrounds. Examples from AB (pink) and wik (black) genetic backgrounds are shown here; large chromosome: **A/C;** small chromosome: **C/T**; the large chromosome SNP is closely linked to the mutation (**Mut**). PCR is used to amplify DNA segments known to contain the SNPs to be screened (2 in this case, hundreds normally) from the pooled F2 mutant and sibling genomic DNA. These DNA fragments are differentially labelled with fluorescent dyes (green for siblings; red for mutants in this example), the labelled DNA from both F2 pools is mixed and hybridised onto a oligonucleotide microarray with complementary sequence for the known SNPs. If a SNP is tightly linked to a mutation then the red mutant pool DNA will hybridise to only one SNP and so there will be one green spot (only the green-fluorescent labelled wik SNP) and one yellow (green sibling wik and red homozygote mutant AB SNP) on the microarray. Unlinked SNPs will always appear as two yellow spots where there is no difference in the level of the marker between mutants and siblings.

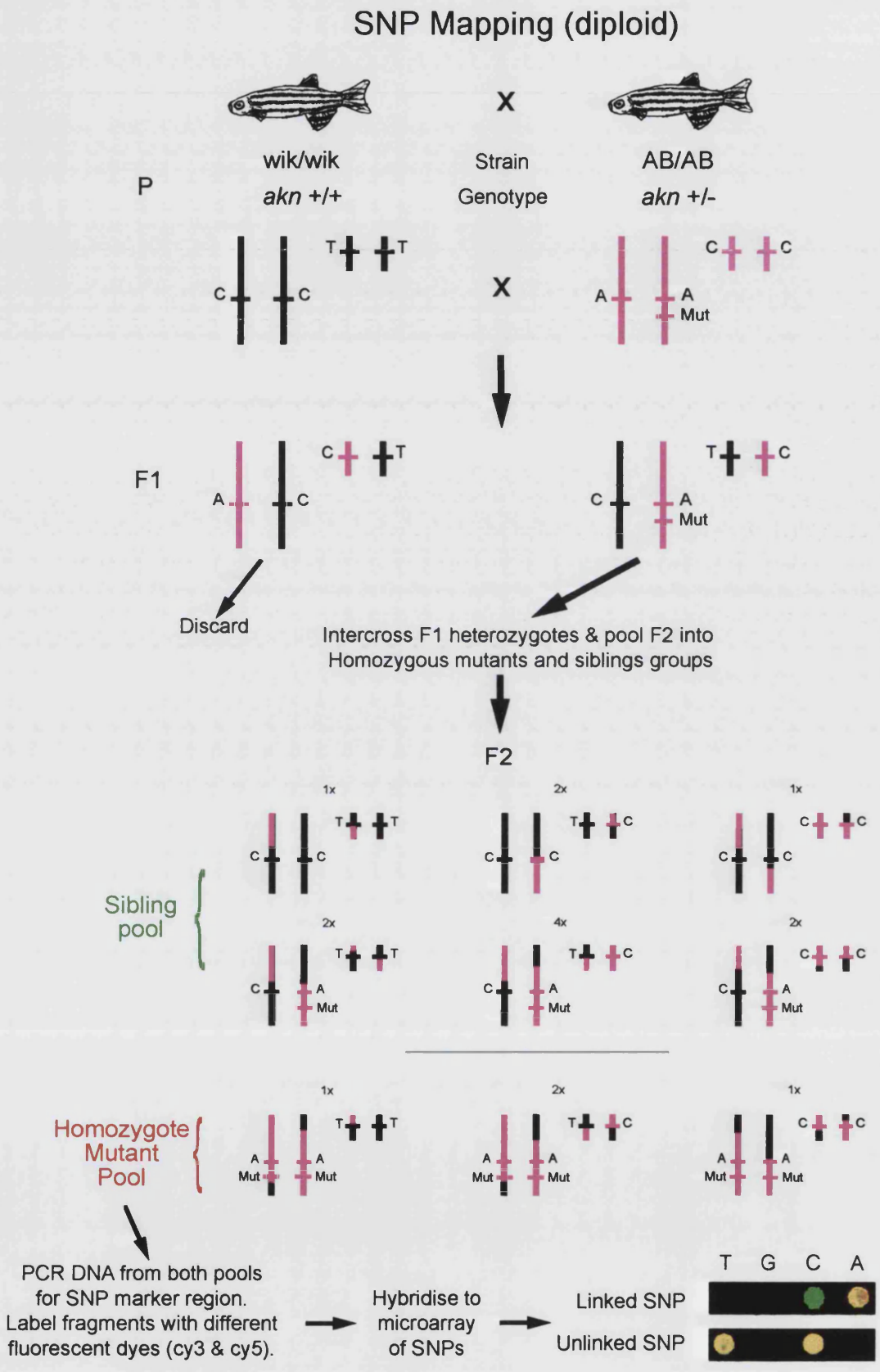
SNP Mapping (diploid)
X
P
wik/wik
akn +/+
Strain
Genotype
AB/AB
akn +/-
X
F1
Discard
Intercross F1 heterozygotes & pool F2 into
Homozygous mutants and siblings groups
F2
Sibling
pool
Homozygote
Mutant
Pool
Mut
PCR DNA from both pools
for SNP marker region.
Label fragments with different
fluorescent dyes (cy3 & cy5).
Hybridise to
microarray
of SNPs
Linked SNP
Unlinked SNP
T G C A

Chapter 10: Discussion

10.1 The consequence of the mutation: A myofibrillogenesis defect

At the time of writing we do not know what the afflicted gene is in *akn*^{u45} mutants. However, what is clear from the results presented here is the cause of the lack of movement in the fish. The myofibrils in the skeletal muscle fail to form correctly. More specifically, the mutants are unable to form ordered arrays of thick filaments which can be correctly integrated to form the A bands of myofibrils. Without the crucial myosin assemblies the myofibrils cannot contract and the fish remains immobile.

A key result is the finding of I-Z-I brushes in the mutant fishes. From the complementation testing of the *akn*^{u45} allele we now know that this is the same gene as *sloth* previously identified in Tübingen. Granato et al (1996) describe *sloth* as possessing a defect in muscle differentiation, meaning it never forms myofibrils. Here I have described TEM and antibody studies on *akn*^{u45} at the same locus, showing part assembly of myofibrils lacking thick filaments. It seems that the muscle cells attempt to form myofibrils but fail to complete this process, because the mutated gene is required for thick filament assembly, integration or stability. Thus, assuming there are no major differences in the type of mutation between the *sloth* alleles (*sloth*^{tu44c} & *sloth*^{tm201}) and *akn*^{u45} the initial suggestion by Granato et al (1996) that the *sloth* mutant fails to differentiate to commence myofibril formation may not be correct.

10.2 Current theories of myofibrillogenesis.

If the *akn*^{u45} gene can be identified, how useful might this mutation be in furthering our understanding of how myofibrils develop? To assess this, I will review here what is currently understood about sarcomere development

The mechanisms of sarcomere contraction were largely understood more than a quater of a century ago (reviewed by Pollard, 2000). Research since then has refined that model and added certain components (e.g. titin). As a result, the contractile apparatus of muscle cells and its activation remain one of the best understood molecular systems in terms of how its functional requirements

determine its structure (Pollard, 2000; Clark et al., 2002). However, the assembly of this beautifully regular structure is only starting to be understood. From many *in vitro* and some *in vivo* studies in the cardiac and skeletal muscles of several species, we now have an idea of the approximate sequence of myofibril assembly are assembled in (Fürst et al., 1989; Schultheiss et al., 1990; van der Loop et al., 1992; Lin et al., 1994; Rhee et al., 1994; LoRusso et al., 1997; Ehler et al., 1999; Van der Ven et al., 1999; Costa et al., 2002; Sanger et al., 2002; White et al., 2003). There are many disagreements between observations in different systems and species (notably between *in vitro* and *in vivo* systems), and for conciseness' sake I will derive a consensus view of the sequence in which molecules appear. This may conceal important species differences.

10.2.1 The sequence of expression of sarcomeric components.

The first sarcomere-associated molecules to be expressed are desmin intermediate filaments (Fürst et al., 1989; Lin et al., 1994; Costa et al., 2002). Actual sarcomere assembly often commences in close proximity to the plasma membrane. This observation in combination with the early expression of cytoskeletal molecules like desmin has led to suggestions that anchorage is important during initial stages of myofibrillogenesis. The actual process of sarcomere assembly commences at the Z-line with the assembly of actin filaments (Ehler et al., 1999; Van der Ven et al., 1999). At this stage, several *in vitro* studies find the appearance of stress fibre-like structures (SFLS)(Dlugosz et al., 1984; Schultheiss et al., 1990) on which subsequent stages of assembly take place. However, some researchers consider that these SFLS structures are an *in vitro* artefact. Complexes form that consist of Z-lines flanked on either side by arrays of thin filaments (I-Z-I brushes) (Fürst et al., 1989; Schultheiss et al., 1990) similar to those seen in akn^{u45} mutants. Titin appears to be incorporated at this stage because Z-line, I band and A-I band area epitopes of the molecule are present (Fürst et al., 1989; Ehler et al., 1999; Van der Ven et al., 1999). There is much controversy over the exact sequence of events that follows (see below). Thick filaments are incorporated, either partly or fully assembled with their M band components (Ehler et al., 1999). At this stage, A band and M band epitopes of titin are also detectable in regular arrays and this may precede A band formation (Fürst et al., 1989; Van der Ven et al., 1999). Following the assembly of sarcomeres the extra-sarcomeric cytoskeletal components such as dystrophin

(Mora et al., 1996) assemble to link the contractile machinery to the cell and to the basal lamina.

Interestingly, this sequence of assembly is corroborated through studies on fish. The electric organs of weakly electric teleosts develop from muscle tissue (Szabo, 1960; Patterson and Zakon, 1996). In the mature electric organs of these fish, remnants of muscle ultrastructure remain (Wachtel, 1964; Schwartz et al., 1975). This may indicate where in the process of muscle differentiation the electrical organ began to change its fate. Thus there is a full spectrum of ultrastructural features in the cells of the electric organs of these fish. They range from disorganised thin filaments seen in all Gymnotids examined: *Gymnotus, Hypopomus, Eigenmannia, Steatogenys and Sternopgyrus,* through I-Z-I brushes similar to those that we see in *akn*^{u45} mutants which are seen in *Gymnarchus niloticus* (group: Mormyriformes), to fully organised sarcomeres with fully integrated thick filaments which are seen in species such as *Gnathonemus petersi* (also group Mormyriformes) (Wachtel, 1964; Schwartz et al., 1975). This variety indicates that the different species have different stalling points in the myofibril assembly programme.

The sequential deposition of sarcomere components seems to imply a requirement to have reached one stage before proceeding to the next. If this were true then one would not expect to see thick filament assembly in the absence of I-Z-I brushes. However, this is not the case, both thick and thin filaments can assemble independently without the presence of the other component (Waterston et al., 1980; Zengel and Epstein, 1980; Mahaffey et al., 1985; O'Donnell and Bernstein, 1988; Epstein and Fischman, 1991; Sehnert et al., 2002) or even in cell-free conditions (Goldfine et al., 1991). In addition, the ordered scaffold of titin, Z-line proteins and M-band proteins can remain in place after the removal of thick and thin filaments (Funatsu et al., 1993). However, interactions between thick and thin filaments, particularly in force generation, are necessary for the assembly of myofibrils with the proper periodicity (Ramachandran et al., 2003)

10.2.2 Models of myofibrillogenesis

Based mainly on *in vitro* observations of myofibrillogenesis sequence, two main models of how myofibrillogenesis is controlled have been proposed (Figure 10.1 **1** & **2**). These are the Holtzer model (Schultheiss et al., 1990) and the Sanger

Figure 10.1 Current models of myofibrillogenesis

1. Holtzer model. Firstly, stress-fibre like structures (SFLS) form from polymerised actin (green). These become organised by Z-line proteins (blue) into non-striated myofibrils (NSMF; similar to I-Z-I brushes). Concurrently with the formation of NSMFs, myosin molecules assemble into thick filaments (brown). The NSMFs and thick filaments then integrate to form striated myofibrils (SMFs) at cell locations dense in cell-adhesive proteins called subsarcolemmal adhesion plaques (SAPs).

2. Sanger 'premyofibril' model. In this model premyofibrils are proposed to form from I-Z-I brushes/complexes and non-muscle myosin (orange). This results in myofibrils lacking thick filaments and having a shorted Z-line to Z-line distance. Progressively the non-muscle myosin is replaced by muscle myosin assembling into thick filaments which expands the Z-line to Z-line distance and striated myofibrils are thus formed.

3. Titin Model. I-Z-I complexes form and are associated with titin (purple) which is not uunfolded as a filament or is incompletely assembled. As the titin molecule is either constructed or unfolded, neighbouring I-Z-I brushes are connected by the titin molecules and M-line proteins (red). This forms a scaffold onto which thick filaments can assemble from individual myosin molecules. Striated myofibrils are this formed.

1. Holtzer Model.

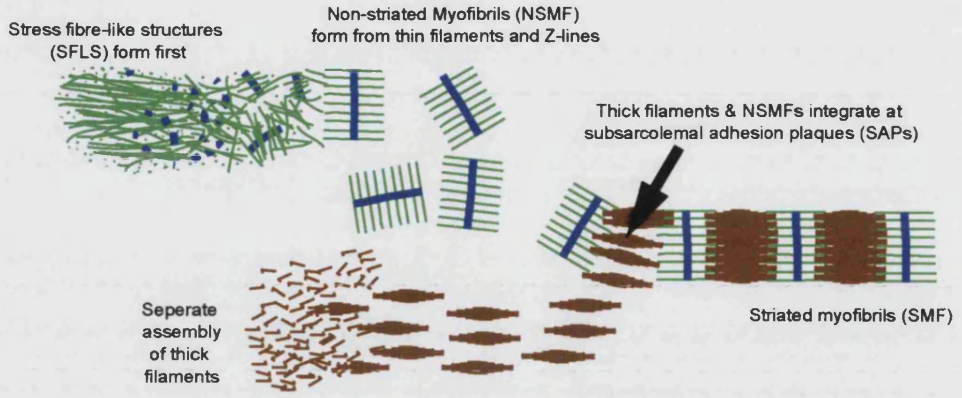

2. Sanger 'premyofibril' model.

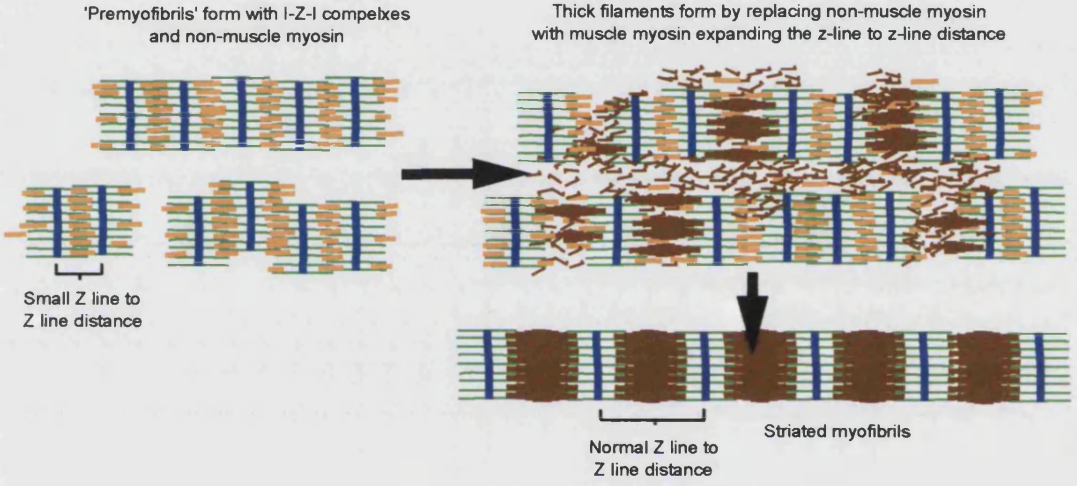

3. Titin model

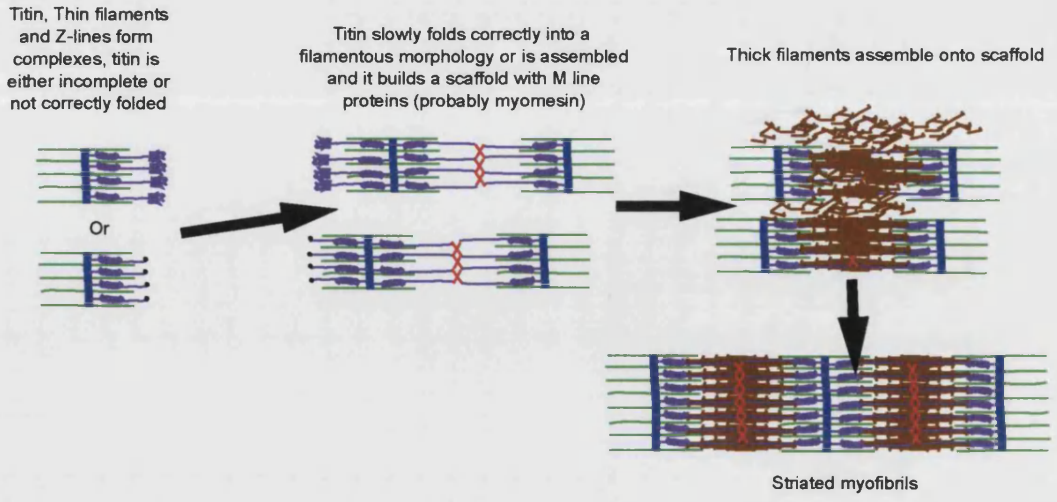

model (Rhee et al., 1994; LoRusso et al., 1997; Sanger et al., 2002). The main difference between the models is the way they propose that thick filaments are incorporated. The Holtzer model proposes that non-striated myofibrils (NSMFs) lacking thick filaments) assemble from stress fibre-like structures (SFLS) and then independently assembled thick filaments are incorporated at sites called sub-sarcolemmal adhesion plaques (SAPs) to form striated myofibrils (SMFs) (Schultheiss et al., 1990). The Sanger theory holds that premyofibrils with a shorter length than mature myofibrils and containing non-muscle isoforms of myosin form first. These then form mature myofibrils through the replacement of the non-muscle myosin with muscle myosin (Rhee et al., 1994; LoRusso et al., 1997; Sanger et al., 2002). Recent evidence from a Drosophila mutant called *zipper*, which lacks non-muscle myosin, shows that this molecule is important for myfibril formation thus supporting the Sanger model (Bloor and Kiehart, 2001).

These two models were based mainly on *in vitro* observations of chick cardiomyocytes and a new model based on *in vivo* observations is emerging, in which the giant molecule titin plays a central role (Ehler et al., 1999) (Figure 5.13 **C**). The full sequence of titin is known, and antibodies against different epitopes distributed along the length of the molecule (Fürst et al., 1988) have revealed its placement in the sarcomere. Because of titin's interactions with molecules in all zones of the sarcomere, the new model views it as a template or scaffold on which other sarcomeric components assemble (Ehler et al., 1999; Gregorio et al., 1999; Trinick and Tskhovrebova, 1999; Van der Ven et al., 1999). Some advocates of this model maintain that the construction of the sarcomere is actually regulated by the lengthy translation of the huge titin sequence (Fulton and L'Ecuyer, 1993; Fulton and Alftine, 1997). The first step in the third model is the formation of a complex comprised of α-actinin, the N-terminus portion of titin and actin filaments (I-Z-I brushes). These complexes are then brought into register probably by the unfolding (or perhaps further translation) of the titin molecule and the antiparallel association of the C-terminus (M-line) region of the now unfolded (or assembled) titin molecules (Ehler et al., 1999; Van der Ven et al., 1999). This fits with the observation of the sequential appearance of titin epitopes (Fürst et al., 1989). The M-line component, myomesin then closes the M-line end of the myofibrillogenesis scaffold and following this, thick filaments integrate into the structure through interaction with the A band region of titin

and additional M-line components (Ehler et al., 1999). In support of the titin template model, recent descriptions of titin mutants and *in vitro* knockout experiments have demonstrated it's crucial role in sarcomere assembly (van der Ven et al., 2000; Xu et al., 2002).

10.2.3 Akineto and thick filament assembly.

In *akn*^{u45} mutants, it appears that the last stage of the process of myofibrillogenesis in which thick filaments are integrated into the sarcomere is defective. The thick filaments are either unstable or fail to assemble. The constituent myosin molecules from which thick filaments are assembled are probably available (from the antibody studies) albeit in reduced number, and it would be of great interest to see whether purified *akn*^{u45} myosin will assemble into thick filaments *in vitro*.

Our understanding of the process of the assembly of thick filaments has recently become substantially clearer because of work initiated in *Caenorhabditis elegans* (Brenner, 1974; Epstein and Thomson, 1974). The *Unc-45* mutant in *C. elegans* has defective thick filament assembly in its body wall muscle (Brenner, 1974; Epstein and Thomson, 1974; Barral et al., 1998; Barral et al., 2002). Recently it has been shown that the *Unc-45* gene is part of a family of genes called the UCS family and that it interacts with myosin where it is thought to act as a chaperone protein or 'assemblase' that assists the assembly of myosin into thick filaments (Barral et al., 1998; Barral et al., 2002). The thick filaments of *C. elegans* differ from those of zebrafish and other vertebrates. They are made from a core of paramyosin and two separate types of myosin: A & B which segregate to different domains of the filament (White et al., 2003). Lack of a functional *Unc-45* molecule causes a major reduction in the number of thick filaments and the filaments that do assemble have a scrambling of the arrangement of myosin domains rendering the filaments unstable (Barral et al., 1998; Barral et al., 2002).

Unc-45 equivalents have now been cloned in many higher vertebrates including zebrafish (Etheridge et al., 2002). In mammals there are two distinct forms of *Unc-45*. One is specifically expressed in striated muscle and the other is more ubiquitous (also called general cell *Unc--45*; gc*Unc-45* : Price et al., 2002). Price et al (2002) also found that there is a distinct difference in the UCS domain in *Unc-45* genes between vertebrates and invertebrates. This could reflect

different requirements of the molecule given the differences in muscle ultrastructure between the respective phyla. For example, vertebrates possess the very large cross-sarcomere titin molecule which contrasts with the smaller invertebrate titin (twitchin/projectin/mini-titin) molecule (Benian et al., 1989; Tskhovrebova and Trinick, 2003). If vertebrates use titin as a template for thick filament synthesis then this appears to have superceded the similar use of paramyosin as a thick filament core in *C. elegans* (White et al., 2003). However, in *Drosophila* titin is also a small molecule but the muscle of *Drosophila,* does not use paramyosin like *C. elegans* and so this model may not hold for all species.

Aside from the *Unc-45* chaperone molecule regulation of thick filament assembly there have been some recent speculations on molecular methods by which other aspects of myofibrillogenesis take place. The recently discovered Z-disc associated molecule obscurin has a calmodulin binding domain and a Rho guanine nucleotide exchange domain suggesting roles in intracellular signalling and sarcomere assembly (Young et al., 2001). Also, the sequencing of the titin molecule (Labeit and Kolmerer, 1995) revealed the presence of a kinase domain in the C terminus M line region. Further characterisation of this domain revels that it is a myosin-light-chain kinase family member and is activated during myofibrillogenesis (Mayans et al., 1998). The target of this kinase is another recently discovered sarcomeric protein called telethonin which strangely in mature myofibrils is a Z-disk protein 1μm away from its kinase in the M-line. However, during myofibrillogenesis telethonin seems to closely associate with the C terminus region of the titin molecule (Mayans et al., 1998). The exact role of this interaction during myofibrillogenesis is unclear but telethonin is interacting with titin at a crucial time of development, and since titin is considered to have an important role in myofibrillogenesis (at least in vertebrates), then this interaction is likely to have some role in the control of myofibril formation.

In view of the large number of different species, culture conditions and cells used in studies of myofibrillogenesis it is hardly surprising that no clear consensus model of how myofibrils are assembled has emerged. The recent advances described above based upon *C. elegans* mutants of *unc-45* are a good step forward to producing a clearer picture of how the thick filaments are constructed not just in invertebrates but in vertebrates also. The lack of thick filaments in akn^{u45} mutants may well provide additional insight into this process

once the affected gene is known. There are considerable differences in the sarcomeric structure of invertebrate and vertebrate muscle. Because of their embryonic accessibility and their genetic pliability zebrafish are a good system to closely examine the process of myofibrillogenesis in a vertebrate system. Indeed, moderate numbers (in comparison to *C. elegans*) of motility and heart mutants have already been identified (Chen et al., 1996; Granato et al., 1996; Stainier et al., 1996) and some have been further characterised (Sehnert et al., 2002; Xu et al., 2002). The ease of phenotypically identifying such mutants is sure to yield many more myofibrillogenesis zebrafish mutants in the future. These mutants, together with the advent of morpholino knockdown methodology means that zebrafish could be an ideal organism to further unravel the complex process by which myofibrils are constructed.

10.3 Possible candidate genes for *akn*^{u45}.

We do not at present know the gene affected in *akn* mutants. However, the structure of the myofibril and its main structural components are well characterised, which permits some speculation over possible genes that may have been affected by the *akn*^{u45} mutation.

The most obvious candidates are structural genes involved with the thick filaments or their assembly. This would include thick filament-associated molecules such as myosin, C-protein, X and H proteins and UNC-45, the A or M band portion of titin might have been affected or M-band proteins like myomesin, Creatine kinase, M-protein could have been affected There are also less obvious candidates like tropomyosin or the troponins which may partictpate in constructing the sarcomere assembly and thus may directly or indirectly affect the building of thick filaments.

The fact that the heart has normal sarcomere formation eliminates some of these from the list but most of these molecules have cardiac and skeletal specific isoforms, so this is not as useful as might be expected. The major M-line components are common between cardiac and skeletal muscle in mammals and thus can probably be eliminated. I hazard that the troponins and tropomyosin can be eliminated because of the observable regularly spaced striations that were visible on the actin filaments of the I-Z-I brushes in *akn*^{u45} mutants. These

probably represent troponin complexes spaced at intervals by tropomyosin molecules bound to the actin. Next, the early mapping data we have indicating that the *akn*^{u45} gene is on linkage group 20 allows us to cautiously eliminate some other candidates. Titin is on linkage group 9 so is unlikely to be the gene affected. By synteny with the Mouse gene the zebrafish unc-45 gene should be on linkage group 3 so this can be tentatively eliminated.

After these eliminations we are left with the following genes: Myosin, C-protein, and X and H proteins. Myosin is an obvious candidate, but the antibody against myosin heavy chains showed that myosin is present in the muscles of *akn*^{u45} mutants, albeit in lower concentration than in wild type siblings. Myosin is a hexamer of a pair of heavy chain molecules and two pairs of light chain molecules. Although Pavlina Haramis found myosin heavy chain protein present in the mutants it might be that the mutation is in one of the light chains. A *Drosophila* mutant in myosin heavy chain (O'Donnell and Bernstein, 1988) has a muscle structural phenotype similar to that in *akn*^{u45} mutants. The indirect flight muscle of the *Drosophila* mutants contains I-Z-I brushes and a total absence of thick filaments. The thick filament accessory proteins C, X and H have much more enigmatic roles during myofibrillogenesis. In adult rabbit muscle they are found in specific locations along the thick filament which is thought to be associated with different types of muscle fibre (Bennett et al., 1986).

Aside from these obvious candidates there remains the more interesting possibility that *akn*^{u45} is a novel gene. Possibly most interesting would be a role similar to that of the UNC-45 protein in chaperoning or aiding in the folding of myofibril components (e.g. M-line proteins or titin) and their correct placement to allow the further construction of the sarcomere. There also remains the possibility that *akn*^{u45} is a transcription factor involved in the control of the expression of one of the above genes.

10.4 Prospects for the Future.

The first mission is to determine the gene affected in *akineto*^{u45} mutants, and this will determine what comes next. Hopefully fine mapping data from my planned work with Will Talbot in Stanford will pinpoint the mutation on genetic map of the zebrafish. In years past, this would have led to chromosome walking and positional cloning. However, the fully sequenced and annotated zebrafish

genome to be released by the Sanger centre will probably allow bioinformatic determination of candidates for the mutation. This could lead to phenotypic rescue testing with BAC injections and the cloning of the affected gene and sequencing of the mutation site from mutants and siblings.

The zebrafish offers a clear way forward to build on findings from worms and flies in the field of myofibrillogensis. It offers two clear advantages over the mouse. Firstly, it can be visualised during early development (particularly during myofibrillogenesis) and secondly, forward genetic screens for novel genes are easily accomplished.

References.

Aggelopoulos N, Parnavelas JG, Edmunds S (1989) Synaptogenesis in the dorsal lateral geniculate nucleus of the rat. Anat Embryol (Berl) 180(3) pp 243-257.

Alberts B, Johnson A, Lewis J, Raff M, Roberts K, Walter P (2002) Molecular biology of the cell. New York: Garland Science.

Amsterdam A, Burgess S, Golling G, Chen W, Sun Z, Townsend K, Farrington S, Haldi M, Hopkins N (1999) A large-scale insertional mutagenesis screen in zebrafish. Genes Dev 13(20) pp 2713-2724.

Amur-Umarjee SG, Hall L, Campagnoni AT (1990) Spatial distribution of mRNAs for myelin proteins in primary cultures of mouse brain. Dev Neurosci 12(4-5) pp 263-272.

Andriezen W (1893) The neuroglia elements in the human brain. Brit Med J 2 pp 227-230.

Ankerhold R, Stuermer CA (1999) Fate of oligodendrocytes during retinal axon degeneration and regeneration in the goldfish visual pathway. J Neurobiol 41(4) pp 572-584.

Bansal R (2002) Fibroblast growth factors and their receptors in oligodendrocyte development: implications for demyelination and remyelination. Dev Neurosci 24(1) pp 35-46.

Bansal R, Pfeiffer SE (1997) FGF-2 converts mature oligodendrocytes to a novel phenotype. J Neurosci Res 50(2) pp 215-228.

Bansal R, Stefansson K, Pfeiffer SE (1992) Proligodendroblast antigen (POA), a developmental antigen expressed by A007/O4-positive oligodendrocyte progenitors prior to the appearance of sulfatide and galactocerebroside. J Neurochem 58(6) pp 2221-2229.

Baron W, Decker L, Colognato H, ffrench-Constant C (2003) Regulation of integrin growth factor interactions in oligodendrocytes by lipid raft microdomains. Curr Biol 13(2) pp 151-155.

Barral JM, Bauer CC, Ortiz I, Epstein HF (1998) Unc-45 mutations in Caenorhabditis elegans implicate a CRO1/She4p-like domain in myosin assembly. J Cell Biol 143(5) pp 1215-1225.

Barral JM, Hutagalung AH, Brinker A, Hartl FU, Epstein HF (2002) Role of the myosin assembly protein UNC-45 as a molecular chaperone for myosin. Science 295(5555) pp 669-671.

Barres BA, Raff MC (1993) Proliferation of oligodendrocyte precursor cells depends on electrical activity in axons. Nature 361(6409) pp 258-260.

Barres BA, Raff MC (1994) Control of oligodendrocyte number in the developing rat optic nerve. Neuron 12(5) pp 935-942.

Barres BA, Koroshetz WJ, Swartz KJ, Chun LL, Corey DP (1990) Ion channel expression by white matter glia: the O-2A glial progenitor cell. Neuron 4(4) pp 507-524.

Barres BA, Hart IK, Coles HS, Burne JF, Voyvodic JT, Richardson WD, Raff MC (1992) Cell death and control of cell survival in the oligodendrocyte lineage. Cell 70(1) pp 31-46.

Barres BA, Schmid R, Sendnter M, Raff MC (1993a) Multiple extracellular signals are required for long-term oligodendrocyte survival. Development 118(1) pp 283-295.

Barres BA, Jacobson R, Schmid R, Sendtner M, Raff MC (1993b) Does oligodendrocyte survival depend upon axons? Curr Biol 3 pp 489-497.

Barres BA, Lazar MA, Raff MC (1994a) A novel role for thyroid hormone, glucocorticoids and retinoic acid in timing oligodendrocyte development. Development 120(5) pp 1097-1108.

Barres BA, Raff MC, Gaese F, Bartke I, Dechant G, Barde YA (1994b) A crucial role for neurotrophin-3 in oligodendrocyte development. Nature 367(6461) pp 371-375.

Barrios A, Poole RJ, Durbin L, Brennan C, Holder N, Wilson SW (2003) Eph/Ephrin signalling regulates mesenchymal to epithelial transition of the paraxial mesoderm during somite morphogenesis. Curr Biol 13(18) pp 1571-1582.

Bartsch U, Kirchhoff F, Schachner M (1990) Highly sialylated N-CAM is expressed in adult mouse optic nerve and retina. J Neurocytol 19(4) pp 550-565.

Baumann N, Pham-Dinh D (2001) Biology of oligodendrocyte and myelin in the mammalian central nervous system. Physiol Rev 81(2) pp 871-927.

Beck KD, Powell-Braxton L, Widmer HR, Valverde J, Hefti F (1995) Igf1 gene disruption results in reduced brain size, CNS hypomyelination, and loss of hippocampal granule and striatal parvalbumin-containing neurons. Neuron 14(4) pp 717-730.

Behra M, Cousin X, Bertrand C, Vonesch JL, Biellmann D, Chatonnet A, Strahle U (2002) Acetylcholinesterase is required for neuronal and muscular development in the zebrafish embryo. Nat Neurosci 5(2) pp 111-118.

Benian GM, Kiff JE, Neckelmann N, Moerman DG, Waterston RH (1989) Sequence of an unusually large protein implicated in regulation of myosin activity in C. elegans. Nature 342(6245) pp 45-50.

Bennett P, Craig R, Starr R, Offer G (1986) The ultrastructural location of C-protein, X-protein and H-protein in rabbit muscle. J Muscle Res Cell Motil 7(6) pp 550-567.

Bierkamp C, Campos-Ortega JA (1993) A zebrafish homologue of the Drosophila neurogenic gene Notch and its pattern of transcription during early embryogenesis. Mech Dev 43(2-3) pp 87-100.

Bloor JW, Kiehart DP (2001) zipper Nonmuscle myosin-II functions downstream of PS2 integrin in Drosophila myogenesis and is necessary for myofibril formation. Dev Biol 239(2) pp 215-228.

Bögler O, Wren D, Barnett SC, Land H, Noble M (1990) Cooperation between two growth factors promotes extended self-renewal and inhibits differentiation of oligodendrocyte-type-2 astrocyte (O-2A) progenitor cells. Proc Natl Acad Sci U S A 87(16) pp 6368-6372.

Bosio A, Binczek E, Stoffel W (1996) Functional breakdown of the lipid bilayer of the myelin membrane in central and peripheral nervous system by disrupted galactocerebroside synthesis. Proc Natl Acad Sci U S A 93(23) pp 13280-13285.

Boss VC, Schmidt JT (1984) Activity and the formation of ocular dominance patches in dually innervated tectum of goldfish. J Neurosci 4(12) pp 2891-2905.

Braford MRJ, Northcutt RG (1983) Organisation of the diencephalon and pretectum of the ray-finned fishes. In: Fish neurobiology (Northcutt RG, Davis Roger E, eds), pp 117-163. Ann Arbor, Mich.: University of Michigan Press.

Braun PE (1984) Molecular organization of myelin. In: Myelin, 2nd Edition (Morell P, ed), pp 97-116. New York ; London: Plenum Press.

Braun PE, Sandillon F, Edwards A, Matthieu JM, Privat A (1988) Immunocytochemical localization by electron microscopy of 2'3'-cyclic nucleotide 3'-phosphodiesterase in developing oligodendrocytes of normal and mutant brain. J Neurosci 8(8) pp 3057-3066.

Bray GM, Villegas-Perez MP, Vidal-Sanz M, Aguayo AJ (1987) The use of peripheral nerve grafts to enhance neuronal survival, promote growth and permit terminal reconnections in the central nervous system of adult rats. J Exp Biol 132 pp 5-19.

Brenner S (1974) The genetics of Caenorhabditis elegans. Genetics 77(1) pp 71-94.

Brody BA, Kinney HC, Kloman AS, Gilles FH (1987) Sequence of central nervous system myelination in human infancy. I. An autopsy study of myelination. J Neuropathol Exp Neurol 46(3) pp 283-301.

Brösamle C, Halpern ME (2002) Characterization of myelination in the developing zebrafish. Glia 39(1) pp 47-57.

Bullard B (1984) A Large Troponin in Asynchronous Insect Flight-Muscle. Journal of Muscle Research and Cell Motility 5(2) pp 196-196.

Bunge MB, Bunge RP, Ris H (1961) Ultrastructural study of remyelination in an experimental lesion in adult cat spinal cord. J Biophys Biochem Cytol 10 p 67.

Bunge MB, Bunge RP, Pappas GD (1962) Electron microscopic demonstrations of connecitons between glia and myelin sheaths in the developing mammalian central nervous system. J Cell Biol 12 p 448.

Burrill JD, Easter SS, Jr. (1994) Development of the retinofugal projections in the embryonic and larval zebrafish (Brachydanio rerio). J Comp Neurol 346(4) pp 583-600.

Butt AM, Ibrahim M, Ruge FM, Berry M (1995) Biochemical subtypes of oligodendrocyte in the anterior medullary velum of the rat as revealed by the monoclonal antibody Rip. Glia 14(3) pp 185-197.

Butt AM, Ibrahim M, Gregson N, Berry M (1998) Differential expression of the L- and S-isoforms of myelin associated glycoprotein (MAG) in oligodendrocyte unit phenotypes in the adult rat anterior medullary velum. J Neurocytol 27(4) pp 271-280.

Buttery PC, ffrench-Constant C (1999) Laminin-2/integrin interactions enhance myelin membrane formation by oligodendrocytes. Mol Cell Neurosci 14(3) pp 199-212.

Cajal SR y (1909) Histologie du système nerveux de l'homme & des vertébrés. Texture of the nervous system of man and the vertebrates. An annotated and edited translation of the original Spanish text with the additions of the French version. 2002. Wien ; New York: Springer.

Cajal SR y (1913a) Sobre un nuevo proceder de impregnación de la neuroglia y sus resultados en los centros nerviosos del hombre y animales. Trab Lab Invest Biol Univ Madrid 11 pp 219-252.

Cajal SR y (1913b) Contribución al conocimiento de la neuroglia del cerebro humano. Trab Lab Invest Biol Univ Madrid 11 pp 255-315.

Calver AR, Hall AC, Yu WP, Walsh FS, Heath JK, Betsholtz C, Richardson WD (1998) Oligodendrocyte population dynamics and the role of PDGF in vivo. Neuron 20(5) pp 869-882.

Campagnoni AT (1988) Molecular biology of myelin proteins from the central nervous system. J Neurochem 51(1) pp 1-14.

Campagnoni AT, Pribyl TM, Campagnoni CW, Kampf K, Amur-Umarjee S, Landry CF, Handley VW, Newman SL, Garbay B, Kitamura K (1993) Structure and developmental regulation of Golli-mbp, a 105-kilobase gene that encompasses the myelin basic protein gene and is expressed in cells in the oligodendrocyte lineage in the brain. J Biol Chem 268(7) pp 4930-4938.

Campagnoni CW, Kampf K, Mason B, Handley VW, Campagnoni AT (1994) Isolation and characterization of a cDNA encoding the zebra finch myelin proteolipid protein. Neurochem Res 19(8) pp 1061-1065.

Campbell G, Kitching J, Anderson PN, Lieberman AR (2003) Effects of PNS and CNS glia on the maturation of regenerating optic nerve axons. submitted to Neuroreport.

Charles P, Hernandez MP, Stankoff B, Aigrot MS, Colin C, Rougon G, Zalc B, Lubetzki C (2000) Negative regulation of central nervous system myelination by polysialylated-neural cell adhesion molecule. Proc Natl Acad Sci U S A 97(13) pp 7585-7590.

Charles P, Reynolds R, Seilhean D, Rougon G, Aigrot MS, Niezgoda A, Zalc B, Lubetzki C (2002) Re-expression of PSA-NCAM by demyelinated axons: an inhibitor of remyelination in multiple sclerosis? Brain 125(Pt 9) pp 1972-1979.

Chen JN, Haffter P, Odenthal J, Vogelsang E, Brand M, van Eeden FJ, Furutani-Seiki M, Granato M, Hammerschmidt M, Heisenberg CP, Jiang YJ, Kane DA, Kelsh RN, Mullins MC, Nusslein-Volhard C (1996) Mutations affecting the cardiovascular system and other internal organs in zebrafish. Development 123 pp 293-302.

Cheng CM, Joncas G, Reinhardt RR, Farrer R, Quarles R, Janssen J, McDonald MP, Crawley JN, Powell-Braxton L, Bondy CA (1998) Biochemical and morphometric analyses show that myelination in the insulin-like growth factor 1 null brain is proportionate to its neuronal composition. J Neurosci 18(15) pp 5673-5681.

Chun M, Falkenthal S (1988) Ifm(2)2 is a myosin heavy chain allele that disrupts myofibrillar assembly only in the indirect flight muscle of Drosophila melanogaster. J Cell Biol 107(6 Pt 2) pp 2613-2621.

Chung K, Coggeshall RE (1984) The postnatal development of the tract of Lissauer in the rat. J Comp Neurol 229(4) pp 471-475.

Clark KA, McElhinny AS, Beckerle MC, Gregorio CC (2002) Striated muscle cytoarchitecture: An Intricate Web of Form and Function. Annu Rev Cell Dev Biol 18 pp 637-706.

Cline HT (1991) Activity-dependent plasticity in the visual systems of frogs and fish. Trends Neurosci 14(3) pp 104-111.

Cline HT, Constantine-Paton M (1989) NMDA receptor antagonists disrupt the retinotectal topographic map. Neuron 3(4) pp 413-426.

Cline HT, Debski EA, Constantine-Paton M (1987) N-methyl-D-aspartate receptor antagonist desegregates eye-specific stripes. Proc Natl Acad Sci U S A 84(12) pp 4342-4345.

Coetzee T, Fujita N, Dupree J, Shi R, Blight A, Suzuki K, Popko B (1996) Myelination in the absence of galactocerebroside and sulfatide: normal

structure with abnormal function and regional instability. Cell 86(2) pp 209-219.

Colello RJ, Devey LR, Imperato E, Pott U (1995) The chronology of oligodendrocyte differentiation in the rat optic nerve: evidence for a signaling step initiating myelination in the CNS. J Neurosci 15(11) pp 7665-7672.

Colman DR, Kreibich G, Frey AB, Sabatini DD (1982) Synthesis and incorporation of myelin polypeptides into CNS myelin. J Cell Biol 95(2 Pt 1) pp 598-608.

Colognato H, Baron W, Avellana-Adalid V, Relvas JB, Baron-Van Evercooren A, Georges-Labouesse E, ffrench-Constant C (2002) CNS integrins switch growth factor signalling to promote target-dependent survival. Nat Cell Biol 4(11) pp 833-841.

Compston A, Zajicek J, Sussman J, Webb A, Hall G, Muir D, Shaw C, Wood A, Scolding N (1997) Glial lineages and myelination in the central nervous system. J Anat 190 (Pt 2) pp 161-200.

Constantine-Paton M, Law MI (1978) Eye-specific termination bands in tecta of three-eyed frogs. Science 202(4368) pp 639-641.

Costa ML, Escaleira RC, Rodrigues VB, Manasfi M, Mermelstein CS (2002) Some distinctive features of zebrafish myogenesis based on unexpected distributions of the muscle cytoskeletal proteins actin, myosin, desmin, alpha-actinin, troponin and titin. Mech Dev 116(1-2) pp 95-104.

Currie PD, Ingham PW (1998) The generation and interpretation of positional information within the vertebrate myotome. Mech Dev 73(1) pp 3-21.

Davis RE, Schlumpf BE (1984) Visual recovery in goldfish following unilateral optic tectum ablation: evidence of competition between optic axons for tectal targets. Behav Brain Res 13(3) pp 287-291.

de Ferra F, Engh H, Hudson L, Kamholz J, Puckett C, Molineaux S, Lazzarini RA (1985) Alternative splicing accounts for the four forms of myelin basic protein. Cell 43(3 Pt 2) pp 721-727.

Debski EA, Cline HT (2002) Activity-dependent mapping in the retinotectal projection. Curr Opin Neurobiol 12(1) pp 93-99.

Deiters O (1865) Untersuchungen uber Gehirn und Ruckenmark des Menschen und der Saugethiere. Posthumously edited by M. Schultze. In, p 318. Braunschweig: F. Vieweg u. Sohn.

Del Rio Hortega P (1920) Estudios sobre la neuroglia. - La microglia y su transformación en células en bastoncito y cuerpos gránulo-adiposos. Trab Lab Invest Biol Univ Madrid 9 pp 1-46.

Del Rio-Hortega P (1919) El 'tercer elemento' de los centos nerviosos. I. La microglia en estado normal. II. - Intervencion de la microglia en los

procesos patologicos. III. Naturaleza probable de la microglia. Bol de la Soc Espanola de la Biol 9 pp 69-120.

Del Rio-Hortega P (1921) Estudios sobre la neuroglia. - La glia de escasas radiciones (oligodendroglia). Boletin del la Real Sociedad Espanola de la Historia Natural 21 pp 63-92.

Demerens C, Stankoff B, Logak M, Anglade P, Allinquant B, Couraud F, Zalc B, Lubetzki C (1996) Induction of myelination in the central nervous system by electrical activity. Proc Natl Acad Sci U S A 93(18) pp 9887-9892.

Dickinson PJ, Fanarraga ML, Griffiths IR, Barrie JM, Kyriakides E, Montague P (1996) Oligodendrocyte progenitors in the embryonic spinal cord express DM-20. Neuropathol Appl Neurobiol 22(3) pp 188-198.

Diehl HJ, Schaich M, Budzinski RM, Stoffel W (1986) Individual exons encode the integral membrane domains of human myelin proteolipid protein. Proc Natl Acad Sci U S A 83(24) pp 9807-9811.

Dlugosz AA, Antin PB, Nachmias VT, Holtzer H (1984) The relationship between stress fiber-like structures and nascent myofibrils in cultured cardiac myocytes. J Cell Biol 99(6) pp 2268-2278.

Driever W, Solnica-Krezel L, Schier AF, Neuhauss SC, Malicki J, Stemple DL, Stainier DY, Zwartkruis F, Abdelilah S, Rangini Z, Belak J, Boggs C (1996) A genetic screen for mutations affecting embryogenesis in zebrafish. Development 123 pp 37-46.

Dugas JC, Milligan BD, Barres BA (2001) Onset of CNS myelination is triggered by target innervation. Soc neurosci abstr 27 p Program No. 900.904.

Duncan D (1934) A relation between axone diameter and myelination as determined by measurement of myelinated spinal root fibres. J Comp Neurol 60 pp 437-471.

Durand B, Gao FB, Raff M (1997) Accumulation of the cyclin-dependent kinase inhibitor p27/Kip1 and the timing of oligodendrocyte differentiation. Embo J 16(2) pp 306-317.

Dusart I, Airaksinen MS, Sotelo C (1997) Purkinje cell survival and axonal regeneration are age dependent: an in vitro study. J Neurosci 17(10) pp 3710-3726.

Easter SS, Jr., Nicola GN (1996) The development of vision in the zebrafish (Danio rerio). Dev Biol 180(2) pp 646-663.

Easter SS, Jr., Nicola GN (1997) The development of eye movements in the zebrafish (Danio rerio). Dev Psychobiol 31(4) pp 267-276.

Easter SS, Jr., Rusoff AC, Kish PE (1981) The growth and organization of the optic nerve and tract in juvenile and adult goldfish. J Neurosci 1(8) pp 793-811.

Ehler E, Rothen BM, Hammerle SP, Komiyama M, Perriard JC (1999) Myofibrillogenesis in the developing chicken heart: assembly of Z-disk, M-line and the thick filaments. J Cell Sci 112 (Pt 10) pp 1529-1539.

Ekker M, Wegner J, Akimenko MA, Westerfield M (1992) Coordinate embryonic expression of three zebrafish engrailed genes. Development 116(4) pp 1001-1010.

Epstein HF, Thomson JN (1974) Temperature-sensitive mutation affecting myofilament assembly in Caenorhabditis elegans. Nature 250(467) pp 579-580.

Epstein HF, Fischman DA (1991) Molecular analysis of protein assembly in muscle development. Science 251(4997) pp 1039-1044.

Espinosa de los Monteros A, Zhang M, De Vellis J (1993) O2A progenitor cells transplanted into the neonatal rat brain develop into oligodendrocytes but not astrocytes. Proc Natl Acad Sci U S A 90(1) pp 50-54.

Etheridge L, Diiorio P, Sagerstrom CG (2002) A zebrafish unc-45-related gene expressed during muscle development. Dev Dyn 224(4) pp 457-460.

Etlinger JD, Zak R, Fischman DA (1976) Compositional studies of myofibrils from rabbit striated muscle. J Cell Biol 68(1) pp 123-141.

Felsenfeld AL, Curry M, Kimmel CB (1991) The fub-1 mutation blocks initial myofibril formation in zebrafish muscle pioneer cells. Dev Biol 148(1) pp 23-30.

Felsenfeld AL, Walker C, Westerfield M, Kimmel C, Streisinger G (1990) Mutations affecting skeletal muscle myofibril structure in the zebrafish. Development 108(3) pp 443-459.

Fernandez PA, Tang DG, Cheng L, Prochiantz A, Mudge AW, Raff MC (2000) Evidence that axon-derived neuregulin promotes oligodendrocyte survival in the developing rat optic nerve. Neuron 28(1) pp 81-90.

Fernandez-Moran H (1950) EM observations on the structure of the myelinated nerve sheath. Exp Cell Res 1 p 143.

Fernandez-Moran H (1954) The submicroscopic structure of nerve fibres. Prog Biophys 4 p 112.

Flechsig P (1901) Developmental (myelinogenetic) localisation of the cerebral cortex in the human subject. Lancet 2 pp 1027-1029.

Flechsig P (1920) Anatomie des Menschlichen Gehirns und Ruckenmarks auf myelogenetischer Grund-lange. Volume 1. Pages 9-37. Leipzig: Thieme.

Fok-Seang J, Miller RH (1994) Distribution and differentiation of A2B5+ glial precursors in the developing rat spinal cord. J Neurosci Res 37(2) pp 219-235.

Fruttiger M, Calver AR, Richardson WD (2000) Platelet-derived growth factor is constitutively secreted from neuronal cell bodies but not from axons. Curr Biol 10(20) pp 1283-1286.

Fruttiger M, Karlsson L, Hall AC, Abramsson A, Calver AR, Bostrom H, Willetts K, Bertold CH, Heath JK, Betsholtz C, Richardson WD (1999) Defective oligodendrocyte development and severe hypomyelination in PDGF-A knockout mice. Development 126(3) pp 457-467.

Fulton AB, L'Ecuyer T (1993) Cotranslational assembly of some cytoskeletal proteins: implications and prospects. J Cell Sci 105 (Pt 4) pp 867-871.

Fulton AB, Alftine C (1997) Organization of protein and mRNA for titin and other myofibril components during myofibrillogenesis in cultured chicken skeletal muscle. Cell Struct Funct 22(1) pp 51-58.

Fulton BP, Burne JF, Raff MC (1992) Visualization of O-2A progenitor cells in developing and adult rat optic nerve by quisqualate-stimulated cobalt uptake. J Neurosci 12(12) pp 4816-4833.

Funatsu T, Kono E, Higuchi H, Kimura S, Ishiwata S, Yoshioka T, Maruyama K, Tsukita S (1993) Elastic filaments in situ in cardiac muscle: deep-etch replica analysis in combination with selective removal of actin and myosin filaments. J Cell Biol 120(3) pp 711-724.

Fürst DO, Osborn M, Weber K (1989) Myogenesis in the mouse embryo: differential onset of expression of myogenic proteins and the involvement of titin in myofibril assembly. J Cell Biol 109(2) pp 517-527.

Fürst DO, Osborn M, Nave R, Weber K (1988) The organization of titin filaments in the half-sarcomere revealed by monoclonal antibodies in immunoelectron microscopy: a map of ten nonrepetitive epitopes starting at the Z line extends close to the M line. J Cell Biol 106(5) pp 1563-1572.

Gallo V, Armstrong RC (1995) Developmental and growth factor-induced regulation of nestin in oligodendrocyte lineage cells. J Neurosci 15(1 Pt 1) pp 394-406.

Gao FB, Durand B, Raff M (1997) Oligodendrocyte precursor cells count time but not cell divisions before differentiation. Curr Biol 7(2) pp 152-155.

Gard AL, Pfeiffer SE (1989) Oligodendrocyte progenitors isolated directly from developing telencephalon at a specific phenotypic stage: myelinogenic potential in a defined environment. Development 106(1) pp 119-132.

Gard AL, Pfeiffer SE (1993) Glial cell mitogens bFGF and PDGF differentially regulate development of O4+GalC- oligodendrocyte progenitors. Dev Biol 159(2) pp 618-630.

Gardinier MV, Macklin WB (1988) Myelin proteolipid protein gene expression in jimpy and jimpy(msd) mice. J Neurochem 51(2) pp 360-369.

Genoud S, Lappe-Siefke C, Goebbels S, Radtke F, Aguet M, Scherer SS, Suter U, Nave KA, Mantei N (2002) Notch1 control of oligodendrocyte differentiation in the spinal cord. J Cell Biol 158(4) pp 709-718.

Geren BB (1954) The formation from the schwann cell surface of myelin in peripheral nerves of chick embryos. Exp Cell Res 7 p 558.

Givogri MI, Costa RM, Schonmann V, Silva AJ, Campagnoni AT, Bongarzone ER (2002) Central nervous system myelination in mice with deficient expression of Notch1 receptor. J Neurosci Res 67(3) pp 309-320.

Goddard DR, Berry M, Butt AM (1999) In vivo actions of fibroblast growth factor-2 and insulin-like growth factor-I on oligodendrocyte development and myelination in the central nervous system. J Neurosci Res 57(1) pp 74-85.

Goldfine SM, Einheber S, Fischman DA (1991) Cell-free incorporation of newly synthesized myosin subunits into thick myofilaments. J Muscle Res Cell Motil 12(2) pp 161-170.

Golgi C (1873) Sulla struttura della sostanza grigia del cervello. Gazzetta Medica Italiana: Lombardia 33 pp 244-246.

Golgi C (1885) Sulla fina anatomia degli organi centrali del sistema nervoso. Reggio Emilia.: Tipografia di Stefano Calderini e Figlio,.

Goll DE, Stromer MH, Robson RM, Luke BM, Hammond KS (1977) Extraction, purification, and localization of alpha-actinin from asynchronous insect flight muscle. In: Insect flight muscle : proceedings of the Oxford Symposium, 3rd-5th April, 1977 (Tregear RT, ed), pp 15-40. Amsterdam ; Oxford: North-Holland.

Gordon AM, Homsher E, Regnier M (2000) Regulation of contraction in striated muscle. Physiol Rev 80(2) pp 853-924.

Gothlin GF (1913) Die doppelbrechenden Eigenschaften des Nervengewebes. K Sven Vetenskapsakad Handl 51(1) p 1.

Grafstein B (1963) Postnatal development of the transcallosal evoked response in the cerebral cortex of the cat. J Neurophysiol 26 pp 79-99.

Granato M, van Eeden FJ, Schach U, Trowe T, Brand M, Furutani-Seiki M, Haffter P, Hammerschmidt M, Heisenberg CP, Jiang YJ, Kane DA, Kelsh RN, Mullins MC, Odenthal J, Nusslein-Volhard C (1996) Genes controlling and mediating locomotion behavior of the zebrafish embryo and larva. Development 123 pp 399-413.

Gregori N, Proschel C, Noble M, Mayer-Proschel M (2002) The tripotential glial-restricted precursor (GRP) cell and glial development in the spinal cord: generation of bipotential oligodendrocyte-type-2 astrocyte progenitor cells and dorsal-ventral differences in GRP cell function. J Neurosci 22(1) pp 248-256.

Gregorio CC, Granzier H, Sorimachi H, Labeit S (1999) Muscle assembly: a titanic achievement? Curr Opin Cell Biol 11(1) pp 18-25.

Grima B, Zelenika D, Pessac B (1992) A novel transcript overlapping the myelin basic protein gene. J Neurochem 59(6) pp 2318-2323.

Grinspan JB, Franceschini B (1995) Platelet-derived growth factor is a survival factor for PSA-NCAM+ oligodendrocyte pre-progenitor cells. J Neurosci Res 41(4) pp 540-551.

Grinspan JB, Stern JL, Pustilnik SM, Pleasure D (1990) Cerebral white matter contains PDGF-responsive precursors to O2A cells. J Neurosci 10(6) pp 1866-1873.

Gyllensten L, Malmfors T (1963) Myelinization of the optic nerve and its dependence on visual function- a quantitative investigation in mice. J embryol exp morphol 2(1) pp 255-266.

Haddon C, Jiang YJ, Smithers L, Lewis J (1998) Delta-Notch signalling and the patterning of sensory cell differentiation in the zebrafish ear: evidence from the mind bomb mutant. Development 125(23) pp 4637-4644.

Haffter P, Granato M, Brand M, Mullins MC, Hammerschmidt M, Kane DA, Odenthal J, van Eeden FJ, Jiang YJ, Heisenberg CP, Kelsh RN, Furutani-Seiki M, Vogelsang E, Beuchle D, Schach U, Fabian C, Nusslein-Volhard C (1996) The identification of genes with unique and essential functions in the development of the zebrafish, Danio rerio. Development 123 pp 1-36.

Hall A, Giese NA, Richardson WD (1996) Spinal cord oligodendrocytes develop from ventrally derived progenitor cells that express PDGF alpha-receptors. Development 122(12) pp 4085-4094.

Hamano K, Iwasaki N, Takeya T, Takita H (1996) A quantitative analysis of rat central nervous system myelination using the immunohistochemical method for MBP. Brain Res Dev Brain Res 93(1-2) pp 18-22.

Hardy R, Reynolds R (1991) Proliferation and differentiation potential of rat forebrain oligodendroglial progenitors both in vitro and in vivo. Development 111(4) pp 1061-1080.

Hardy RJ, Friedrich VL, Jr. (1996) Progressive remodeling of the oligodendrocyte process arbor during myelinogenesis. Dev Neurosci 18(4) pp 243-254.

Hardy RJ, Lazzarini RA, Colman DR, Friedrich VL, Jr. (1996) Cytoplasmic and nuclear localization of myelin basic proteins reveals heterogeneity among oligodendrocytes. J Neurosci Res 46(2) pp 246-257.

Hart IK, Richardson WD, Bolsover SR, Raff MC (1989) PDGF and intracellular signaling in the timing of oligodendrocyte differentiation. J Cell Biol 109(6 Pt 2) pp 3411-3417.

Hatta K, Bremiller R, Westerfield M, Kimmel CB (1991) Diversity of expression of engrailed-like antigens in zebrafish. Development 112(3) pp 821-832.

Haug H, Kolln M, Rast A (1976) The postnatal development of myelinated nerve fibres in the visual cortex of the cat: a stereological and electron microscopical investigation. Cell Tissue Res 167(2) pp 265-288.

Hayes WP, Meyer RL (1989) Impulse blockade by intraocular tetrodotoxin during optic regeneration in goldfish: HRP-EM evidence that the formation of normal numbers of optic synapses and the elimination of exuberant optic fibers is activity independent. J Neurosci 9(4) pp 1414-1423.

He W, Ingraham C, Rising L, Goderie S, Temple S (2001) Multipotent stem cells from the mouse basal forebrain contribute GABAergic neurons and oligodendrocytes to the cerebral cortex during embryogenesis. J Neurosci 21(22) pp 8854-8862.

Herrera J, Yang H, Zhang SC, Proschel C, Tresco P, Duncan ID, Luskin M, Mayer-Proschel M (2001) Embryonic-derived glial-restricted precursor cells (GRP cells) can differentiate into astrocytes and oligodendrocytes in vivo. Exp Neurol 171(1) pp 11-21.

Hieber V, Agranoff BW, Goldman D (1992) Target-dependent regulation of retinal nicotinic acetylcholine receptor and tubulin RNAs during optic nerve regeneration in goldfish. J Neurochem 58(3) pp 1009-1015.

Hildebrand C, Remahl S, Persson H, Bjartmar C (1993) Myelinated nerve fibres in the CNS. Prog Neurobiol 40(3) pp 319-384.

Holley SA, Geisler R, Nusslein-Volhard C (2000) Control of her1 expression during zebrafish somitogenesis by a delta-dependent oscillator and an independent wave-front activity. Genes Dev 14(13) pp 1678-1690.

Hoover F, Hankin MH, Radel JD, Reese JS, Goldman D (1997) Axon-target interactions maintain synaptic gene expression in retinae transplanted to intracranial regions of the rat. Brain Res Mol Brain Res 51(1-2) pp 123-132.

Hudson LD (1990) Molecular Biology of myelin proteins in the central and peripheral nervous systems. Sems Neurosci 2 pp 483-496.

Hughes SM, Cho M, Karsch-Mizrachi I, Travis M, Silberstein L, Leinwand LA, Blau HM (1993) Three slow myosin heavy chains sequentially expressed in developing mammalian skeletal muscle. Dev Biol 158(1) pp 183-199.

Hunt D, Coffin RS, Anderson PN (2002) The Nogo receptor, its ligands and axonal regeneration in the spinal cord; A review. J Neurocytol 31(2) pp 93-120.

Ikenaka K, Kagawa T, Mikoshiba K (1992) Selective expression of DM-20, an alternatively spliced myelin proteolipid protein gene product, in developing nervous system and in nonglial cells. J Neurochem 58(6) pp 2248-2253.

Itoh M, Kim CH, Palardy G, Oda T, Jiang YJ, Maust D, Yeo SY, Lorick K, Wright GJ, Ariza-McNaughton L, Weissman AM, Lewis J, Chandrasekharappa

SC, Chitnis AB (2003) Mind bomb is a ubiquitin ligase that is essential for efficient activation of Notch signaling by Delta. Dev Cell 4(1) pp 67-82.

Jeserich G (1981) A morphological and biochemical study of myelinogenesis in fish brain. Dev Neurosci 4(5) pp 373-381.

Jeserich G (1982) Ingrowth of optic nerve fibers and onset of myelin ensheathment in the optic tectum of the trout (*Salmo gairdneri*). Cell Tissue Res 227(1) pp 201-211.

Jeserich G (1983) Protein analysis of myelin isolated from the CNS of fish: developmental and species comparisons. Neurochem Res 8(8) pp 957-970.

Jeserich G, Rahmann H (1977) Larval synaptogenesis in the optic tectum of the rainbow trout (*Salmo gairdneri*, Rich). IRCS Medical science 5 p 128.

Jeserich G, Waehneldt TV (1986) Characterization of antibodies against major fish CNS myelin proteins: immunoblot analysis and immunohistochemical localization of 36K and IP2 proteins in trout nerve tissue. J Neurosci Res 15(2) pp 147-158.

Jeserich G, Strelau J, Lanwert C (1997) Partial characterization of the 5'-flanking region of trout IP: a Po-like gene containing a PLP-like promoter. J Neurosci Res 50(5) pp 781-790.

Jiang YJ, Aerne BL, Smithers L, Haddon C, Ish-Horowicz D, Lewis J (2000) Notch signalling and the synchronization of the somite segmentation clock. Nature 408(6811) pp 475-479.

John GR, Shankar SL, Shafit-Zagardo B, Massimi A, Lee SC, Raine CS, Brosnan CF (2002) Multiple sclerosis: re-expression of a developmental pathway that restricts oligodendrocyte maturation. Nat Med 8(10) pp 1115-1121.

Kessaris N, Pringle N, Richardson WD (2001) Ventral neurogenesis and the neuron-glial switch. Neuron 31(5) pp 677-680.

Kim JY, Sun Q, Oglesbee M, Yoon SO (2003) The role of ErbB2 Signalling in the onset of terminal differentiation of oligodendrocytes *in vivo*. J Neurosci 23(13) pp 5561-5571.

Kimmel CB, Ballard WW, Kimmel SR, Ullmann B, Schilling TF (1995) Stages of embryonic development of the zebrafish. Dev Dyn 203(3) pp 253-310.

Kirschner DA, Blaurock AE (1992) Organisation, phylogenetic variations and dynamic transitions of myelin. In: Myelin : Biology and Chemistry (Martenson Russell E, ed), pp 1-53. Boca Raton FL USA: CRC Press.

Knapp PE, Skoff RP, Sprinkle TJ (1988) Differential expression of galactocerebroside, myelin basic protein, and 2',3'-cyclic nucleotide 3'-phosphohydrolase during development of oligodendrocytes in vitro. J Neurosci Res 21(2-4) pp 249-259.

Kölliker A (1893) Handbuch der Gewebelehre des Menschen. Volume 2, 2 Edition. Leipzig: Wilhem Englemann.

Kondo T, Raff M (2000a) Basic helix-loop-helix proteins and the timing of oligodendrocyte differentiation. Development 127(14) pp 2989-2998.

Kondo T, Raff M (2000b) The Id4 HLH protein and the timing of oligodendrocyte differentiation. Embo J 19(9) pp 1998-2007.

Kronquist KE, Crandall BF, Macklin WB, Campagnoni AT (1987) Expression of myelin proteins in the developing human spinal cord: cloning and sequencing of human proteolipid protein cDNA. J Neurosci Res 18(3) pp 395-401.

Kruger M, Wright J, Wang K (1991) Nebulin as a length regulator of thin filaments of vertebrate skeletal muscles: correlation of thin filament length, nebulin size, and epitope profile. J Cell Biol 115(1) pp 97-107.

Labeit S, Kolmerer B (1995) Titins: giant proteins in charge of muscle ultrastructure and elasticity. Science 270(5234) pp 293-296.

Labeit S, Kolmerer B, Linke WA (1997) The giant protein titin. Emerging roles in physiology and pathophysiology. Circ Res 80(2) pp 290-294.

Landry CF, Watson JB, Kashima T, Campagnoni AT (1994) Cellular influences on RNA sorting in neurons and glia: an in situ hybridization histochemical study. Brain Res Mol Brain Res 27(1) pp 1-11.

Langworthy OR (1933) Development of behaviour patterns and myelinization of the nervous system in the Human fetus and infant. Contrib Embryol 26(139) pp 1-65.

Lantermann AJ (1877) Ueber den feineren Bau der markhaltigen Nervenfasern. Arch Mikrosk Anat Entwicklungsmech 13 pp 1-8.

Lappe-Siefke C, Goebbels S, Gravel M, Nicksch E, Lee J, Braun PE, Griffiths IR, Nave KA (2003) Disruption of Cnp1 uncouples oligodendroglial functions in axonal support and myelination. Nat Genet 33(3) pp 366-374.

Lee AG (2001) Myelin: Delivery by raft. Curr Biol 11(2) pp R60-62.

Lees MB, Brostoff SW (1984) Proteins of myelin. In: Myelin, 2nd Edition (Morell P, ed), pp 197-217. New York ; London: Plenum Press.

Levine RL, Jacobson M (1975) Discontinuous mapping of retina onto tectum innervated by both eyes. Brain Res 98(1) pp 172-176.

LeVine SM, Wong D, Macklin WB (1990) Developmental expression of proteolipid protein and DM20 mRNAs and proteins in the rat brain. Dev Neurosci 12(4-5) pp 235-250.

Lewis J (2003) Autoinhibition with transcriptional delay: a simple mechanism for the zebrafish somitogenesis oscillator. Curr Biol 13(16) pp 1398-1408.

Lin Z, Lu MH, Schultheiss T, Choi J, Holtzer S, DiLullo C, Fischman DA, Holtzer H (1994) Sequential appearance of muscle-specific proteins in myoblasts as a function of time after cell division: evidence for a conserved myoblast differentiation program in skeletal muscle. Cell Motil Cytoskeleton 29(1) pp 1-19.

Looney GA, Elberger AJ (1986) Myelination of the corpus callosum in the cat: time course, topography, and functional implications. J Comp Neurol 248(3) pp 336-347.

LoRusso SM, Rhee D, Sanger JM, Sanger JW (1997) Premyofibrils in spreading adult cardiomyocytes in tissue culture: evidence for reexpression of the embryonic program for myofibrillogenesis in adult cells. Cell Motil Cytoskeleton 37(3) pp 183-198.

Lu QR, Sun T, Zhu Z, Ma N, Garcia M, Stiles CD, Rowitch DH (2002) Common developmental requirement for Olig function indicates a motor neuron/oligodendrocyte connection. Cell 109(1) pp 75-86.

Lu QR, Yuk D, Alberta JA, Zhu Z, Pawlitzky I, Chan J, McMahon AP, Stiles CD, Rowitch DH (2000) Sonic hedgehog--regulated oligodendrocyte lineage genes encoding bHLH proteins in the mammalian central nervous system. Neuron 25(2) pp 317-329.

Lund RD, Lund JS (1972) Development of synaptic patterns in the superior colliculus of the rat. Brain Res 42(1) pp 1-20.

Lunn ER, Perry VH, Brown MC, Rosen H, Gordon S (1989) Absence of Wallerian Degeneration does not Hinder Regeneration in Peripheral Nerve. Eur J Neurosci 1(1) pp 27-33.

Mack TG, Reiner M, Beirowski B, Mi W, Emanuelli M, Wagner D, Thomson D, Gillingwater T, Court F, Conforti L, Fernando FS, Tarlton A, Andressen C, Addicks K, Magni G, Ribchester RR, Perry VH, Coleman MP (2001) Wallerian degeneration of injured axons and synapses is delayed by a Ube4b/Nmnat chimeric gene. Nat Neurosci 4(12) pp 1199-1206.

Macklin WB (1992) The Myelin Proteolipid Protein Gene and its Expression. In: Myelin : biology and chemistry (Martenson RE, ed). Boca Raton, Ann Arbor, London, Tokyo: CRC Press.

Macklin WB, Campagnoni CW, Deininger PL, Gardinier MV (1987) Structure and expression of the mouse myelin proteolipid protein gene. J Neurosci Res 18(3) pp 383-394.

Mahaffey JW, Coutu MD, Fyrberg EA, Inwood W (1985) The flightless Drosophila mutant raised has two distinct genetic lesions affecting accumulation of myofibrillar proteins in flight muscles. Cell 40(1) pp 101-110.

Maier CE, Miller RH (1997) Notochord is essential for oligodendrocyte development in Xenopus spinal cord. J Neurosci Res 47(4) pp 361-371.

Marcus J, Popko B (2002) Galactolipids are molecular determinants of myelin development and axo-glial organization. Biochim Biophys Acta 1573(3) pp 406-413.

Marotte LR (1980) Goldfish retinotectal system: continuing development and synaptogenesis. J Comp Neurol 193(2) pp 319-334.

Martonosi AN (2000) Animal electricity, Ca2+ and muscle contraction. A brief history of muscle research. Acta Biochim Pol 47(3) pp 493-516.

Maruyama K (1997) Connectin/titin, giant elastic protein of muscle. Faseb J 11(5) pp 341-345.

Maruyama K, Murakami F, Ohashi K (1977) Connectin, an elastic protein of muscle. Comparative Biochemistry. J Biochem (Tokyo) 82(2) pp 339-345.

Matthews MA, Duncan D (1971) A quantitative study of morphological changes accompanying the initiation and progress of myelin production in the dorsal funiculus of the rat spinal cord. J Comp Neurol 142(1) pp 1-22.

Mayans O, van der Ven PF, Wilm M, Mues A, Young P, Furst DO, Wilmanns M, Gautel M (1998) Structural basis for activation of the titin kinase domain during myofibrillogenesis. Nature 395(6705) pp 863-869.

McKinnon RD, Smith C, Behar T, Smith T, Dubois-Dalcq M (1993) Distinct effects of bFGF and PDGF on oligodendrocyte progenitor cells. Glia 7(3) pp 245-254.

Meyer RL (1980) Mapping the normal and regenerating retinotectal projection of goldfish with autoradiographic methods. J Comp Neurol 189(2) pp 273-289.

Meyer RL (1983) Tetrodotoxin inhibits the formation of refined retinotopography in goldfish. Brain Res 282(3) pp 293-298.

Meyer-Franke A, Shen S, Barres BA (1999) Astrocytes induce oligodendrocyte processes to align with and adhere to axons. Mol Cell Neurosci 14(4-5) pp 385-397.

Miller RH (2002) Regulation of oligodendrocyte development in the vertebrate CNS. Prog Neurobiol 67(6) pp 451-467.

Moll W, Lanwert C, Jeserich G (2003) Molecular cloning, tissue expression, and partial characterization of the major fish CNS myelin protein 36k. Glia 44(1) pp 57-66.

Mora M, Di Blasi C, Barresi R, Morandi L, Brambati B, Jarre L, Cornelio F (1996) Developmental expression of dystrophin, dystrophin-associated glycoproteins and other membrane cytoskeletal proteins in human skeletal and heart muscle. Brain Res Dev Brain Res 91(1) pp 70-82.

Morin-Kensicki EM, Eisen JS (1997) Sclerotome development and peripheral nervous system segmentation in embryonic zebrafish. Development 124(1) pp 159-167.

Morris J, Jeserich G, Kinter K, Trapp B (2003) The novel teleost myelin protein, 36K, is a member of the short-chain dehydrogenase family. In: 3rd European Conference on Zebrafish and Medaka Genetics and Development (Rosa F, ed), pp P-125. Paris.

Mudhar HS, Pollock RA, Wang C, Stiles CD, Richardson WD (1993) PDGF and its receptors in the developing rodent retina and optic nerve. Development 118(2) pp 539-552.

Mullins MC, Hammerschmidt M, Haffter P, Nusslein-Volhard C (1994) Large-scale mutagenesis in the zebrafish: in search of genes controlling development in a vertebrate. Curr Biol 4(3) pp 189-202.

Murray M (1976) Regeneration of retinal axons into the goldfish optic tectum. J Comp Neurol 168(2) pp 175-195.

Nagashima K (1979) Ultrastructural study of myelinating cells and sub-pial astrocytes in developing rat spinal cord. J Neurol Sci 44(1) pp 1-12.

Nave KA (2001) Myelin-specific genes and their mutations in the mouse. In: Glial cell development : basic principles and clinical relevance (Jessen Kristjan R, Richardson William D, eds), pp 177-208. Oxford ; New York: Oxford University Press.

Nave KA, Lai C, Bloom FE, Milner RJ (1987) Splice site selection in the proteolipid protein (PLP) gene transcript and primary structure of the DM-20 protein of central nervous system myelin. Proc Natl Acad Sci U S A 84(16) pp 5665-5669.

Nishiyama A, Lin XH, Giese N, Heldin CH, Stallcup WB (1996a) Co-localization of NG2 proteoglycan and PDGF alpha-receptor on O2A progenitor cells in the developing rat brain. J Neurosci Res 43(3) pp 299-314.

Nishiyama A, Lin XH, Giese N, Heldin CH, Stallcup WB (1996b) Interaction between NG2 proteoglycan and PDGF alpha-receptor on O2A progenitor cells is required for optimal response to PDGF. J Neurosci Res 43(3) pp 315-330.

Noble M, Murray K, Stroobant P, Waterfield MD, Riddle P (1988) Platelet-derived growth factor promotes division and motility and inhibits premature differentiation of the oligodendrocyte/type-2 astrocyte progenitor cell. Nature 333(6173) pp 560-562.

Nona SN, Thomlinson AM, Bartlett CA, Scholes J (2000) Schwann cells in the regenerating fish optic nerve: evidence that CNS axons, not the glia, determine when myelin formation begins. J Neurocytol 29(4) pp 285-300.

Nona SN, Duncan A, Stafford CA, Maggs A, Jeserich G, Cronly-Dillon JR (1992) Myelination of regenerated axons in goldfish optic nerve by Schwann cells. J Neurocytol 21(6) pp 391-401.

Northcutt RG, Wulliman MF (1987) The visual system in teleost fishes: morphological patterns and trends. In: Sensory biology of aquatic animals. (Atema JF, Popper AN, Tavloga WN, eds), pp 515-552. New York: Springer-Verlag.

Norton WT, Cammer W (1984) Isolation and characterization of myelin. In: Myelin, 2nd Edition (Morell P, ed), pp 147-195. New York ; London: Plenum Press.

O'Donnell PT, Bernstein SI (1988) Molecular and ultrastructural defects in a Drosophila myosin heavy chain mutant: differential effects on muscle function produced by similar thick filament abnormalities. J Cell Biol 107(6 Pt 2) pp 2601-2612.

Ohara O, Dorit RL, Gilbert W (1989) One-sided polymerase chain reaction: the amplification of cDNA. Proc Natl Acad Sci U S A 86(15) pp 5673-5677.

Olivier C, Cobos I, Perez Villegas EM, Spassky N, Zalc B, Martinez S, Thomas JL (2001) Monofocal origin of telencephalic oligodendrocytes in the anterior entopeduncular area of the chick embryo. Development 128(10) pp 1757-1769.

Olson MD, Meyer RL (1991) The effect of TTX-activity blockade and total darkness on the formation of retinotopy in the goldfish retinotectal projection. J Comp Neurol 303(3) pp 412-423.

Omlin FX, Webster HD, Palkovits CG, Cohen SR (1982) Immunocytochemical localization of basic protein in major dense line regions of central and peripheral myelin. J Cell Biol 95(1) pp 242-248.

Ono K, Bansal R, Payne J, Rutishauser U, Miller RH (1995) Early development and dispersal of oligodendrocyte precursors in the embryonic chick spinal cord. Development 121(6) pp 1743-1754.

Oppenheim RW (1991) Cell death during development of the nervous system. Annu Rev Neurosci 14 pp 453-501.

Orentas DM, Miller RH (1996) The origin of spinal cord oligodendrocytes is dependent on local influences from the notochord. Dev Biol 177(1) pp 43-53.

Oumesmar BN, Vignais L, Duhamel-Clerin E, Avellana-Adalid V, Rougon G, Baron-Van Evercooren A (1995) Expression of the highly polysialylated neural cell adhesion molecule during postnatal myelination and following chemically induced demyelination of the adult mouse spinal cord. Eur J Neurosci 7(3) pp 480-491.

Park HC, Appel B (2003) Delta-Notch signaling regulates oligodendrocyte specification. Development 130(16) pp 3747-3755.

Park SK, Miller R, Krane I, Vartanian T (2001) The erbB2 gene is required for the development of terminally differentiated spinal cord oligodendrocytes. J Cell Biol 154(6) pp 1245-1258.

Patterson JM, Zakon HH (1996) Differential expression of proteins in muscle and electric organ, a muscle derivative. J Comp Neurol 370(3) pp 367-376.

Paus T, Collins DL, Evans AC, Leonard G, Pike B, Zijdenbos A (2001) Maturation of white matter in the human brain: a review of magnetic resonance studies. Brain Res Bull 54(3) pp 255-266.

Paus T, Zijdenbos A, Worsley K, Collins DL, Blumenthal J, Giedd JN, Rapoport JL, Evans AC (1999) Structural maturation of neural pathways in children and adolescents: in vivo study. Science 283(5409) pp 1908-1911.

Peachey LD (1965) The sarcoplasmic reticulum and transverse tubules of the frog's sartorius. J Cell Biol 25(3) pp Suppl:209-231.

Pellegrino RG, Spencer PS (1985) Schwann cell mitosis in response to regenerating peripheral axons in vivo. Brain Res 341(1) pp 16-25.

Penfield W (1924) Oligodendroglia and its relation to classical neuroglia. Brain 47 pp 430-452.

Penfield W (1932) Neuroglia, Normal and pathological. In: Cytology & cellular pathology of the nervous system (Penfield W, ed), pp 423-479. New York,: P.B. Hoeber Inc.

Perez Villegas EM, Olivier C, Spassky N, Poncet C, Cochard P, Zalc B, Thomas JL, Martinez S (1999) Early specification of oligodendrocytes in the chick embryonic brain. Dev Biol 216(1) pp 98-113.

Perry GW, Burmeister DW, Grafstein B (1987) Fast axonally transported proteins in regenerating goldfish optic axons. J Neurosci 7(3) pp 792-806.

Perry GW, Burmeister DW, Grafstein B (1990) Effect of target removal on goldfish optic nerve regeneration: analysis of fast axonally transported proteins. J Neurosci 10(10) pp 3439-3448.

Peters A (1960) The formation and structure of myelin sheaths in the central nervous system. J Biophys Biochem Cytol 8 pp 431-446.

Peters A (1962) Myelinogenesis in the central nervous system. In: Proceedings, IV international congress of neuropathology (Munich 1961) (Jacob H, ed), pp 50-54. Stuttgart: Thieme.

Peters A (1964) Observations on the connexions between myelin sheaths and glial cells in the optic nerve of young rats. J Anat 98 p 125.

Peters A, Palay SL, Webster HdeF. (1991) The fine structure of the nervous system : neurons and their supporting cells, 3rd Edition. New York, Oxford: Oxford University Press.

Pfeiffer SE, Warrington AE, Bansal R (1993) The oligodendrocyte and it's many cellular processes. Trends Cell Biol 3 pp 191-197.

Phillips GN, Jr., Fillers JP, Cohen C (1986) Tropomyosin crystal structure and muscle regulation. J Mol Biol 192(1) pp 111-131.

Piatigorsky J, Wistow GJ (1989) Enzyme/crystallins: gene sharing as an evolutionary strategy. Cell 57(2) pp 197-199.

Pollard TD (2000) Reflections on a quarter century of research on contractile systems. Trends Biochem Sci 25(12) pp 607-611.

Popko B (2003) Myelin: not just a conduit for conduction. Nat Genet 33(3) pp 327-328.

Porzio MA, Pearson AM (1977) Improved resolution of myofibrillar proteins with sodium dodecyl sulfate-polyacrylamide gel electrophoresis. Biochim Biophys Acta 490(1) pp 27-34.

Potter JD, Gergely J (1974) Troponin, tropomyosin, and actin interactions in the Ca2+ regulation of muscle contraction. Biochemistry 13(13) pp 2697-2703.

Pribyl TM, Campagnoni CW, Kampf K, Kashima T, Handley VW, McMahon J, Campagnoni AT (1993) The human myelin basic protein gene is included within a 179-kilobase transcription unit: expression in the immune and central nervous systems. Proc Natl Acad Sci U S A 90(22) pp 10695-10699.

Pribyl TM, Campagnoni CW, Kampf K, Ellison JA, Landry CF, Kashima T, McMahon J, Campagnoni AT (1996) Expression of the myelin basic protein gene locus in neurons and oligodendrocytes in the human fetal central nervous system. J Comp Neurol 374(3) pp 342-353.

Price MG, Landsverk ML, Barral JM, Epstein HF (2002) Two mammalian UNC-45 isoforms are related to distinct cytoskeletal and muscle-specific functions. J Cell Sci 115(Pt 21) pp 4013-4023.

Pringle NP, Richardson WD (1993) A singularity of PDGF alpha-receptor expression in the dorsoventral axis of the neural tube may define the origin of the oligodendrocyte lineage. Development 117(2) pp 525-533.

Pringle NP, Mudhar HS, Collarini EJ, Richardson WD (1992) PDGF receptors in the rat CNS: during late neurogenesis, PDGF alpha-receptor expression appears to be restricted to glial cells of the oligodendrocyte lineage. Development 115(2) pp 535-551.

Privat A, Jacque C, Bourre JM, Dupouey P, Baumann N (1979) Absence of the major dense line in myelin of the mutant mouse "shiverer". Neurosci Lett 12(1) pp 107-112.

Raff MC, Williams BP, Miller RH (1984) The in vitro differentiation of a bipotential glial progenitor cell. Embo J 3(8) pp 1857-1864.

Raff MC, Durand B, Gao FB (1998) Cell number control and timing in animal development: the oligodendrocyte cell lineage. Int J Dev Biol 42(3 Spec No) pp 263-267.

Raff MC, Lillien LE, Richardson WD, Burne JF, Noble MD (1988) Platelet-derived growth factor from astrocytes drives the clock that times oligodendrocyte development in culture. Nature 333(6173) pp 562-565.

Rager GH (1980) Development of the retinotectal projection in the chicken. Adv Anat Embryol Cell Biol 63 pp 1-90.

Raine C, S (1984) Morphology of myelin and myelination. In: Myelin, 2nd Edition (Morell P, ed), pp 1-41. New York ; London: Plenum Press.

Ramachandran I, Terry M, Ferrari MB (2003) Skeletal muscle myosin cross-bridge cycling is necessary for myofibrillogenesis. Cell Motil Cytoskeleton 55(1) pp 61-72.

Rankin EC, Cook JE (1986) Topographic refinement of the regenerating retinotectal projection of the goldfish in standard laboratory conditions: a quantitative WGA-HRP study. Exp Brain Res 63(2) pp 409-420.

Ranvier LA (1872) Recherches sur l'histologie et la physiologie des nerfs. Arch Physiol Norm Pathol 4 pp 129-149.

Ranvier LA (1878) leçons sur l'histologie du système Nerveux. Paris: F. Savy.

Rao MS, Mayer-Proschel M (1997) Glial-restricted precursors are derived from multipotent neuroepithelial stem cells. Dev Biol 188(1) pp 48-63.

Rao MS, Noble M, Mayer-Proschel M (1998) A tripotential glial precursor cell is present in the developing spinal cord. Proc Natl Acad Sci U S A 95(7) pp 3996-4001.

Relvas JB, Setzu A, Baron W, Buttery PC, LaFlamme SE, Franklin RJ, ffrench-Constant C (2001) Expression of dominant-negative and chimeric subunits reveals an essential role for beta1 integrin during myelination. Curr Biol 11(13) pp 1039-1043.

Remahl S, Hildebrand C (1990) Relation between axons and oligodendroglial cells during initial myelination. I. The glial unit. J Neurocytol 19(3) pp 313-328.

Remahl S, Hildebrand C (1990) Relations between axons and oligodendroglial cells during initial myelination. II. The individual axon. J Neurocytol 19(6) pp 883-898.

Reynolds R, Wilkin GP (1988) Development of macroglial cells in rat cerebellum. II. An in situ immunohistochemical study of oligodendroglial lineage from precursor to mature myelinating cell. Development 102(2) pp 409-425.

Rhee D, Sanger JM, Sanger JW (1994) The premyofibril: evidence for its role in myofibrillogenesis. Cell Motil Cytoskeleton 28(1) pp 1-24.

Richardson PM, McGuinness UM, Aguayo AJ (1980) Axons from CNS neurons regenerate into PNS grafts. Nature 284(5753) pp 264-265.

Richardson WD (2001) Oligodendrocyte Development. In: Glial cell development : basic principles and clinical relevance (Jessen Kristjan R, Richardson William D, eds), pp 21-54. Oxford ; New York: Oxford University Press.

Richardson WD, Pringle N, Mosley MJ, Westermark B, Dubois-Dalcq M (1988) A role for platelet-derived growth factor in normal gliogenesis in the central nervous system. Cell 53(2) pp 309-319.

Richardson WD, Smith HK, Sun T, Pringle NP, Hall A, Woodruff R (2000) Oligodendrocyte lineage and the motor neuron connection. Glia 29(2) pp 136-142.

Rios E, Pizarro G (1991) Voltage sensor of excitation-contraction coupling in skeletal muscle. Physiol Rev 71(3) pp 849-908.

Roach A, Takahashi N, Pravtcheva D, Ruddle F, Hood L (1985) Chromosomal mapping of mouse myelin basic protein gene and structure and transcription of the partially deleted gene in shiverer mutant mice. Cell 42(1) pp 149-155.

Robertson WF (1897) The normal histology and pathology of the neuroglia (in relation specially to mental Diseases). Journal of Mental science 43 pp 733-752.

Robertson WF (1900) A microscopic demonstration of the normal and pathological Histology of mesoglia cells. Journal of Mental science 46 p 724.

Robinson S, Miller R (1996) Environmental enhancement of growth factor-mediated oligodendrocyte precursor proliferation. Mol Cell Neurosci 8(1) pp 38-52.

Robinson S, Tani M, Strieter RM, Ransohoff RM, Miller RH (1998) The chemokine growth-regulated oncogene-alpha promotes spinal cord oligodendrocyte precursor proliferation. J Neurosci 18(24) pp 10457-10463.

Rodriguez-Pena A (1999) Oligodendrocyte development and thyroid hormone. J Neurobiol 40(4) pp 497-512.

Rogister B, Ben-Hur T, Dubois-Dalcq M (1999) From neural stem cells to myelinating oligodendrocytes. Mol Cell Neurosci 14(4-5) pp 287-300.

Rosenbluth J (1980) Peripheral myelin in the mouse mutant Shiverer. J Comp Neurol 193(3) pp 729-739.

Roy S, Wolff C, Ingham PW (2001) The u-boot mutation identifies a Hedgehog-regulated myogenic switch for fiber-type diversification in the zebrafish embryo. Genes Dev 15(12) pp 1563-1576.

Rozeik C, Von Keyserlingk D (1987) The sequence of myelination in the brainstem of the rat monitored by myelin basic protein immunohistochemistry. Dev Brain Res 35 pp 183-190.

Sanger JW, Chowrashi P, Shaner NC, Spalthoff S, Wang J, Freeman NL, Sanger JM (2002) Myofibrillogenesis in skeletal muscle cells. Clin Orthop (403 Suppl) pp S153-162.

Sarlieve LL, Fabre M, Susz J, Matthieu JM (1983) Investigations on myelination in vitro: IV. "Myelin-like" or premyelin structures in cultures of dissociated brain cells from 14--15-day-old embryonic mice. J Neurosci Res 10(2) pp 191-210.

Schachner M, Bartsch U (2000) Multiple functions of the myelin-associated glycoprotein MAG (siglec-4a) in formation and maintenance of myelin. Glia 29(2) pp 154-165.

Scherer WJ, Udin SB (1989) N-methyl-D-aspartate antagonists prevent interaction of binocular maps in Xenopus tectum. J Neurosci 9(11) pp 3837-3843.

Schmidt HD (1874) on the construction of the dark or double bordered nerve fibre. Mon Microsc, J (London) 11 pp 200-221.

Schmidt JT (1990) Long-term potentiation and activity-dependent retinotopic sharpening in the regenerating retinotectal projection of goldfish: common sensitive period and sensitivity to NMDA blockers. J Neurosci 10(1) pp 233-246.

Schmitt FO, Bear RS (1939) The ultrastructure of the nerve axon sheath. Biol Rev 14 p 27.

Schmitt FO, Bear RS, Clark GL (1935) X-ray diffraction studies on nerve. Radiology 25 p 131.

Schmitt FO, Bear RS, Palmer JJ (1941) X-ray diffraction studies of the nerve myelin sheath. J Cell Comp Physiol 18 p 31.

Schnadelbach O, Ozen I, Blaschuk OW, Meyer RL, Fawcett JW (2001) N-cadherin is involved in axon-oligodendrocyte contact and myelination. Mol Cell Neurosci 17(6) pp 1084-1093.

Scholes J (1981) Ribbon optic nerves and axonal growth in the retinal projection to the tectum. In: Development in the nervous system. (Garrod DR, Fieldman JD, eds), pp 181-214. Cambridge: Cambridge university press.

Scholes J (1991) The design of the optic nerve in fish. Vis Neurosci 7(1-2) pp 129-139.

Schreyer DJ, Jones EG (1982) Growth and target finding by axons of the corticospinal tract in prenatal and postnatal rats. Neuroscience 7(8) pp 1837-1853.

Schultheiss T, Lin ZX, Lu MH, Murray J, Fischman DA, Weber K, Masaki T, Imamura M, Holtzer H (1990) Differential distribution of subsets of myofibrillar proteins in cardiac nonstriated and striated myofibrils. J Cell Biol 110(4) pp 1159-1172.

Schwab ME, Schnell L (1989) Region-specific appearance of myelin constituents in the developing rat spinal cord. J Neurocytol 18(2) pp 161-169.

Schwann T (1839) Mikroskopische Untersuchungen uber die Uebereinstimmung in der Struktur und dem Wachsthum der Thiere und Pflanzen. Berlin: Reimer.

Schwartz IR, Pappas GD, Bennett MV (1975) The fine structure of electrocytes in weakly electric teleosts. J Neurocytol 4(1) pp 87-114.

Sefton AJ, Lam K (1984) Quantitative and morphological studies on developing optic axons in normal and enucleated albino rats. Exp Brain Res 57(1) pp 107-117.

Seggie J, Berry M (1972) Ontogeny of interhemispheric evoked potentials in the rat: significance of myelination of the corpus callosum. Exp Neurol 35(2) pp 215-232.

Sehnert AJ, Huq A, Weinstein BM, Walker C, Fishman M, Stainier DY (2002) Cardiac troponin T is essential in sarcomere assembly and cardiac contractility. Nat Genet 31(1) pp 106-110.

Sharma SC (1973) Anomalous retinal projection after removal of contralateral optic tectum in adult goldfish. Exp Neurol 41(3) pp 661-669.

Shrager P, Novakovic SD (1995) Control of myelination, axonal growth, and synapse formation in spinal cord explants by ion channels and electrical activity. Brain Res Dev Brain Res 88(1) pp 68-78.

Simon DK, Prusky GT, O'Leary DD, Constantine-Paton M (1992) N-methyl-D-aspartate receptor antagonists disrupt the formation of a mammalian neural map. Proc Natl Acad Sci U S A 89(22) pp 10593-10597.

Sjostrand FS (1949) EM study of the retinal rods in the Guinea pig eye. J Cell Comp Physiol 33 p 383.

Skoff RP (1978) The pattern of myelination along the developing rat optic nerve. Neurosci Lett 7(2-3) pp 191-196.

Skoff RP, Price DL, Stocks A (1976a) Electron microscopic autoradiographic studies of gliogenesis in rat optic nerve. I. Cell proliferation. J Comp Neurol 169(3) pp 291-312.

Skoff RP, Price DL, Stocks A (1976b) Electron microscopic autoradiographic studies of gliogenesis in rat optic nerve. II. Time of origin. J Comp Neurol 169(3) pp 313-334.

Skoff RP, Toland D, Nast E (1980) Pattern of myelination and distribution of neuroglial cells along the developing optic system of the rat and rabbit. J Comp Neurol 191(2) pp 237-253.

Small RK, Riddle P, Noble M (1987) Evidence for migration of oligodendrocyte--type-2 astrocyte progenitor cells into the developing rat optic nerve. Nature 328(6126) pp 155-157.

Somjen GG (1988) Nervenkitt: notes on the history of the concept of neuroglia. Glia 1(1) pp 2-9.

Sommer I, Schachner M (1981) Monoclonal antibodies (O1 to O4) to oligodendrocyte cell surfaces: an immunocytological study in the central nervous system. Dev Biol 83(2) pp 311-327.

Spassky N, Heydon K, Mangatal A, Jankovski A, Olivier C, Queraud-Lesaux F, Goujet-Zalc C, Thomas JL, Zalc B (2001) Sonic hedgehog-dependent emergence of oligodendrocytes in the telencephalon: evidence for a source of oligodendrocytes in the olfactory bulb that is independent of PDGFRalpha signaling. Development 128(24) pp 4993-5004.

Spassky N, Goujet-Zalc C, Parmantier E, Olivier C, Martinez S, Ivanova A, Ikenaka K, Macklin W, Cerruti I, Zalc B, Thomas JL (1998) Multiple restricted origin of oligodendrocytes. J Neurosci 18(20) pp 8331-8343.

Speidel CC (1964) *In Vivo* Studies of Myelinated Nerve Fibres. Int Rev Cytol 16 pp 173-231.

Sperry RW (1948) Patterning of central synapses in regeneration of the optic nerve in Teleosts. Physiol Zoöl 21 pp 351-361.

Springer AD, Cohen SM (1981) Optic fiber segregation in goldfish with two eyes innervating one tectal lobe. Brain Res 225(1) pp 23-36.

Squire JM (1997) Architecture and function in the muscle sarcomere. Curr Opin Struct Biol 7(2) pp 247-257.

Stainier DY, Fouquet B, Chen JN, Warren KS, Weinstein BM, Meiler SE, Mohideen MA, Neuhauss SC, Solnica-Krezel L, Schier AF, Zwartkruis F, Stemple DL, Malicki J, Driever W, Fishman MC (1996) Mutations affecting the formation and function of the cardiovascular system in the zebrafish embryo. Development 123 pp 285-292.

Stensaas LJ (1977) The ultrastructure of astrocytes, oligodendrocytes, and microglia in the optic nerve of urodele amphibians (A. punctatum, T. pyrrhogaster, T. viridescens). J Neurocytol 6(3) pp 269-286.

Stevens B, Porta S, Haak LL, Gallo V, Fields RD (2002) Adenosine: a neuron-glial transmitter promoting myelination in the CNS in response to action potentials. Neuron 36(5) pp 855-868.

Stickney HL, Barresi MJ, Devoto SH (2000) Somite development in zebrafish. Dev Dyn 219(3) pp 287-303.

Stickney HL, Schmutz J, Woods IG, Holtzer CC, Dickson MC, Kelly PD, Myers RM, Talbot WS (2002) Rapid mapping of zebrafish mutations with SNPs and oligonucleotide microarrays. Genome Res 12(12) pp 1929-1934.

Streisinger G, Walker C, Dower N, Knauber D, Singer F (1981) Production of clones of homozygous diploid zebra fish (Brachydanio rerio). Nature 291(5813) pp 293-296.

Stuermer CA (1988) Retinotopic organization of the developing retinotectal projection in the zebrafish embryo. J Neurosci 8(12) pp 4513-4530.

Stuermer CA, Easter SS, Jr. (1984) A comparison of the normal and regenerated retinotectal pathways of goldfish. J Comp Neurol 223(1) pp 57-76.

Sun T, Pringle NP, Hardy AP, Richardson WD, Smith HK (1998) Pax6 influences the time and site of origin of glial precursors in the ventral neural tube. Mol Cell Neurosci 12(4-5) pp 228-239.

Suzuki M, Raisman G (1992) The glial framework of central white matter tracts: segmented rows of contiguous interfascicular oligodendrocytes and solitary astrocytes give rise to a continuous meshwork of transverse and longitudinal processes in the adult rat fimbria. Glia 6(3) pp 222-235.

Suzuki M, Raisman G (1994) Multifocal pattern of postnatal development of the macroglial framework of the rat fimbria. Glia 12(4) pp 294-308.

Szabo T (1960) Development of the electric organ of mormyridae. Nature 188 pp 760-762.

Takahashi N, Roach A, Teplow DB, Prusiner SB, Hood L (1985) Cloning and characterization of the myelin basic protein gene from mouse: one gene can encode both 14 kd and 18.5 kd MBPs by alternate use of exons. Cell 42(1) pp 139-148.

Tauber H, Waehneldt TV, Neuhoff V (1980) Myelination in rabbit optic nerves is accelerated by artificial eye opening. Neurosci Lett 16(3) pp 235-238.

Tekki-Kessaris N, Woodruff R, Hall AC, Gaffield W, Kimura S, Stiles CD, Rowitch DH, Richardson WD (2001) Hedgehog-dependent oligodendrocyte lineage specification in the telencephalon. Development 128(13) pp 2545-2554.

Temple S, Raff MC (1985) Differentiation of a bipotential glial progenitor cell in a single cell microculture. Nature 313(5999) pp 223-225.

Thisse C, Thisse B, Schilling TF, Postlethwait JH (1993) Structure of the zebrafish snail1 gene and its expression in wild-type, spadetail and no tail mutant embryos. Development 119(4) pp 1203-1215.

Timsit S, Martinez S, Allinquant B, Peyron F, Puelles L, Zalc B (1995) Oligodendrocytes originate in a restricted zone of the embryonic ventral neural tube defined by DM-20 mRNA expression. J Neurosci 15(2) pp 1012-1024.

Timsit SG, Bally-Cuif L, Colman DR, Zalc B (1992) DM-20 mRNA is expressed during the embryonic development of the nervous system of the mouse. J Neurochem 58(3) pp 1172-1175.

Tokumoto YM, Apperly JA, Gao FB, Raff MC (2002) Posttranscriptional regulation of p18 and p27 Cdk inhibitor proteins and the timing of oligodendrocyte differentiation. Dev Biol 245(1) pp 224-234.

Trapp BD, Bernier L, Andrews SB, Colman DR (1988) Cellular and subcellular distribution of 2',3'-cyclic nucleotide 3'-phosphodiesterase and its mRNA in the rat central nervous system. J Neurochem 51(3) pp 859-868.

Trapp BD, Nishiyama A, Cheng D, Macklin W (1997) Differentiation and death of premyelinating oligodendrocytes in developing rodent brain. J Cell Biol 137(2) pp 459-468.

Trapp BD, Moench T, Pulley M, Barbosa E, Tennekoon G, Griffin J (1987) Spatial segregation of mRNA encoding myelin-specific proteins. Proc Natl Acad Sci U S A 84(21) pp 7773-7777.

Trinick J (1994) Titin and nebulin: protein rulers in muscle? Trends Biochem Sci 19(10) pp 405-409.

Trinick J, Tskhovrebova L (1999) Titin: a molecular control freak. Trends Cell Biol 9(10) pp 377-380.

Tsai HH, Frost E, To V, Robinson S, Ffrench-Constant C, Geertman R, Ransohoff RM, Miller RH (2002) The chemokine receptor CXCR2 controls positioning of oligodendrocyte precursors in developing spinal cord by arresting their migration. Cell 110(3) pp 373-383.

Tskhovrebova L, Trinick J (2002) Role of titin in vertebrate striated muscle. Philos Trans R Soc Lond B Biol Sci 357(1418) pp 199-206.

Tskhovrebova L, Trinick J (2003) Titin: Properties and family relationships. Nature Rev Mol Cell Biol 4 pp 679-689.

Udin SB, Scherer WJ, Constantine-Paton M (1992) Physiological effects of chronic and acute application of N-methyl-D-aspartate and 5-amino-phosphonovaleric acid to the optic tectum of Rana pipiens frogs. Neuroscience 49(3) pp 739-747.

Vale RD, Milligan RA (2000) The way things move: looking under the hood of molecular motor proteins. Science 288(5463) pp 88-95.

Van der Knaap MS, Valk J (1995) Myelination and retarded myelination. In: Magnetic resonance of myelin, myelination, and myelin disorders (Van der Knaap MS, Valk J, eds), pp 31-57. Berlin ; [London]: Springer.

van der Loop FT, Schaart G, Langmann W, Ramaekers FC, Viebahn C (1992) Expression and organization of muscle specific proteins during the early developmental stages of the rabbit heart. Anat Embryol (Berl) 185(5) pp 439-450.

Van der Ven PF, Ehler E, Perriard JC, Furst DO (1999) Thick filament assembly occurs after the formation of a cytoskeletal scaffold. J Muscle Res Cell Motil 20(5-6) pp 569-579.

van der Ven PF, Bartsch JW, Gautel M, Jockusch H, Furst DO (2000) A functional knock-out of titin results in defective myofibril assembly. J Cell Sci 113 (Pt 8) pp 1405-1414.

van Straaten HW, Hekking JW, Thors F, Wiertz-Hoessels EL, Drukker J (1985a) Induction of an additional floor plate in the neural tube. Acta Morphol Neerl Scand 23(2) pp 91-97.

van Straaten HW, Thors F, Wiertz-Hoessels L, Hekking J, Drukker J (1985b) Effect of a notochordal implant on the early morphogenesis of the neural tube and neuroblasts: histometrical and histological results. Dev Biol 110(1) pp 247-254.

Vanegas, H. (1984) Comparative neurology of the optic tectum. New York ; London: Plenum Press.

Vartanian T, Fischbach G, Miller R (1999) Failure of spinal cord oligodendrocyte development in mice lacking neuregulin. Proc Natl Acad Sci U S A 96(2) pp 731-735.

Vernier JM (1969) Table chronologique du développment embryonnaire de la truite arc-en-ciel, *Salmo gairdneri* Rich.1836. Ann d'embryologie et de Morphogenèse 2(4) pp 495-520.

Vidal-Sanz M, Bray GM, Villegas-Perez MP, Thanos S, Aguayo AJ (1987) Axonal regeneration and synapse formation in the superior colliculus by retinal ganglion cells in the adult rat. J Neurosci 7(9) pp 2894-2909.

Virchow R (1846) Uber das granulirte Ansehen der Wandungen der Gehirnventrikel. Allg Ztschr f Psychiat 3 pp 242-250.

Virchow R (1854) Ueber das ausgebreitete Vorkommen einer dem Nervenmark analogen Substanz in den tierischen Geweben. Virchows Arch Pathol Anat 6 p 562.

Virchow R (1858) Cellularpathologie in ihre Begrundung auf physiologische und pathologische Gewebelehre. Berlin: A. Hirschwald, Berlin.

Vogt C, Vogt O (1908) Die myelo-architektonischen Rindenfelder des Menschen. Neurol Centralbl 27 p 137.

von Monakow C (1900) Ueber die Projektions und Associationszentren im Grosshirn. Monatschr f Psychiat 8 p 405.

von Monakow C (1910) Demonstration von makro- und mikroskopischen Praeparaten. Neurol Centralbl 29 p 110.

Voyvodic JT (1989) Target size regulates calibre and myelination of sympathetic axons. Nature 342(6248) pp 430-433.

Wachtel AM (1964) The ultrastructural relationships of electric organs and muscle. 1. Filamentous systems. J Morphol 114 pp 325-359.

Waehneldt TV, Jeserich G (1984) Biochemical characterization of the central nervous system myelin proteins of the rainbow trout, Salmo gairdneri. Brain Res 309(1) pp 127-134.

Waehneldt TV, Stoklas S, Jeserich G, Matthieu JM (1986) Central nervous system myelin of teleosts: comparative electrophoretic analysis of its proteins by staining and immunoblotting. Comp Biochem Physiol B 84(3) pp 273-278.

Wang K, McClure J, Tu A (1979) Titin: major myofibrillar components of striated muscle. Proc Natl Acad Sci U S A 76(8) pp 3698-3702.

Wang K, Ramirez-Mitchell R, Palter D (1984) Titin is an extraordinarily long, flexible, and slender myofibrillar protein. Proc Natl Acad Sci U S A 81(12) pp 3685-3689.

Wang S, Sdrulla A, Johnson JE, Yokota Y, Barres BA (2001) A role for the helix-loop-helix protein Id2 in the control of oligodendrocyte development. Neuron 29(3) pp 603-614.

Wang S, Sdrulla AD, diSibio G, Bush G, Nofziger D, Hicks C, Weinmaster G, Barres BA (1998) Notch receptor activation inhibits oligodendrocyte differentiation. Neuron 21(1) pp 63-75.

Warrington AE, Barbarese E, Pfeiffer SE (1993) Differential myelinogenic capacity of specific developmental stages of the oligodendrocyte lineage upon transplantation into hypomyelinating hosts. J Neurosci Res 34(1) pp 1-13.

Warton SS, McCart R (1989) Synaptogenesis in the stratum griseum superficiale of the rat superior colliculus. Synapse 3(2) pp 136-148.

Waterston RH, Thomson JN, Brenner S (1980) Mutants with altered muscle structure of Caenorhabditis elegans. Dev Biol 77(2) pp 271-302.

Webster Hd, Martin R, O'Connell MF (1973) The relationships between interphase Schwann cells and axons before myelination: a quantitative electron microscopic study. Dev Biol 32(2) pp 401-416.

Weigert, C. (1895) Beiträge zur Kenntnis der normalen menschlichen Neuroglia. Frankfurt a. M.: M. Diesterweg.

Weinberg ES, Allende ML, Kelly CS, Abdelhamid A, Murakami T, Andermann P, Doerre OG, Grunwald DJ, Riggleman B (1996) Developmental regulation of zebrafish MyoD in wild-type, no tail and spadetail embryos. Development 122(1) pp 271-280.

Westerfield M (2000) The zebrafish book. A guide for the laboratory use of zebrafish (Danio rerio). 4th Edition: University of Oregon Press, Eugene. U.S.A.

Westin J, Lardelli M (1997) Three novel Notch genes in zebrafish: implications for vertebrate Notch gene evolution and function. Dev Genes Evol 207 pp 51-63.

White GE, Petry CM, Schachat F (2003) The pathway of myofibrillogenesis determines the interrelationship between myosin and paramyosin synthesis in Caenorhabditis elegans. J Exp Biol 206(Pt 11) pp 1899-1906.

Whiting A, Wardale J, Trinick J (1989) Does titin regulate the length of muscle thick filaments? J Mol Biol 205(1) pp 263-268.

Wilson SW, Ross LS, Parrett T, Easter SS, Jr. (1990) The development of a simple scaffold of axon tracts in the brain of the embryonic zebrafish, Brachydanio rerio. Development 108(1) pp 121-145.

Windebank AJ, Wood P, Bunge RP, Dyck PJ (1985) Myelination determines the caliber of dorsal root ganglion neurons in culture. J Neurosci 5(6) pp 1563-1569.

Windle WF (1958) Biology of neuroglia : [proceedings of a conference held in Bethesda, Md., in March 1956, and sponsored by the National Advisory Neurological Diseases and Blindness Council]. Springfield, IL USA: Charles C. Thomas.

Wolff C, Roy S, Ingham PW (2003) Multiple muscle cell identities induced by distinct levels and timing of hedgehog activity in the zebrafish embryo. Curr Biol 13(14) pp 1169-1181.

Wye-Dvorak J, Marotte LR, Mark RF (1979) Retinotectal reorganization in goldfish--I. Effects of season, lighting conditions and size of fish. Neuroscience 4(6) pp 789-802.

Wyllie DJ, Mathie A, Symonds CJ, Cull-Candy SG (1991) Activation of glutamate receptors and glutamate uptake in identified macroglial cells in rat cerebellar cultures. J Physiol 432 pp 235-258.

Xu X, Meiler SE, Zhong TP, Mohideen M, Crossley DA, Burggren WW, Fishman MC (2002) Cardiomyopathy in zebrafish due to mutation in an alternatively spliced exon of titin. Nat Genet 30(2) pp 205-209.

Xu Y, He J, Wang X, Lim TM, Gong Z (2000) Asynchronous activation of 10 muscle-specific protein (MSP) genes during zebrafish somitogenesis. Dev Dyn 219(2) pp 201-215.

Yakovlev PI, Lecours A-R (1967) The myelogenetic cycles of regional maturation of the brain. In: Regional development of the brain in early life, A symposium. (Minkowski A, ed), pp 3-70. Oxford & Edinburgh: Blackwell Scientific Publications.

Yamada T, Placzek M, Tanaka H, Dodd J, Jessell TM (1991) Control of cell pattern in the developing nervous system: polarizing activity of the floor plate and notochord. Cell 64(3) pp 635-647.

Yeh HJ, Ruit KG, Wang YX, Parks WC, Snider WD, Deuel TF (1991) PDGF A-chain gene is expressed by mammalian neurons during development and in maturity. Cell 64(1) pp 209-216.

Yoon MG (1976) Progress of topographic regulation of the visual projection in the halved optic tectum of adult goldfish. J Physiol 257(3) pp 621-643.

Yoshida M, Colman DR (1996) Parallel evolution and coexpression of the proteolipid proteins and protein zero in vertebrate myelin. Neuron 16(6) pp 1115-1126.

Young P, Ehler E, Gautel M (2001) Obscurin, a giant sarcomeric Rho guanine nucleotide exchange factor protein involved in sarcomere assembly. J Cell Biol 154(1) pp 123-136.

Yu WP, Collarini EJ, Pringle NP, Richardson WD (1994) Embryonic expression of myelin genes: evidence for a focal source of oligodendrocyte precursors in the ventricular zone of the neural tube. Neuron 12(6) pp 1353-1362.

Zelenika D, Grima B, Pessac B (1993) A new family of transcripts of the myelin basic protein gene: expression in brain and in immune system. J Neurochem 60(4) pp 1574-1577.

Zengel JM, Epstein HF (1980) Identification of genetic elements associated with muscle structure in the nematode Caenorhabditis elegans. Cell Motil 1(1) pp 73-97.

Zhou Q, Choi G, Anderson DJ (2001) The bHLH transcription factor Olig2 promotes oligodendrocyte differentiation in collaboration with Nkx2.2. Neuron 31(5) pp 791-807.

Zimprich F, Ashworth R, Bolsover S (1998) Real-time measurements of calcium dynamics in neurons developing in situ within zebrafish embryos. Pflugers Arch 436(3) pp 489-493.